Université de Montréal

The Multifaceted Proprotein Convertases PC7 and Furin: Identification of New Substrates and Physiological Relevance

Par

Stéphanie Duval

Biologie Moléculaire, Faculté de médecine

Thèse présentée en vue de l'obtention du grade de *Philosophiae doctor* (Ph.D) en

Biologie moléculaire, option médecine cellulaire et moléculaire

Avril 2020

Résumé

Les proprotéines convertases (PCs) sont responsables de la maturation de plusieurs protéines précurseurs et sont impliquées dans divers processus biologiques importants. Durant les 30 dernières années, plusieurs études sur les PCs se sont traduites en succès cliniques, toutefois les fonctions spécifiques de PC7 demeurent obscures. Afin de comprendre PC7 et d'identifier de nouveaux substrats, nous avons généré une analyse protéomique des protéines sécrétées dans les cellules HuH7. Cette analyse nous a permis d'identifier deux protéines transmembranaires de fonctions inconnues: CASC4 et GPP130/GOLIM4. Au cours de cette thèse, nous nous sommes aussi intéressé au rôle de PC7 dans les troubles comportementaux, grâce à un substrat connu, BDNF.

Dans le chapitre premier, je présenterai une revue de la littérature portant entre autres sur les PCs. Dans le chapitre II, l'étude de CASC4 nous a permis de démontrer que cette protéine est clivée au site $KR_{66}\downarrow NS$ par PC7 et Furin dans des compartiments cellulaires acides. Comme CASC4 a été rapporté dans des études de cancer du sein, nous avons généré des cellules MDA-MB-231 exprimant CASC4 de type sauvage et avons démontré une diminution significative de la migration et de l'invasion cellulaire. Ce phénotype est causé notamment par une augmentation du nombre de complexes d'adhésion focale et peut être contrecarré par la surexpression d'une protéine CASC4 mutante ayant un site de clivage optimale par PC7/Furin ou encore en exprimant une protéine contenant uniquement le domaine clivé N-terminal. Finalement, des résultats provenant de base de données de patients atteint de cancer du sein ont démontrés que

l'expression élevé des gènes *CASC4* et *PCSK7* corrélaient à un mauvais prognostique, tandis qu'une expression élevée de *CASC4* mais faible de *PCSK7* était associée un meilleur prognostique.

Dans le chapitre III, nous avons démontré que GPP130 est aussi clivé par PC7 et Furin mais au niveau des motifs H_{67}RSRLEK$_{73}$↓SL et K_{274}PTR$_{277}$↓EV dans les endosomes/TGN ou à la membrane plasmique. Récemment, GPP130 a été rapporté comme étant impliqué dans la prolifération cellulaire de cancers de la tête et du cou. Nos analyses provenant de la banque de données cBioPortal ont montré que le gène *GPP130/GOLIM4* était surexprimé dans 35% des cas de cancer du poumon. Nous avons aussi montré qu'une réduction de GPP130 dans les cellules de cancer de poumon A549 augmente légèrement la prolifération cellulaire. Nous étudions actuellement l'hypothèse que GPP130 transporterait des cargos qui pourraient influencer la prolifération cellulaire.

Finalement, durant le chapitre IV de cette thèse, nous avons poursuivi les études comportementales chez les souris PC7 KO afin d'investiguer si ces souris seraient protégées d'un effet anxiogène causé par l'obésité induite par l'alimentation. Nous avons montré que les souris PC7 KO ont une tendance à être moins affectées par la diète riche en gras saturé. Nous avons aussi montré que les souris PC7 ont une réponse déficiente face au stress.

En conclusion, nos travaux de recherche ont permis d'identifier de nouveaux substrats de PC7 afin de mieux comprendre son rôle biologique, mais aussi de soulevé l'importance de PC7 dans les troubles comportementaux.

Mots-clés : Protéolyse fonctionnelle, proprotéine convertase, modification post-traductionnelle, CASC4, GPP130, cancer, BDNF, comportement, anxiété, stress

Abstract

The proprotein convertases (PCs) are responsible for the maturation of precursor proteins and are involved in multiple biological processes. Over the past 30 years, the PCs have had great translational achievements, but the physiological roles of PC7, the seventh member of the family, are still obscure. Searching for new PC7 substrates, a quantitative proteomics screen for selective enrichment of N-glycosylated polypeptides secreted from hepatic HuH7 cells identified two type-II transmembrane-proteins of unknown function(s): Cancer Susceptibility Candidate 4 (CASC4) and Golgi Phosphoprotein of 130 kDa (GPP130/GOLIM4). The chapters II and III of this thesis will focus on the investigation of CASC4 and GPP130 shedding by PC7 and Furin, and their corresponding physiological functions. In chapter IV we pursued the PC7 KO mice behavior phenotyping.

Concentrating on CASC4 in chapter II, its mutagenesis characterized the PC7/Furin-shedding site to occur at $KR_{66}\downarrow NS$, in HEK293 cells. We further defined PC7 and Furin activity and demonstrated that CASC4 shedding occurs in acidic endosomes and/or trans-Golgi Network. Since CASC4 has been reported in breast cancer studies, we generated MDA-MB-231 cells stably expressing CASC4 WT and we showed a significant reduction of migration and invasion, caused by an increased number of paxillin-positive focal adhesions. This phenotype was reversed in cells overexpressing an optimally PC7/Furin-cleaved CASC4 mutant, or upon overexpression of CASC4 N-terminal domain. In accord, breast cancer patients' datasets show that high CASC4 and PCSK7 expression levels predict a significantly worse prognosis compared to high CASC4 but low PCSK7 levels.

In chapter III, we demonstrated that GPP130 is also cleaved by PC7 and Furin at similar and distinct motifs (H_{67}RSRLEK_{73}↓SL and K_{274}PTR_{277}↓EV) within acidic endosomes or at the TGN. GPP130 is predicted to be trafficking cargos and is responsible for the binding and retrograde trafficking of the Shiga toxin. In addition, GPP130 was recently reported to be implicated in cell proliferation in head and neck cancer cells. Our analysis from cBioPortal for Cancer Genomics has shown that the *GPP130/GOLIM4* gene is amplified in up to 35% of the patients with lung cancer. During this chapter we also showed that GPP130 knockdown in A549 cells slightly increases cell proliferation. We are currently investigating that GPP130 transports important cargos that would influence cell proliferation.

Finally, during the chapter IV of this thesis we have pursued the characterization of the PC7 KO mice anxiolytic phenotype that was previously described, and we investigated a possible protection from diet-induced obesity anxiety-like behavior. Interestingly, we have shown that the PC7 KO mice have a tendency to be less affected by the saturated high-fat anxiogenic diet. Also, we showed that the PC7 KO mice have an impaired stress-coping response that will need further investigations.

In conclusion, we identified new PC7 substrates to better understand its biology but we also investigated more deeply known substrates, such as BDNF in the PC7 KO mice to fully grasp the physiological functions of this enigmatic proprotein convertase.

Keywords Proteolysis, proprotein convertase, post-translational modifications, CASC4, GPP130, cancer, cell migration, BDNF, anxiety, stress.

Table of contents

List of tables

List of figures

List of abbreviations

ACTH: Adrenocorticotrophic hormone
ACC: Anterior cingulate cortex
ADAM: A desintegrin and metalloprotease
AgRP: Agouti-related protein
AP: Adaptor protein
Arf: ADP-ribosylation factor
ARC: Arcuate nucleus of the hypothalamus
Apo: Apolipoprotein
APP: Amyloid precursor protein
aa: Amino acids

BACE: β-site APP-cleaving enzyme
BDNF: Brain-derived-neurotrophic-factor
BFA: Brefeldin A
BiP: Binding immunoglobulin protein
BMP: Bone morphogenic protein
β-MSH: β-melanocyte-stimulating hormone
β-LPH: β-lipotropin

CART: Cocaine- and Amphetamine-Regulated Transcript
CASC4: Cancer susceptibility candidate 4
Ca2+: Calcium
CCK: Cholecystokinin
CDG: Congenital disorders of glycosylation
CMK: Chloromethylketone
COG: Conserved oligomeric Golgi
CT: Cytosolic tail

DA: Dopamine

EEA1: Early endosome antigen 1
EGF: Epidermal growth factor
EMT: Epithelial-mesenchymal transition
endoH: Endoglycosidase H
EPM: Elevated plus maze test
ER: Endoplasmic reticulum
ER: Estrogen receptor

FA: Focal adhesion
FST: Force swim test

GBP: Guanylate-binding protein
GEF: Guanine nucleotide exchange factor
GGA: Golgi-associated γ-ear-containing ARF binding protein
GOF: Gain of function
GPP130: Golgi phosphoprotein of 130 kDa
GRASP: Golgi Reassembly Stacking Proteins
GTP: Guanine triphosphate
GWAS: Genome-wide association studies
γ-LPH: γ-lipotropin

HER: Human epidermal growth factor receptor
HIV: Human immunodeficiency virus
HPA: Hypothalamic-pituitary-adrenal
HSPG: Heparan sulfate proteoglycan

IGFR: Insulin-like growth factor

KLK: Kalikrein
KO: Knockout

LDLR: Low-density lipoprotein receptor
LHA: Lateral hypothalamic area
LPC: Lymphoma proprotein convertase
LTM: Long-term memory

MBT: Marble burying test
MERS-Cov: Middle east respiratory syndrome
MMP: Matrix Metalloproteinase
MPR: Mannose-6-phosphate receptor
Mn2+: Manganese
MVB: Multivesicular bodies

NAc: Nucleus accumbens
ND: Normal diet
NGF: Nerve growth factor
NORM: Novel object recognition memory
NPY: Neuropeptide Y

NTD: N-terminal domain

OCD: Obsessive-compulsive disorder
OFC: Orbitofrontal cortex
OFT: Open-field test

PACE4: Paired basic amino acid cleaving enzyme 4
PACS-1: Phosphofurin acidic cluster sortin protein 1
PAR-1: Proteinase-activated receptor-1
PC: Proprotein convertase
PCSK: Proprotein convertase subtilisin kexin
PC7: Proprotein convertase 7
PFC: Prefrontal cortex
PNGaseF: Peptide-N4-(N-acetyl-beta-glucosaminyl) asparagine amidase
PM: Plasma membrane
POMC: Pro-Opiomelanocortin
PR: Progesterone receptor
PTM: Post-translational modification

Rab: Ras-associated binding
RER: Respiratory exchange rate

SARS-Cov: Severe acute respiratory syndrome -coronavirus
sdLDL: Small dense low-density lipoprotein
siRNA: Small interference RNA
SKI-1/S1P: Subtilisin kexin isoenzyme-1/site-1 protease
SNP: Single nucleotide polymorphism
SOCE: Store-operated calcium entry
SP: Signal peptide
SREBP: Sterol regulatory element binding proteins
STM: Short term memory
STRING: Search tool for the retrieval of interacting genes/proteins

TAILS: Terminal amine isotopic labeling of substrates
TfR1: Transferrin receptor 1
TG: Triglycerides
TGF: Transforming growth factor
TGN: Trans-Golgi Network
TM: Transmembrane domain
TRH: Thyrotropin-releasing hormone
TrKB: Tropomyosin receptor kinase beta

VEGF/VEGFR: Vascular endothelial growth factor/receptor
VTA: Ventral tegmental area

WT: Wild type

Life, finds a way

-Dr Ian Malcolm

Acknowledgements

I would like to thank my director, Dr Nabil G. Seidah, for welcoming me into his lab when I was a master's student and allowing me to stay for my Ph.D. It was a great adventure to be part of Dr Seidah's lab for the past few years. We certainly had some ups and downs, but I can say that I have progressed both professionally and personally during my time in Dr Seidah's lab. I would also like to thank Dr Annik Prat, for her rigorous mind but also for her advices on maintaining a balanced life. I also want to thank LoreleÏ, who showed me the way in the lab when I arrived and was an important part of the social life in the lab. Many thanks to the lab members, Julie always pushing me to be stronger, Emma for your positive attitude, Edwidge for our early morning conversations, Josée for cloning advices, Ann for keeping the lab together and Brigitte for everything really. All the lab members of course for their support and good spirit around the lab. I also want to thank my IRCM friends and colleagues that became my Montreal family, particularly Virginie for psychological support, I am lucky to have you around, and Dan who's been a great mentor and friend. I also want to thank Léa, the mouse whisperer. Huge recognition for Dominic Fillion for always being available and keen to help. I also want to thank my thesis committee members for their guidance during the past 5 years, with a special thanks to Dr JF Côté for being very supportive. Finally, I want to thank my thesis evaluation committee: Dr Hideto Takahashi, Dr Stephane Lefrançois, Dr Melkam Kebede and Dr Richard Bertrand for taking the time to read and evaluate this thesis.

On a personal note, I want to thank my family who always supported me and made me believe I could do this. My mom, for showing me how to be a strong independent woman and my dad for teaching me discipline and hard work. I also want to thank my friends in Quebec City, for still being around even though I more or less ignored them for the past 5 years…

Lastly, I want to thank my partner Jérémy for all those Saturday night dates at the IRCM's cafeteria between experiments and the long walks on the Mont-Royal. I would not have done a thesis writing marathon in quarantine with anyone else.

Chapter I. Introduction

1.1 General introduction

The secretory proprotein convertases (PCs) consist of a family of 9 serine proteases (PC1, PC2, Furin, PC4, PC5, PACE4, PC7, SKI-1/S1P and PCSK9) responsible for the maturation of a wide variety of precursor proteins and therefore enable their activation, inactivation and sometimes generate peptide fragments endowed with novel functions. To better understand the biological functions of the 7th member PC7, we have generated a proteomics screen to identify new PC7 substrates. In this thesis, we have investigated the biological roles of novel PC7 and Furin substrates as well as pursued the analysis of the PC7 knockout (KO) mice phenotypes.

To have a better appreciation of the proprotein convertases' relevance in biology and before diving into the experimental chapters, important definitions, mechanisms of action and key examples of proteolysis will be discussed. Finally, since the main goals of this thesis led to the identification of two Golgi proteins as novel substrates, a brief introduction to the Golgi structure, Golgi-resident proteins and their role in maintaining cellular homeostasis will be presented.

1.1.1 Post-translational modifications

The proteome in a living cell is vastly more elaborate than the number of proteins predicted by the known coding genes. Encoding a restricted number of genes and modulating the nascent transcribed mRNA or translated proteins are not only adding layers of complexity, but also allow for a more diverse genome and genome products. Diversity is the ability to adjust the genome and inherently protein functions in order to adapt and face different intracellular and extracellular stimuli and environment changes.

Amongst the ~20 000 genes in the human genome, it is estimated that there are about 4000 secretory proteins that traffic through the lumen of the endoplasmic reticulum (ER) to reach their final destination (1). It is therefore not surprising to find quality control enzymes in the secretory pathway in addition to enzymes responsible for a wide variety of post-translational modifications (PTMs) (2). PTMs govern protein outcomes by influencing not only their conformation but also their localization, interactions, and activities (3). This highlights the capacity of the cells to generate various end products from the same backbone in order to satisfy cellular acute needs

and maintain homeostasis. Tremendous amount of work has been done over the past decades to understand the biological mechanisms generated by the ≈ 200 PTMs estimated. These PTMs include: phosphorylation (serine, threonine or tyrosine), glycosylation (asparagine, serine/threonine); tyrosine sulphation, protein lipidation and/or prenylation; serine/threonine octanoylation; amino-terminal acetylation; N-terminal pyroglutamate formation; histone modifications such as lysine methylation, ubiquitylation; protein sumoylation, protein palmitoylation, proteolysis and carboxy-terminal amidation (4). Reversible and irreversible PTMs are key to adapt and control multiple cellular events such as modulating chromatin architecture, receptor tyrosine kinase signaling cascade and protein localization.

1.1.1.1 Post-translational modifications as biomarkers

The functional consequences of many aberrant protein modifications in multiple diseases has led to a rising interest in clinical and pharmaceutical research to target the PTMs machinery (5). It is now evident that PTMs are not only a fascinating fundamental research field but also provide evident examples of clinical importance, as discussed below (6). Many of the above listed PTMs are very dynamic and can widely vary between healthy and disease states. Phosphorylation is one of the most abundant PTM and according to the phosphosite database, there are over 350 proteins with modified PTMs in diseases state (5). Indeed, dysregulation of many proteins, such as Tau or α-synuclein have been highlighted since the 1980's to be important in neurodegenerative diseases such as Alzheimer's disease and Parkinson's disease, respectively. Modified patterns of phosphorylation has also been reported in other diseases ranging from acute myeloid leukaemia in bone marrow cells (AML) (7) to cardiovascular diseases (8). New tools to quantitively study profiles or patterns of PTMs by mass spectrometry are being developed and are rapidly emerging such as glycoproteomics. Glycosylation is the addition of oliogosaccharides to proteins (asparagine (N-glycans) or serine and/or threonine (O-monosaccharides and O-glycans). Adequate glycosylation is necessary for proper folding of proteins, stability and their function (2, 9). Because the addition of oligosaccharides is a multi-step procedure, many diseases have been described caused by mutations along the pathway. Accordingly, important defects in N-glycosylation are observed in a disease called Congenital disorders of glycosylation (CDG) and leads to mental and psychomotor retardation. Understanding glycobiology is relevant in many

physiological contexts, it can be used for instance in screening for glycated haemoglobin in diabetes (10), or can influence breast cancer progression (11). Finally, Table 1.1 is depicting examples of common reversible and irreversible PTMs in different clinically relevant settings that could represent critical biomarkers (5).

Table 1.1 Examples of reversible and irreversible PTMs considered for biomarkers in clinic

PTM	Protein example	Disease	Reference
Phosphorylation	Tau	Alzheimer's disease	(12)
	X box-binding protein 1 (NFX1)	Breast cancer	(13)
	α-synuclein	Parkinson's disease	(14)
N-Glycosylation	GP73	Hepatocellular carcinomas	(15)
	prostaglandin-H2 D-isomerase (PTGDS)	Prostate cancer	(16)
	CD59	Glucose handling	(17)
	Multiple aberrant N-glycosylation profiles	Schizophrenia	(18, 19)
Ubiquitinylation	UPS unique profiles	Leukemia	(20)
		Alzheimer's disease	(21)

1.2 Proteolysis: More than just trash bin enzymes

In biological chemistry, proteolysis can be simply defined as the enzymatic hydrolysis of a peptide bond by enzymes called proteases (22). As the chemistry suggests, this PTM is an irreversible mechanism. By its very irremediable nature, proteolysis is sometimes referred to as a deleterious mechanism (*i.e.* protein degradation by ubiquitin-proteasome system (23)), but it is in fact a ubiquitous PTMs responsible for the generation of diverse protein fragments that influences proteins biological function, localization and stability (24).

1.2.1 Learning from the bakers' yeast

The mechanistic understanding of proteolysis catalytic activity in mammalian cells was originally performed in the unicellular eukaryote *Saccharomyces cerevisiae* (the bakers' yeast). The seminal work by the Thorner group in yeast in the early 1980s have explained the protein maturation processes that were suggested during the characterization of proinsulin but where low

abundance of endogenous proteins rendered research technically difficult. The main conclusions from work on the α-mating factor in yeast originated from the deduction that the actual sequence of the gene was longer than the secreted bioactive polypeptide (25, 26). Accordingly, primary observations in the protein structure revealed that precursor genes had specific sequences referred to as "space segments" which will later be described as recognition motifs/cleavage motifs. Also, precursor proteins trafficking through the secretory pathway that were blocked in different organelles with specific inhibitors shown different molecular weight (27), suggesting that a certain maturation or processing was happening. They elegantly demonstrated that yeast *ste13* (dipeptidyl aminopeptidase) deficient strains were generating intermediate protein molecules in size and in biological activity (25). These original observations led to the conclusions that the precursor proteins were not processed correctly, hence the *ste13* mutants were interfering with the aminopeptidase enzymatic activity. They further demonstrated other functional consequences from this aberrant protein maturation by rationalizing that Kex2 mutants were incapable to process the prepro-α-mating factor needed for mating which thereby explained the sterile phenotype observed in the yeast Kex2 mutant (28). This way, they identified the enzymes responsible for the processing of the yeast prepro-α-factor; kex2 (25) and discovered the yeast homologue of the proprotein convertase Furin, one of the most studied protease with many biological functions and clinical applications (29).

1.2.2 The prohormone theory

Almost 20 years before Kex2 was identified for its role in processing precursors in yeast, Chrétien *et al*. introduced the prohormone theory (30). This theory stipulates that a biologically active peptide hormone comes from a larger polypeptide precursor. This statement was based on the observation that β-lipotropin (β-LPH) and γ-lipotropin (γ-LPH) contained a segment of identical sequence to β-melanocyte-stimulating hormone (β-MSH), a shorter peptide identified in 1955 (31). In support for the theory, they soon demonstrated that the β-MSH had the lipolytic and melanophore-stimulating activities (32). It took 24 years of sequencing to put all the pieces together to finally elucidate the Pro-Opiomelanocortin (POMC)-related peptides, which will soon become the model of prohormones (32). This ground-breaking achievement was done at a time where sequencing techniques were just starting (33, 34). Many other examples came to further

corroborate the theory when cloning and sequencing of neurohormones showed that active peptides seemed "contained" in bigger polypeptides and flanked by basic residues (35). Hence reinforcing that for a limited number of genes, many more bioactive peptides could be generated.

1.2.3 Proinsulin characterization

It is impossible to discuss the prohormone theory without acknowledging the work done on pro-insulin around the same period when the prohormone theory was enunciated. During the 1950's, it was a subject of active debate to understand and demonstrate how insulin is synthesized. Speculations such as that active insulin comes from two separate genes "glued" by disulfide bonds post-transcriptionally were proposed. Nevertheless, the mystery of the origin of insulin, first sequenced by Sanger in 1959 (33), was solved almost a decade later when Chance and Steiner published the characterization of the maturation of proinsulin. It was thus shown that proinsulin, the precursor of insulin, is processed into bio-active insulin following endoproteolysis at pairs of basic residues (36, 37). Steiner further demonstrated that proinsulin has very low biological activity but can be converted into active insulin after incubation with trypsin *in vitro* (38, 39). A timeline from the first gene sequenced (β-MSH) to the discovery of proprotein convertases and PCSK9 in 2003 by the laboratory of Dr Seidah is depicted on Figure 1.1. To conclude, insulin maturation is another pioneer example of precursor protein maturation and really paved the way for many more processing enzymes and substrates to be discovered. Indeed, many aspects of proteolysis such as enzyme classifications, substrate recognition and specificity emerged from these early studies on the α-mating factor, the prohormone theory and proinsulin characterization.

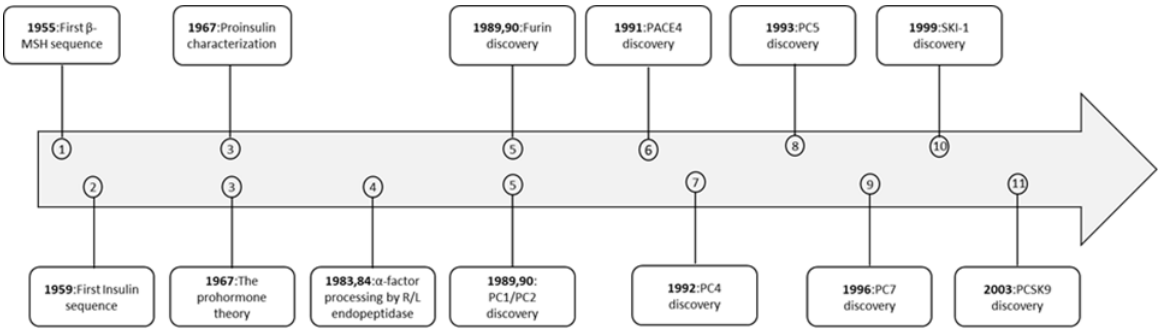

Figure 1.1. Timeline of selected proteases discovery.

Representation of the discovery of the first gene sequenced (β-MSH) in 1955 in a sequential order until the discovery of PCSK9 in 2003.

1.2.4 Proteases classifications and substrates' specificity

In humans, there are approximately 588 genes coding for proteases (24, 40) and based on the nature of their catalytic sites, they can be classified into 5 distinct groups: aspartic, metallo, cysteine, serine and threonine proteases, Figure 1.2. The first two classes of enzymes use a water molecule as a nucleophile in the peptide bond cleavage reaction, but the three remaining classes use a nucleophile catalytic amino-acid residue (*i.e.* Serine, Cysteine or Threonine) present in their active sites (40). Interestingly, metalloproteases and serine proteases have the most members in their family, and the threonine and aspartic proteases have the lowest number of members probably due to their high degree of specialization (40). These five different classes of proteases can also be grouped according to their sequence homologies and/or to the similarities between their three-dimensional (3D) folding (22).

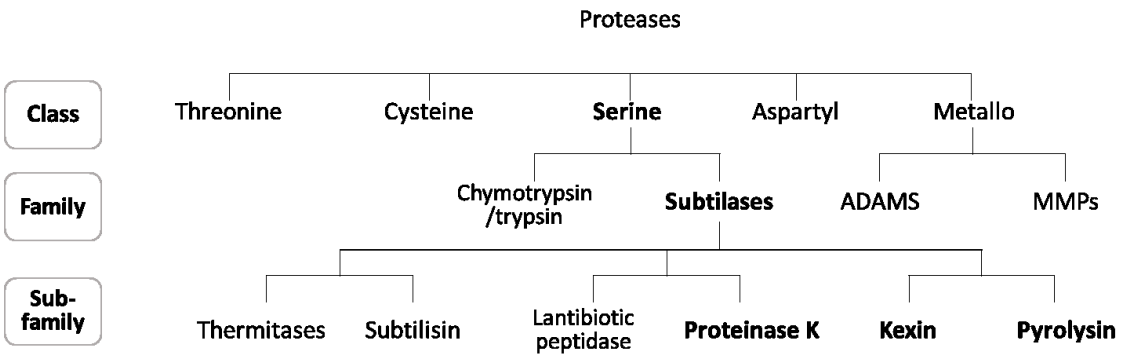

Figure 1.2. Proteases classification based on their catalytic domain.

Family tree is based on the homology of their catalytic domain. Adapted from Seidah and Chrétien 1999.

Substrates recognition and specificity have evolved in a way that enzymes are capable of targeting a wide variety of different substrates, hence allowing for a greater diversity of biological outcomes (41). A persevering area of research in the field of proteolysis is to understand a protease substrates' specificity. It is a very active area of investigation because a better understanding of the specialization of an enzyme for its target substrates will not only help to understand the protease biological functions, but it will also help in designing more specific enzymatic inhibitors. A great amount of information can be found looking at the crystal structure of an enzyme. For instance, the differences in substrates specificity between the proprotein convertase Furin, its yeast homolog kexin and subtilisin serine proteases have been highlighted when the crystal structures were solved (29) and has served as a good example to understand substrates specificity. Indeed the comparison between the structures allow us to observe differences in the substrates recognition pockets, rendering unique recognition properties (29). In fact, a closer look at the catalytic subunit of the crystal structures confirms a strong specificity for arginine in P_1 in Furin and Kex2 but not for subtilisin. Components of the enzymatic fold such as the shape and the distance accessible for the substrates, as well as specific contacts possible between the enzyme and the substrates side chains dictates a protease preference for substrates (29). Also, the specificity for the different residues around the substrate's cleavage site comes

from availability of the catalytic subunits grooves and different types of interactions, either elaborate machinery or looser interactions (29, 42).

The nomenclature P1-, P1'-, and S1-, S1'- originates from studies investigating the active site of the protease papain in relationship to its substrate, and can be appreciated in Figure 1.3 (43, 44). In the original work from Schechter and Berger, the authors described the residues around the enzyme catalytic active site as "subsites" grooves, hence the reference to S1, S2, S3 (…) and S1', S2', S3' since they started counting the residues from both sides of the catalytic site. The binding site on the substrates where hydrolysis occurs is referred to as the 'point of cleavage' therefore the P1, P2, P3 (…) and P1', P2', P3' (…) nomenclature, which it still currently used today.

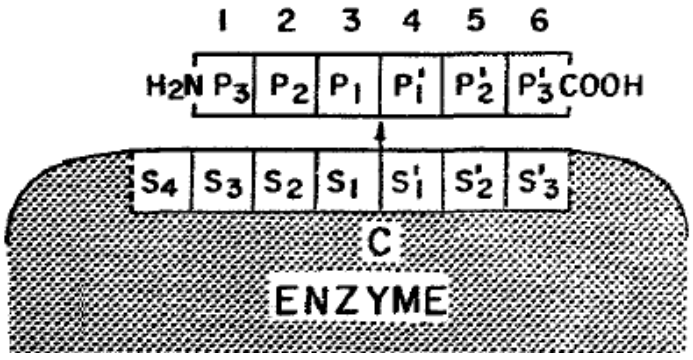

Figure 1.3. Nomenclature of the protease-substrate complex.

Design of the suggested nomenclature P3- P3' for the substrate side chain, and S4-S3' of the catalytic subunit of the enzyme. C: Catalytic subunit. Adapted from Schechter *et al*., 1967 (44).

Specificity for different substrates can also be appreciated *in vitro*, by performing kinetics analysis. Diverse tools used to screen for proteases substrates specificity, such as artificial peptide mapping have made it possible to decipher optimal substrate recognition sequences for processing enzymes. In search for the best way to characterize a protease substrates' specificity, many techniques have been developed and can be grouped into two categories: proteomic approaches and chemical tools (45). Those two broad categories are composed of multiple ways to identify not only the cleavage sites, which is critical, but has also led to identification of new

substrates. A very interesting approach for the identification of novel protease substrates with broad or unknown cleavage site specificity is the recently developed terminal amine isotopic labeling of substrates (TAILS) strategy. It is based on the idea that distinguishing the N-termini of a full length protein from a N-termini generated from a cleavage product, with differential isotope labelling, should give information not only on the substrates cleaved but also the cleavage sites (46). This strategy thus allows the identification of new substrates and/or their predicted cleavage sites without having to manually annotate the identified peptides for cleavage consensus motifs, which is a great technique for proteases without known cleavage motifs.

In conclusion, because of its irreversible nature, peptide-bond proteolysis needs to be tightly controlled in order to avoid derailed protein maturation. It is now evident that proteases biological functions go way beyond protein degradation to generated backbone material for novel protein synthesis (47). There is a wide spectrum of biological processes where proteolysis is essential to maintain cellular integrity, and sometimes this regulation happens is a not-so-convenient place as inside the lipid bilayer of the cell membrane.

1.2.5 Regulated intramembrane proteolysis and proteolytic ectodomain shedding

The idea that a protease trapped inside a lipid bilayer is able to recognize and cleave specific substrates is quite extraordinary, yet regulated intramembrane proteolysis of membrane proteins is a key mechanism in cell biology (48, 49). For example, the rhomboids are the most well understood intramembrane proteases and are actually the most prevalent membrane proteins across all living organism (50). The physiological roles of the rhomboids have been linked to multiple fields of biology, from development to diabetes (51), but understanding how a membrane-trapped enzyme is regulated and coordinates processing of specific substrates remains a challenging area of research. Also, many cases of intramembrane proteolysis is preceded by an ectodomain shedding often realized by members of the ADAM (a desintegrin/metalloprotease) family or aspartyl proteases (BACE1, BACE2), which subsequently allows the transmembrane domain to be accessible for an intramembrane protease (52). One of the most studied examples is the amyloid precursor protein (APP) because of its connection to

Alzheimer's disease. Interestingly, the role of the full-length APP is still not fully understood but its shedding is one of the most studied shedding events because of the generation of neurotoxic amyloid-β (Aβ) aggregates in the brain (53). To summarize the shedding event leading to deleterious Aβ formation, the first step is the shedding in the N-terminal region of APP by a β-secretase (BACE1 or BACE2/aspartyl protease). Following this cleavage, the transmembrane domain is now accessible for a second cleavage by γ-secretase within its transmembrane domain. This leads to the formation of heterogenous Aβ entities of different sizes, ranging from 37 to 43 amino acids (aa) with the major product being Aβ40 and the minor being Aβ42 (52). Albeit being the minor form, this Aβ42 product is thought to be one of the causative fragments of Alzheimer's disease (52). The remaining APP intracellular domain is then released into the cytosol to be degraded but signalling functions of this entities are subject of ongoing debates. Indeed, both the cleaved form and the membrane bound form of the intracellular domain have been shown to retrotranslocate into the nucleus to have transcriptional activity (54, 55). On the other hand, the α-secretase (ADAM10, ADAM17) shedding of APP prevents the formation of the pathogenic Aβ, and the ectodomain released from the α-secretase shedding was also demonstrated to have neuroprotective effects (56, 57). Accordingly, a recent report has demonstrated that the shed APP binds the sushi domain of the gamma-aminobutyric acid type B receptor subunit 1a (GABAB1a receptor) in hippocampal synapses which leads to suppressed synaptic transmission and enhances short-term facilitation (58). Finally, APP mutations around or in the cleavage sites are associated with rare familial forms of Alzheimer's disease (52). This sequential cleavage events of APP and the demonstrated roles (either detrimental or protective) of the different specific cleavage products is a great demonstration that proteolysis has drastic consequences and needs to be regulated.

Previously portrayed as a means for the cell to adapt to extracellular stimuli by adjusting the levels of membrane proteins available at a given time, proteolytic ectodomain shedding is also controlling the activity of multiple membrane proteins (59). The definition of shedding is the cleavage of a transmembrane protein (either single pass, GPI-anchored and/or multiple transmembrane domains) by a protease (called sheddases in this case)(59). The cleavage on the juxtamembrane (the region next to its transmembrane domain) typically occurs within 10-35 aa

of the transmembrane domain or even within the transmembrane domain, but more distant shedding is also possible (59). This shedding results in two distinct entities, one soluble extracellular domain (ectodomain), and a membrane-bound fragment (60-62). Contrary to what shedding was previously referred to, that ectodomain shedding is occurring solely at the plasma membrane (62), it is now becoming clear that shedding can occur in many cellular compartments of the secretory pathway, hence influencing protein functions at different levels (59). Indeed, the functional consequences of this shedding can be grouped in three different categories; The first mechanism is shedding of a full-length transmembrane protein that will inactivate its function. This mechanism will not only lead to cleaved protein fragments that will be directly targeted for degradation, in some cases the released fragment can act as a decoy receptor, which can also dampen signaling (*i.e.* B cell maturation antigens) (63). The second mechanism is the activation of membrane proteins, *via* release of a biologically active fragment from the parent protein. It is also interesting to note that in some cases the full length and the shed products have opposite roles in signaling events. Finally, the third mechanism is shedding that allows subsequent cleavage by regulated intramembrane proteolysis. One typical example, other than APP, is the Notch receptor where Notch is endocytosed with its ligand allowing for ADAM10 first cleavage and is followed by a γ-secretase second processing, which releases a small intracellular domain fragment (NICD) that can now act as a transcriptional activator (64). Figure 1.4 is a schematic representation of the three mechanistic consequences of shedding.

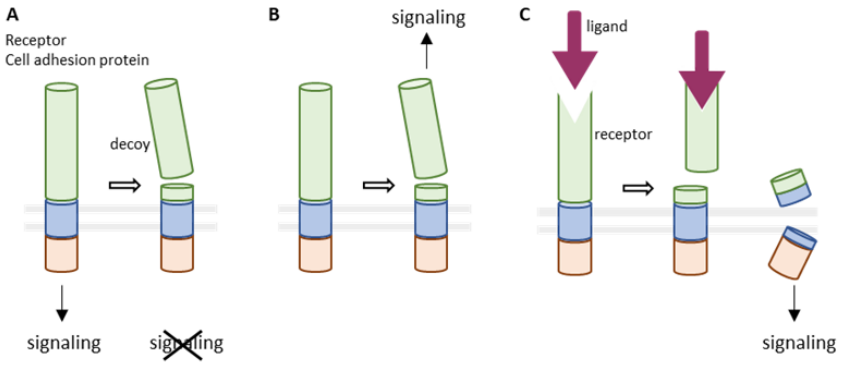

Figure 1.4. Consequences of proteolytic ectodomain shedding.

A) Shedding inactivates the function. B) Shedding generates biologically active molecules. C) Shedding allows subsequent cleavage. Adapted from Lichtenthaler *et al*., 2018.

1.3 Serine proteases: Evolutionary blockbusters

1.3.1 Classification:

Before presenting the proprotein convertases, it would first be necessary to address the catalytic activity of this class of enzymes, as well as other well-known examples of serine proteases. Serine proteases represent one third of known proteases (~175 members), most of them are secreted (*i.e.* thrombin) but a fraction of them are membrane-bound (type-I , type-II or via GPI-anchorage) (65, 66). Serine proteases can be classified into six different families; chymotrypsin/trypsin, subtilisin-like, carboxypeptidase C, D-Ala-D-Ala peptidase A, repressor Lexa and the ATP-dependent serine peptidase, based on their substrates specificity and organization of their catalytic subunits (43, 67). Within these families, the two largest groups are: proteases related to trypsin/chymotrypsin and those similar to bacterial subtilisin (called subtilases) (43). Trypsin-like proteases (such as tryptases, matriptases, kallikreins and granzymes) cleave proteins at arginines or lysines (68). Chymotrypsin-like proteases cleave proteins at the C-terminus of phenylalanine, tyrosine, Leucine or tryptophan (69). For the subtilisin group, bacterial subtilases cleave after multiple residues, but the Kexin-like members of the subtilase family are more specific to basic residues as they only cleave after monobasic/dibasic/multiple basic residues (70, 71).

1.3.2 Catalytic mechanism

The catalytic mechanism of serine proteases is based on an evolutionary conserved catalytic triad, which coordinates a nucleophilic attack on the substrates carbonyl atom (72). In brief, the serine residue is bringing the nucleophilic hydroxyl to attack the scissile bon, the histidine acts as the catalytic base when deprotonation of the nucleophilic serine, with the help of the aspartate that stabilizes the positive charge on the histidine (73). The scissile bond attack generates a build-up of negative charges on the carbonyl oxygen, this situation is stabilized by an "oxyanion hole", giving hydrogen bond donors to the carbonyl oxygen. From this, the substrate is bound to the enzyme and the first step of catalysis (acylation) can happen. Following this first step, a product is released from the substrate which then leaves the serine covalently linked, as an ester, to the polypeptide chain and is referred to acyl enzyme intermediate. This intermediate is then deacylated by a water molecule, hence generating the N-terminal cleavage product (73).

Interestingly, this catalytic triad is found in four different protein folds, thereby showcasing an important evolutionary pressure that happened in four different independent situations (74). The Figure 1.5 is depicting catalytic mechanisms within four different enzymatic groups to compare endopeptidase mechanisms (75).

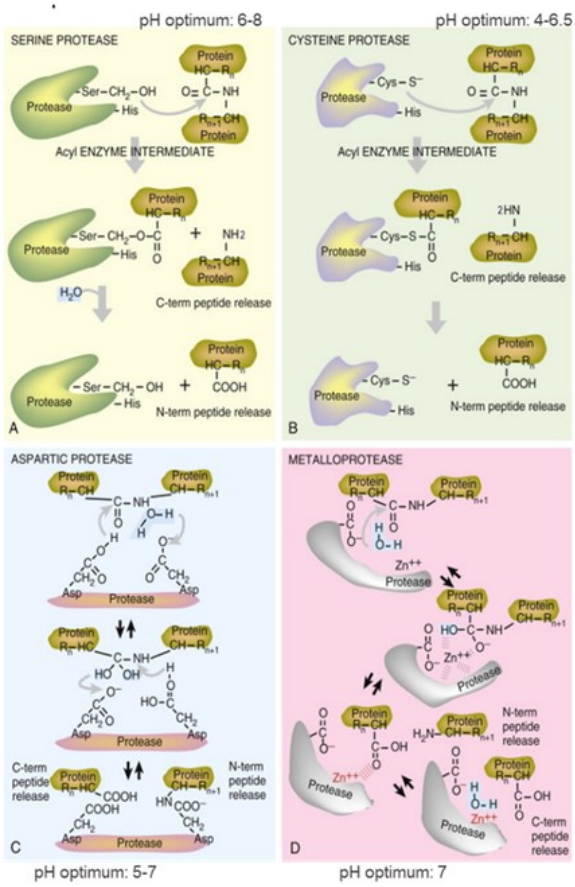

Figure 1.5. Endopeptidase catalytic activity.

A) Serine proteases cleave peptide bonds by forming an acyl enzyme intermediate. The active-site serine bonds temporarily with the amino-terminal fragment of the cleaved protein. B) Cysteine proteases use a similar mechanism to serine proteases but use active-site cysteines. C) Aspartic proteases have two active-site aspartic acids that hydrolysis the substrate protein. D) Metalloproteases use metal ions (Zn^{2+}) to hydrolyze their substrates. Different pH requirements for adequate enzymatic activity is also depicted. From Clark *et al.*, 2016 (75).

1.3.3 Serine proteases in health and diseases

It is now well established that serine proteases are important in many fields of biology such as digestion, blood coagulation, apoptosis, immunity and fertilisation (76). Many serine proteases are involved to maintain homeostasis in healthy individuals such as in the hemostasis cascade, namely thrombin and factor X (77). In fact, almost all the hemostatic enzymes are serine proteases (77). Another well known serine protease is trypsin, which is secreted by the pancreas and helps in digestion by cleaving larger polypeptides after arginine or lysine into smaller fragments (78, 79). Many serine proteases are also widely studied in immune regulation and infectious diseases (69). Regarding immune regulation, serine proteases are implicated in inflammation, pathogen clearance and apoptosis (80). For example, both the cytotoxic T lymphocytes and natural killer cells in human secrete five types (A, B, H, K, M) of the serine protease granzymes, which help in the killing of infected and/or tumour cells (81).

Also, since they are responsible for the activation of numerous growth factor ligands and receptors (82), promoting epithelial to mesenchymal transition (EMT) (82) and activating extracellular matrix metalloproteinase remodeling proteins (*i.e* MMP14 (83)), serine proteases have been extensively studied in the context of cancer. Overexpression of many membrane-bound serine proteases have been found in different types of cancers (82). Type-II serine proteases such as matriptases, hepsin and prostatin have been studied extensively in various cancers such as breast cancer and head and neck cancers (84).

One of the well-known proteases studied in cancer, other than the proprotein convertases, which will be discussed below, are the kallikrein serine proteases (chymotrypsin-like) (85). The kallikrein (*KLK*) family of genes is the most abundant proteases group of the human genome with 15 members (*KLK1-KLK15*) (86). In normal physiology, kallikreins function in harmony in diverse physiological systems, *e.g.* skin epidermis. However, loss-of-function of an important natural inhibitor of these enzymes, the lympho-epithelial Kazal-type inhibitor (LEKTI), results in dramatic consequences that are found in a genetic disease known as Netherton syndrome, where the patients have impaired keratinisation and aberrant skin barriers (85), likely due to derailed proteases activity. Another clinically important area of research related to the kallikrein enzymes

is in ovarian cancer (87-91). The clinical relevance of the kallikrein enzymes in ovarian cancer is very diverse, where KLK5-7 high expression seems to be providing unfavorable outcomes, but KLK11 and KLK14 increased expression seems to be favorable (85). Overall, various expression levels of the different kallikreins in ovarian cancer illustrates the complexity of studying a rich proteolytic network in a disease context. Further studies will be needed in order to better understand the physiological relevance of these enzymes and their targeted substrates in hope of finding novel diagnostic tools and treatment strategies.

1.4 The proprotein convertases

1.4.1 Putting all the pieces to the puzzle together

The first proprotein convertases (PCs) were identified and characterized in a quest to find the enzymes responsible for transforming or *converting*, precursor proteins into bioactive peptides (92). The idea was incubating in the minds of many international scientists since the mid 1960s in response to the pro-hormone theory developed around these years (31,33,38). Multiple discoveries paved the way to the identification of the nine members of the proprotein convertase family, an adventure that lasted 23 years.

As mentioned before, it is really the identification of the archetypical serine proteinase Kex*2* in yeast, which reported that this enzyme is related to bacterial subtilases, and not to the trypsin-chemotrypsin fold (93, 94), that really kicked-off the race to identify other proteolytic enzymes. Previous failed attempts at identification of the mammalian members using degenerate primers derived from bacterial serine proteases of the chymotrypsin-trypsin catalytic active site were suddenly explained. Further evidences came from the demonstration that many precursor proteins were matured into their bioactive entities when overexpressing the yeast kexin (*i.e.* adrenocorticotropic hormone (ACTH)) (95), but not all of the substrates (*i.e.* pro-somatostatin) (96), which pointed towards potential mammalian homologues that could have similar but somewhat different substrate specificities. From there on, the identification of a mammalian homologue of the yeast kexin, called Furin, (97) was really a breakthrough and was accompanied by the simultaneous discovery of two neuroendocrine PCs, namely PC1 and PC2 (94, 98-100).

Over the next 13 years a total of nine subtilisin-like secretory serine proprotein convertases were identified, with the first seven being basic-amino acid specific convertases: PC1, PC2, Furin, PC4, PC5A/B, PACE4 and PC7; while the 8th member (site-1 protease or SKI-1) (101), is a pyrolysin-like homologue of subtilisin. The last member PCSK9 was characterized in Dr Seidah's laboratory in 2003 (102), has no other catalytic activity than the autocatalytic cleavage of its pro-segment in the endoplasmic reticulum (ER).

1.4.2 Conserved structure and zymogen activation

The PCs share remarkable similarity in their primary structure, especially in the subtilisin-like catalytic domain containing the catalytic triad (Asp, His and Ser, and the Asn of the oxyanion hole) (4). Indeed, based on over 150 proprotein convertase sequences aligned and analyzed from different species, the sequences of the active sites are 95% conserved (103). The first seven PCs cleave (↓) precursor proteins at specific single or paired basic aa within the motif (R/K)-(2X)$_n$-(R/K)↓, where n = 0-3 spacer aa (4). Other common PC features include a signal peptide that allows entry of the proteins in the secretory pathway, a prosegment that is necessary for proper folding and can act as a inhibitor, a P-domain that stabilizes the catalytic pocket and also regulates the enzyme calcium dependence as well as the pH sensitivity, and a C-terminal domain that contains unique information dictating the trafficking route and localization of the protein (4, 104).

The zymogen processing of the secretory PCs begins in the ER, following removal of the signal peptide by the signal peptide peptidase (4). The next step is the protein folding, which is regulated by the N-terminal pro-segment (intramolecular chaperone and inhibitor) and results in the autocatalytic cleavage of the pro-segment. These events will release from the ER the PCs in an active conformation that remain attached to their inhibitory prosegments, as a controlled inhibitory mechanism until the cognate subcellular localization is achieved (4). In fact, different PCs will lose their inhibitory prosegments in different target organelles, in order to maintain limited proteolysis of substrates. The sections bellow will discuss distinct maturation mechanisms, trafficking properties, specific substrates and associated biological roles of the nine proprotein convertases, with a deliberate emphasis on Furin and PC7, which are the focus of this

thesis. Figure 1.6 depicts selected major physiological contributions of the nine proprotein convertase in humans.

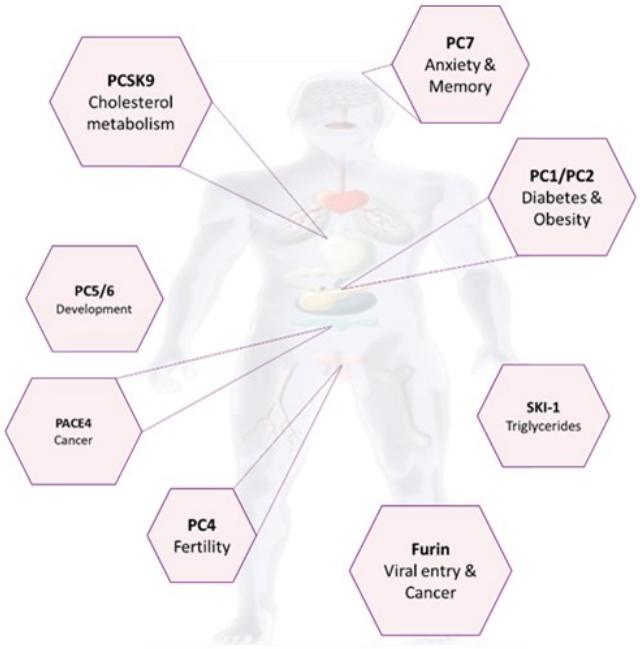

Figure 1.6. Proprotein convertases in health and diseases.

Schematic representation of selected proprotein convertases' roles in health and disease states.

1.4.3 PC1 and PC2: The neuroendocrine enzymes

ProPC2 is the only convertase that is activated by the removal of an inhibitory chaperone called 7B2. Indeed, proPC2 remains bound to its chaperone 7B2 (105) until it reaches immature secretory granules and can then get autocatalytically activated (106, 107). PC1 and PC2 are found in immature and dense-core granules of neural and neuroendocrine cells, which explains why they are responsible for the maturation of most prohormones in the regulated secretory pathway (108, 109). The regulated secretory pathway, as opposed to the constitutive secretory pathway, is composed of secretory granules that store bioactive hormones, which are secreted in response to various stimuli (110). The localization of PC1 and PC2 in the endocrine and neural granules helped to decipher their functions. In the brain, they are highly expressed in hypothalamus (111), but are also found in cerebral cortex, hippocampus and cerebellum (112-114). Whereas in the peripheral tissues, PC1/2 are mainly localized in adrenal medulla, pituitary, thyroid gland,

pancreas (β-cells) and small intestine (109, 115-117). From earlier studies in mice, it was established that PC1 was responsible for a wide range of precursor prohormones, from POMC to proinsulin. Interestingly, PC1 is capable of processing independently precursor proteins into a bioactive entity such as the generation of ACTH from POMC (118), but sometimes it requires the subsequent activity of PC2 (*e.g.* in the case of proinsulin and thyrotropin-releasing hormone (TRH)) (4, 119, 120).

The physiological relevance of PC1/PC2 was predictable from their tissue localization (*i.e.* neural and endocrine cells) and was confirmed in multiple knockout (KO) models in mice. The remarkable phenotypes of PC1 KO mice were: severe dwarfism likely due to impaired growth hormone releasing hormone (GHRH) (121), proopiomelanocortin, proinsulin and proglucagon processing. The PC2 KO mice displayed chronic fasting hypoglycaemia and lower circulating glucagon (122, 123). Patients with mutations in the *PCSK1 or PCSK2* genes have multiple phenotypes that are anticipated from the mice studies. Indeed, the first patient with a heterozygous mutation in *PCSK1* exhibited severe hypoglycaemia, impaired adrenal and thyroid functions, hypogonadotropic hypogonadism and severe obesity (124). Accordingly, the clinical phenotypes of PC1 deficiency also include polyuria/polydipsia, malabsorptive diarrhea, hypotyroism and hypocortisolism (125) and obesity (126, 127).

1.4.4 PC4 and the male contraceptive speculations

Like the other proprotein convertases PC4 is synthesized as a zymogen but unlike the other convertases PC4 is trapped in the ER *via* interaction with the chaperone glucose-regulated protein 78/immunoglobulin heavy chain binding protein (GRP78/BiP) in somatic cells (128). This binding leads to an impossibility to activate proPC4 to PC4 in non-germline cells, suggesting highly specialized biological functions in gonadal tissues. Also different from the other PCs, after the first autocatalytic cleavage of its prosegment, PC4 does not need a secondary cleavage, since no apparent second cleavage site is detected. Hence, the prosegment might be separated early in the secretory pathway like PC7 (129).

The confined tissue localisation of PC4 to gonads limits its cellular targets and therefore its biological functions *in vivo*. Indeed, being solely expressed in the testicular germ line pachytene

spermatocytes and round spermatids cells in males (130, 131), and in the placenta and ovaries in females (132), its contribution to fertility were anticipated. Accordingly, *PCSK4*-deficient male mice showed subfertility, and it was suggested to be caused by egg-binding lower capacity, accelerated capacitation and precocious acrosomal reaction (131). Albeit these drastic phenotypes observed in mice and their related consequences to the comprehension of fertility, very little is known about endogenous PC4 substrates within the testis or placenta. Nevertheless, *in vitro* analysis demonstrated that PC4 was capable of cleaving proIGF-1/-2 as well as propituitary adenylate cyclase activating polypeptide (proPACAP) (133). Also, a more recent report suggested that the infertility phenotype observed in the *PCSK4*-null mice were in part due to the lower maturation of ADAM2, a protein implicated in the sperm-egg plasma membrane interaction (134-136).

1.4.5 PC5A, PC5B

The *PCSK5* gene is broadly expressed, with enriched tissues such as the adrenal cortex, intestine, kidneys and ovaries (137, 138). Unlike the other PCs, the *PCSK5* gene encodes two alternatively spliced mRNAs, which results in two very distinct products, one being a widely expressed 913 amino acid soluble protein (PC5A) that can be located at the plasma membrane by its interaction with heparan sulphate proteoglycans (HSPGs) (139) and a type-I transmembrane of 1860 amino acid protein mostly found in gut (140, 141).

The *PCSK5* KO mice have also been very informative in the characterization of the physiological functions and related substrates. Indeed, *PCSK5* KO mice die at birth and show a drastic phenotype of considerable defects in anteroposterior axis such as extrathoracic and lumbar vertebrae, and they are also missing kidneys and their tails (142). Interestingly, the connection between the *Gdf11* KO mice, that also lack their tails (143), led to the demonstration that GDF11 is a PC5 substrate (136) and is possibly causing the anteroposterior patterning gross defects (144). In humans, intronic *PCSK5* SNPs have been associated with low circulating levels of high-density lipoproteins (145). In addition, PC5, as well as Furin, are found in atherosclerotic lesions in humans and are up-regulated after vascular injuries in animal models (146). Interestingly, PC5 is believed to have some protective role in intestine-related adenocarcinomas, as mice lacking

PC5 in enterocytes displayed more tumours (147). Also, recent reports have demonstrated a role for PC5 in bone, as it is was shown to be responsible for osteopontin cleavage. Osteopontin has a role in bone mineralization, cell adhesion and migration, and accordingly *PCSK5* epiblast-specific conditional knockout mice displayed smaller bone size and delayed ossification (148). Finally, the specific function(s) of PC5B in the gut where it is most abundant is still obscure.

1.4.6 PACE4

PACE4 is secreted, and like PC5 (139), it is widely expressed and binds HSPGs at the cell surface of the cells and in the extracellular matrix (149) by its cysteine-rich domain (150). A few substrates have been demonstrated for PACE4 *in vivo*, such as nodal and lefty, two TGFβ-like proteins important during development, and are also substrates redundant with Furin (151). Other known substrates are ADAMTS-4 (152) , angiopoietin-like 3 (153) and the accessory viral protein of HIV-1 Vpr (154). Similar to PC5, the *PCSK6* (the PACE4 gene) KO mice display growth defect, but contrary to PC5, the *PCSK6* KO mice die embryonically at day 14 in 25% of the cases and have cardiac malformations, as well as bone morphogenetic defects (155).

Unsurprisingly, PACE4 has also been extensively studied in the context of cancer development, more precisely in prostate cancer. As mentioned above, it is now well understood that PCs play an important role at different levels of cancer progression, and the clinical relevance of PACE4 inhibition in therapeutic avenues is a good example. Original works from the group of Dr Robert Day demonstrated that amongst all the PCs, *PACE4/PCSK6* is a unique PC overexpressed at mRNA levels in prostate cancer (156). This study elegantly demonstrated for the first time that specifically inhibiting PACE4 in DU145 prostate cancer cells significantly reduced proliferation *in vitro* and in xenograft mouse models (156). This seminal work was deemed extremely promising for patients and led to rapidly evolving endeavors aiming to develop PACE4 inhibitors. Further studies have also demonstrated that PACE4 is also critical during cancer progression *via* the generation of very oncogenic alternatively spliced isoforms occurring in prostate cancer cells, which is referred to as an oncogenic "switch" and was suggested to also occur in other cancers (157).

1.4.7 Furin

1.4.7.1 Trafficking

Furin is a ubiquitously expressed enzyme, which is activated by removal of its prodomain in the *trans*-Golgi network (TGN) (158), and can be shed from the majority of the cells (159). Because Furin is implicated in a multitude of physiological processes, from development to viral infection, it is crucial to properly understand its activation. In that sense, a lot of work has been done to map its trafficking and binding partners. Being localized in the TGN at steady-state, a central hub for sorting proteins to many destinations (*i.e.* cell surface, endosomes and lysosomes) (160), its trafficking/ zymogen activation needs to be tightly controlled (161). Furin localization in the TGN is regulated by its cytoplasmic tail, more precisely a bipartite motif composed of a (EECPpSDpSEEDE) casein kinase 2 (CK2)-phosphorylated acidic residue cluster and two hydrophobic motifs (YKGL and LI) (162-164). Importantly, this bipartite motif is responsible for two different trafficking movements. The hydrophobic motifs (YKGL and LI) are needed for Furin budding from TGN to endosome, *via* binding to the adaptor protein AP-1 (165), but the YKGL motif is also responsible for its endocytosis by binding the µ2 subunit of the adaptor protein AP-2 (165) . On the other hand, the phosphorylated acidic cluster is recognized by the sorting protein PACS-1 and therefore is important in the retrieval from endosome back to the TGN (166). Overall, Furin is in the TGN at steady state, but can move to the plasma membrane (PM) and recycle back to the TGN following its endocytosis from the PM, thus encountering multiple substrates along the way, explaining why it is involved in a wide range of processing and physiological activities at the TGN, cell surface and endosomes (158).

1.4.7.2 Substrates/Biological functions: Development

Emphasising its requirement in multiple biological processes, *Furin* KO mice are embryonically lethal at day 11, likely due to haemo-dynamic insufficiency and cardiac defects (167). In brief, different steps of extra-embryonic tissue development as well as cardiogenic mesoderm formation requires Furin to generate adequate vascularisation, ventral closure, heart-looping and axial rotation (167). The defects observed in aberrant symmetry in the embryos are due to a reduction in Furin-activated growth factors nodal and lefty (167, 168). Other growth factors are

processed by Furin, such as TGFβ, which will be discussed below in the cancer-related section, as well as bone morphogenetic protein-4 (BMP-4) (169). The cardiac defects in Furin KO mice are associated with loss of bone morphogenic protein 10 (BMP10) processing (170). Another important step of embryogenesis involving Furin is the formation of adequate synaptic complexes. Accordingly, Furin was shown to be the main protease activating the archetypical neurotrophin pro-β-nerve growth factor (pro-β-NGF) (161). Interestingly, neurotrophins are synthesized as proproteins, and accumulating evidences are demonstrating that the pro-form and the mature form of these proteins have opposite signaling consequences namely neural growth or cell death (171). Another interesting regulation mediated by Furin activation is the first cleavage event in Notch signaling (172). Furin cleavage of Notch transmembrane domain leads to its second cleavage by γ-secretase and the release of an intramembrane fragment that will act a as transcriptional regulator for C-promoter binding factor/Suppressor of hairless/LAG-1 (CSL), leading to gene transcription implicated in cell to cell communication during development (173). This contrast with the function of uncleaved Notch that inhibits cell differentiation (174). In addition, many important Furin physiological functions were highlighted from studies in mice using the Mx1-Cre transgene systems to generated Furin knockdowns (KDs) in specific tissues. Analysis from these mice, especially the liver-Knockdown mice were the first evidences that Furin had redundant functions with other PCs (175).

In addition to mice studies, mutations within cleavage motifs of different substrates have been found in patients and are suggested to have clinical consequences. An interesting example is the cleavage and inactivation by Furin of phosphate-regulating hormone fibroblast growth factor 23 (FGF23), a protein secreted from osteoblasts and osteocytes that regulates the reabsorption of phosphate and catabolism of 1,25-dihydroxyvitamin D_3 in the kidneys (176). Furin inactivates FGF23 by cleavage at the motif $R_{176}HTR_{179}{\downarrow}S_{180}AE_{182}$. Gain-of-function (GOF) mutations in FGF23 have been identified in patients with autosomal dominant hypophosphatemic rickets (ADHR), where the arginine residues within the cleavage motif are mutated, thereby resulting in an uncleavable and more stable hormone (177). Also, the threonine 178 within the above cleavage motif can also be O-glycosylated, which blocks the Furin cleavage, and results in a more biologically active hormone. Accordingly, inactivating mutations in the N-

acetylgalactosaminyltransferase 3 (GalNAcT3) prevents FGF23 O-glycosylation and increases Furin cleavage of FGF23 at $Arg_{179}\downarrow$ (178). In addition, it was recently demonstrated that the serine 180 could also be phosphorylated by the secretory kinase FAM20C (179), which in turn blocks the O-glycosylation and makes the cleavage by Furin more favorable and therefore inactivates FGF23 (180). This former example reveals the complexity of the post translational network in order to finely regulate precursor protein functions.

1.4.7.3 Substrates/Biological functions: Cancer

Overexpression of Furin in multiple cancers have led to detailed investigations of Furin activity and targeted substrates susceptible to modulate cancer progression (83). Furin is mainly responsible for the activation of matrix metalloproteases (MMPs), a group of proteins responsible for the degradation of extracellular matrix, thereby facilitating cell invasion and migration, but also growth factors, cell-adhesion molecules and angiogenic and lyphangiogenic factors. Table 1.2 summarizes how Furin overexpression impacts a variety of cancers, with the associated phenotypes and the candidate substrates. One of the archetypical examples of Furin's role in cancer, is its regulation of TGFβ. The transforming growth factors (TGFs) were originally identified as potent molecules capable of inducing the anchorage-independent growth transformation of rat fibroblasts in 1981 (181). Since then, the subject of TGFβ in cell proliferation, cell adhesion, organization and programmed cell death has been well documented (182), but its involvement in cancer progression still remains controversial. Indeed, opposite results can be found in the literature about the direct roles of TGFβ. This cytokine acts as a suppressor in pre-malignant state, but helps in tumour growth and metastasis in later stages (183). It was also demonstrated that Furin activates TGFβ and that active TGFβ is promoting the expression of metalloproteinases and integrins (184). Other Furin substrates that are contributing to cancer include the well-known metalloproteases ADAM10 and ADAM17, two proteases with important roles both in development and cancer (185). Another key example is the Furin-activation of MMP-14, a proteases that once activated is capable of cleaving collagen 1 (186) and is also important in the first step of maturation of another MMP, MMP-2 (187). Finally, Furin also plays a role in activating cell-adhesion molecules such as N-cadherin and E-cadherin, important proteins in cell to cell interactions but that can also mediate signaling (188).

Interestingly, while Furin activates N-cadherin, PC5A inactivates it by cleavage at an alternative site (188).

Table 1.2. Selected Furin implication in various cancers and the related substrates

Cancer types	Phenotypes	Furin substrates	References
Lung Carcinomas, non small cells, lung squamous cell carcinomas, adenocarcinomas	Invasive potential	IGF-1R	(189)
Head and neck squamous carcinomas	Aggressiveness	MMP14	(190)
Head and neck squamous carcinomas	Cell proliferation, tumorigenicity invasiveness	TGFβ, MMP14, IGF1R, VEGF-C	(191)
Squamous cell carcinomas of the oral cavity and oesophagus and laryngeal	Invasiveness	VEGF-C, MMP14	(192, 193)
Breast	oestrogen dependency oestrogen resistance invasiveness	MMP14, MMP2, MMP9, PDGF-A, IGF1R	(194-196)
Endometrial, cervical and ovarian	Motility, tumour growth	-	(197)
Gastro-intestinal track	Invasiveness, tumour growth, vascularization metastasis, proliferation	IGF1R, PDGF-A, PTHrP	(195)
Sarcomas	Motility, invasiveness tumour growth,	IGF1R, MMP14,	(198)
Brain and central nervous system	Malignancy, proliferation invasiveness, tumour size	IR, TGFβ, MMP14	(199)
Skin	SCC formation	-	(200)
Hepatocellular carcinomas		Glypican-3	(201)

1.4.7.4 Substrates/Biological functions: Viral infection

In order to invade host cells, virus need to fuse at the plasma membrane and to do so, proper maturation of viral surface glycoproteins is needed, a step that is often realized by the proprotein convertases. In addition, many studies have highlighted that Furin and PC7 are the PCs mostly involved in this process (202). This maturation step not only allows the virion to fuse but also activates the virus and is therefore a virulence-activating step (203). Interestingly, in situations promoting viral infections, Furin and PC7 expression have been demonstrated to be upregulated (204). As a particularly relevant example of the PCs implication in viral entry, the wild-type H5N1 avian influenza virus is pathogenic for chickens, but not for humans, although the emergence of a mutant form with a RERR insertion in the gene sequence had transformed the virus in a highly

pathogenic form for both humans and chickens. The insertion revealed a ~5 fold increase in cleavage efficiency and is suggested to be responsible for the high infectivity of the virus (202). Although other PCs can mature viral proteins, Furin is the well-known PC able to mature viral glycoproteins (203). Indeed, during human immunodeficiency virus type 1 (HIV-1) viral infection the glycoprotein gp160 needs to be processed into gp120 and gp41 by Furin, and also PC7 but to a lesser extent (205, 206). Other than HIV-1 glycoproteins, Furin and other PCs have been studied in the context of many more viruses such as Ebola (207), Marburg (208) and the influenza virus (209). Very recently, Furin has been proposed to possibly play a major role in the activation of the cell surface protein-S of the highly pathogenic SARS-CoV-2 implicated in the COVID-19 pandemic (210).

1.4.7.5 Furin Inhibitors

Because Furin cleavage and maturation activities can be pathogenic in cancer and in viral entry, targeting Furin with different inhibition strategies is an active area of research. Table 1.3 summarizes different inhibitor strategies exploited over the years. They fall into five broad categories: 1) protein-based, 2) peptide-based, 3) peptidomimetic Furin inhibitors, 4) natural inhibitors, and 5) Furin siRNA on patients-derived cells (211). For the protein-based category, one of the most important inhibitors is the artificial α-1 antitrypsin Portland (α-PDX), and the strategy is based on the natural serum protease inhibitor (α-1 antitrypsin). Adding a RIPR site into the AIPM sequence generates an inhibitor that forms a tetrahedral adduct with the Furin active site's serine (212). The peptide-based inhibitors were developed following an amidated and acetylated synthetic L- and D-hexapeptide combinatorial libraries screen and are usually referred to as the polybasic peptides or polyarginines (213). For the peptidomimetic Furin inhibitors, a chloromethylketone (CMK) moiety was added to a multibasic substrate, which create a peptide that interact with the active site Ser, and blocks its activity (214). The natural inhibitors are proteins that have been demonstrated to inhibit Furin, namely PAR1, GBP2 and GBP5. The protease activated receptor 1 (PAR1), inhibit Furin's cleavage of HIV-1 gp160 into gp120/gp41 by retaining Furin in the TGN in an inactive state (215). The cytosolic restriction factors induced by interferon (GBP2 and GBP5) also inhibit Furin by retaining it in an inactive form in the early Golgi compartments and thereby inhibit the processing of multiple viral and cancer related proteins

Table 1.3. Furin inhibitors

	Abbreviation	Applications	References
Peptide-based inhibitors	α-1-PDX	Inhibition of processing of gp160 and measles virus-fo	(212)
		limits joint inflammation	US0127396
		(PD-1) repression +cytotoxic T lymphocytes exhaustion	(216)
	Acyclic mini-PDX	N/A	(217)
	Cyclic mini-PDX	N/A	(217)
	OMTKY3 (variant A15R, T17K, L18R)	N/A	(218)
	6R	gp160 processing inhibition	(213, 219)
		supress HIV infection of T-cells and macrophages	(219)
		inhibits latent TGFβ activation *in vitro*	(219)
	D6R	protective effect against anthrax toxemia	(220)
		blocks activation of PEA	(220)
	D9R	protective effect against anthrax toxemia	(220, 221)
		reduction of *P.aeruginosa* ocular infection	(221, 222)
	H5N1 derived peptide	PA83 cleavage inhibition	WO023306
		protective effect against anthrax toxemia	WO023306
		blocks activation of PEA	WO023306
	Ac-RXXT-NH_2	blocks hemagglutinin-mediated fusogenicity	(223)
		protects from Shiga toxin	(223)
	H_2N-C8-RXXT	protective effect against anthrax toxemia	(224)
	name	Applications	
Protein natural inhibitors	PAR1	reduced processing of gp160	(204)
	GBP2/5	inhibition of processing of avian influenza and HIV glycoproteins	(225)
		inhibition of processing of Zika virus, measles and Marburg virus	(225)
		inhibition of processing of GPC3 and MMP14	(225)
	Abbreviation	Applications	References
Autologous cancer cell vaccine	FANG vaccine	double lifespan survival of colorectal, melanoma and ovarian cancer patients	(226)

(such as MMP14) (225). Interestingly, these natural inhibitors have in common that they seem to sequester Furin away from their substrates. But other possible mechanisms are also reported for GBP2/5 Furin inhibition such as interfering with Furin expression itself (225). Lastly, the autologous tumour-based FANG vaccine combines Furin-knockdown and granulocyte-macrophage colony-stimulating factor (GM-CSF) overexpression in patient-derived cancer cells and the infusion of the modified cells into the patients in order to boost their immune system (226). It is a dual strategy; on one hand the goal is to block the immunosuppressive effects of mature TGBβ activated by Furin by using an siRNA approach targeting Furin. On the other hand the strategy is to boost the immune response using GM-CSF overexpression (which primes T-cells and increases the recruitment of dendritic cells) resulting in an increase in anti-tumoral response (226).

1.4.8 PC7/PCSK7: Identification and structure

In 1996, a few years after the identification of the first mammalian proprotein processing enzymes, the PCSK7 gene was discovered in a chromosomal translocation breakpoint t(1 l;14(q23;q32)) occurring in a high grade lymphoma (227). In previous studies aiming to identify new gene targets of chromosome translocation occurring during acute leukemia, the chromosome 11q23 was reported to have high incidence of abnormalities, especially in Hodgkin's disease (228, 229). The authors concluded that this region, the chromosome 11q23, coincidently the PCSK7 chromosome, have consistent degree of abnormalities occurring in lymphomas (227). Using the genomic sequencing tools available at the time, a potential coding sequence was identified from germline cosmid (cos6) around a chromosomal breakpoint. Using that sequence cDNA as a probe to screen a library from Jurkat cell line, several cDNAs were identified with promising open reading frames encoding a sequence for a new convertase member with homology with Furin. Hence, the identification of the seventh member of the proprotein convertase family originated from a genetic rearrangement occurring in human lymphoma, therefore PC7 has been referred to as Lymphoma Proprotein Convertase (LPC) in its early days. This latter study also highlighted a very interesting and still understudied matter regarding the PCSK7 gene, which is the duplication of exons 13 to 17, 60 Kb downstream of PCSK7 coding region. Indeed, the exons 13-17 are reversed and duplicated, but no detailed investigations as of

now have demonstrated the possible transcriptional regulation roles of the duplicated region of the gene. Nevertheless, preliminary studies are suggesting that this duplication could act as a microRNA to regulate the *PCSK7* gene in *cis*, and possibly other genes, in *trans*, but these are just speculations for now.

Independently, the complete cDNA sequence of PC7 was simultaneously identified by Seidah *et al*. using RT- PCR on RNA isolated from rat pituitary extracts and screening rat spleen and PC12 cells *Agtll* cDNA libraries (230). The data from this original study revealed multiple key characteristics of rat PC7; that it is a type-I membrane-bound protein, has a signal peptide and a pro domain involved in the zymogen activation with an autocatalytic cleavage site Arg-Ala-Lys-$Arg_{104}\downarrow$ similar to the other PCs. The deduced protein sequence also highlighted the catalytic site (His_{191}, Ser_{369}, Asp_{150} and Asn_{292}) and even predicted four N-glycosylation sites (Asn_{130}, Asn_{138}, Asn_{204}, and $Asn_{474)}$, and a Tyr sulfation at $Tyr_{621.}$ Investigations looking more closely at the cytosolic tail of PC7 will demonstrate that some residues, often conserved in different species, are critical for its trafficking and therefore its activity and will be discussed below. Finally, phylogenic analysis also represented PC7 as structurally the closest member of the mammalian PCs to yeast kexin and as the most ancient and highly conserved member of the PC-family (4).

1.4.8.1 Tissue distribution

Like other members of the convertase family, PC7 mRNA and protein levels are found ubiquitously throughout the body (4). Also, Northern blots from different rat, mouse and human cell lines revealed that the levels of PC7 are the highest in gonadotrophs (αT3-1), corticortroph (AtT20) and somatomammotroph (GH4C1) cell lines, pointing towards biological relevance in pituitary-related substrates/hormones (4). Other cell lines had significant levels of PC7 such as insulinomas cells (Rim5F and βTC-3), the adrenal cortex (Y1), pheochromocytoma-derived (PC12), the fibroblasts (Ltk) and the colon carcinoma cell line (LoVo) (230). *In vivo* analysis in rats showed that PC7 mRNAs is rich in the liver, thymus, colon, kidney, testis and in the brain (*e.g.* hippocampus, amygdala and pituitary) (230).

1.4.8.2 Trafficking

PC7 was discovered almost 25 years ago but a lot is left to learn about its specific trafficking and zymogen activation. In recent years, multiple studies have attempted to unravel the PC7-specific trafficking route in the hope of understanding how this convertase is different from Furin and the other PCs. These studies would potentially direct to specific substrate recognition and novel biological roles. One key feature that makes PC7 different from the other PCs is its zymogen activation. Indeed, like PC4, it does not require a second cleavage for the removal of its inhibitory prosegment after the first autocatalytic cleavage at $RRAKR_{141}\downarrow$ (in human PC7) in the ER (129). Following its first cleavage, the prosegment remains attached non-covalently, as a heterodimer consisting of the inhibitory prosegment with mature PC7 (prosegment-PC7), as evidenced by co-immunoprecipitation (129). The prosegment was also detected in the media (129), suggesting that PC7 prosegment is secreted and could have a function in the media. In addition, *in vitro* experiments demonstrated that the optimal pH for its activity is neutral (6-7) and that calcium is necessary and acts as a cofactor for the reaction, like the other PCs.

Multiple evidences have shown that PC7 accumulates in the ER and the TGN on its way to the plasma membrane, where a small fraction is found at steady state (~10%) (129, 231). An unconventional route has also been suggested since PC7 was found at the plasma membrane after brefeldin A treatment (129), which blocks protein transport from the ER to the Golgi. Also, swapping the transmembrane domain (TM) of Furin with the one of PC7 directs Furin to plasma membrane via an unconventional pathway, indicating that important information is contained specifically in the TM of PC7 for its trafficking to the plasma membrane but further investigations of this pathway have not been fully characterized yet (129, 232). Elucidating PC7 trafficking in the secretory pathway still contain missing pieces, but different motifs are emerging to better define and distinguish this enzyme from the other PCs. Figure 1.7 is a schematic representation comparing the trafficking pathways used by PC7 and Furin. As mentioned above, PC7 cytosolic tail contains specific information for its targeting to its final destinations. Amongst those features, the cytosolic tail of PC7 contains two cysteines palmitoylations, Cys_{699} and Cys_{704}, which may be important for enrichment in PM microdomains important for Anthrax toxin activation (233) but not for most other substrates (234, 235). These two potential palmitoylated-cysteine did not

show importance in PC7 trafficking to the TGN if mutated alone (236), but they were shown recently to be important, in combination with a novel basic cluster H_{708}RSRKAK$_{714}$ for endosome to TGN transport (237). It was also demonstrated that internalization from the plasma membrane to the endosomes is dependant on clathrin-coated vesicles via the internalization motifs PLC$_{726}$ in PC7's cytosolic tail. However, the association of these motifs with adaptor proteins or regulators of endocytosis have not been fully characterized (231, 237, 238). Lastly, works by our group have also shown that in addition to the PLC motif and the basic cluster, the motif ExExxxL$_{725}$ in PC7 cytosolic tail is not only required for its internalization but also its activity to cleave and shed the type-II membrane bound human transferrin receptor (hTfR1). Indeed, we have showed that the ExxExxxL$_{725}$ motif binds the cytosolic adaptor protein AP-2 (239), which is a main actor in the trafficking of endocytic vesicles from the plasma membrane to the endosomes (240). The PC7-AP-2 binding is abrogated when PC7 is mutated at the ExxExxxL$_{725}$ motif, more precisely when changed into AxAxxxA$_{725}$. Different point mutations in the former motifs also cause PC7 to accumulate at the plasma membrane and have significant decreases in enzymatic activity, reported by the decrease in the cleavage of hTfR1 (239). We believe that the ExxExxxL$_{725}$ motif best represents the endocytosis function previously attributed to the PLC$_{726}$ motif.

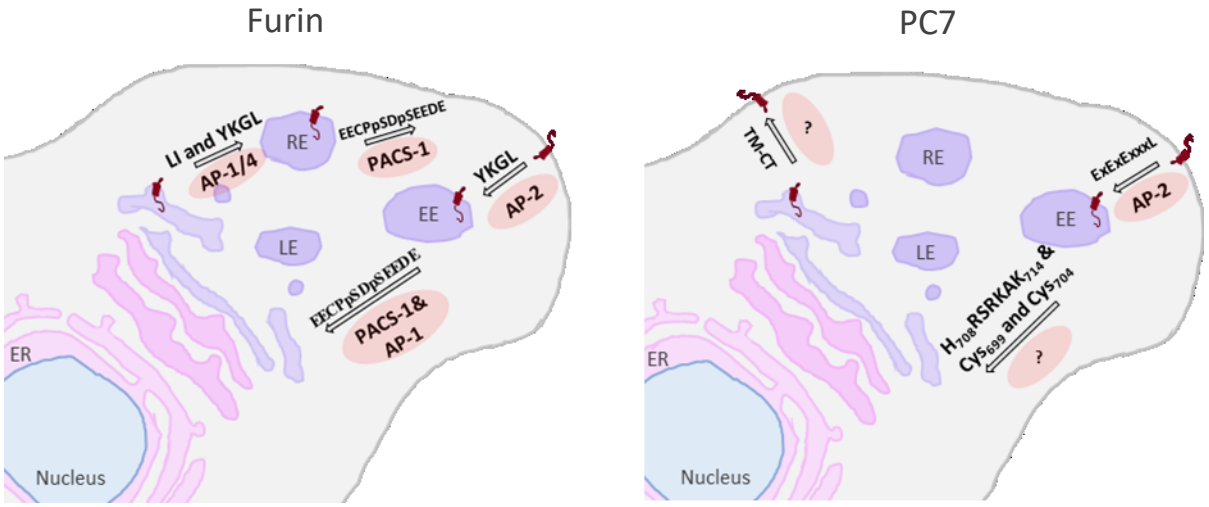

Figure 1.7. Comparison between Furin and PC7 trafficking signatures.

PC7 or Furin proteins are depicted in dark red. Relevant Furin or PC7 motifs are written in black, important trafficking binding partners are within pink circles.

Finally, the previous studies have investigated PC7 trafficking under conditions where PC7 is overexpressed to facilitate wild type (WT) and mutant PC7 immunofluorescence detection or to analyze the maturation of overexpressed substrates. It is necessary to mention that trafficking of proteins can be affected by over-abundant quantities of exogenous proteins and could lead to mislocalization (241). Indeed, it was reported by Ginefra *et al.*, 2018 that subcellular localization and related endoproteolytic activity results may vary when using the overexpression strategy (238). Therefore, using overexpression is necessary for dissecting the protein domains and motifs, but whether it is completely translatable *in vivo* on endogenous levels of a convertase remains to be proven. Taken together, these observations demonstrated that PC7 is ubiquitously expressed, but it's distinct trafficking signature likely suggests specific protein interactions and physiological functions.

1.4.8.3 Substrates and biological functions

The only specific PC7 substrate is the human transferrin receptor 1 (hTfR1) (235), a protein reported from a genome-wide association study (GWAS) that was interested in finding genes associated with iron metabolism and that directly linked the levels of soluble transferrin receptor with the *PCSK7* gene locus (242). It was one of the first human mutations or SNPs associated with PC7 function in humans, but it was just the tip of the iceberg as other genomics studies revealed PC7 functions that will be discussed in a section below. To summarize the hTfR1 conclusions, PC7 is responsible for the shedding of the receptor at the $KTECER_{100}\downarrow LA$, this cleavage occurs at 12 amino acids from the C-terminus of the transmembrane domain, which is a typical shedding architecture (59). Therefore PC7-shedding of the transferrin receptor 1 will influence the bioavailability of the full-length receptor at the cell surface of enterocytes, hence modulate iron entry (235). Accordingly, it was demonstrated that removing iron from the media of a hepatocellular cell line resulted in a down-regulation of *PCSK7* at the mRNA levels (235). For almost 25 years, PC7 was considered to have substrate redundancies with other enzymes because no specific substrate was identified, but the study on the transferrin receptor 1 was really an important step which suggested that PC7 could have its own physiological functions by cleaving specific substrates. In addition, recent reports demonstrating that PC7 has a unique

trafficking signature and a different cell compartmentalization suggested that PC7 could interact with different proteins than the other PCs depending on the cell type or the cellular context. Taken these data together and considering that PC7 is well conserved and broadly expressed in many tissues, these evidences would support that PC7 could have other PC7-specfic substrates, and possibly acts as a more general sheddase. This hypothesis and its validation are the basis of the first part of this thesis (see Chapter II) which aims to identify new specific PC7 substrates shed into the media.

Albeit having identified only one specific substrate so far, other PC7 substrates have been reported *in vitro* and *in vivo*, but these proteins can also be cleaved by other proprotein convertases (redundancy) or other proteases. Based on over 100 peptide cleavages, the consensus substrate cleavage motif is depicted at Figure 1.8. PC7 known substrates have been demonstrated experimentally from cultured human cell lines, mouse, rat or zebrafish models and like Furin they fall in three broad categories: development, immunity/inflammation and cancer.

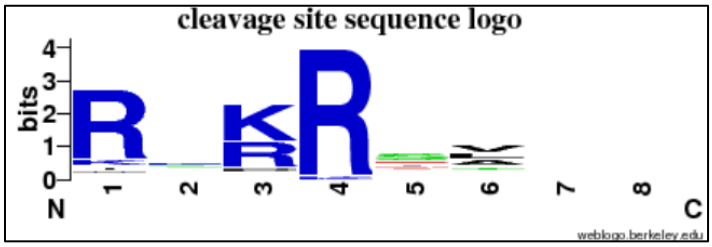

Figure 1.8. PC7 cleavage site preference.

Cleavage site pattern is represented based on 116 substrate cleavages. The cleavage site logo was generated from the MEROPS peptidases database (22).

4.3.8.4 Substrates and biological functions: Development

As it will be discussed below, the PC7 KO mice are viable and do not harbour any growth defects, hence PC7 role in development could seem secondary. Yet, studies in Xenopus and zebrafish have highlighted unique roles for PC7 in embryogenesis and early development. Accordingly, *PCSK7* is expressed in early development in zebrafish and when inhibited, using antisense morpholino oligonucleotides, apparent growth defects were shown in different organs such as the brain, eyes and auditory vesicles which led to embryonic death within 7 days post-fertilization (243). These

developmental defects in the PCSK7 morphants were attributed to aberrant processing of the growth factor TGFβ, hence demonstrating a non-redundant function for PC7 in the development of the zebrafish. Similarly, inhibiting PCSK7 in xenopus at the 2-4 cell stage during development is also generating severe developmental defects such as disruption of head and eye formation (244). The associated phenotypes in xenopus were rationalized by a reduction in multiple bone morphogenetic protein (BMP) family members such as Sox2, Pax6 and Opsin, which are known to be targeted by PC7 (244). Other precursor proteins that are relevant in development such as the Vascular endothelial growth factor-C (VEGF-C) (245), platelet-derived growth factor (PDGF) (246), parathyroid hormone precursor (247), cholecystokinin (CCK) (248), Notch1 (172), E-cadherin (249), proEGF (234) and Angiopoietin-like protein 4 (ANGPTL4) (250) have been reported to be cleaved by PC7 but are also cleaved by other PCs.

1.4.8.5 Substrates and biological functions: Cancer

Similar to Furin's role in cancer progression, PC7 is also implicated in the maturation and activation of multiple growth factors and matrix metalloproteases such as disintegrin metalloproteinase domain-containing protein 10 precursor (ADAM10) (251). As the critical importance of such maturation in cancer progression was discussed above, it will not be discussed further in this section. Nevertheless, shRNA specifically against PCSK7 in prostate cancer cells have shown significant growth inhibition *in vitro* (252). Also, in colorectal cancer, it was shown that overexpression of the general PC-inhibitor α1-PDX led to a significant reduction of metastatic potential of human colorectal tumor cells (253).

1.4.8.6 Substrates and biological functions: Immunity/Inflammation

When rat PC7 sequence and tissue distribution was identified in 1996, one of the most abundant tissue expressing PC7 mRNA was the thymus (230), hence potentially uncovering important physiological roles in the immune system. Indeed, it was recently demonstrated that PC7 and Furin are significantly expressed in lymphocyte T regulators (Treg) and T effectors (Tefs), and that they cleave Foxp3, a transcription factor essential for the Treg function (254). Taken together, these investigations point towards a possible role for PC7 in autoimmune, inflammatory or in infection diseases, but further investigations are clearly needed. Lastly, as mentioned above for

Furin, PC7 is also involved in the processing of viral surface proteins and their activation such as the Chikungunya virus (CHIKV) E2 glycoprotein (255), SARS corona virus S-protein (256), SARS-CoV (257) and HIV-gp160 (258).

1.4.8.7 PC7 KO mice

As discussed for the other PCs, the generation of KO mice have often allowed the identification of their physiological functions. The majority of the proprotein convertases mice models with reduced levels or knockout gene expressions displayed apparent phenotypes, which have given strong clues to identify the substrates responsible for the phenotypes. Some of the best examples consist of Furin in development *via* aberrant growth factors activation, or the obesity and hypoglycaemia phenotype observed in the *PCSK2* KO mice *via* maturation defects of insulin and glucagon. On the other hand, finding PC7 specific substrates is a laborious task since the knockout mice are viable, with no gross physical malformations. Hence, PC7 has been categorized as an enzyme that shares substrates with other PCs, especially Furin. While those redundancies can be appreciated as a strong evolutionary survival mechanism, considering that PCs regulate many essential biological processes, the idea of studying the activity of a redundant protein can be somewhat unappealing. This was the case, until our group ventured into the characterization of the PC7 KO mice more thoroughly and performed behavioural assays. The results from these tests revealed that the PC7 KO mice are healthy but display an anxiolytic phenotype and episodic memory defects (259). These phenotypes are thought to be caused by a reduction in the maturation of proBrain-Derived-Neurotrophic-Factor (proBDNF) into mature(mBDNF) in various regions of the brain, such as hypothalamus and amygdala. proBNDF and mBDNF have different signalling pathways in the central nervous system by binding different receptors (Figure 1.9) (260). MatureBDNF was originally believed to be the only bioactive entity, but it was shown that proBDNF also had signaling properties via p75NTR and sortilin which could induce apoptosis (171, 261). The proportion of mBDNF and proBDNF needs to be balanced for proper neuronal growth and synapse plasticity (260). Hence, it is proposed that in the PC7 KO mice the observed ~40-45% decrease in the maturation of proBDNF may have led to an aberrant and imbalanced signaling at the synapses (259) through impaired signaling from the tyrosine kinase beta receptor (TrkB). Accordingly, the PC7 KO phenotypes were rescued by using injections 1h before the behavior

tests of a brain-penetrable BDNF receptor (TrkB) agonist 7,8-dihydroxyflavone (DHF). Importantly, PC7 is not the only enzyme that can process proBDNF, as it is also cleaved by Furin and PC1 at the same motif $RVRR_{130}\downarrow$ (262-264), possibly explaining why the mice are viable. Interestingly, recent work has shown that diet-induced obesity is inducing anxiety-like behavior in mice, in part by the increased maturation of BDNF and other signaling molecules, such as p-CREB and ΔFos, in the reward circuit of the brain (265).The demonstration of a link between mood disorders and PC7 is not a surprise considering the observation of *PCSK7* mRNA expression in different regions of the brain (230) but also, is coherent with previous results from the zebrafish (243) and Xenopus (244) where silencing the *PCSK7* gene in early development led to severe brain and eye defects and lethality. While the conclusions from the behavioral assays were promising, future work will be needed to better understand how the *PCSK7* gene can affect mood, anxiety and possibly other cognitive performance. The investigation of *PCSK7* SNPs in humans could also reveal potential susceptibility genes for mood disorders and/or candidate treatments for patients in the future.

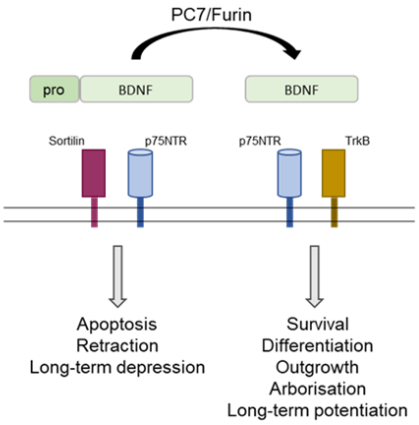

Figure 1.9. Differential signaling of proBDNF and mBDNF.

Both proBDNF and mBDNF are biologically active. Functional consequences of the different signaling are depicted. Adapted from Deinhardt *et al.*, 2014.

1.4.8.7.1 Diet and mood disorders

It is well established that undernutrition have severe consequences on health, but overcomption of food in our contemporary societies is generating different types of health issues. There is more and more evidences supporting a role for the diet in the modulation of psychological, metabolic

and emotional health (266). Indeed, there is an increase of ~25% in the odds of developing mood and anxiety disorders in obese individuals (267). Also, the consumption of appetizing high-fat and high-sugar content foods is stimulating the reward circuit in the brain and leads to rearrangement of the neural circuits which can be similar to drug consumption (265). To better understand the intimate relationship between diet, mood and behavior it is important to consider the composition of the diet, the dietary habits and the related consequences on mood and behavior.

The multiple types of dietary fats available can be regrouped in three broad categories, saturated, monounsaturated and polyunsaturated fatty acids (PUFA). Briefly, typical Western diet is rich in saturated fats, such as palm oil, and its consumption have higher incidence of depression (268). On the other hand, consumption of unsaturated fats such as in the Mediteranean diet shows lower incidence of depression (269). Also, reduced comsomption of PUFA, such as fish oil, is associated with higher risk of depression (270). In addition, there is a positive correlation between depressive symptoms and saturated fats consumption, and a negative correlation with monounsaturated fats consumption (271).

It is a complex interplay of neuronal signals that governs food intake in response to both physiological cues and supraphysiological cues within the reward system, see figure 1.10. Briefly, the arcuate nucleus (ARC) and the lateral hypothalamic area (LHA) of the hypothalamus are the primary neurons integrating information about energy balance and coordinating the signals from the anorexigenic αMSH/CART neurons and orexigenic NPY/AgRP neuropeptides (272). The LHA is consolidating the energy deficiency cues and signals to the mesolimbic reward pathway to stimulate feeding behavior (273). On the other hand, sensory inputs such as olfactory or visual can trigger food consumption independantly of energy requirements. Indeed, these sensory inputs from palatable foods are related to the insula wich with the orbitofrontal cortex (OFC), anterior cingulate cortex (ACC) and amygdala will assess the reward value and drive food consumption. This mechanism also relies on the connections with the nucleus accumbens (NAc) and the ventral tegmental area (VTA) of the mesolimbic reward circuit (273). The mesolimbic reward circuit is therefore responsible for motivation and feeding behaviors and is composed of domapine (DA) neurons which transmit signals related to food seeking and eating (273). The mechanisms by which the different types of dietary fats influence mood disorders and

particularly anxiety and depression is related to neuroadaptations in the reward circuit in part *via* changes in dopamine signaling (274) and particularly in the nucleus accumbens (275). Accordingly, dopamine receptor regulating inhibitory mechanisms within the reward circuit is decreased in obese rodents, which contributes to the vulnerability of diet-induced compulsive eating (276). These compulsive behaviors are also observed in humans and the deficit in inhibitory signals of mesolimbic dopamine system is suggested to compensate its desensitization (277, 278).

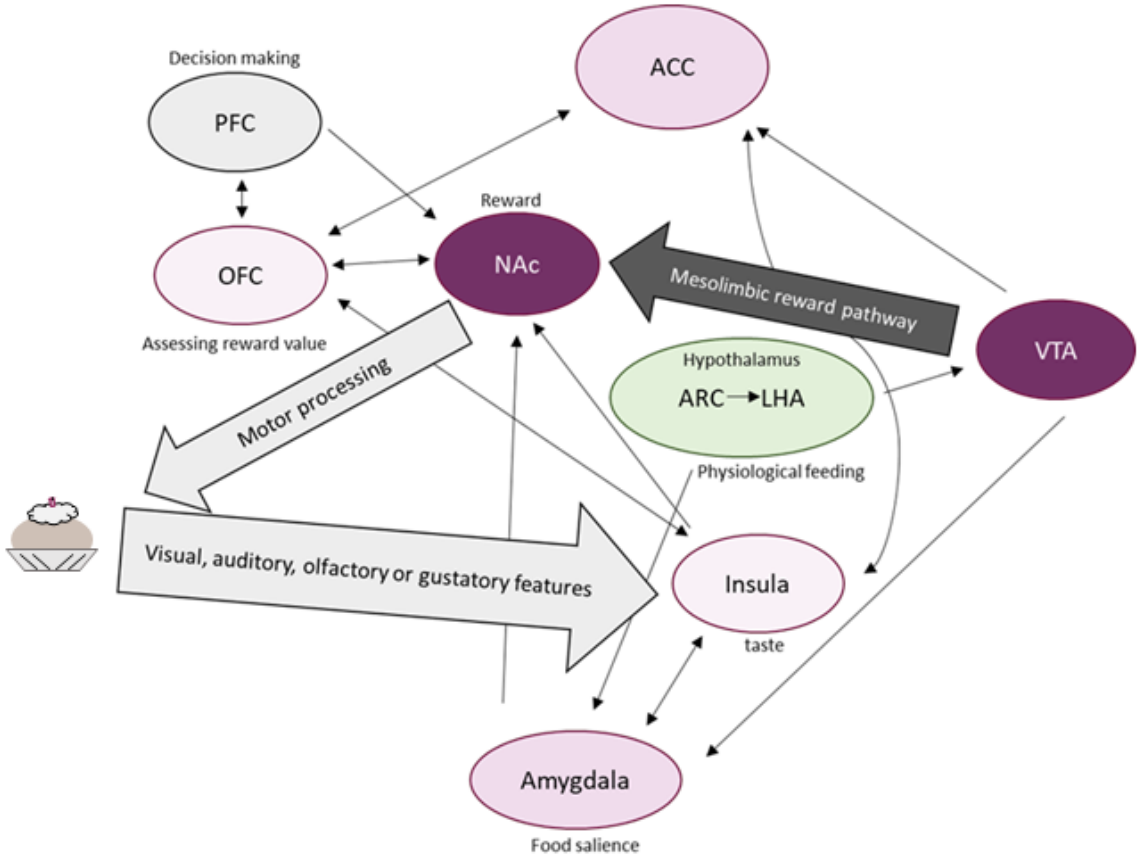

Figure 1.10. Interplay of neuronal signals driving food intake.

In purple are depicted supraphysiological feeding and mesolimbic reward pathway, in green is depicted the physiological feeding pathway. PFC: prefrontal cortex, NAc: Nucleus accumbens, VTA: Ventral tegmental area, OFC: orbitofrontal cortex, ACC: anterior cingulate cortex. ARC: arcuate nucleus of the hypothalamus, LHA: lateral hypothalamic area. Adapted from Leigh S.J. *et al.*, 2018 (273).

In addition, low-grade persistent inflammation in obese individuals results in high levels of circulating inflammatory cytokines and inflammatory markers such as C-reactive protein which correlates with higher prevelence of depression symptoms in humans (279-281). In rodents, HFD consumption is also activating an immune reaction in the hypothalamus and hippocampus (282-284). Lasty, it was recently showed that the chronic consumption (12 weeks) of saturated fat (from palm oil) and monounsaturated fat (from olive oil) both resulted in obesity in mice, but only the saturated fat diet generated increased inflammation in the nucleus accumbens accompanied by anxiodepressive behavior (268).

Of note, the duration of consumption of these HFDs is critical, as short-term consumption can have opposite results as a chronic consumption, as reported by opposing results in the litterature (266). Indeed, an earlier study reported that high-fat diet feeding during only 1 week was inducing an anxiolytic phenotype in mice (285). Conversly, high-fat diet feeding has been reported multiple times to be anxiogenic in mice (266) and a time-dependant opposite effect of the HFD on anxiety-like behavior was demonstrated recently (286). Indeed, it was shown that a 'short-term' HFD feeding during 5 weeks was anxiolytic as observed by the mice spending significantly more time in the open arms of the elevated-plus maze (EPM) test (286). During the same study, a 8-week HFD feeding was not showing any-behavioral changes, likely due to a moderate increased in body weight gain. Lastly, the 15-week high-fat diet was shown to generate diet-induced obesity anxietly-like behavior in mice as they had a significant decrease in time spent in the center of the open-field test (OFT) (286).

Importantly, high-sugar diet is also contributing to mood disorders in mice, as it was demonstrated that high sucrose diet feeding to mice led to decrease time in the light chamber during the light/dark box behavior assay (287). High-sugar diet consequences have been particularly studied following its withdrawal, and the associated anxiety phenotypes were similar to those observed when withdrawal of addictive drugs (288). Finaly, the combination of high fat and high sugar diet in the so called 'Western-style diet' is also influencing mood disorders and learning abilities (289). Indeed, mice fed a high fat high sugar diet for only 3 weeks showed increased anxiety behavior in the Barnes maze, and was correlated with increased in hyppocampal BDNF (289). In line with this, feeding of a high-fat and high-sugar diet in mice for a

short period of time (5 to 20 days) impairs hippocampal-dependant memory, even prior to body weight gain (290). Accordingly, Beilharz *et al.* demonstrated that the memory deficit were associated with an increase in hippocampal inflammation markers TNF-α and IL-1β as well as an oxidative stress marker NRF1 (290). In addition, longer exposure (60 weeks) to high-fat high-sugar diet also impairs short-term memorry, as demonstrated by a lower percentage of alternations during the Y-maze behavior test (291). Finaly, coherent with the pre-clinical litterature, memory impairment were also observed in humans fed high-fat high-sugar diets, as observed by a decrease in hippocampal-dependent learning and memory tests (292).

Mood disorders and obesity are two major public health concerns. To better understand the neural circuit rearrangements in the diet-induced obesity phenotypes (265) as well as the interplay between proBDNF and matureBDNF in the PC7 KO mice, we have undertaken a study interested in the possible protective effect in the PC7 KO mice from anxiety-like behavior when challenged with a high fat diet. The background information, project layout and results are discussed in Chapter IV of this thesis.

1.4.8.8. Human mutations, GWAS and SNPs

The unique PC7-specific substrate was identified following a GWAS study which helped to connect PC7 to iron metabolism. Therefore, the idea of identifying other biological functions from human genomic analyses is very possible. Indeed, when studying the literature, we can find publications that have linked the *PCSK7* gene locus to insulin resistance, triglycerides and non-alcoholic fatty liver disease (NAFLD). Indeed, because of its previous link to iron metabolism, the variant rs236918 in the *PCSK7* gene was analysed in a meta-analysis for liver cirrhosis and fibrosis and was positively associated as a risk factor for cirrhosis in hereditary hemochromatosis patients with a *HFE* C282Y mutation (293). Other metabolic diseases have been linked to this *PCSK7* rs236918 variant, such as a GWAS investigating the effect of a weight-loss diet on insulin resistance. In this weight-loss trial, the PCSK7 rs236918 G allele was significantly associated with a decrease in fasting insulin in the high dietary CHO-intake group, reporting for the first time a link between *PCSK7* genotype and insulin sensitivity in white Americans (294). A second GWAS have linked two other *PCSK7* SNPs (possibly resulting in a PC7 gain-of-function or higher levels),

the rs508487 and rs236911 with increased triglycerides and sdLDL (295). Also, recent data from a study aiming at identifying genes linked with coronary heart diseases have correlated the *PCSK7* gene with the levels of high-density lipoproteins (HDL) and triglycerides (TGs). In this study, the variant R504H (rs142953140) has been associated with a significant increase (40%) of HDL and a decrease (30%) of TG (296). Interestingly, the R504H mutation does not affect the enzymatic activity of PC7 on TfR1 (297). Also, some previously reported mutations in the *PCSK7* gene (D186G, R316C, and L506P) as well as the rs508487 variants were all proven to be loss-of-function mutations, at least regarding the shedding of TfR1 (297). Finally, the coronary heart disease study (296) highlighted the *PCSK7* gene locus in close proximity to the apolipoprotein locus (Figure 1.11). These original observations suggested a possible association between PC7 and the apolipoproteins, which resulted in the discovery of a novel PC7 non-enzymatic function by our group.

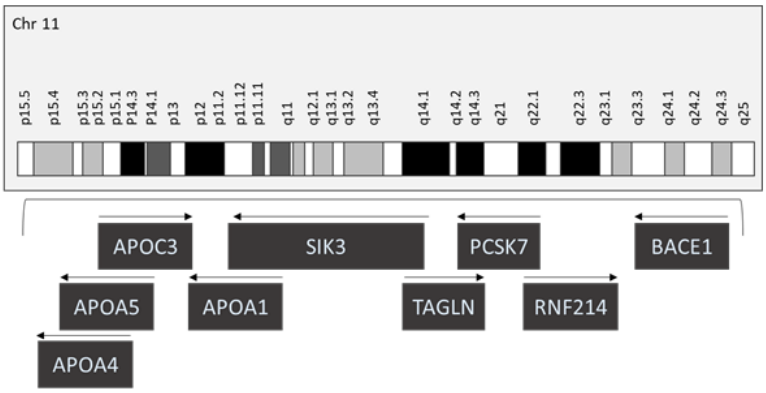

Figure 1.11. The *PCSK7* gene locus is in close proximity to the apolipoproteins.

Depicted is the chromosome 11 and the reported genes surrounding *PCSK7*.

1.4.8.9 Non-enzymatic functions: Apoa5 and HIF-1α

The proximity of the apolipoproteins locus to the *PCSK7* gene, as well as the linkage disequilibrium with the apolipoprotein A-V (apoA-V) promoter variant rs662799 (295) which was previously associated with elevated TG-levels, gave us confidence that PC7 could be involved in lipid metabolism. The first hypothesis was that PC7 might cleave apoA-V and therefore modulate its activity as an activator of lipoprotein lipase (LpL) (298). This first hypothesis turned out to be

incorrect. Surprisingly, instead of generating a cleaved fragment, PC7 overexpression led to reduced apoA-V protein levels (299). From this first observation and subsequent work in mice, our group have identified one of the first non-enzymatic functions of PC7 implicated with lipid metabolism. Indeed, we demonstrated in HuH7 cells that in a bafilomycin A1-dependent pathway, PC7 binds apoA-V in an acidic compartment, which leads to its degradation in lysosomes. Hence, this novel mechanism regulates the levels of cellular and secreted apoA-V and was further confirmed in mice fed a high fat diet (HFD), where plasma apoA-V levels and adipose LpL-activity are increased compared to WT mice (299). In addition, the adipocytes from these mice displayed a tendency for hypertrophy with enhanced TG content (299). In conclusion from this study, we demonstrated a first mechanistic link between PC7 and lipid metabolism *via* its activity on regulating apoA-V levels which corroborates previous reported genomic associations. Related work from our lab have also shown that the PC7 KO mice on normal diet have high TG levels and decreased apolipoprotein B (apoB) levels in the plasma, *unpublished data*. Preliminary results of this ongoing work show that PC7 interacts with apoB and could act as a chaperone to maintain its proper folding before its secretion from the liver. In conclusion, with our demonstration of PC7 implication in lipid metabolism, we are strongly interested in investigating therapeutic avenues for TG lowering and cirrhosis using the PC7 KO mice model.

Another non-enzymatic PC7 function was demonstrated a few years before our observations of the link between PC7 and the apolipoprotein locus and is related to the interplay between PCs and the hypoxia-inducible factor 1α (HIF-1α). It is well established that hypoxia-inducible factor-1α is induced in hypoxic intratumoral conditions (300). One of the many transcriptional targets of HIF1-α is Furin, which in response to hypoxia has been demonstrated to translocated from endosome to the plasma membrane (301, 302). In line with these observations, it was shown that *Furin* mRNA was upregulated in oxygen-deficient cells (301, 303). Reciprocally, it was recently demonstrated that both *Furin* and *PCSK7* siRNAs were increasing HIF-1α protein *via* activation of its translation, which in turn increase the production of VEGF-A, possibly highlighting another non-enzymatic PC7 and Furin activity (304).

1.4.9 Subtilisin kexin isozyme-1 (SKI-1)

SKI-1 is like the other convertases in its zymogen activation, it needs a second cleavage in the ER in order to be released as an active enzyme, after a primarily cleavage at three internal sites within its prosegment (101, 305, 306). Like many of the other convertases, SK1-1 is ubiquitously expressed (4, 307) and is located intracellularly in the *cis* and *medial* Golgi, but can also be found in endosomes or lysosomes (308). Unlike the first seventh PCs, SKI-1 cleaves precursor proteins at the C-terminal end of the motif: RX(L/V/I)X↓, where X is any amino acids, except proline or cysteine (309, 310). Some of SKI-1 well characterized substrates are the SREBPs, ATF6 and CREBS transcription factors (311, 312), pointing towards a relevance for this enzyme in cholesterol regulation. In fact, the suggested phenotypes from these substrate were confirmed in mice lacking ~80% SKI-1 in the liver, were they displayed a ~50% decrease in circulating triglycerides and cholesterol, explained by a significant decrease of the nuclear levels SREPBs and their target gene expressions (313). Like Furin, PC5 and PACE4; SKI-1 KO mice die embryonically, but in 25% of the cases at the blastocyte stage from a malformation in the epiblast (314). Other known SKI-1 substrates are BDNF (251), Glc-NAc-phosphotransferase and viral glycoproteins (e.g., lassa and Crimean Congo hemorrhagic fever virus) (309, 315, 316).

1.4.10 PCSK9: from bench to bedside

As mentioned in the introduction of this section on the proprotein convertases, PCSK9 has no other substrates than itself and importantly following its autocatalytic cleavage, PCSK9 remains as an inactive protease (317). Interestingly, before PCSK9 earned its fame from being an excellent drug target for lowering plasma LDL-cholesterol, it was called neural apoptosis regulated convertase 1, or NARC1 for short. Searching the patent literature revealed that the same gene was identified in a screen for genes upregulated during induced neural apoptosis (Millenum patent no. WO 01/57081 A2; and Eli Lilly, LP251 patent no. WO 02/14358 A2). But the work from Dr Seidah's laboratory have clearly identified and characterized this new enzyme as the last member of the proprotein convertase family, hence its name PCSK9 (102). The original work on PCSK9 demonstrated that this enzyme was rich in the hepatocytes, kidneys, intestinal ileum, colon epithelia and in the embryonic brain neurons in mice (102). The authors referred PCSK9 as

important in proliferating and differentiating cells. Rapidly, the discovery of patients with autosomal dominant hypercholesterolemia with missense mutation in the *PCSK9* gene (318) led to a shift from neural development investigations to LDL-cholesterol metabolism. Indeed, PCSK9 is now the third gene locus associated with autosomal dominant hypercholesterolemia, along with the low-density lipoprotein receptor (LDLR) and apoB (318). Briefly, PCSK9 is mainly expressed and secreted by the liver, binds LDLR and targets it for degradation, resulting in increase concentration of LDL in circulation which causes atherosclerosis plaque accumulations (319). Therefore, strategies aiming at blocking PCSK9 activity will increase the bio-disponibility of the LDLR at the cell surface hence decreasing the LDL in circulation (LDL-C) and decreasing the atherosclerosis plaque formation. The strategy has been working extremely well as multiple clinical studies have successfully shown a significant reduction of cardiovascular accidents in patients treated with PCSK9 monoclonal antibodies (320). Indeed, evolocumab and alirocumab are two monoclonal antibodies against PCSK9 commercially available and subcutaneous injections in patients every 2-4 weeks have shown a decrease in ~60% of LDL-C and a 15-20% decrease in cardiovascular events (320). Pharmaceutical companies have soon jumped into the field, and now PCSK9-targeting strategies is a multi-billion-dollar industry and they have diversified their approaches ranging from monoclonal antibodies, antisense oligonucleotides (ASOs), to vaccines and more (321). PCSK9 targeting therapies have been extensively studied for the past 10-years (320) and the different approaches and the long term repercussions of inhibiting PCSK9 on patients (*e.g*. the emerging concerns related to diabetes mellitus or the role of PCSK9 in other tissue than the liver) go beyond the scope of this introduction and will not be discussed further.

1.5. Identification of new PC7 substrates: Mass spectrometry identifies two new proteins shed by PC7

As mentioned in the previous section on proprotein convertases, multiple PC-specific substrates have been identified and their related biological consequences have been well characterized. Some therapies involving PCs have even reached translational success in the clinic. One main issue regarding the biological roles of the seventh member of the family, PC7, is that we lack

information about specific substrates, we therefore aimed at identifying new substrates using a N-glycoproteome enrichment mass spectrometry approach. In this section, the interest of investigating N-glycoproteins and the strategies available for enrichment will be addressed. Also, the structure, trafficking and potential biological functions of two new PC7 substrates identified with this screen will be discussed. Other members of their gene family will also be discussed as it might shed light into the identification of the biological functions of the novel substrates. Before reviewing the literature on the two new substrates that we identified, a brief description of the method used by mass spectrometry to identify the substrates, the rationale behind it, as well as other available options and their advantages/disadvantages will be addressed.

1.5.1 Techniques for glycoprotein enrichment and analysis

Analysing and quantifying the repertoire of proteins and their associated post-translational modifications in a dynamic system is key to our understanding of a protein function or its involvement in a disease state (322). To do so, many tools and strategies have been developed over the years. The most common proteomics approach is the bottom-up (or shotgun) proteomics (323, 324). This technique is an indirect measurement of peptides from proteolytic digestion of proteins, often using trypsin because of its Arg & Lys cleavage specificity (325), but sometimes endoproteinase Lys-C, endoproteinase Glu-C or elastase can be used. The digested peptide solution is then analysed by liquid chromatography coupled to a tandem mass spectrometer detector (LC-MS/MS) (322). To do the proper quantification, the samples are usually compared by relative quantification between non labeling and labelled samples, (i.*e.* isotope-labeled *vs* label-free).

The interest of studying protein N-glycosylation is growing both from a fundamental and a clinal perspective. As mentioned above, N-glycosylation is a very important and ubiquitous PTMs in normal state but also play a major role in various diseases such as cancer and inflammatory diseases (326). Better methods to analyze the N-glycoproteome will improve the detection in various disease states since it will enhance the quantification of secreted proteins, which is in line with our own interests for finding new PC substrates. Indeed, the N-glycosyltransferases and sugar trimming enzymes are located in the ER and in the Golgi and will therefore attach their

complex series of glycan on this motif sequence N-X-[S/T] (where X represents any amino acid except Pro or Cys) to proteins trafficking through the secretory pathway such as: secreted proteins, luminal domain of membrane bound proteins or the extracellular part of plasma membrane proteins (327). Liquid chromatography coupled to high-resolution mass spectrometry (LC-MS) technologies have been used profusely throughout the past years for large scale screening of N-glycosylated proteins but inherent issues such as the chemistry complexity of the oligosaccharides attached and the low expression of multiple N-glycoproteins makes the analysis very difficult (327, 328). To circumvent the low abundant nature of glyco-proteomics analysis caused by the poor ionization capacity due to the highly hydrophilic characteristics of glycans, enrichment techniques have been developed. In addition, the MS/MS fragmentation is often used sequentially to assess information on both the peptides backbone as well as the glycosylation sites (322).

The different glycopeptides enrichment techniques available are based on the following methods: lectin affinity chromatographic, covalent hydrazide chemistry, immunoprecipitation, hydrophilic interaction liquid chromatography, click chemistry, covalent boronic acid chemistry and electrostatic repulsion interaction chromatography. For the lectin affinity chromatographic enrichment, different lectins will bind specifically glycans *via* hydrogen bonds and hydrophilic interactions with sugars (329). One important drawback from lectin affinity enrichment is that lectins binds specifically a unique type of glycopeptides hence only a specific saccharide will be purified, hence to overcome this a combination of different lectins is often used in the experiment (322). The covalent hydrazide chemistry consists of first oxidizing the glycopeptides to form aldehydes, which will then be bound covalently to a solid hydrazide support. This step will allow glycopeptides to stay on the support while non-glycopeptides will be washed-off after a tryptic digestion. Albeit an efficient purification strategy, using this technique will provide information only about the sites of the glycosylated residues and not the glycan structures (330). Immunoprecipitation enrichment necessitates the use of specific antibodies that recognize specific glycopeptides, hence is a more expensive technique (331). The hydrophilic interaction liquid chromatography enrichment technique is similar to the hydrazide enrichment because it is using the hydroxyl group formed on the glycans to bind a cellulose stationary phase *via*

hydrophilic interactions. One of the positive sides of this technique is that it successfully remove non-specific peptides from the samples (322). Click chemistry has been around for over 20 years (332), and as the name suggests, the chemical reactions referred to as 'click chemistry' are fast, easy to perform, reaction products are easy to purify and should produce a high yield. In brief, there is a first step of metabolic labelling were glycan residues are modified to azides and inserted into the cell membranes. The click chemistry (copper-catalyzed azide-alkyne cycloaddition) will allow the glycoproteins to be bound to the membranes, so after the cytosolic proteins removal, the glycoproteins should be enriched/purified (332). Boronic acid chemistry enrichment uses the boronic acid to bind covalently 1–2 and 1–3 cis-diol groups of peptides which creates a cyclic bronate ester. The wash step will remove all the non-covalently bond peptides (330). The last strategy is the electrostatic repulsion hydrophilic interaction chromatography, which is using a silica-based stationary phase composed of different positive functional groups. Negative charges on the sialic acid will be attracted and retained to the positive stationary phase, and in addition a hydrophilic reaction will happen between the glycan and the functional group (333).

1.5.1.1 Our strategy

In line with the challenges raised previously, we have developed a technique to analyse only secreted and membrane N-glycoproteins to circumvent the low abundance of glycosylated proteins. The technique we used is based on the hydrazide chemistry with an optimized protein solubilization protocol using high concentration of detergent (Sodium dodecyl sulfate (SDS) and Triton X-100). The high concentration of detergent helps in dissolving hydrophobic membrane proteins and increases the yield of membrane proteins (334, 335). In addition, the selective isolation of N-glycosylated proteins was performed using the hydrophilic interaction chromatography solid phase interaction (HILIC SPE) which has the additional benefits of removing the detergents and allows the site-specific glycan compositions (335). Following N-glycosylation purification, the captured glycoproteins were denatured, alkylated and trypsin-digested on beads releasing the non-glycosylated peptides first, following by elution with Peptide-N4-(N-acetyl-beta-glucosaminyl) asparagine amidase (PNGase F). The digested peptides were then labeled with light and heavy demethylation reagents, mixed and analyzed by RP-HPLC coupled to a high resolution LTQ-Orbitrap mass spectrometer.

1.5.2 The substrates identified: Golgi phosphoprotein of 130 kDa (GPP130/GOLIM4) and Cancer susceptibility candidate 4 (CASC4)

From our N-glycosylated enrichment screen, we found 645 and 867 glycosylated peptides enriched from the media of HEK293 and HuH7 respectively. We then compared secreted proteins that were quantitatively enriched in cells overexpressing PC7 to those of the empty vector control expressing cells. We have narrowed our analysis to proteins harboring consensus PC cleavage motifs (R/K)-Xn-(R/K) ↓ and found 18 and 10 proteins identified as enriched in our samples with potential cleavage sites in HEK293 and HuH7 respectively. In our analysis, we detected positive controls such as human transferrin receptor 1 (235, 239), ADAM17 (336) and sortilin (259), and also two novel potential substrates: GPP130 and CASC4. These two proteins are interesting because they are both type-II transmembrane proteins (similar to TfR1), located in the secretory pathway and have unknown biological functions. Interestingly, they are also part of a group of proteins from the GOLM1 family, Golgi-resident proteins that are believed to be carrying cargos along the secretory pathway. Before reviewing the literature about GPP130 and CASC4, the structure and function of the Golgi will be presented, in hope of shedding light on potential functions for these two poorly characterized proteins in this highly organized organelle.

1.5.3 The Golgi apparatus

1.5.3.1 Structure and function

The Golgi apparatus is a very busy and elaborate organelle, it is where many PTMs occurs, proteins traffic and are being sorted to their final destinations (337). During protein trafficking from the *cis*-Golgi to the TGN, proteins will undergo glycan remodeling, complex oligosaccharide synthesis and finally packaging and transport to final destinations (338, 339). The Golgi apparatus is composed of different stacks of flattened cisternae interconnected with tubular structures consisting of the *cis*, *medial*, *trans* and *trans*-Golgi Network (TGN) (340, 341). In addition to these, the ER-Golgi intermediate compartment (ERGIC) is a structure localized between the ER and the Golgi. To define the different Golgi cisternae's it is traditionally stipulated that the separation occurs according to the composition of the set of enzymes within each cisternae (342). Each Golgi cisternae's have distinct functions and inherently, they have different structure and composition.

Accordingly, experimental evidences performed by density gradient fractionation and immunolocalization have demonstrated that specific enzymes locate preferentially to specific cisternae (343). For example, first steps of glycosylation enzymes are located on the *cis* side of the Golgi such as α1,2 mannosidase I , whereas the beta 1,2 N-acetylglucosaminyltransferase I (NAGT I) and α 1,3-1,6 mannosidase II (Mann II) only reside in the medial and *trans* cisternae (344). Hence the concentration gradient of enzymes and their specific localization offer biochemical evidences of the distinct functions occurring in the four different cisternaes, but on the other hand this definition does not offer a clear and precise organelle physical separation. In accord with this argument, a recent view is instead separating the different cisternaes according to the type of trafficking mechanism used for importing and exporting proteins (343).

1.5.3.2 Golgi trafficking

The theories regarding protein transport through the Golgi is still a subject of active debate (345, 346). The two theories are the cisternal maturation model (347, 348), *vs* the vesicular transport model (349, 350). In the cisternal maturation model, the cargos do not leave the lumen of the cisternaes but instead the cisternaes progressively mature from the *cis* to *trans* direction, consequently, the resident proteins, such as glycosyltransferases are then retrieved by retrograde trafficking (351). On the other hand, the vesicular model stipulates that the Golgi cisternae are stable but that the cargos traffic *via* budding from one cisternae to another (350).

Vesicular trafficking is a mechanism that relies on the coordination of multiple elements: a coat complex for sorting and vesicle formation, Rab GTPases, adaptor proteins, tethering proteins and SNARE complex (352). Briefly for the coat proteins, COPII vesicles are carrying cargos from the ER to the *cis*-Golgi and are also critical in the fusion of the ERGIC compartment (353, 354). In contrast, the COPI vesicles transport cargos from the *cis*-Golgi to the ER, but they also act between different Golgi cisternaes (354). The clathrin-coated vesicles are responsible for the transport from the TGN to endosomes and lysosomes/vacuoles, as well as for the recycling of proteins from old to nascent TGN cisternae (355). Also, clathrin-coated vesicles are necessary for endocytosis at the plasma membrane (356).

The Rab GTPases are considered to be the master regulators of vesicular trafficking. There are ~60 Rabs in human, and about 1/3 are located at the Golgi membranes. These include but is not limited to: Rab1, Rab2, Rab8, Rab18, Rab43, Rab6/41 and Rab30 (357). Rab proteins cycle between nucleotide-bound membrane-associated and free states. Once activated they will target different effector proteins depending on the location and the pathways (357). They regulate the activity of many downstream effectors implicated in tethering complexes and scaffolding (357).

In addition to the golgins mentioned previously (358), another important group of proteins involved in tethering is the Conserved Oligomeric Complex (COG complex) (359, 360). These proteins can interact with SNARES, Rabs, coil-coil tethers and coat proteins and are important for vesicle formation during retrograde trafficking within the Golgi (359, 360). Interestingly in humans, the COG-congenital disorder of glycosylation (COG-CDG) is a severe disease that affects a multitude of systems (359). It was recently rationalized that patients with COG-CDG have underglycosylated proteins causing a plethora of defects in multiple pathways, but also these patients have trafficking defects caused by aberrant COG complex function, leading to problems in Golgi structure and protein secretion (359).

SNARE proteins are responsible for the fusion of vesicle, the last step in vesicle movement (361). It is proposed that the v-SNARE on the vesicle side is interacting with the t-SNARE on the target membrane compartment and forms a complex called trans-SNARE which generates a driving force to fuse two lipid bilayers together (361, 362).

The GGAs, or Golgi-localized, γ-ear-containing ADP ribosylation factor (Arf)-binding proteins, are a family of three monomeric clathrin adaptor proteins implicated in the traffic of proteins from TGN to endosomes (363, 364). The GGAs have four domains, VHS (Vps27, Hrs and STAM), GAT (GGA and TOM1), a flexible hinge-like domain and a ear region homologous to AP-1γ-1 ear domain (365). Accordingly, the different domains have been shown to bind different targets, for example the VHS domain was demonstrated to be recognizing dileucine acidic-cluster sorting signals on MPRs and sortilin (366, 367). The GAT domain is binding the GTPase Arf1 which helps in the GGAs recruitment to the TGN membranes (368) and the hinge-like domain is necessary for clathrin recruitment (369).

The adaptor protein complexes (AP-1 to AP-5) are heterotetrameric complexes consisting of two large subunits (either β1-5, or α, γ, δ, ε, ζ), one μ(1-5) subunit and a small σ(1-5) subunit (370). They are responsible for the trafficking of proteins along the secretory and endocytic pathway by recognition *via* their μ and σ subunits of specific motifs on the cytosolic tails of targeted proteins. AP-1 is localized to the TGN and to recycling endosomes and is involved in bidirectional transport as well as basolateral sorting in polarized cells. AP-2 is responsible for clathrin-dependant internalization from the plasma membrane into endocytic compartments. AP-3 is in the TGN/early endosomes and is responsible for transport to late endosome/lysosomes. AP-4 is in the TGN and is responsible for transport to the endosomes. Finally, AP-5 is a more recently described adaptor protein and its trafficking is still unclear, although it was recently demonstrated to be involved in late endosome/lysosome homeostasis (371, 372).

1.5.3.3 Golgi matrix proteins: The Golgi Reassembly Stacking Proteins (GRASPs)

Many investigations have led to a better understanding of the unique architecture and dynamic organization of the Golgi. Indeed, keeping the Golgi's integrity is important for proper maturation, traffic and sorting of proteins. The Golgi Reassembly Stacking Proteins (GRASPs) are Golgi matrix proteins implicated in the structure formation and stacking of Golgi cisternae (373). They are located on the periphery of the Golgi and form *trans* oligomers via their GRASP domains which thereby glues the cisternae together into stacks and stacks into ribbon (373). The best characterized GRAPs proteins are GRASP55 and GRASP65 for their roles in Golgi stacking (374), ribbon-linking (375), cargo transportation (376), cell cycle regulation (377), but even autophagy (378) and apoptosis (379). For example, GRASP55 and GRASP65 were showed to be implicated in Golgi disassembly and reassembly during mitosis (380, 381). Indeed, a sequential order of signaling events during mitosis leads to unlinking and partitioning of the Golgi stacks in order to divide into daughter cells (380, 381). As mentioned above, the GRASP activities go beyond Golgi stacking, as a study by Xiang *et al.* showed that silencing either one or multiple GRAPS proteins leads to faster protein trafficking which in turn impair protein glycosylation and sorting (382). Therefore, GRASPs are Golgi stacking proteins but are also required for the proper transport of cargos to final destinations. Figure 1.12 is a schematic representation showing that deficient GRASPs proteins impairs not only the structure of the Golgi but also protein glycosylation (383).

Other roles have been identified for these Golgi resident proteins such as unconventional protein secretion (384). Finally, the regulation to maintain Golgi stacks connected also involves components of the Golgi nucleated-microtubules and the centrosome (385).

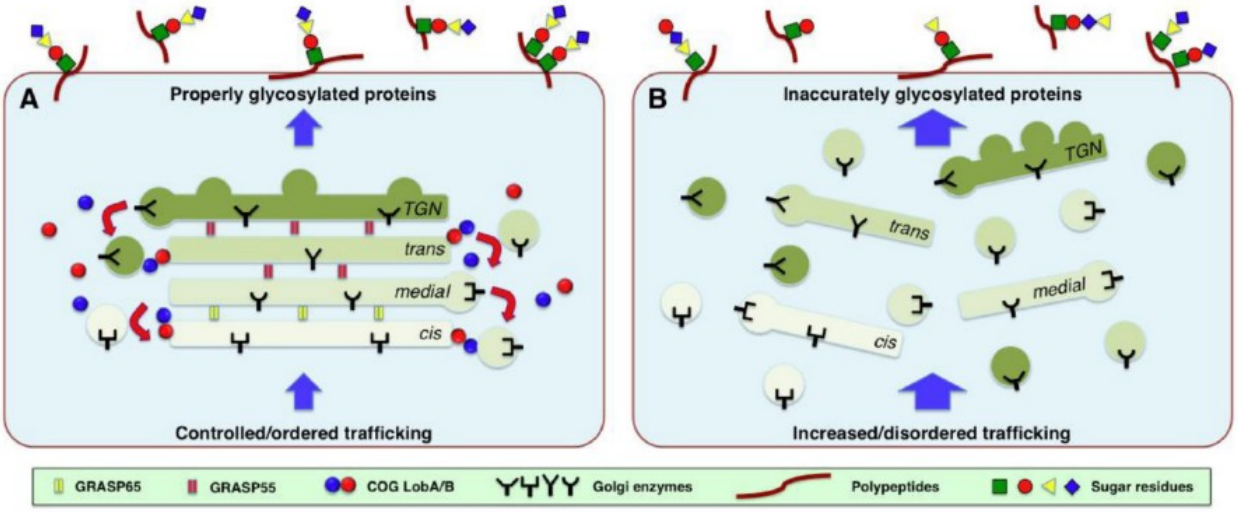

Figure 1.12. Regulated trafficking in the Golgi is essential for proper protein glycosylation.

A) GRASP proteins are needed for maintaining proper environment for glycosylation enzymes, ensuring proper cargo trafficking through the Golgi stacks and restricting vesicle budding to Golgi borders. B) Impaired protein glycosylation as a consequence of GRASP disruption. From Zhang X. *et al.*, 2016. (386)

1.5.3.4 Golgi matrix proteins: Golgins

Golgins are a family of Golgi matrix proteins implicated in maintenance of the Golgi structure and vesicle tethering (387). It is a group of proteins that are Golgi-bound either by direct anchoring of their transmembrane domain or *via* binding to a GTPase at the Golgi such as Arf1 or Rab6 (388). The golgins harbour long coil-coil cytoplasmic domains which are projected into the surrounding cytoplasm and are well suited to capture/tether membranes or cytoskeletal elements (389). Accordingly, golgins are defined as tethering proteins, hence they are involved

in vesicle trafficking, Golgi architecture and positioning (358). Amongst the well-known golgins are GM130, giantin and Golgin-97 (389). The golgins are also described to bind specific GRASP proteins, *i.e.* GM130 binding to GRASP65 in the *cis* Golgi is necessary for proper glycosylation and enzymes distribution (383). Other important golgin members are the GRIP domain proteins, they localize to the TGN via their GRIP domain and are implicated in Golgi organization, *i.e.*GCC185 is a protein that when depleted causes *cis* and *trans* Golgi fragmentation (390, 391). Interestingly, GCC185 was recently described to be involved in actin-dependant Golgi ribbon dispersal via the protein ITSN-1, a guanine nucleotide exchange factor of Cdc42 (392).

1.5.3.3 Golgi structure and function in diseases:

1.5.3.3.1 Alzheimer's disease

Alzheimer's disease is a neurodegenerative disease that is described as a progressive loss of cognition and memory (393). Like mentioned previously, amyloid beta precursor (APP) is cleaved and its end products (Aβ) aggregates are one of the causes of Alzheimer's disease (53). Interestingly, these Aβ aggregates are likely to cause Golgi fragmentation (394), a clinical occurrence observed in the neurons of early stages of the disease (395). The Golgi fragmentation is a result of GRASP65 Golgi stacking and ribbon formation inhibition caused by cdk5 phosphorylation of GRASP65 (394). These results suggested that inhibiting GRAPS65 phosphorylation could block Golgi fragmentation in AD patients (396), as a potential therapeutic avenue.

1.5.3.3.2 Parkinson's disease

Parkinson's disease is described as a progressive mid-brain dopamine neurons loss and α-synuclein aggregates within Lewis bodies (397, 398). α-synuclein aggregates correlates with Golgi fragmentation in early stages of Parkinson's disease (399). It was suggested that the α-synuclein aggregates are causing a ER to Golgi transport inhibition (400) which can cause neuronal degeneration .

1.5.3.3.3 Amyotrophic Lateral Sclerosis (ALS)

Amyotrophic Lateral sclerosis is a neurodegenerative disease targeting the motor neurons where fragmented Golgi has been reported. Multiple proteins have been linked to aberrant sorting and secretory trafficking leading to Golgi fragmentation such as SOD1, TDP-43 and FUS (401). Indeed, it was demonstrated that SOD1 is causing Golgi fragmentation in part by inhibiting the ER to Golgi v-SNARES GS15 and GS28 (402) within motor neurons.

1.5.3.3.4 Cancer

Golgi integrity and polarized secretion is necessary for directional migration (403) and evidences demonstrating that the Golgi is a signaling hub regulating cell migration in cancer cells are accumulating. Accordingly, Golgi resident proteins have been shown to be involved in multiple steps during cancer progression. Two interesting examples are the golgins GM130 and GOLPH3. About GM130, its role in cancer cell migration have been reported because of its binding to the small GTPase Cdc42, a regulator of cytoskeleton organization and cell polarity. It was shown that inhibition of GM130 led to the decrease of the Golgi-localized Cdc42 (404). Importantly, active Cdc42 at the Golgi is necessary for proper cell polarity and inherently directional cell migration (405). GOLPH3 was one of the first peripheral Golgi protein to be identified for its role in cancer (406). Indeed, it is located to the Golgi via binding to the Golgi membrane lipid phosphatidylinositol-4-phosphate (PtdIns(4)P). GOLPH3 was also shown to bind myosin MYO18A and to act as a mediator between the Golgi membrane lipids and the actin structure, see Figure 1.13, which favors vesicle budding, trafficking and consequently protein secretion (407, 408). It is now well established that GOLPH3 is a main actor in cancer by increasing directional secretion (409), but subsequent studies have also connected GOLPH3 to DNA damage (410). Another well known protein that was reported to have a crucial role in directional migration is golgin-160, this protein was demonstrated to be inducing Golgi apparatus dispersal when silenced and was one of the first evidence for Golgi positioning in directed secretion, cell polarity, and directional migration (411). In line with this original observation, a recent publication confirmed the role of golgin-160 in gliomas cell lines U251, where using lentivirus to decrease golgin-160 severely impaired migration and invasion of these cells (412).

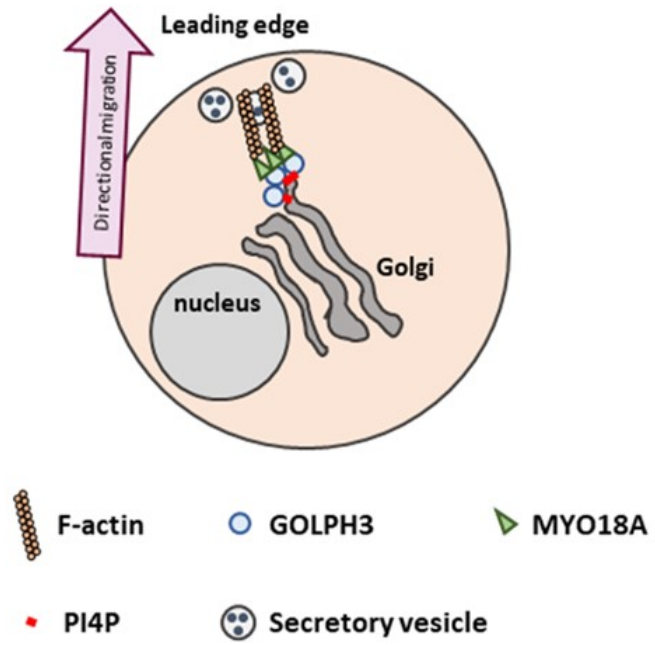

Figure 1.13. GOLPH3 bridges phosphatidylinositol-4-phosphate and actin to reorient the Golgi and promote directional migration.

Overexpression of GOLPH3 is driving Golgi reorientation towards the leading edge, increases the protein traffic from the Golgi to the plasma membrane and specifically towards the cell front. Adapted from Xing M. *et al.*, 2016 (408).

1.5.3.3.5 Cell migration

As mention in the previous section, it is becoming more and more clear that Golgi proteins have an important role to play in cell polarity and cell migration, which when dysregulated can lead to derailed cell migration and metastasis in cancer. To better appreciate the chapter II of this thesis, which is regarding cell migration, a few mechanisms will be presented in this section, with a particular focus on the Golgi apparatus and the cytoskeleton interplay during migration.

The force generate for migration comes mostly from the actin cytoskeleton, and more precisely the actin filaments (340). Cell motility is possible because of repeated cycles of protrusion attachments at the cell front combined with retraction and detachment at the rear (340). In migrating cells, stronger traction and adhesion at the front in comparison to the rear is needed for cell movement (342). Important structures composing the cytoskeleton are mechanosensitive such as stress fibers which are actin bundles associated with myosin II, α-actinin and cytoskeletal

proteins (342) that are connecting the extracellular matrix to focal adhesions (343). Focal adhesions are complexes localized at the plasma membrane that associate on one hand extracellular matrix *via* integrin binding, and on the other hand connect with the actin cytoskeleton *via* focal adhesions associated proteins such as paxillin (344), Figure 1.14. Paxillin is an adaptor protein localized at the focal adhesion complex and is required for focal adhesion turnover on the leading edge of the cell during migration (345). Paxillin is also capable of regulating actin remodeling and focal adhesion turnovers by acting on RhoA- and Rac1-GTPase signaling, which drastically influences cell migration (346). Importantly, too many stress fibers and focal adhesions assembly can also impede cell movement by generating stronger adhesion.

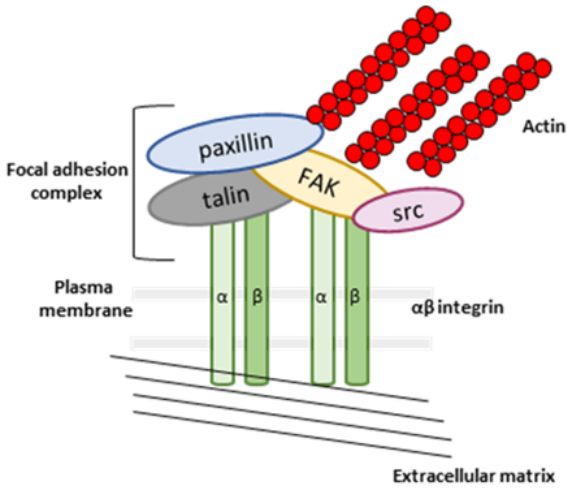

Figure 1.14. Focal adhesions are complex structures that connect the actin cytoskeleton to the extracellular matrix.

Depicted are main components of focal adhesions such as paxillin, talin, src and integrins linking the extracellular matrix with the actin cytoskeleton. Adapted from Deakin N. *et al.*, 2008 (413).

In conclusion for this part, the Golgi resident proteins have been highlighted at multiple occasions for important roles during cancer progression. These observations have inspired our group to further study the two uncharacterized Golgi proteins identified in our screen and highlight novel protein functions with relevance to cancer.

1.5.4 Cancer Susceptibility Candidate (CASC4)

1.5.4.1 Structure and function

CASC4 is an uncharacterized protein, it was identified in a cDNA library screen for new candidate gene overexpressed along with the oncogenic receptor HER^{2+} (414). Like the transferrin receptor 1 and GPP130, CASC4 is a type-II transmembrane domain protein, has a short 13 aa cytosolic tail, a 20 aa transmembrane domain and a luminal domain, Figure 1.15 It is predicted to be Golgi localized, but no publications have addressed its specific localization, or biological functions yet. The only available information about CASC4 is related to its aberrant splicing events in breast cancer and in glioblastomas (415, 416). Indeed, a study investigating the splicing factor SRSF1 identified CASC4 as a downstream target of the SRSF1 splicing machinery, leading to the inclusion of the exon 9 in the protein which corresponds to the full-length isoform (415). Additionally, short isoforms were also observed in patient-derived glioblastoma cells, compared to control cells (416). It is noteworthy to mention that in the glioblastoma study, two other candidate genes were significantly aberrantly spliced; p53 and APP, two well known proteins with undisputable biological roles in cancer (417, 418).

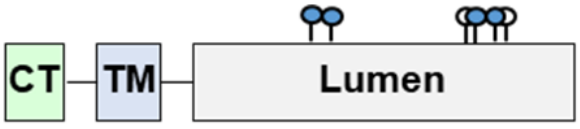

Figure 1.15. Schematic representation of CASC4 structure.

Depicted are the cytosolic tail (CT), the transmembrane domain (TM) and the luminal domain. The blue circles are depicting potential N-glycosylation sites and the white circles are depicting potential O-glycosylation sites.

1.5.5 Golgi phosphoprotein of 130 kDa (GPP130/GOLIM4)

1.5.5.1 Structure and trafficking

GPP130 is a type-II transmembrane domain with a small cytosolic tail (12 aa), a 20 aa long transmembrane domain and a luminal domain containing endosomal and Golgi-retrieval determinants (241, 419). As mentioned in the previous section, Golgi resident proteins that traffic through the secretory pathway and leave the Golgi need a particular signature to allow retrieval back to the Golgi, their home location (419). Accordingly, investigations of GPP130 luminal domain have demonstrated, using different deletion constructs and pH disrupting drugs such as monensin, that the coil-coil domain in the juxtamembrane region is necessary and sufficient for pH-sensitive Golgi localization as well as endosome to Golgi retrieval (419). More specifically, two amino acid stretches (aa 176-248 and 38-107) on the luminal domain were shown to be involved in Golgi localization, and another stretch (aa 80-175) is needed for endosome localization (419). Interestingly, for Golgi exit, many signals on the cytosolic tail of transmembrane proteins are known, but for the Golgi retrieval, proteins tend to rely on short sequences in their transmembrane domain (*i.e*. glycosyltransferases) (420), as for GPP130 it depends on key luminal domains. Figure 1.16 represents a cartoon of the GPP130 structure with its associated localization determinants. GPP130 is also different from other Golgi resident proteins because upon pH disruption it relocalizes from endosomes and plasma membrane, and cycles back to the Golgi *via* the late endosome independent TGN38/46 bypass pathway (421). The TGN38/46 pathway is a trafficking route from the plasma membrane to endosomes that bypasses late endosomal compartments, hence avoids possible degradation, and trafficking back to the Golgi (422).

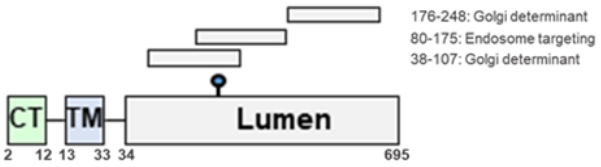

Figure 1.16 Schematic representation of GPP130 structure.

Depicted are the cytosolic tail (CT), the transmembrane domain (TM) and the luminal domain. The blue circle is depicting a potential N-glycosylation site.

1.5.5.2 Shiga Toxin and manganese

Toxins have been reported to use the bypass pathway as a mean to enter the cell, traffic to the ER and deploy their cytotoxic effects while escaping degradation in acidic endosomes/lysosomes (423, 424). It was hypothesised that GPP130, which was demonstrated to traffic through the bypass pathway, could influence the Shiga toxin sorting from early endosomes. Accordingly, inhibition of GPP130 led to Shiga toxin endosome-retrieval blockage (423). Further studies have confirmed the GPP130 and Shiga toxin interaction, as well as the trafficking mechanism. In brief, Shiga-like toxins consist of a monomeric A-subunit that is bound to a homopentameric B-subunit (425). The A-subunit is responsible for its toxic effects, as it contains the enzymatic activity (426), whereas the B-subunit bind the glycolipid globotriaosylceramide at the plasma membrane to enable its internalization (427-429). Following its internalization, the B-subunit of the toxin binds GPP130 in early endosomes specifically on the residues 46 to 55 (sequence VALKYQQ) in the juxtamembrane region of GPP130 (430). Interestingly, it was further demonstrated that treatment with manganese (Mn^{2+}) induces the oligomerization of GPP130 and its localization to multivesicular bodies before being rerouted to degradation in lysosomes (431). As it was demonstrated for its subcellular localization determinants, its luminal domain is required for the Mn^{2+} sensitivity but not its cytosolic tail (431). Moreover, it was further demonstrated that the Mn^{2+}-induced GPP130 oligomerization redistribution is clathrin and GGA1-dependent (432). Additionally, the sorting of oligomerized GPP130 into clathrin and GGAs vesicles from the Golgi towards lysosomes also requires the membrane-spanning receptor sortilin (433), which is a sorting receptor that is known to bind cargos on its luminal domain and also bind GGA1 and

clathrin on its cytoplasmic domain (434). Finally, it was recently suggested that the adaptor protein AP-5 ζ is involved in GPP130 endosome to Golgi retrieval via binding to sortilin (372). In this study, they used a CRISPR-Cas9 to knockout the AP-5 ζ subunit and observed aberrant relocalization of proteins retrieval from endosome back to Golgi, including GPP130 and cation-independent mannose 6-phosphate receptor (CIMPR) (372). In conclusion, in the past 10 years, the dissection of GPP130 domains and cluster residues, as well as its sensitivity to Mn^{2+} exposure have led to a better understanding of the trafficking of this Golgi protein.

1.5.5.3 Biological functions; Cancer

Because of its role during infection by Escherichia coli-produced Shiga toxin and its interesting trafficking route, most of the work on GPP130 is related to its retrograde trafficking in the context of toxin degradation. However, it was recently reported that GPP130 can influence cell survival and proliferation *in vitro* in head and neck cancer cell lines. Indeed, using a siRNA knockdown approach, it was demonstrated that silencing of GPP130 significantly reduces cell proliferation, causes a cell cycle arrest and induces apoptosis (435). It is also suggested that knockdown of GPP130 decreases the expression of cell cycle genes such as MDM2 and CDK6. In that sense, it is not surprising that the *GPP130/GOLIM4* gene can be amplified until almost 35% in lung cancer patients analysed in clinical cancer genomics studies, see Figure 1.17.

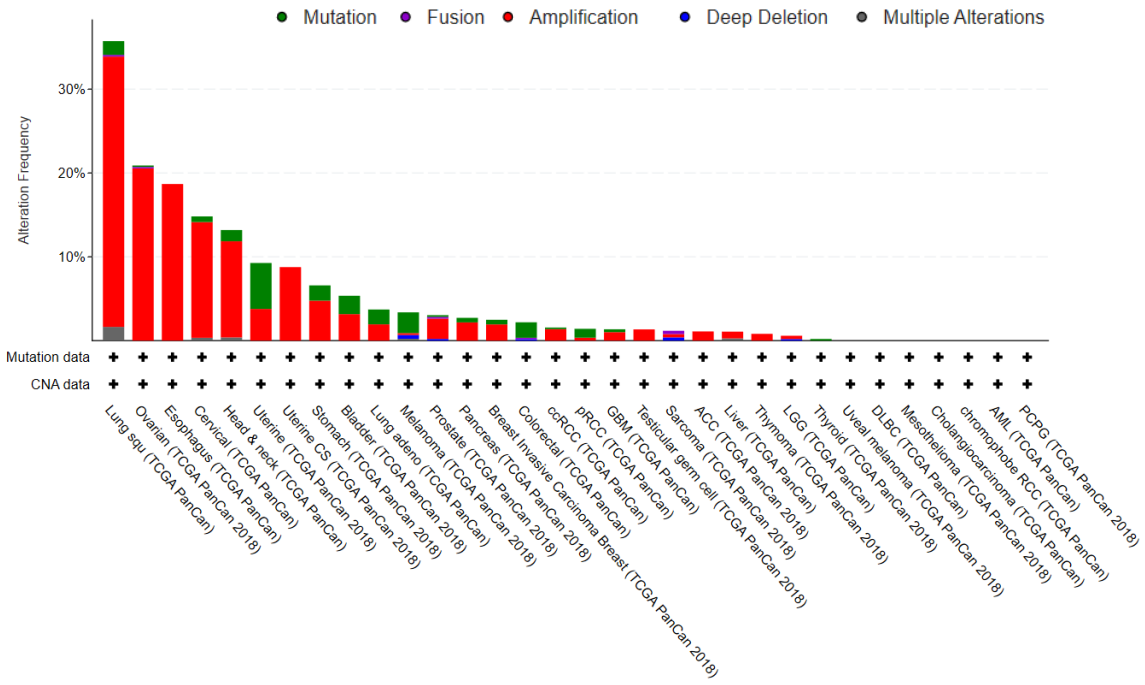

Figure 1.17. *GPP130/GOLIM4* gene expression in different cancers.

Summary of clinical data from cBioPortal for Cancer Genomics.

Other Golgi resident proteins have been previously linked to cancer as mentioned previously, another interesting example is GP73, which is structurally similar to GPP130 and is used as a biomarker in the clinic for multiple liver diseases (436, 437). Indeed, GP73 has attracted a lot of attention in the past because of its increased expression and associated abundance in the plasma in diverse liver disease states establishing a good monitoring tool in the clinic (438). Nevertheless, GP73 biological functions are still poorly characterized, only a few publications have addressed its potential role in disease progression, mainly in the context of hepatocellular carcinomas. Interestingly, it was recently demonstrated that GP73 could carry the metalloprotease MMP-7 as a cargo, and would facilitate its secretion, hence favouring cell invasion in hepatocellular carcinoma cells (439).

In conclusion, the work on proprotein convertases from the past 30 years have highlighted a family of enzymes regulating physiological functions from embryogenesis to viral entry. Both in health and in disease states, investigating the mechanisms of action of these converting enzymes and their specific substrates enabled a better understanding of these secretory proteases. This thesis project will now try to elucidate the biological roles of CASC4 and GPP130, two poorly characterized Golgi-resident proteins, and to define how their maturation by PC7 and Furin will modulate their functions.

1.6. Hypotheses and Objectives

Chapter II & III

Hypothesis: The proprotein convertases have been well characterized in health and diseases. The identification of new PC7 substrates will help the discovery of new physiological functions.

Chapter II. Cancer Susceptibility Candidate 4 (CASC4) Processing by PC7 and Furin Reveals a Novel Secretory Protein Implicated in Cancer Progression

Objective 1. Identification of PC7 new substrates by mass spectrometry and validation of the candidates.

Objective 2. Investigate CASC4 shedding by PC7 and Furin in the secretory pathway.

Objective 3. Since CASC4 was identified as a candidate gene in cancer (breast and glioblastoma), we aim to elucidate its functions in cancer progression.

Objective 4. Investigate how is the shedding by convertases modulating CASC4 activity.

Chapter III. Shedding of GPP130 by PC7 and Furin sheds light on a Golgi-resident protein with a unique trafficking pathway

Objective 1. Investigate GPP130 shedding by PC7 and Furin in the secretory pathway.

Objective 2. Investigate how is the shedding by convertases modulating GPP130 activity.

Objective 3. Shed light on an uncharacterized Golgi protein with gene amplifications in multiple cancers.

Chapter IV. Are PC7 KO mice protected from diet-induced obesity anxiety-like behavior?

Hypothesis: PC7 participates in proBDNF processing and diet-induced obesity anxiety-like behaviors increases BDNF in the reward circuit: PC7 KO mice should be protected from diet-induced obesity anxiety-like behavior.

Objectives 1. Perform behavioral assays on WT and PC7 KO mice chronically exposed to a saturated high-fat diet.

Objective 2. Investigate the maturation of BDNF in different areas of the mice brain.

Chapter II

Shedding of Cancer Susceptibility Candidate 4 (CASC4) by the Convertases PC7/Furin Unravels a Novel Secretory Protein Implicated in Cancer Progression

(Manuscript *accepted* for Cell Death & Disease, July 2020)

2.1 Résumé:

Durant ce deuxième chapitre nous nous intéresserons à l'étude de CASC4, un premier substrat de PC7 identifié dans notre analyse protéomique. Nous avons démontré que cette protéine est clivée au site $KR_{66}\downarrow NS$ par PC7 et Furin dans des compartiments cellulaires acides. Comme CASC4 a été rapporté dans des études de cancer du sein, nous avons généré des cellules MDA-MB-231 exprimant CASC4 de type sauvage et avons démontré une diminution significative de la migration et de l'invasion cellulaire. Ce phénotype est causé notamment par une augmentation du nombre de complexes d'adhésion focale et peut être contrecarré par la surexpression d'une protéine CASC4 mutante ayant un site de clivage optimale par PC7/Furin ou encore en exprimant une protéine contenant uniquement le domaine clivé N-terminal. Finalement, des résultats provenant de base de données de patients atteint de cancer du sein ont démontrés que l'expression élevé des gènes *CASC4* et *PCSK7* corrélaient à un mauvais prognostique, tandis qu'une expression élevée de *CASC4* mais faible de *PCSK7* était associée un meilleur prognostique.

2.2 Contributions to the chapter:

Conceptualization: Nabil G. Seidah and Stéphanie Duval

Performing experiments: Stéphanie Duval performed most of the experiments, except the mass spectrometry performed by R. Chen, J. Mayne, D. Seebun and D. Figeys. I E. Elkholi performed bioinformatics analysis and A. Abu-Thuraia performed Figure 2.6A.

Result analysis: Stéphanie Duval, Jean-François Côté and Nabil G. Seidah

Writing of the manuscript: Stéphanie Duval and Nabil G. Seidah

Supervision: Nabil G. Seidah

Manuscript #	CDDIS-20-0998
Current Revision #	0
Submission Date	10th Mar 20
Current Stage	Under Consideration
Title	Shedding of Cancer Susceptibility Candidate 4 (CASC4) by the Convertases PC7/Furin Unravels a Novel Secretory Protein Implicated in Cancer Progression
Running Title	Role of PC7/Furin cleavage of CASC4 in Cancer
Manuscript Type	Article

2.3 Manuscript #1

Shedding of Cancer Susceptibility Candidate 4 (CASC4) by the Convertases PC7/Furin Unravels a Novel Secretory Protein Implicated in Cancer Progression

Stephanie Duval[1], Afnan Abu-Thuraia[2], Islam E. Elkholi[2], Rui Chen[3], Deeptee Seebun[3], Janice Mayne[3], Jean-François Côté[2], Daniel Figeys[3], and Nabil G. Seidah*[,1]

[1] Laboratory of Biochemical Neuroendocrinology, Montreal Clinical Research Institute (IRCM; affiliated to the University of Montreal), 110 Pine Ave West, Montreal, QC, H2W1R7, Canada

[2] Laboratory of Cytoskeletal Organization and Cell Migration, Montreal Clinical Research Institute (IRCM; affiliated to the University of Montreal), 110 Pine Ave West, Montreal, QC, H2W1R7, Canada

[3] Ottawa Institute of Systems Biology and Department of Biochemistry, Microbiology and Immunology, Faculty of Medicine, University of Ottawa, Ottawa, ON, K1H8M5, Canada

*Corresponding author: Nabil G. Seidah, Montreal Clinical Research Institute, 110 Pine Ave West, Montreal, QC, H2W1R7 Canada.

Tel: 517-987-5609;

E-mail: seidahn@ircm.qc.ca

Running Title: **Role of PC7/Furin cleavage of CASC4 in Cancer**

2.3.1 Abstract

The proprotein convertases (PCs) are responsible for the maturation of precursor proteins and are involved in multiple and critical biological processes. Over the past 30 years, the PCs have had great translational achievements, but the physiological roles of PC7, the seventh member of the family, are still obscure. Searching for new substrates of PC7, a quantitative proteomics screen for selective enrichment of N-glycosylated polypeptides secreted from hepatic HuH7 cells identified two human type-II transmembrane-proteins of unknown function(s): Cancer Susceptibility Candidate 4 (CASC4) and Golgi Phosphoprotein of 130 kDa (GPP130/GOLIM4). Concentrating on CASC4, its mutagenesis characterized the PC7/Furin-shedding site to occur at $KR_{66}\downarrow$NS, in HEK293 cells. We defined PC7 and Furin trafficking and activity and demonstrated that CASC4 shedding occurs in acidic endosomes and/or in the trans-Golgi Network, respectively. Our data unraveled a cancer-protective role for CASC4, because siRNA silencing of endogenous CASC4 expression in the invasive triple-negative breast cancer human cell line MDA-MB-231 resulted in a significantly increased cellular migration and invasion. Conversely, MDA-MB-231 cells stably expressing CASC4 exhibited reduced migration and invasion, which can be explained by an increased number of paxillin-positive focal adhesions. This phenotypic cancer-protective role of CASC4 is reversed in cells overexpressing an optimally PC7/Furin-cleaved CASC4 mutant, or upon overexpression of the N-terminally convertase-generated membrane-bound segment. This phenotype was associated with increased formation of podosome-like structures, especially evident in cells overexpressing the N-terminal fragment. In accord, breast cancer patients' datasets show that high CASC4 and PCSK7 expression levels predict a significantly worse prognosis compared to high CASC4 but low PCSK7 levels. In conclusion, CASC4 shedding not only disrupts its anti-migratory/invasive role, but also generates a membrane-bound fragment that drastically modifies the actin cytoskeleton, resulting in an enhanced cellular migration and invasion. This phenotype might be clinically relevant in the prognosis of breast cancer patients.

2.3.2 Introduction

The proprotein convertases (PCs) constitute a family of nine serine secretory proteases that regulate diverse biological processes in both health and disease states (440). By irreversible proteolysis, PCs are responsible for the activation or inactivation of a variety of precursor proteins, such as growth factors, hormones, receptors and adhesion molecules (440). Such cleavage or shedding events may also result in the generation of cleaved entities with distinct novel functions. The first seven PCs cleave (↓) precursor proteins at specific single or paired basic amino acid (aa) within the motif (R/K)-$(2X)_n$-(R/K)↓, where n = 0-3 spacer aa (441). Because of their roles in the processing of many critical secretory substrates, e.g. activation of TGF-β (442) and matrix metalloproteases (443), PCs, such as Furin, PC5, PACE4 and PC7 were implicated in cancer/metastasis (444-446).

The seventh member of the family (PC7; gene *PCSK7*) is a ubiquitously expressed protease that often shares substrates with other PCs, especially Furin (440, 447). Recent work by our group identified the type-II transmembrane human transferrin receptor 1 (TfR1) as the first PC7-specific substrate (235). In contrast to Furin (448), following PC7 internalization from the cell-surface (449), it primarily cleaves substrates in early endosomes (450). To better understand the PC7 biology and pathophysiology we undertook an unbiased quantitative proteomics screen of N-glycosylated secreted products from hepatic HuH7 cells overexpressing PC7. This screen led us to identify two shed type-II transmembrane-proteins of unknown biological functions: Cancer Susceptibility Candidate 4 (CASC4) (451), and Golgi Phosphoprotein of 130 kDa (GPP130/GOLIM4) (241). *CASC4* was originally identified in a breast cancer screen in the context of $HER2^+$ overexpression (451). More recently, *CASC4* was also shown to be aberrantly spliced in breast cancer (452) and glioblastoma (416), however, the functional consequences of the spliced isoforms were not defined. In addition, a significant increase in secreted (shed) sCASC4 was found upon analysis of the N-glycosylated secretome from highly metastatic breast cancer cell lines (453).

In this study, we demonstrated that PC7 and Furin specifically shed CASC4 in post-ER acidic compartments, generating an N-terminal membrane-bound domain (NTD) and a secreted C-

terminal fragment. Using triple negative breast cancer MDA-MB-231 cells stably expressing CASC4 or its selected mutants, we demonstrated that wild type (WT) CASC4 enhances cell adhesion by increasing the number of focal adhesions (FA) and actin stress fibers, and that its shedding by PC7/Furin abrogates this phenotype. We then showed that the PC7/Furin-generated NTD induced the formation of podosome-like structures, implicated in invasion (454, 455). These results provide a novel unique mechanistic rationale for the functions of CASC4 and its shedding by PCs, which impact cellular migration and invasion.

2.3.3 Materials and methods

2.3.3.1 Glyco-proteomic analysis of secretome from HEK293 and HuH7 cells overexpressing PC7

Transient transfection: HEK293 cells (obtained from ATCC) and HuH7 (obtained from the JCRB) were maintained in 5% CO2 at 37°C were seeded at 6X105 cells in 6-well plates and grown to 80% confluency in Dulbecco's modified Eagle medium (DMEM; Invitrogen) supplemented with 10% (v/v) fetal bovine serum (FBS; Invitrogen), 1 mm sodium pyruvate (Life Technologies) and 28 μg/ml gentamycin (Millipore-Sigma). Cells were transiently transfected with plasmid pIRES2 containing cDNA encoding human PC7 at 2ug and as control pIRES2 empty vector. Transfections were carried out following Lipofectamine 3000 (Invitrogen) recommended protocols with a 1μg:1μl ratio of DNA to Lipofectamine reagent in OPTI-MEM media (Invitrogen) for HEK293 cells and 1:4 for HuH7 cells. Six hours post transfection, media was replaced by 2 mL of fresh OPTI-MEM media. At 24h post media change, spent media was collected, centrifuged at 16,000 Xg for 2 min to remove cellular debris and supernatants stored at -80°C.

Enrichment of secreted glycoproteome: Spent media from transient transfections of PC7 and empty vector were concentrated and equilibrated in 8M urea by ultracentrifugation using Amicon Ultra-15 centrifugal filter units (3 kDa cut-off, MilliporeSigma). A total of 500 ug of proteins were used for glycoprotein enrichment. Proteins were digested with trypsin as described in (335). Briefly, proteins were reduced with 10 mM dithiothreitol (DTT) at 56°C for 45 min, alkylated with 20 mM iodoacetamide (IAA) at room temperature for 1h and digested with trypsin at a 1:50 ratio at 37°C overnight. Glycopeptides were enriched by hydrophilic interaction

chromatography solid phase extraction (HILIC-SPE) as described in (335). Following capture, and washes to remove non-glycosylated peptides, the enriched glycopeptides were eluted from column and dried by vacuum centrifugation. The enriched fraction was deglycosylated using 50 units of PNGaseF (New England Biolabs) in 50 μl 100 mM ammonium bicarbonate at 37°C overnight.

LC-MS/MS Analysis and Database Search: Deglycosylated peptides were analyzed with an HPLC-MS/MS as per (335), using Q Exactive mass spectrometer (ThermoFisher Scientific Inc.) (ThermoFisher). The instrument method consisted of one full MS scan from 300 to 1800 m/z followed by data-dependent MS/MS scan of the 12 most intense ions, a dynamic exclusion repeat count of 2, and repeat exclusion duration of 30. Data files were processed with MaxQuant (1.2.2.5). The resulting precursor masses were matched to the IPI human database (version 3.68, 87,061 entries), and included the standard MaxQuant contaminant database. Mass tolerances were 6 ppm and 0.05 Da for the precursor and fragment, respectively. Enzyme specificity was set as KR/P, and a maximum of two missed cleavages was allowed. Cysteine residue was set as a static modification of 57.0215 Da, and the methionine oxidation and asparagine deamination were set as a variable modification of 15.9949 Da and 0.9840 Da, respectively. The false discovery rate cut-offs for both peptides and proteins were set at 1%. The protein group file was imported into Perseus (version 1.2.0.17) where identifications from contaminants and reversed databases were removed. Label free quantification was carried out and significant changes in proteins were determined by two-sided T-tests.

2.3.3.2 Plasmids

Human GPP130 WT (Thermo Scientific, Open Bioscience), CASC4 WT (Thermo Scientific, Open Bioscience) and its mutants (R60A, R62A, K65A, R66A, $AA_{65/66}$, NTD, SP-ΔTM-CASC4 and 5REL) were subcloned, with a V5 tag at the C-terminus into pIRES2-EGFP vector (Clontech). All constructions (human transferrin receptor 1, human Furin, mouse PC5A, mouse PC5B, human PACE4, full-length human PC7, soluble rat PC7, soluble human PC7 and Sar1P-(H79G) were cloned in pIRES2-EGFP vector (Clontech).

2.3.3.3 Cell Culture, Transfections, and Cell Treatments

HEK293 cells were grown in Dulbecco's modified Eagle's medium (DMEM, Invitrogen) with 10% fetal bovine serum (FBS, Invitrogen), CHO-ldlD cells were grown in DMEM/F12 medium with 10% FBS, MDA-MB-231 cells were grown in Dulbecco's modified Eagle's medium (DMEM, Invitrogen) with 10% fetal bovine serum (FBS, Invitrogen), MCF10a cells were grown in MEGM Mammary Epithelial Cell Growth Medium BulletKit from Lonza (Catalog #: CC-3150) + 5% horse serum. All cells were maintained at 37°C under 5% CO. HEK293 cells were co-transfected with equimolar quantities (0,5µg) of each plasmid using Jetprime Polyplus, CHO-ldlD cells were transfected with equimolar quantities (1,0µg) of each plasmid using FuGene HD, using manufacturer's instructions. MDA-MB-231 cells were transfected using GenJet^{TM} In Vitro DNA Transfection Reagent for MDA-MB231 Cells (SignaGen Laboratories) with equimolar quantities of plasmids (1.5-2 µg) using manufacturer's instructions. At 24h post-transfection, cells were washed in serum-free medium followed by an additional 20h alone or in incubation with 2.5 µg/mL brefeldin A (BFA; Calbiochem) or 20mM ammonium chloride (NH_4Cl; Sigma). For Endo H and PGNase F treatments, cell lysates were incubated with endoglycosidase H (endoH) or Peptide-N-Glycosidase F (PGNase F) for 1h at 37°C (New England Biolabs), cells and media were collected for western blot analysis.

2.3.3.4 siRNAs and quantitative RT-qPCR

A pool of four siRNAs against human CASC4 and a scrambled siRNA (Dharmacon; siGENOME SMARTpool) were transfected with a final 100 nM concentration, using DhamaFECT4 transfection reagent (Dharmacon), using the manufacturer's protocol. Total RNA extraction was performed using 1 mL Trizol reagent (Invitrogen) according to the manufacturer's instructions. Real-time PCR was carried out using Viia7 System (Applied Biosystems). Reactions were run in duplicate for each independent experiment. Human TATA-box binding protein (hTBP) gene was used as an internal control to normalize the variability in expression levels. Supplemental Table 2.3 summaries oligonucleotide sequences used for human *CASC4*, human *PCSK7* and human *Furin*.

2.3.3.5 Affinity-precipitation of GTP-Rho/Cdc42

MDA-MB-231 cells were washed with ice-cold Phosphate-buffered saline and lysed in Cytoskeleton Lysis Buffer (50 mM Tris pH 7.5, 10 mM MgCl2, 0.5 M NaCl, and 2% Igepal). Cell lysates were clarified by centrifugation at 10 000 g at 4°C for 1 min, and equal protein concentrations from the different cell lysates were incubated with GST–RBD (25 µg) or GST-PAK (10 µg) beads at 4°C for 60 min. The beads were washed two times with washing buffer (25 mM Tris pH 7.5, 30 mM MgCl2, 40 mM NaCl). Bound Rho/Cdc42 proteins were detected by Western blotting using a monoclonal antibody against RhoA/Cdc42 (Cytoskeleton). Densitometry analysis was performed using Image J software (National Institutes of Health). The amount of RBD-bound Rho was normalized to the total amount of Rho/Cdc42 in cell lysates for the comparison of Rho activity (level of GTPbound Rho/Cdc42) in the different samples.

2.3.3.6 Western blot analysis and antibodies

Cells were lysed in cold Radio-Immunoprecipitation Assay (RIPA) buffer (100mM Tris-HCL pH 8, 300mM NaCl, 0,2% SDS, 2% NP-40, 1% Na deoxycholate) containing protease inhibitors (Roche Applied Bioscience). Proteins were analysed by SDS-PAGE on 8-12% Tris-Glycine and transferred on a nitrocellulose membrane (GE Healthcare Life Science, No. 10600003) followed by 1h blocking in Li-Cor blocking buffer (Li-Cor) or in 5% milk in TBST-T. Membranes were then incubated with primary antibody overnight. Proteins were visualized using mouse anti-V5 (1/2000, Invitrogen), rabbit anti-PC7 (1:10,000, homemade or 1:5000 Cell Signaling Technologies), Furin (1:5000, Invitrogen), rabbit anti β-actin (1:5,000, Sigma-Aldrich), p-paxillin(Y118) (ThermoFisher), paxillin (Transduction laboratories), CASC4 (1:500, Abcam), Cdc42 (1:250, Cytoskeleton), RhoA (1:500, Cytoskeleton), or a horseradish peroxidase (HRP)-conjugated mAb V5 (1:10,000, Sigma-Aldrich), or anti-Flag M2 HRP (1:3000) (Sigma-Aldrich. Bound primary antibodies were detected with corresponding species-specific fluorescent anti-mouse antibody 680 (Mandel) (1:10 000) or anti-rabbit Ab 800 (Mandel), and revealed using LiCor Bioscience, or with corresponding species-specific HRP-labelled secondary antibodies (1:10,000, Invitrogen) and revealed by enhanced chemiluminescence (ECL; Amersham). Quantifications were done using Image Studio Lite v.4.0 and Image J software (National Institutes of Health).

2.3.3.7 Boyden Migration and Invasion Assays

For migration assays, $1x10^5$ cells were seeded into a transwell (6.5mm, Polycarbonate membrane 0.8µM, VWR) and allowed to migrate towards 10% FBS DMEM medium into the lower chamber as a chemoattractant during 6h. For invasion, $5x10^4$ cells were seeded into a Matrigel matrix (Corning) and allowed to invade during 16h towards 10% FBS DMEM medium into the lower chamber. After migration/invasion, cells were aspirated from the transwell and the membranes were washed before fixation by paraformaldehyde (4%) (Thermo Scientific) for 10 min. Following fixation, membranes were washed 3 times and mounted onto a microscope slide (Fisher Scientific) with ProLong Gold antifade with DAPI (Invitrogen) to stain for nucleus. The fixed membranes were analyzed by a DMRB microscope at 20X, 10 pictures were taken per conditions and counted for nucleus.

2.3.3.8 Wound Healing Assay

Confluent monolayer of cells was scratched with a 200µl-pipette tip to generate a scratch wound. To evaluate the distance travelled by the cells, pictures were taken with a Leica microscope at 6h and 12h post-scratch. Images were analyzed using Image J software (National Institutes of Health).

2.3.3.9 Microscopy Analysis and Antibodies

For F-actin staining, cells were seeded on Fibronectin (Sigma) coated (20µg/ml) glass coverslip into 24 well plates and grown for 48h. Cells were then fixed with warm paraformaldehyde (4%) for 20 min and permeabilized with PBS 1X + Triton 0.1%. Followed permeabilization, cells were stained for primary antibodies: paxillin (Transduction laboratories), anti-LDLR (R&D systems), anti-Golgin 97 (Santa Cruz Biotechnology), V5 (Invitrogen), TKS5 (MilliporeSigma) for 1 hour followed by fluorescent corresponding secondary antibodies or fluorescent coupled 555-Phalloidin to stain for F-actin for 30 minutes. Coverslips were then mounted on microscope slide (Fisher Scientific) with ProLong Gold antifade with DAPI (Invitrogen) to stain for nucleus. Co-localization of fluorescently labeled protein was quantified with IMARIS analysis software (8.2.1) along with aXTension script named Colocalize Spots. We used the same approach as mentioned in Rajan *et al*. (456). Positive signals were found using the Imaris function spots from each

fluorescent marker images. The spot diameter used was 1.2 µm with the same quality factor for each image. The Colocalize Spots script considers co-localization between two spots when their center to center distance is equal of inferior to 0.8 µm. Focal adhesion quantifications were done using Image J software (National Institutes of Health) with a program previously described (457).

2.3.3.10 Clinical data analysis

METABRIC (458, 459) and TCGA (460) datasets were accessed through the cBioPortal online platform (461, 462). To investigate the correlation between the CASC4 and PCSK7 mRNA levels, the plot tool was used. To correlate the association of CASC4 and PCSK7 mRNA expression levels with the survival rate in the METABRIC dataset, the expression level values of both genes (in z-scores) were downloaded for the whole dataset. Threshold of z-score =/higher than 1 is used to identify patients with high expression of PCSK7 or CASC4 and threshold of z-score =/lower than -1 is used to identify patients with low expression of PCSK7. All raw data (with samples IDs) used in generating these analyses are in Supplemental Figure 2.2.

2.3.4 Results

2.3.4.1 Mass spectrometry identifies two novel type-II transmembrane proteins cleaved by PC7

To identify novel PC7 specific substrates, we used a mass spectrometry approach that analyses affinity purified N-glycoproteins secreted in the media (Figure 2.1A). Analysis of secreted N-glycosylated products by this procedure avoids the limitations of the low concentrations of proteins of interest, high abundance of non-glycosylated plasma proteins in the incubation medium, or contamination by cytosolic proteins released from broken cells (463). Indeed, we selectively enriched samples for N-glycosylated peptides using hydrophilic interaction chromatography solid phase micro-extraction (HILIC SPE), before analyzing them by HPLC-ESI-MSMS (Figure 2.1A). Accordingly, we compared the quantitative changes of 645 and 867 enriched glycosylated tryptic peptides from the spent media of human embryonic kidney cells (HEK293) and human hepatic (HuH7) cells, both endogenously expressing TfR1, overexpressing either human PC7 or an empty vector (EV) control, respectively (Figure 2.1B). From HEK293 spent media with PC7, 19 glycopeptides had significantly enhanced levels, 18 of which exhibited potential PC-

cleavage sites (K/R)-(2Xn)-(K/R)↓(Table 2.1) (440). From the HuH7 spent media with PC7, 33 glycopeptides had significantly enhanced levels and an additional 12 glycopeptides were only observed with PC7 expression (Table 2.2). Of these, only 10 parent glycoproteins exhibited potential PC-cleavage sites. These results allowed us to confirm previously known PC7 substrates, such as ADAM17 (336), Sortilin (447) and human TFR1 (235), as well the identification of two novel substrates, the type-II transmembrane proteins CASC4 and GPP130/GOLIM4 (Supplemental Tables 2.1 and 2.2 and Figure 2.1C).

In order to confirm that CASC4 and GPP130 were cleaved by PC7, we co-expressed in HEK293 cells cDNAs coding for V5-tagged TfR1, CASC4 or GPP130 with those encoding PC7 or an empty vector control (Figure 2.1D). Compared to control conditions, Western blot (WB) analyses revealed the presence of secreted products (sCASC4 and sGPP130, or as control sTFR1) from cells co-expressing PC7, confirming that the membrane bound CASC4 and GPP130 are shed by PC7, similarly to TfR1. In view of the connection of CASC4 to cancer (*see later*), in this study, we concentrated on the consequences of the shedding and functional modulation of CASC4 by PCs in details.

2.3.4.2 CASC4 is shed by PC7 and Furin

To assess if CASC4 shedding is specific to PC7, in HEK293 cells we co-expressed CASC4 with all the basic amino acid specific PCs (Furin, PC5A, PC5B, PACE4 and PC7) (440), or with an empty vector control. WB analysis revealed the presence of a fragment released only in the media of cells expressing PC7 or Furin, but not from cells overexpressing the other PCs (Figure 2.1E). Interestingly, the molecular sizes of the PC7 and Furin shed products are similar (Figure 2.1E), suggesting that they cleave CASC4 at, or close to, the same site. To further characterize the difference between the observed ~66 kDa and ~75 kDa CASC4 cellular proteins (Figures 2.1D, E), we treated the cell lysates with endoglycosidase H (endo H) that cleaves immature, mannose-rich sugars which are added on proteins as a post-translational modifications early in the secretory pathway (464), or with PNGase F, which cleaves both immature and mature N-linked oligosaccharides which are modified on proteins in post endoplasmic reticulum (ER) compartments (465) (Figure 2.1F). The data demonstrated that the ~66 kDa CASC4 is likely to

reside in the ER, since its apparent molecular size is reduced to ~61 kDa (*; ER-CASC4) when treated with endo H. We also noticed the presence of a residual amount of ~66 kDa CASC4 after endo H digestion, suggesting the presence of an O-glycosylated form that is not N-glycosylated. Indeed, the mature ~75 kDa CASC4 protein (#; mat-CASC4) is insensitive to endoH, suggesting it has exited the ER, but its size is reduced to both ~61 and ~66 kDa upon PGNase F digestion. As expected from the zymogen activation of Furin in the trans-Golgi network (TGN) (238, 466) and that of PC7 occurring in early endosomes (235, 450), only the ~75 kDa mat-CASC4 is processed by either PC7 or Furin (Figures 2.1D, E).

Immunofluorescence staining of HeLa cells revealed that CASC4 co-localizes with the TGN marker Golgin-97 (yellow arrows, Figure 2.1G). When cells were stained under non-permeabilized conditions, CASC4 is only detected at the cell-surface, co-localizing with the cell-surface marker low-density-lipoprotein-receptor (LDLR) (yellow arrows, Figure 2.1H). Interestingly, we observed a change in cell morphology upon CASC4 expression, providing a clue to elucidate a novel biological function of CASC4.

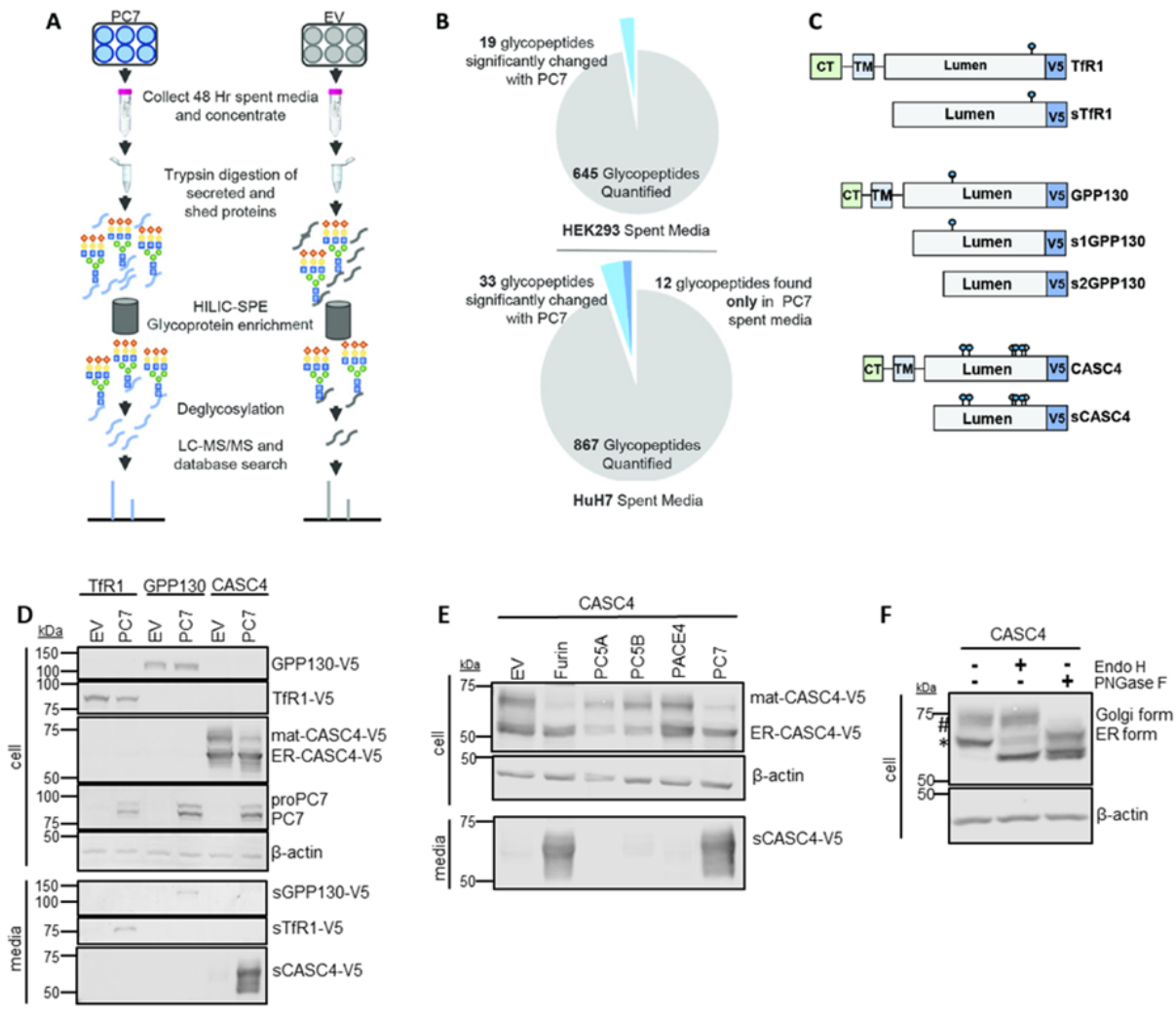
A
PC7
EV
Collect 48 Hr spent media and concentrate
Trypsin digestion of secreted and shed proteins
HILIC-SPE Glycoprotein enrichment
Deglycosylation
LC-MS/MS and database search
B
19 glycopeptides significantly changed with PC7
645 Glycopeptides Quantified
HEK293 Spent Media
33 glycopeptides significantly changed with PC7
12 glycopeptides found only in PC7 spent media
867 Glycopeptides Quantified
HuH7 Spent Media
C
CT
TM
Lumen
V5
TfR1
sTfR1
GPP130
s1GPP130
s2GPP130
CASC4
sCASC4
D
TfR1
GPP130
CASC4
kDa
EV
PC7
cell
media
GPP130-V5
TfR1-V5
mat-CASC4-V5
ER-CASC4-V5
proPC7
PC7
β-actin
sGPP130-V5
sTfR1-V5
sCASC4-V5
E
CASC4
Furin
PC5A
PC5B
PACE4
mat-CASC4-V5
ER-CASC4-V5
β-actin
sCASC4-V5
F
Endo H
PNGase F
Golgi form
ER form
β-actin

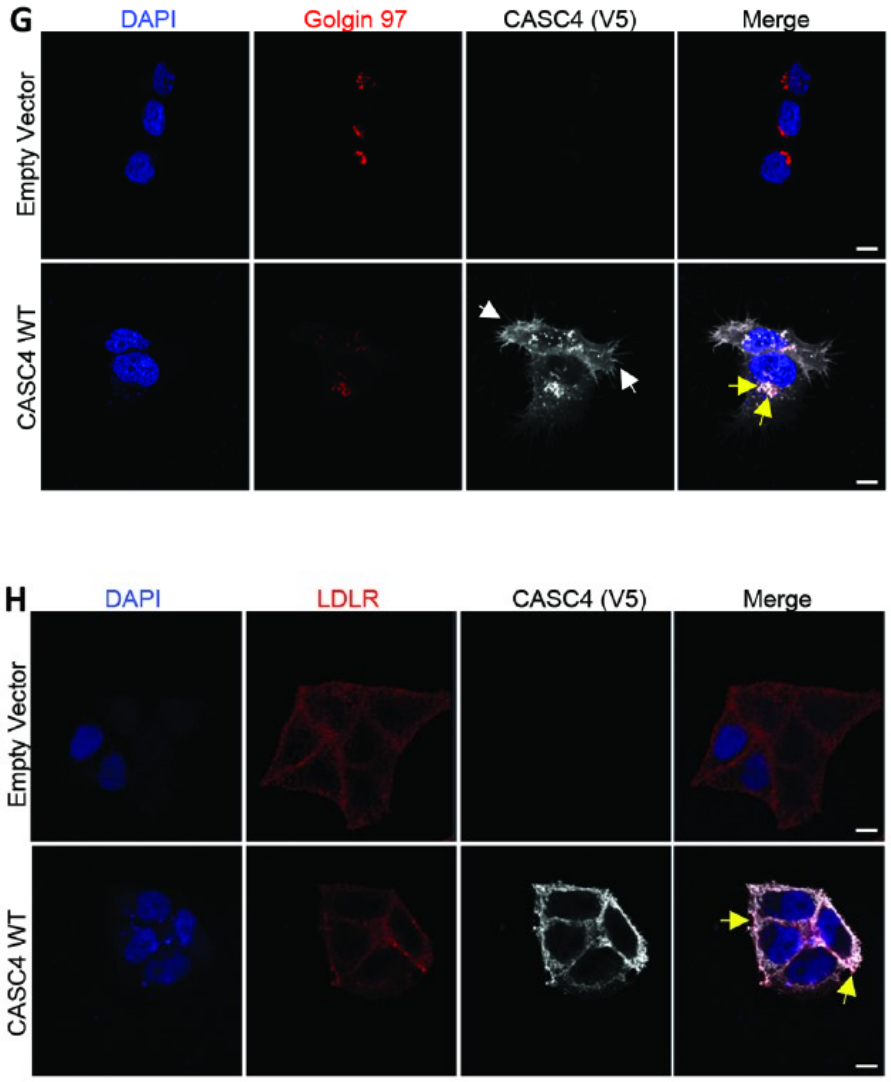

Figure 2.1. Mass Spectrometry Identifies two type-II transmembrane proteins shed by PC7 and Furin.

A) Schematic representation of the mass spectrometry strategy. The media from HEK or HuH7 cells overexpressing PC7 or empty vector were analyzed by LC-ESI-MS/MS and screened for quantitative changes in N-glycosylated soluble proteins. B) Quantitative changes of 645 and 867 enriched glycosylated tryptic peptides from the spent media of HEK293 and HuH7 cells. C) Schematic representation of human transferrin receptor 1 (TfR1), Golgi Phosphoprotein of 130 kDa (GPP130), and Cancer Susceptibility Candidate 4 (CASC4) identified in the analysis. Depicted are the cytosolic tail (CT), the transmembrane domain (TM), the luminal domain and the C-terminal V5-tag. The blue circles are depicting potential N-glycosylation sites and the white circles are depicting potential O-glycosylation sites. D) Western blot analysis of cell lysates and media from HEK293 cells expressing TfR1-V5, GPP130-V5 or CASC4-V5, with either empty pIRES-empty vector or hPC7. E) Western blot analysis of cell lysates and media from HEK293 cells expressing

CASC4-V5 with all the basic aa PCs. F) Western blot analysis of cell lysates from HEK293 expressing CASC4-V5 treated with endo H or PNGase F. G) Immunofluorescence analysis of permeabilized HeLa cells overexpressing CASC4-V5 colocalizing (yellow arrows) with Golgin-97, or in non-permeabilized cells with LDLR (H). These results are representative of three independent experiments. Scale: 10µm.

2.3.4.3 CASC4 cleavage by PC7 and Furin occurs at $Arg_{66}\downarrow$

Because PC7 and Furin cleave substrates after single or paired basic amino acids (aa) (440), we mutated the basic aa in the proposed P1-P2 (467) dibasic motif **$KR_{66}\downarrow$**, as well as the putative P5 **R_{60}** and P7 **R_{62}** sites into alanine (Figures 2.2A, B). WB analyses of HEK293 cells co-expressing PC7 or Furin with WT CASC4 or its Ala-mutants R60A, R62A, K65A or R66A, demonstrated that the K65A and especially R66A variants are resistant to shedding by PC7 and Furin (Figure 2.2B), while the other mutants did not affect shedding. To further emphasize that **$KR_{66}\downarrow$** is the shedding site, we generated CASC4 mutant proteins harboring an optimized PC-site $RRRRR_{66}$EL (440, 468) (called 5REL), or a PC-non-cleavable $AA_{65/66}$ site. Accordingly, in HEK293 cells, processing of the CASC4-$AA_{65/66}$ mutant protein was impaired compared to WT (Figures 2.2C, D). Expression of the 5REL mutant generated a soluble fragment, even when overexpressed with an empty vector control (Figures 2.2C, D), with an apparent molecular size similar to the PC7/Furin-cleaved form of WT-CASC4, supporting that **$KR_{66}\downarrow$** is the shedding site. To demonstrate that the heterogeneity of the secreted forms of CASC4 is due to O-glycosylation (Figure 2.2C), we co-expressed CASC4-WT and its mutants 5REL and $AA_{65/66}$ in CHO-ldlD cells, which are deficient in UDP-N-acetylgalactosamine (469), and therefore cannot O-glycosylate proteins. As expected, the secreted sCASC4 now migrates as a sharp protein band (~61 kDa), confirming the O-glycosylation of CASC4 (Figure 2.2E). Taken together, these data confirm that CASC4 cleavage occurs at **$KR_{66}\downarrow$**NS, which generates a secreted luminal domain and a short N-terminal domain (NTD) composed of the cytosolic tail and transmembrane domain.

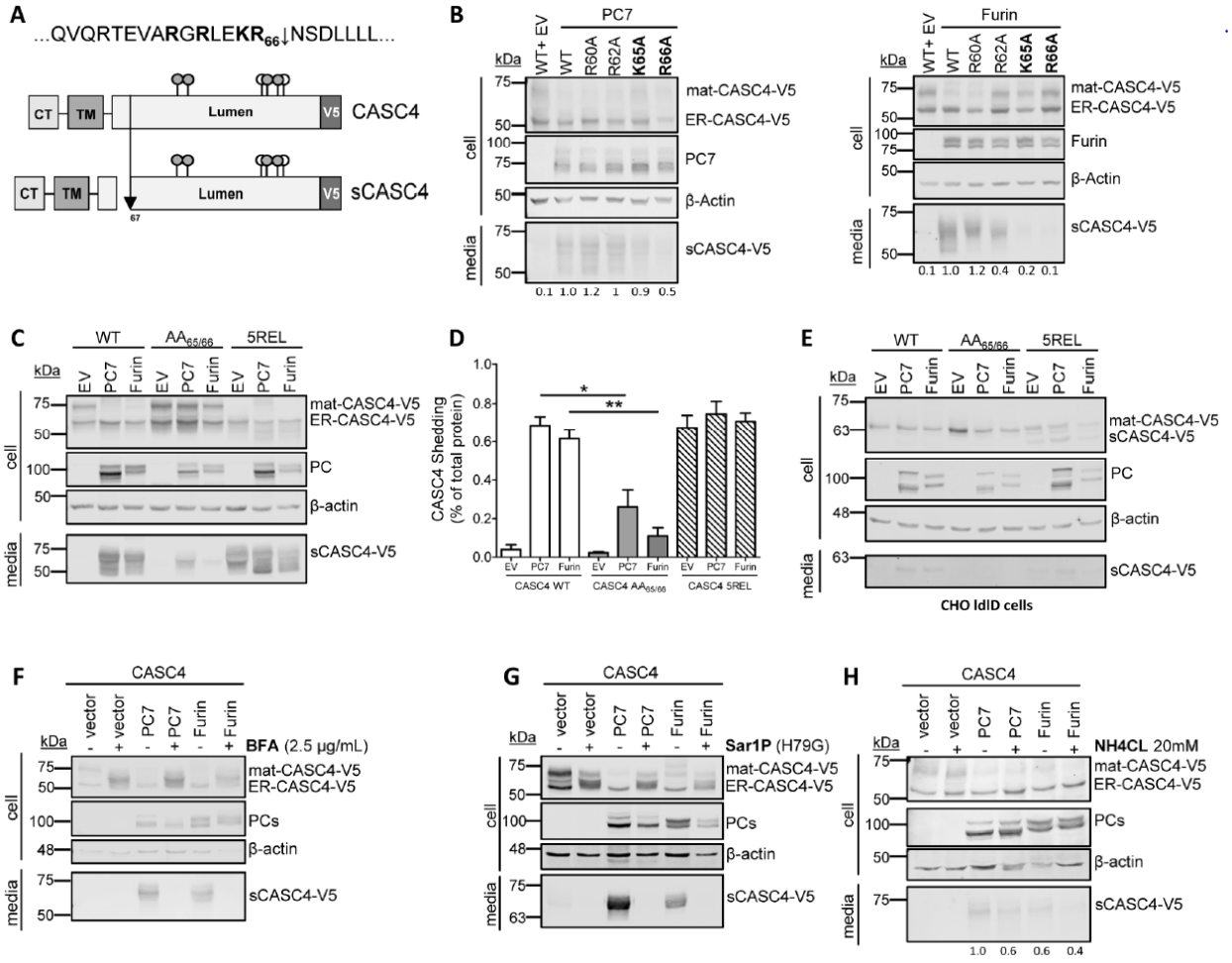

Figure 2.2. CASC4 Cleavage by PC7 and Furin occurs after Arg_{66}↓ in acidic compartment.
A) Schematic representation of the predicted cleavage site KR_{66}↓ generating a N-terminal fragment and a luminal domain. The grey circles are depicting potential N-glycosylation sites and the white circles are depicting O-glycosylation sites. B) Western blot analysis of cell lysates and media from HEK293 cells overexpressing CASC4-V5 WT and different point mutation (R60A, R62A, K65A or R66A) co-expressed with either pIRES-empty vector or with hPC7 or hFurin. C-D) Western blot analysis and quantifications of cell lysates and media from HEK293 cells overexpressing CASC4-V5 WT, CASC4 5REL optimally cleaved mutant or a PC-non-cleavable $AA_{65/66}$ site, co-expressed with either pIRES-empty vector or with hPC7 or hFurin. E) Western blot analysis of cell lysates and media from CHO ldlD cells overexpressing CASC4-V5 WT, CASC4 5REL optimally cleaved mutant or a PC-non-cleavable $AA_{65/66}$ site, co-expressed with either pIRES-empty vector or with hPC7 or hFurin. F) Western blot analysis of cells lysates and media from HEK293 cells overexpressing CASC4-V5 WT, pIRES-empty vector, and hPC7 or hFurin treated with Brefeldin A (2.5µg/mL) or Nh_4Cl (20mM) (G). H) Western blot analysis of cell lysates and media from HEK293 cells overexpressing CASC4-V5 WT, pIRES-empty vector, dominant negative Sar1P-(H79G), and/or with hPC7 or hFurin. These results are representative of three independent experiments. Error bars indicate averaged values ± standard error of the mean (SEM). P values: *, $p \leq 0.05$, **, $p < 0.01$, (Student's *t*-test).

2.3.4.4 Shedding occurs in acidic compartments of the secretory pathway

Shedding of CASC4 by PC7 and Furin occurs in a post-ER compartment, since it was abrogated when HEK293 cells were incubated with Brefeldin A (Figure 2.2F), which blocks the transport of proteins from the ER to the TGN (470). The same conclusion was reached upon expression of the dominant-negative Sar1p-(H79G) (Figure 2.2G), a GTP-restricted mutant that blocks COP-II vesicle formation [21]. Hence, proper COP-II vesicle formation and trafficking from the ER to the Golgi is necessary for PC7 and Furin to shed CASC4. We next used the alkalizing agent ammonium chloride (NH_4Cl), to block the acidification of intracellular compartments and demonstrated that shedding of CASC4 was also impaired (Figure 2.2H), suggesting that that CASC4 shedding occurs in an acidic post-ER compartment(s), likely in endosomes and/or the TGN, as described for the shedding of hTfR1 by PC7 (235, 450), and for Furin-substrates (238, 448).

2.3.4.5 CASC4 is expressed in metastatic breast cancer cells and its association with PC7 predicts poor prognosis in breast cancer patients.

CASC4 is an uncharacterized protein reported to be associated with a potentially bad prognosis in breast cancer (451), and its gene is aberrantly spliced in breast cancer cells (452). In addition, metastatic MDA-MB-453 triple negative breast cancer cells exhibit increased levels of secreted sCASC4 compared to non-cancerous breast cell lines (453). This motivated us to investigate the potential biological role of the PC7-CASC4 association in the context of breast cancer. First, we interrogated the METABRIC clinical dataset, the largest breast cancer dataset encompassing genomic data from ~2500 samples. Although *CASC4* mRNA levels showed a significant negative correlation with those of *PCSK7* (Figure 2.3A), the expression levels of the latter could differentiate the survival rate of the patients with high CASC4 levels (Figure 2.3B). Indeed, patients with high *CASC4* and high *PCSK7* expression levels had a significantly worse prognosis that those with high *CASC4* but low *PCSK7* mRNA levels (Figure 2.3B).

Second, we analyzed the expression levels of *CASC4*, *PCSK7* and *Furin* mRNA levels in MCF10a (human non-cancerous breast epithelial cell line) *versus* MDA-MB-231 (highly metastatic triple negative breast cancer cell line) cells by qPCR. The three genes are ~2-2.5-fold more expressed in MCF10a *versus* MDA-MB-231 (Figure 2.3C). However, at the protein level, WB analysis revealed

that while CASC4 is similarly expressed in both cell lines, its shedding into the media was mostly observed in MDA-MB-231 cells (Figure 2.3D). In addition, the protein expression levels of PC7 and Furin were similar in both cells (Figure 2.3D). We suggest that the TGN localization of CASC4 (Figure 2.1G) and that of the active form of its processing enzymes (450) may provide a favorable environment to allow its shedding in MDA-MB-231 cells compared to MCF10a cells. Altogether these data suggest that the PC7-CASC4 association and specifically the PC7-mediated shedding of CASC4 might have functional consequences in terms of breast cancer aggressiveness (i.e., metastasis).

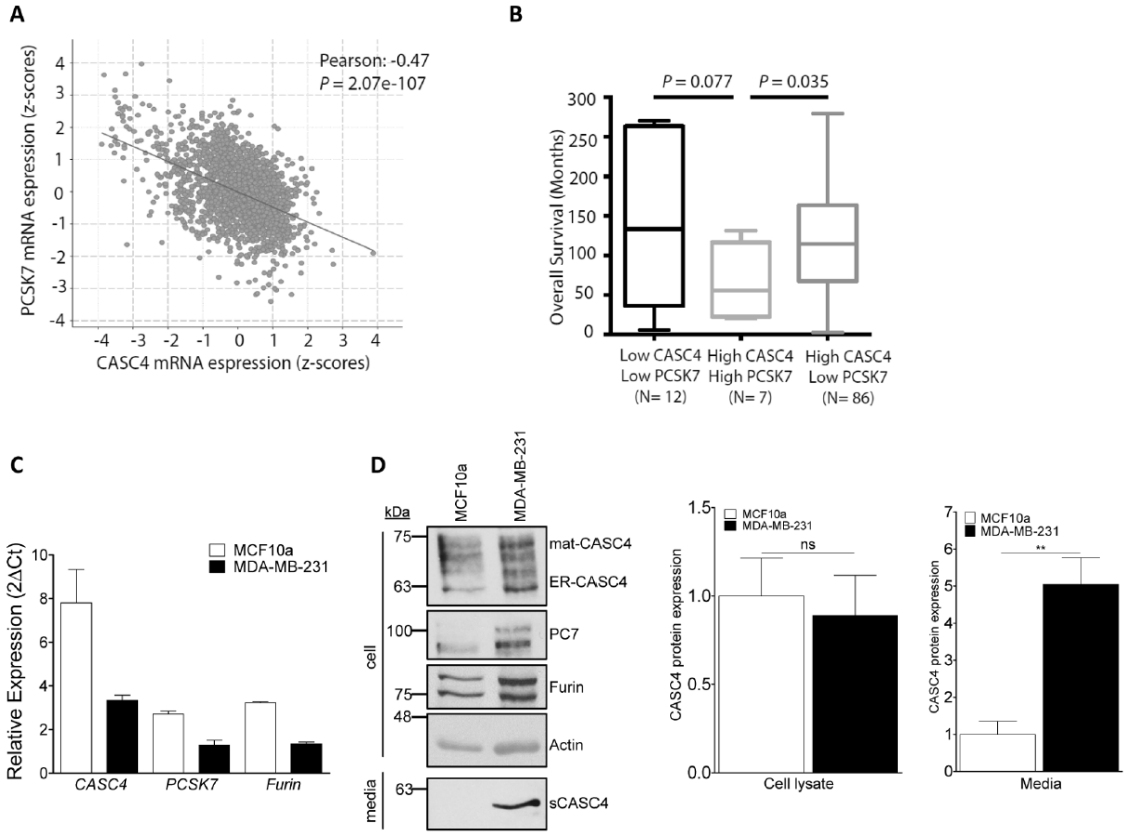

Figure 2.3. CASC4 association with PC7 predicts poor prognosis in breast cancer patients.
A) Correlation of CASC4 and PCSK7 mRNA expression levels (in z-scores) in the METABRIC patients' dataset. B) Association of the expression levels of CASC4 and PCSK7 genes with the survival patients' rate. C) qPCR analysis of hCASC4, hPCSK7 and hFurin in MCF10a and MDA-MB-231 cells. D) Western blot analysis and quantifications of cell lysates from MCF10a or MDA-MB-231 cells. P values: **, p <0.01, n.s. : not significant (Student's t-test).

2.3.4.6 CASC4 modulates cell migration and invasion

The cytoskeletal extensions observed upon overexpression of CASC4 in Hela cells (Figure 2.1G), and the correlation between PCSK7-CASC4 mRNA levels with breast cancer patients' survival (Figures 2.3A, B) suggested that CASC4 may impact cell migration and invasion, two essential steps of the metastatic process. We thus investigated whether siRNA knockdown of CASC4 alters cell migration and invasion in MDA-MB-231 cells. The siRNA-induced silencing was efficient since it reduced by ≥80% endogenous CASC4 protein, as observed by WB (Figure 2.4A) and immunofluorescence (Figure 2.4B). Depletion of CASC4 resulted in a significant increase in cell migration (+30%) and invasion (+60%) as assessed by Boyden Migration and Invasion Assays, respectively (Figures 2.4C-F). These results suggest that expression of CASC4 in MDA-MB-231 cells reduces their cell migration and invasion potential.

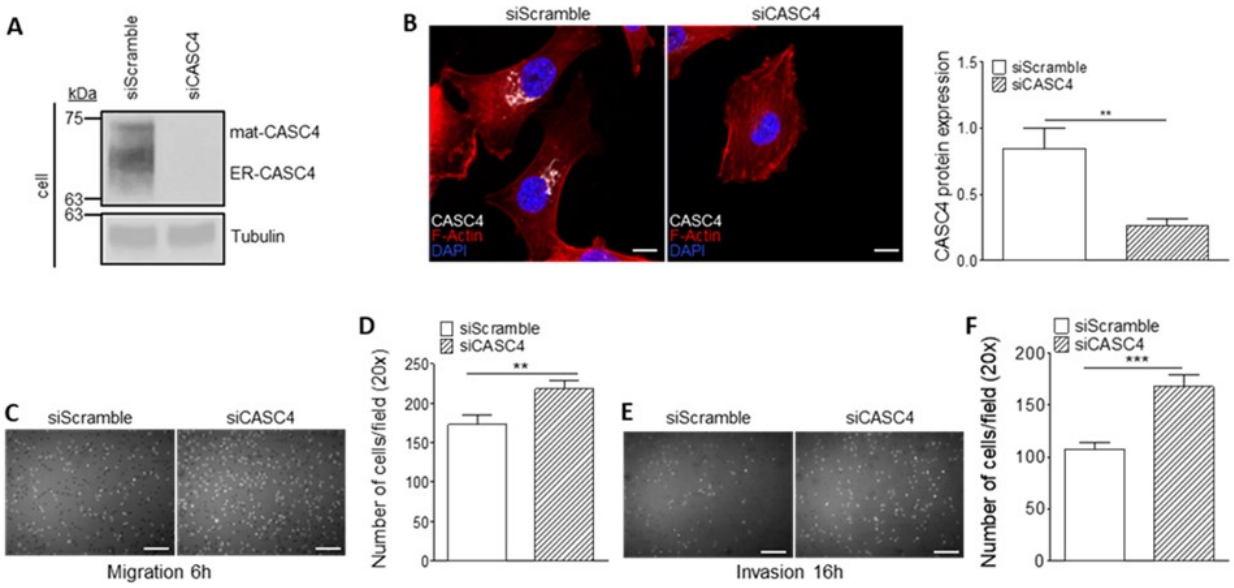

Figure 2.4. CASC4 knockdown increases migration and invasion in MDA-MB-231 metastatic breast cancer cells.

A) Western blot analysis and quantification of cell lysates from MDA-MB-231 cells after 48h siRNA knockdown of endogenous CASC4. B) Immunofluorescence analysis of MDA-MB-231 cells after 48h siRNA knockdown of endogenous CASC4 stained for CASC4 (white labeling), phalloidin (red labeling) and nucleus stained with DAPI (blue labeling). The ability of MDA-MB-231 cells, after 48h siRNA knockdown of endogenous CASC4 to migrate (6h) (C-D) or invade (16h) (E-F) was assessed by counting the number of cells stained with DAPI on the underside of a polycarbonate membrane under a phase contrast microscope (20x). These results are representative of at least three independent experiments. Error bars indicate averaged values ± standard error of the mean (SEM). P values: **, p <0.01, ***, p ≤ 0.001, (Student's *t*-test). Scale: 10µm.

Accordingly, we generated MDA-MB-231 cells stably expressing CASC4-WT, CASC4-5REL (with the constitutively PC-cleaved $RRRRR_{66}\downarrow EL$ motif), or an empty vector control (Figure 2.5A). We confirmed the protein expression in these cells by WB analysis (Figure 2.5B). Since the lack of CASC4 expression resulted in enhanced migration and invasion (Figures 2.4C-F), we evaluated the migration potential of the stable cell lines first by using a wound healing assay. Compared to control or cells expressing CASC4-5REL, only expression of CASC4-WT resulted in significant inhibition of wound closure post-scratching, especially evident after 12h (Figures 2.5C, D). In complementary Boyden Migration and Invasion Assays (Figures 5E-H), CASC4-WT overexpression significantly reduced cell migration (-50%) and invasion (-70%), supporting a role of CASC4 as a negative regulator of cellular movement. Although overexpression of CASC4-5REL did not show a significant migration phenotype (Figures 2.5E, F), its effect on invasion was intermediate between WT and control (Figures 2.5G, H). Taken together, these data suggest that CASC4 represses cellular migration, possibly by acting on key players orchestrating the cellular architecture, and that CASC4 shedding by PCs largely prevents this effect.

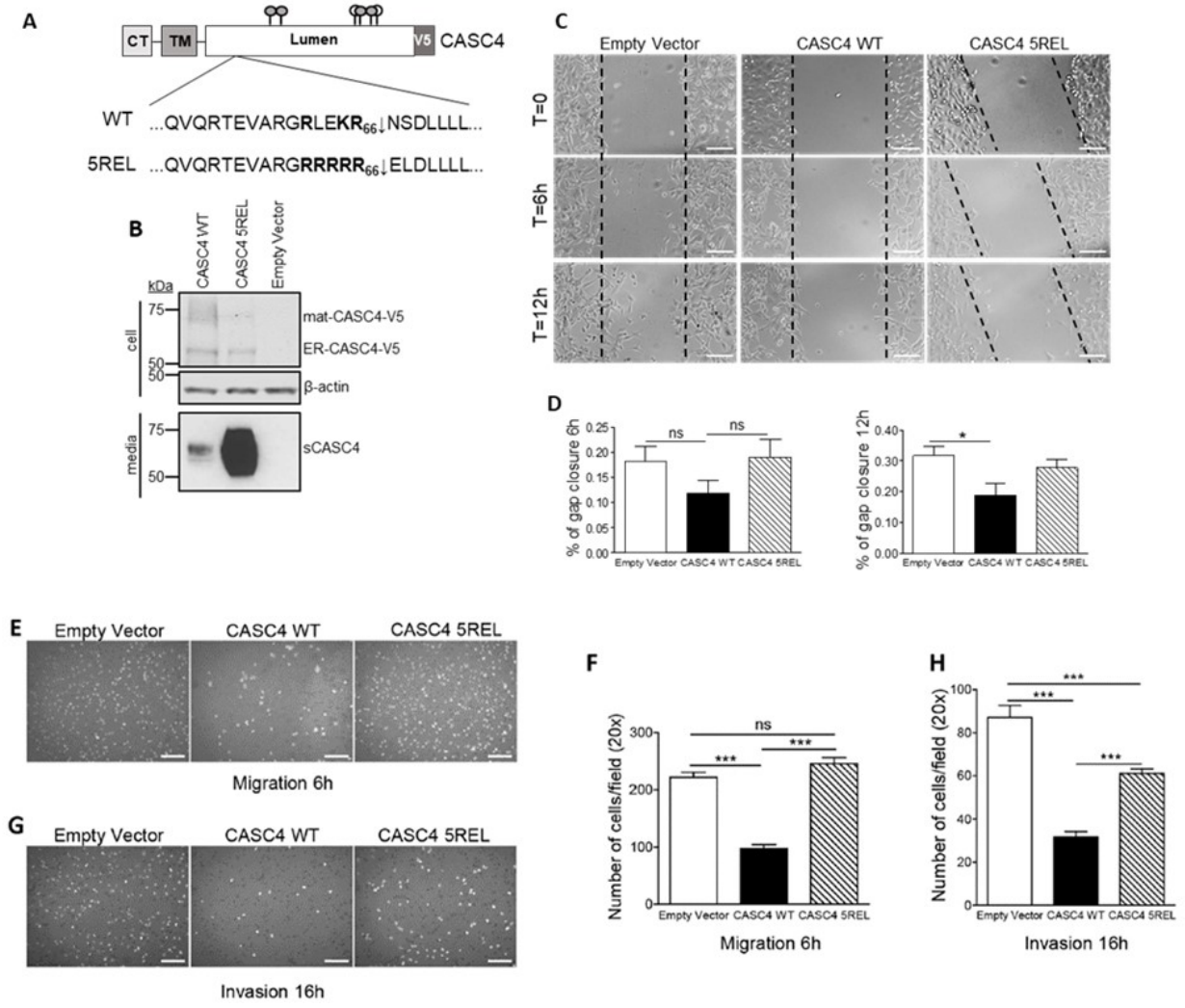

Figure 2.5. CASC4 overexpression decreases cell migration and invasion.

A) Schematic representation of CASC4 WT and amino acid mutations used for the generation MDA-MB-231 stable cells. B) Western blot analysis of lysates from MDA-MB-231 stable cells expressing pIRES-empty vector, CASC4 WT-V5 or CASC4 5REL-V5. C-D) Wound healing assay images and quantifications after 6h, 12h post cell monolayer scratching in MDA-MB-231 stable cell lines. E-H) The ability of MDA-MB-231 stable cells to migrate (6h) (E-F) or invade (16h) (G-H) was assessed by counting the number of cells stained with DAPI on the underside of a polycarbonate membrane under a phase contrast microscope (20x). These results are representative of at least three independent experiments. Error bars indicate averaged values ± standard error of the mean (SEM). P values: *, $p \leq 0.05$, ***, $p \leq 0.001$, n.s. : not significant (Student's *t*-test).

2.3.4.7 CASC4 enhances the number of focal adhesion (FA) formation and impairs Cdc42 activation

To investigate how CASC4 interferes with cellular migration/invasion, we analyzed the actin architecture and focal adhesions by immunofluorescence for phalloidin- and paxillin-staining, respectively. Interestingly, CASC4-WT cells exhibited a higher number and a trend for larger paxillin-positive focal adhesion complexes (Figures 2.6A, B), as well as ~3-fold more Tyr_{118}-phosphorylated paxillin (Figure 2.6C). In addition, the overall architecture of CASC4-WT cells was severely impaired, as evidenced by the induction of actin stress fibers at the expense of cortical actin (Figure 2.6A). This architectural cellular phenotype could explain the observed reduced migration observed in CASC4-WT cells (Figures 2.5 C-H). The actin architecture in cells expressing CASC4-REL, while also severely disrupted, exhibited a very different phenotype with a completely disorganized paxillin staining (Figure 2.6A).

We next characterized in our stable cell lines the activation/inactivation of Rho GTPases, which are molecular switches that control actin cytoskeleton and focal adhesion dynamics (471),(472). The levels of the active forms of the Rho GTPases Cdc42 and RhoA implicated in focal adhesion turnover (473, 474) were quantified by specific GST pull-downs. The data revealed a significant decrease in the levels of active Cdc42 in cells overexpressing CASC4-WT, compared to empty vector and CASC4-5REL, whereas those of active RhoA remained unchanged (Figure 2.6D). This suggests that CASC4-WT, but not CASC4-5REL, blunts the activation of Cdc42, resulting in increased assembly of focal adhesion and stress fibers (Figure 2.6A).

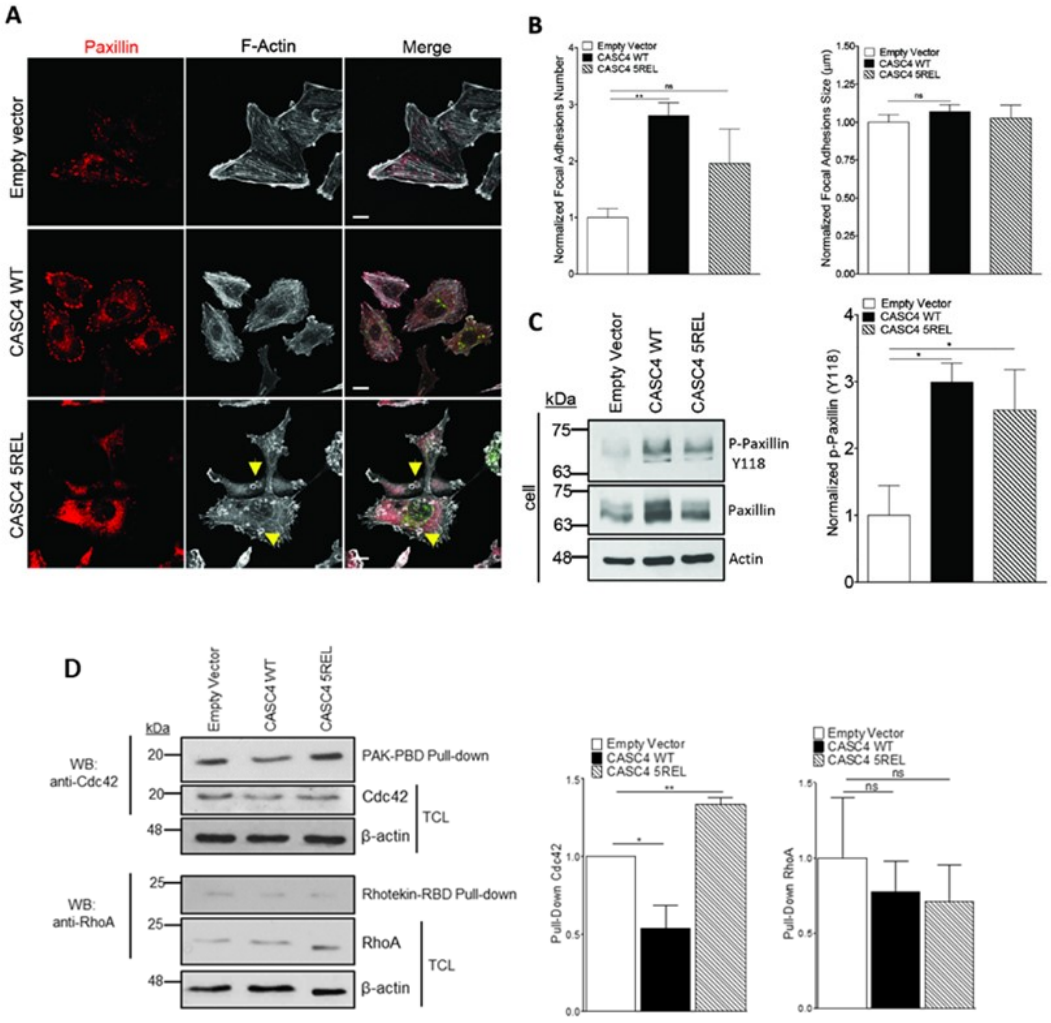

Figure 2.6. CASC4 enhances focal adhesions and perturbs actin architecture.
A) Immunofluorescence analysis of stable MDA-MB-231 cell lines expressing pIRES-empty vector, CASC4 WT or CASC4 5REL stained for focal adhesion marker (Paxillin; red labeling), phalloidin (F-actin; white labeling), and V5 (green labeling). Yellow arrows are highlighting round actin circles generated in cells expressing CASC4 5REL. B) Quantifications of focal adhesions (Paxillin positive areas) number and size. C) Western blot analysis and quantifications of cell lysates from MDA-MB-231 stable cells showing endogenous paxillin and p-paxillin (Y118). D) Western blot analysis and quantification of cells lysates from MDA-MB-231 stable cells incubated with the indicated GST-fusion proteins bound to Glutathione beads. The precipitated proteins were detected by immunoblotting with anti-cdc42 or anti-RhoA antibodies. TCL: total cell lysate. These results are representative of at least three independent experiments. Error bars indicate averaged values ± standard error of the mean (SEM). P values: *, $p \leq 0.05$ **, $p < 0.01$, n.s: not significant (Student's *t*-test). Scale: 10µm.

2.3.4.8 CASC4 N-terminal domain (NTD) impairs actin organization and induces invadopodia-like structures

Notably, cells expressing CASC4-5REL presented round actin rings (depicted with yellow arrows) (Figure 2.6A). These structures are reminiscent of circular dorsal ruffles, actin structures present on the dorsal surface of cells in response to stimuli (i.e., EGF, PDGF) (475), and/or invadosomes (invadopodias/podosomes) structures implicated in actin remodeling and invasion in both cancerous (invadopodias) and non-cancerous cells (podosomes) (454, 455). Since co-localization of F-actin with protein tyrosine kinase substrate 5 (Tks5) and extracellular matrix degradation can define invadosomes (455), we characterized these structures by immunofluorescence staining for F-actin and Tks5. The data showed that Tks5 staining co-localizes (yellow arrows) with the F-actin structures in CASC4 5REL cells (Figures 2.7A, B), suggesting that these actin structures were invadopodias/podosomes. We next investigated whether the NTD or the C-terminal luminal fragment generated by PC7/Furin is/are implicated in invadopodias induction. Thus, we generated two constructs, one with a stop codon at 11-residues after the shedding site (aa 1-77, likely processed at $Arg_{66}\downarrow$), to create an artificial NTD fragment, and another secretory protein mimicking the luminal shed domain with an N-terminal PCSK9 signal peptide (SP) (476) fused to Asn_{67} following the shedding site at Arg_{66} (SP-ΔTM) (Figure 2.7C). We confirmed the expression of these constructs in MDA-MB-231 cells by WB analyses (Figure 2.7D) and immunocytochemistry (Supplemental Figure 2.1). We next assessed the presence of the actin rings structures in cells expressing the different constructs by immunofluorescence (Figure 2.7E). Cells expressing the 5REL and especially the membrane bound NTD constructs exhibit the presence of round actin structures co-localizing with Tks5 (yellow arrows). To test the NTD role in inducing invadopodias formation, likely influencing migration/invasion, we transiently expressed all constructs in MDA-MB-231 cells and performed Boyden Invasion and Migration assays. First, we showed that the double Ala-mutant of the shedding site (CASC4 $AA_{65/66}$, Figure 2.2C) is ~2-fold more active in reducing invasion than the WT-CASC4 (Figures 2.7H, I), supporting the protective role of full length CASC4. In contrast, expression of the NTD significantly enhanced migration/invasion, whereas expression of the SP-ΔTM mutant had no effect (Figures 2.7F-I). Thus, the N-terminal

fragment generated upon shedding of CASC4 is mainly responsible for the cytoskeletal disruption observed in the CASC4-5REL cells.

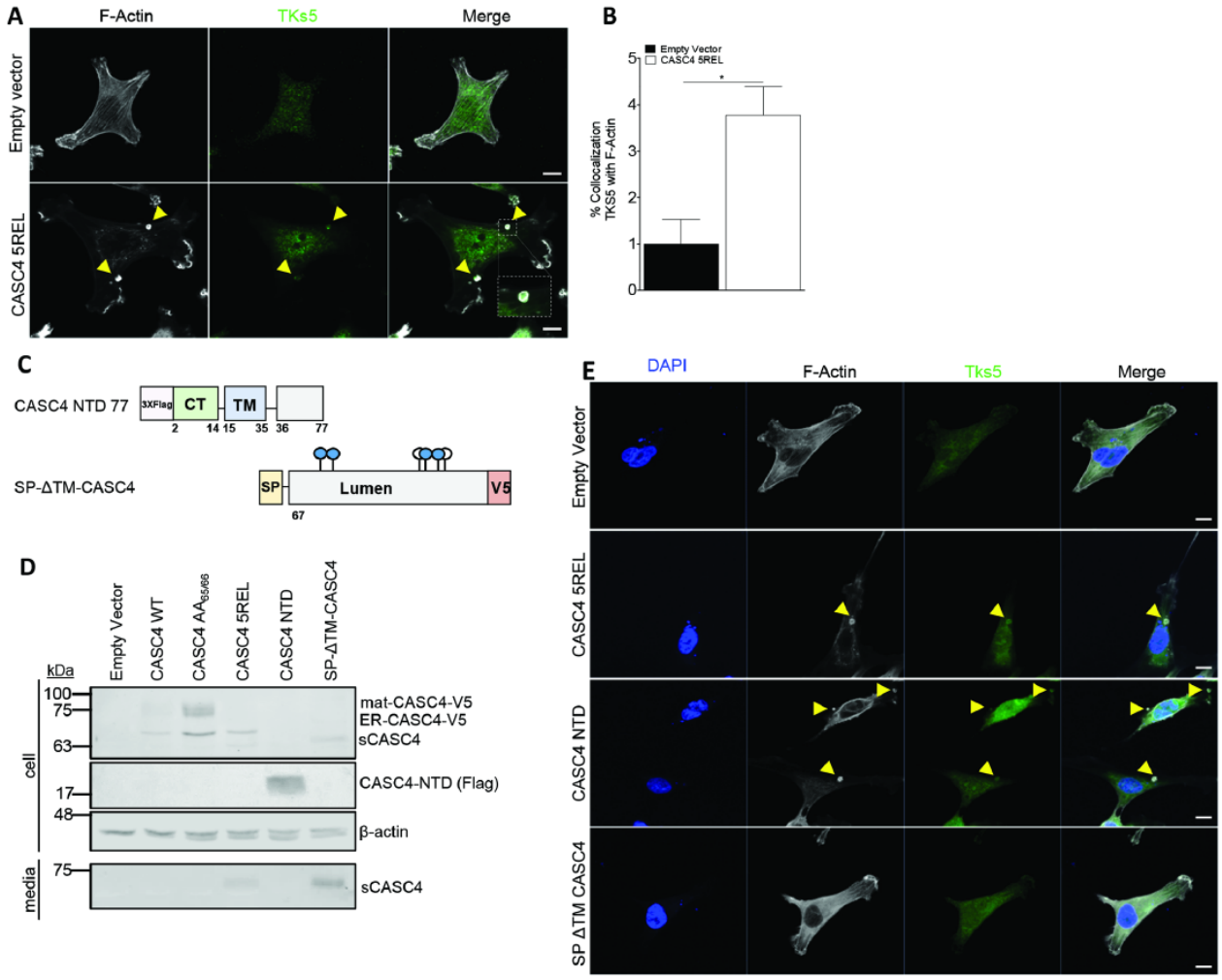

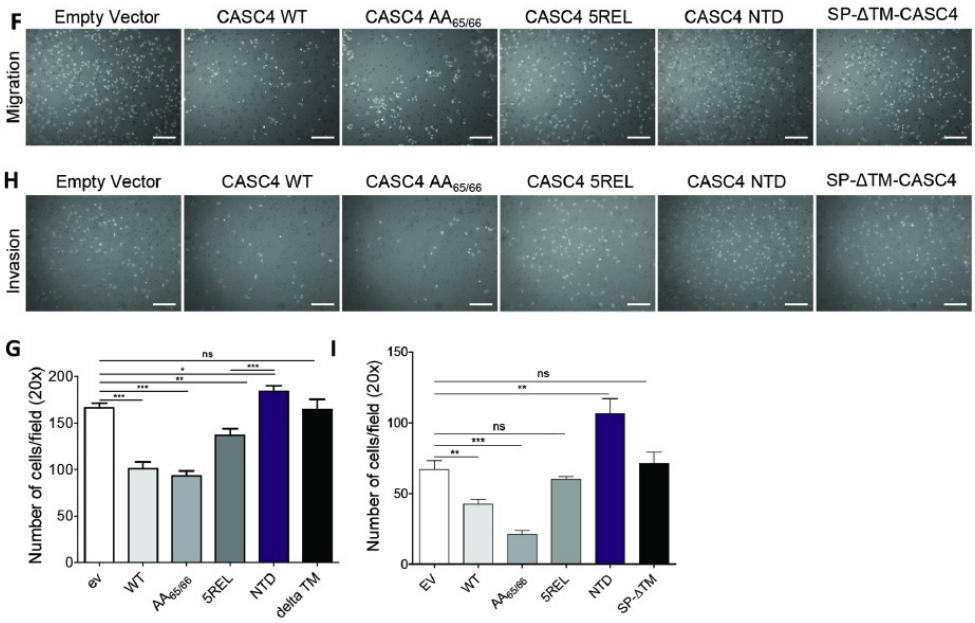

Figure 2.7. CASC4 N-terminal domain (NTD) induces podosome-like structures.
(A-B) Immunofluorescence analysis and quantification of MDA-MB-231 stable cells stained for phalloidin (F-actin; white labeling) or tyrosine kinase substrate 5 (TKS5; green labeling). C) Schematic representation of CASC4 truncated mutant (NTD) with a 3Xflag in N-terminal and SP-ΔTM-CASC4 with a V5 in C-terminal. The blue circles are depicting potential N-glycosylation sites and the white circles are depicting O-glycosylation sites. D) Western blot analysis of cell lysates and media from MDA-MB-231 cells transiently transfected with different CASC4 constructs. E) Immunofluorescence analysis of transiently transfected MDA-MB-231 cells stained for phalloidin (F-actin; white labeling), tyrosine kinase substrate 5 TKS5 (green labeling) and nucleus stained with DAPI (blue labeling). Yellow arrows represent colocalization between F-actin and TKS5. The ability of transiently transfected MDA-MB-231 cells to migrate (6h) (E-F) or invade (16h) (G-H) was assessed by counting the number of cells stained with DAPI on the underside of a polycarbonate membrane under a phase contrast microscope (20x).These results are representative of at least three independent experiments. Error bars indicate averaged values ± standard error of the mean (SEM). P values: *, $p \leq 0.05$, **, $p < 0.01$, ***, $p \leq 0.001$ n.s : not significant (Student's *t*-test). Scale: 10µm.

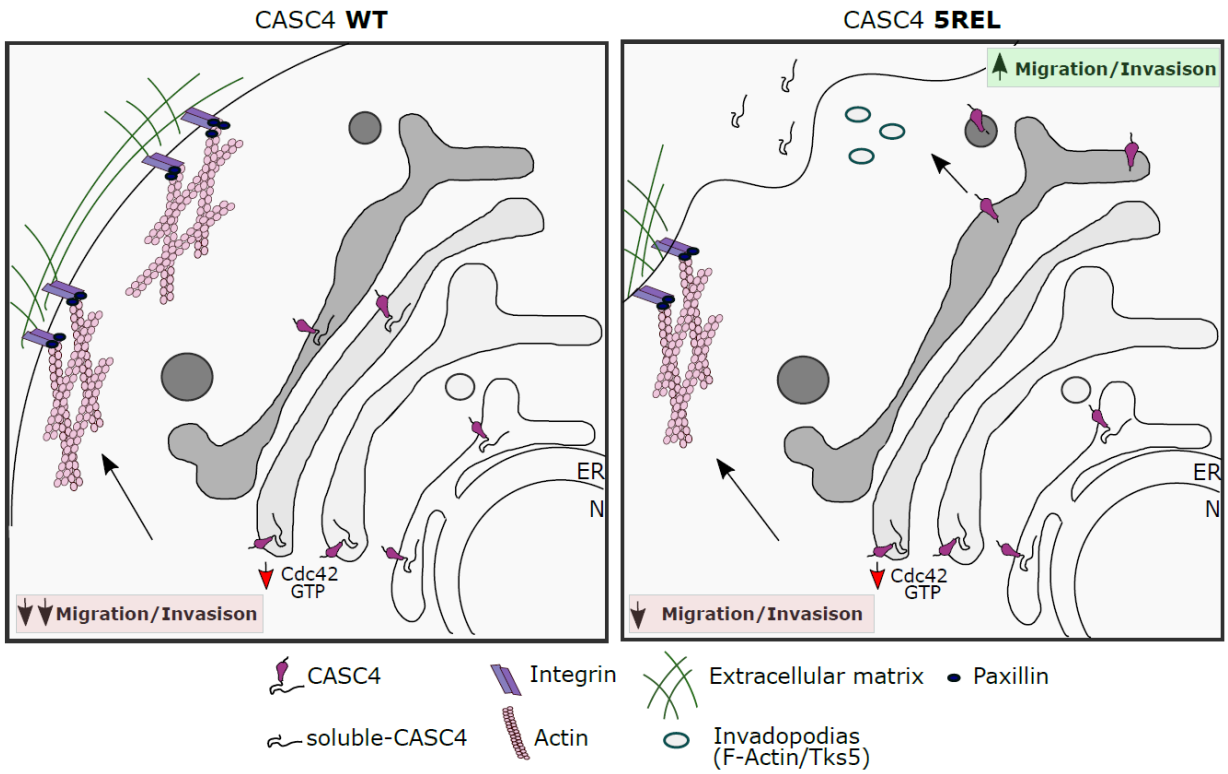

Figure 2.8. Schematic representation of CASC4 biological functions along the secretory pathway.

Depicted are full-length CASC4 WT in the early secretory pathway interfering with the Rho GTPase Cdc42-GTP activation. The decrease in Cdc42 activation results in increased paxillin positive staining focal adhesions which slows down migration (left panel). The dual roles for CASC4 5REL functions are depicted as the protein remain full-length (CASC4 WT) in the early secretory pathway, but is shed trafficking along the secretory pathway which generates membrane-bound N-terminal domain (NTD) which induces the formation of podosome-like structures (right panel) and increases migration, which results in an intermediate migratory phenotype.

Table 2.1: Glycopeptides significantly enriched from the spent media of HEK293 cells overexpressing human proprotein convertase 7.

Protein ID	Gene ID	Protein Name	Ratio glycopeptide intensity PC7/EV	N-linked glycopeptide identified
P02786	TFRC	Transferrin receptor protein 1	52.81106	KDFEDLYTPVNGSIVIVR
P02786	TFRC	Transferrin receptor protein 1	29.93287	KQNNGAFNETLFR
Q13433	SLC39A6	Zinc transporter ZIP6	7.908147	YGENNSLSVEGFR
Q13433	SLC39A6	Zinc transporter ZIP6	2.976814	KTNESVSEPR
Q16549	PCSK7	Proprotein convertase subtilisin/kexin type 7	NFEVS	CAGEIAAVPNNSFCAVGVAYGSR
Q16549	PCSK7	Proprotein convertase subtilisin/kexin type 7	NFEVS	DINVTGVWERNVTGR
Q16549	PCSK7	Proprotein convertase subtilisin/kexin type 7	NFEVS	DINVTGVWERNVTGR
P49641	MAN2A2	Alpha-mannosidase 2x	12.52052	NLGFNCTTSQGK
P55268	LAMB2	Laminin subunit beta-2	4.758911	NTSAASTAQLVEATEELRR
A2RU67	KIAA1467	Uncharacterized protein KIAA1467	15.38932	APDSNCSNLLITTR
Q96MM7	HS6ST2	Heparan-sulfate 6-O-sulfotransferase 2	3.47587	YNFTRGDLLR
Q9UK76	HN1	Hematological and neurological expressed 1 protein	NFEVS	GVDPNSRNSSR
Q9UK76	HN1	Hematological and neurological expressed 1 protein	NFEVS	VLRPPGGGSNFSLGFDEPTEQPVRK
Q8WXG9	GPR98	G-protein coupled receptor 98	0.125277	ISEENTTAR
P10253	GAA	Lysosomal alpha-glucosidase	3.670205	NNTIVNELVR
O75976	CPD	Carboxypeptidase D	7.709885	NNSNNFDLNR
Q9H8M5	CNNM2	Metal transporter CNNM2	11.78985	VYGQNINNETWSR
Q6P4E1	CASC4	Protein CASC4	9.046698	QEDQLQDYRKNNTYLVK
P18850	ATF6	Cyclic AMP-dependent transcription factor ATF-6 alpha	NFEVS	DHLLLPATTHNKTTRPK

NFEV: Glycopeptide not identified from HEK293 spent media transfected with empty vector as control and significantly different from media from PC7 expressing cells. Significance defined as $p<0.05$ by Student's t-Test.

Table 2.2: Glycopeptides significantly enriched from the spent media of HuH7 cells overexpressing human proprotein convertase 7.

Protein ID	Gene ID	Protein Name	Ratio glyco-peptide intensity PC7/EV	N-linked glycopeptides identified
P78536	ADAM17	Disintegrin and metalloproteinase domain-containing protein 17	4.92	SEDIKNVSR
Q15758	ASCT2	Sodium-dependent neutral amino acid transporter type 2	5.79	SYSTTYEERNITGTR
Q15904	ATP6AP1	Protein XAP-3	5.54	EIKINASIPAIIIIR
Q8NBJ4	C9orf155	Golgi membrane protein 1	2.04	IYQDEKAVIVNNITTGER
G5E934	CASC4	Cancer susceptibility candidate gene 4 protein	NFEVS	QEDQIQDYRKNNTYIVK
Q9UBG0	CLEC13E	C-type lectin domain family 13 member E	0.69	WNDSPCNQSIPSICK
O75976	CPD	Carboxypeptidase D	2.9	IINTTDVYIIPSINPDGFER
O75976	CPD	Carboxypeptidase D	2.2	GYNPVTKNVTVK
A9R9N7	DADB-123	Major histocompatibility complex, class I, A	3.25	GYYNQSEAGSHTVQR
O43909	EXTL1L	Exostosin-like 3	NFEVS	KSDTQNIIYNVSTGR
Q06828	FM	Collagen-binding 59 kDa protein	0.68	IYIDHNNITR
P10253	GAA	70 kDa lysosomal alpha-glucosidase	2.29	GVFITNETGQPIIGK
Q99988	GDF15	Growth/differentiation factor 15	1.21	IRANQSWEDSNTDIVPAPAVR
F6S8M0	GNS	Glucosamine-6-sulfatase	NFEVS	ASIITGKYPHNHHVVNNTIEGNCSSK
Q9Y4L1	GRP170	150 kDa oxygen-regulated protein	NFEVS	DKNGTRAEPPINASASDQGEK
E9PDY5	HS6ST2	Heparan-sulfate 6-O-sulfotransferase 2	NFEVS	FVPRYNFTRGDIIR
P10809	HSP60	60 kDa chaperonin	NFEVS	VTDAINATR
Q92626	KIAA0230	Melanoma-associated antigen MG50	13.04	QGEHISNSTSAFSTR
P11047	LAMB2	Laminin B2 chain	0.03	IQRVNNTISSQISR
Q13433	LIV1	Estrogen-regulated protein LIV-1	NFEVS	KTNESVSEPR
Q9H9K5	LP9056	Uncharacterized protein LP9056	0.86	AIINISK
Q16549	PCSK7	Subtilisin/kexin-like protease PC7	NFEVS	DINVTGVWER
Q16549	PCSK7	Subtilisin/kexin-like protease PC7	NFEVS	RSPGRDINVTGVWER
Q16549	PCSK7	Subtilisin/kexin-like protease PC7	NFEVS	SPGRDINVTGVWERNVTGR
Q16549	PCSK7	Subtilisin/kexin-like protease PC7	NFEVS	SPGRDINVTGVWER
P78395	MAPE	Melanoma antigen preferentially expressed in tumors	28.07	IPTIAKFSPYIGQMINIR
P08195-4	MDU1	4F2 cell-surface antigen heavy chain	5.08	DIENIKDASSFIAEWQNITK
P54802	NAGLU	Alpha-N-acetylglucosaminidase	0.68	SVYNCSGEACR
P47972	NPTX2	Neuronal pentraxin II	9.26	KVAEIEDEKSIIHNETSAHR
P02787	PRO1400	Beta-1 metal-binding globulin	2.82	IIRQQQHIFGSNVTDCSGNFCIFR
Q99523	SORT1	100 kDa NT receptor	NFEVS	DITDIINNTFIR
P02786	TFRC	Transferrin receptor protein 1	35.88	KQNNGAFNETIFR
P02786	TFRC	Transferrin receptor protein 1	NFEVS	DFEDIYTPVNGSIVIVR
P51884	LDC	Keratan sulfate proteoglycan lumican	NFEV	KLHINHNNLTESVGPLPK
P02786	TFRC	Transferrin receptor protein 1	NFEV	KDFEDLYTPVNGSIVIVR
P18850	ATF6	Activating transcription factor 6 alpha	NFEV	DHLLLPATTHNKTTRPK
Q9H8M5	ACDP2	Ancient conserved domain-containing protein 2	NFEV	VYGQNINNETWSR
Q96TA2	FTSH1	ATP-dependent metalloprotease FtsH1	NFEV	SVEIDNKNK
Q96J84-2	KIRREL	Kin of irregular chiasm-like protein 1	NFEV	IDGGPVILLQAGTPHNLTCR
O00461	GPP130	Golgi-localized phosphoprotein of 130 kDa	NFEV	KPDPAEQQNVTQVAHSPQGYNTAR
	/GIMPC			
E7ETH0	CFI	C3B/C4B inactivator	NFEV	SIPACVPWSPYIFQPNDTCIVSGWGR
G5E934	CASC4	Cancer susceptibility candidate gene 4 protein	NFEV	KNNTYLVK
P02787	PRO1400	Beta-1 metal-binding globulin	NFEV	CGLVPVLAENYNKSDNCEDTPEAGYFAIAVVK
P02786	TFRC	Transferrin receptor protein 1	NFEV	QNNGAFNETLFR
P23142-4	CTA-941F9	Fibulin 1	NFEV	CATPHGDNASIEATFVK

NFEV: Glycopeptide not identified from HuH7 spent media transfected with empty vector as control. NFEVS: Not found in EV and significant from PC7 spent media. Significance defined as $p<0.05$ by Student's t-Test

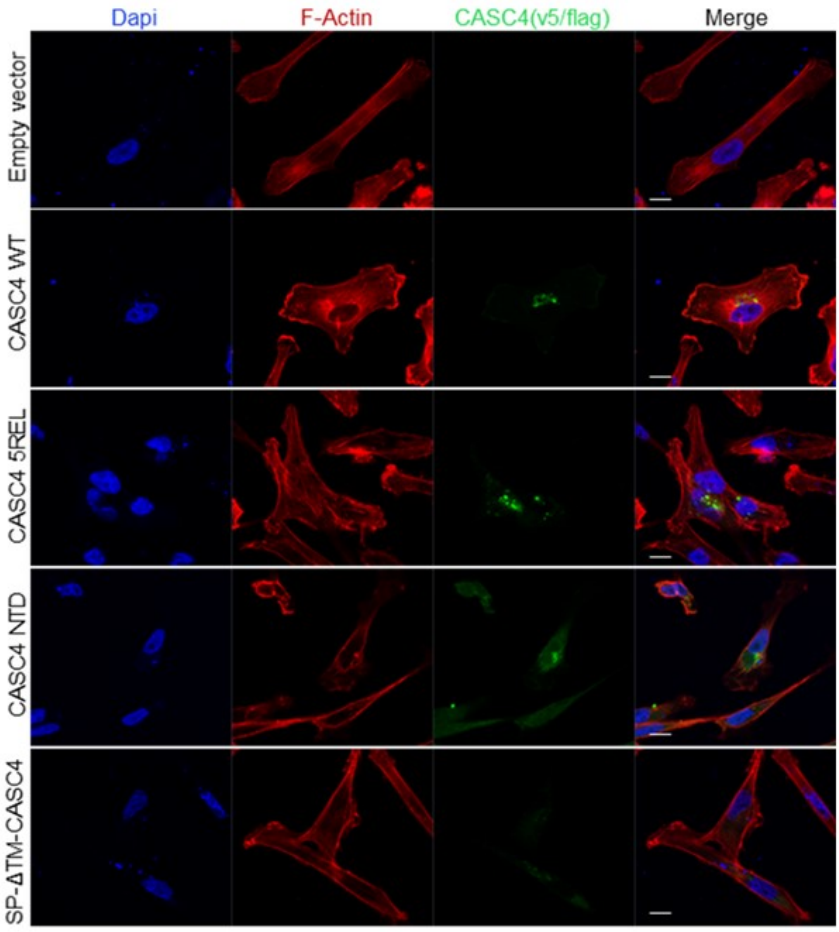

Supplemental Figure 2.1. CASC4-NTD and SP-ΔTM-CASC4 are well expressed in MDA-MB-231 cells.

Immunofluorescence analysis of transiently transfected MDA-MB-231 cells stained for phalloidin (F-actin; white labeling), CASC4 (V5 or Flag tags) (green labeling) and nucleus stained with DAPI (blue labeling). Scale: 10µm

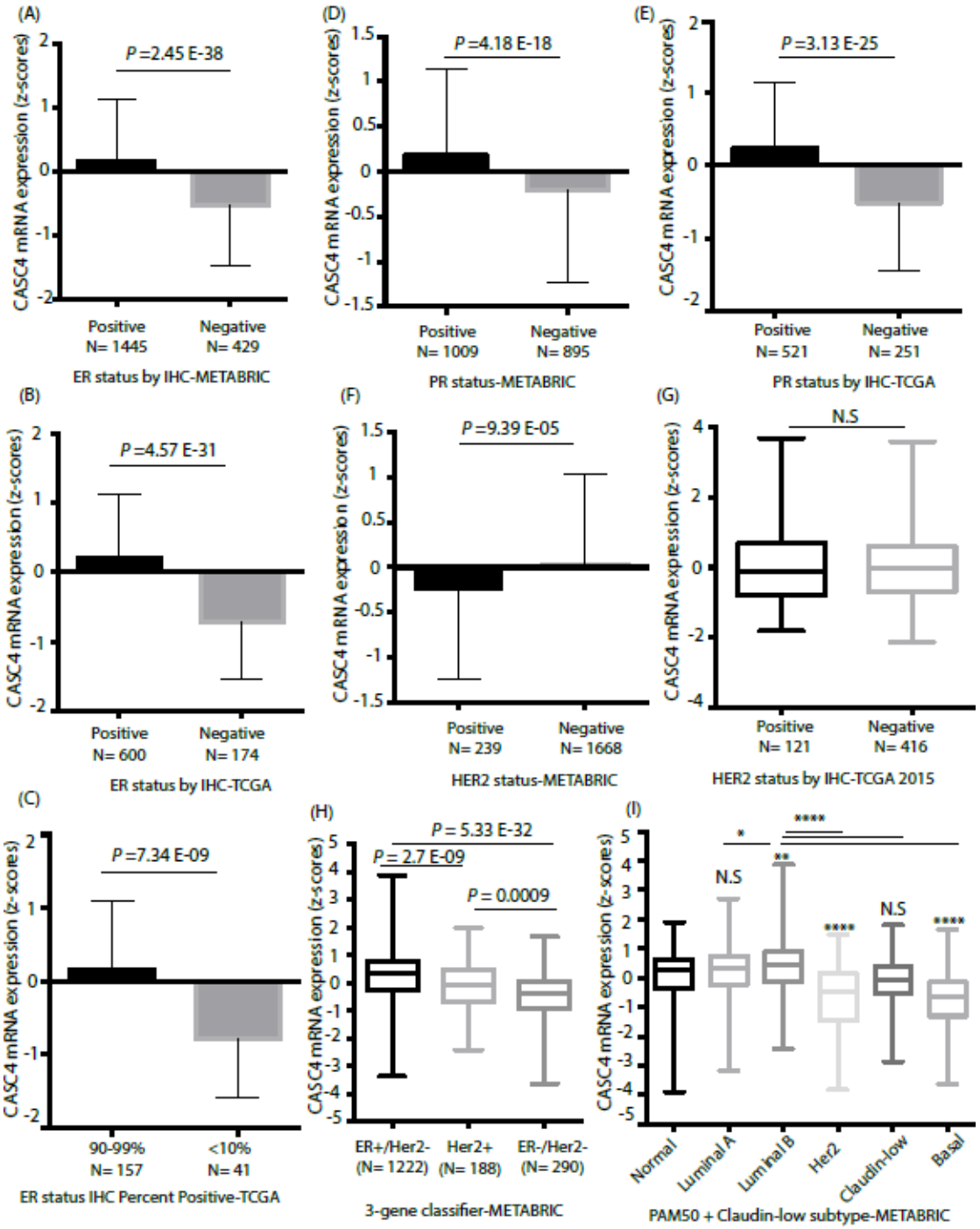

Supplemental Figure 2.2. METABRIC and TCGA patients' raw data.
Raw data (with samples IDs) used to investigate the correlation between CASC4 mRNA levels in METABRIC and TCGA patients' datasets. PR=Progesterone receptor, ER=Estrogen receptor.

http://canprovar2.zhang-lab.org/chr/chr11.php

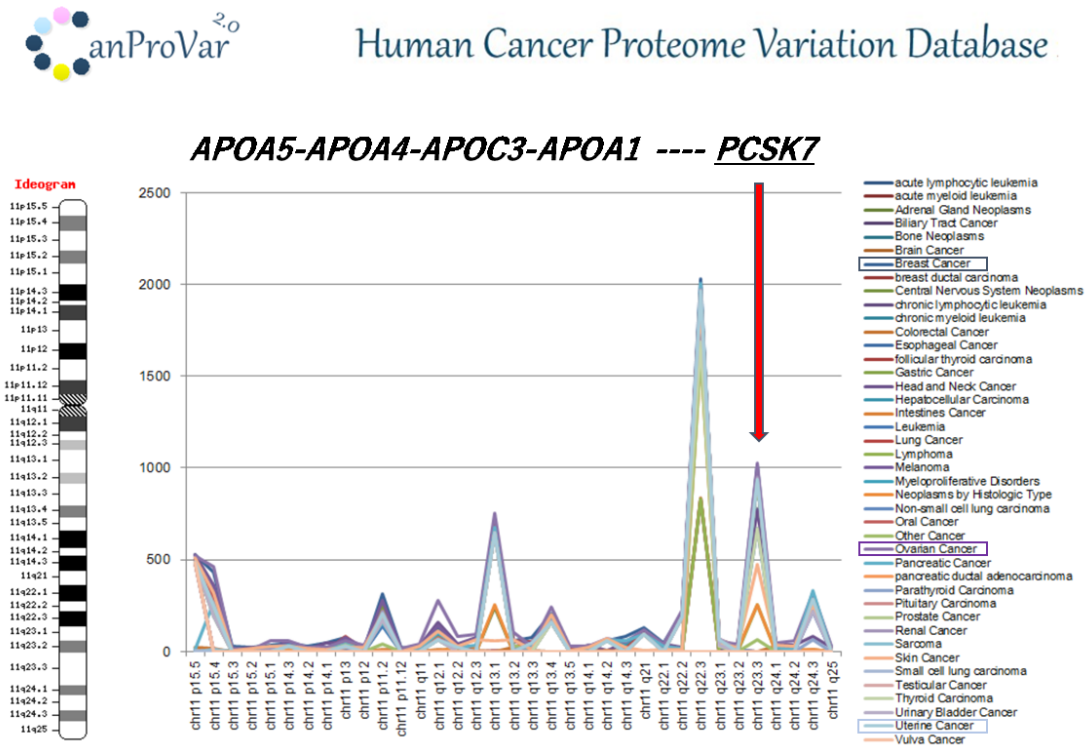

Supplemental Figure 2.3. Cancer locus PCSK7.
Map of the chromosome 11 with different cancer incidence, where PC7 is highlighted in ovarian, breast and uterine cancer and is located in close proximity with the apolipoprotein locus.

Supplemental Table 2.1. Oligonucleotides for RT-quantitative PCR.

Gene	Forward	Reverse
CASC4	GAAGAACCCTCAAGCAATCATATTC	CCTGCATCACCACCTCTTTTG
PCSK7	GGACCTACAGGCTTGTCATC	CCACTCATGGCACTCTCTAACA
Furin	CACCAGCGAAGCCAACAACT	TGCCATAGAGTACGAGGGTGAA

2.3.5 Discussion

The proprotein convertases play key roles in both health and disease states by cleavage of precursor proteins (440), which results in the bioactivation of proteins, but sometimes may also generate cleaved products endowed with novel functions (59, 477). While the roles of Furin in proliferative and infectious diseases have been extensively characterized (83, 210, 216, 448, 478), those of PC7 are barely defined (235, 447, 450). One of the specific functions of PC7 is the shedding of the human type-II TfR1 (235), resulting in the secretion of a circulating sTfR1 that correlates with iron deficiency (479). These data and those of the present study suggest that PC7 may shed several type-II transmembrane-proteins, and would not represent a rare phenomenon, but rather provide a mechanism to modulate their functions and possibly generate new ones.

A proteomic screen from the media of HuH7 cells identified three shed type-II transmembrane-proteins, TfR1, as well as CASC4 and GPP130. We demonstrated that only PC7 and Furin can shed CASC4 at $Arg_{66}\downarrow$ and GPP130 (*not shown*) in post-ER acidic compartments. This CASC4 cleavage generates an N-terminal membrane-bound fragment (NTD; aa 2-65) and a secreted C-terminal fragment starting at Asn_{67}. The only available information on CASC4 is its association with $HER2^{+}$ overexpression and its differential splicing in breast cancer (451, 452) and glioblastoma (416). Our METABRIC data indicated that patients with high *PCSK7* and high *CASC4* had significantly worse prognosis than those with high *CASC4* but low *PCSK7*. In addition, we demonstrated that endogenous shedding of CASC4 is only observed in triple negative breast cancer cells MDA-MB-231. We thus hypothesized that CASC4 and its shedding are relevant in breast cancer aggressiveness/metastasis. Initial evidence revealed that knockdown of CASC4 mRNA significantly increased cell migration and invasion, suggesting a protective role of CASC4.

To explore the functional consequences of CASC4 shedding, we generated three cells lines expressing either a control empty vector, CASC4-WT or CASC4-5REL. The data revealed that overexpressed CASC4 enhanced the number of focal adhesions, in part by blunting the activation of the Rho GTPase Cdc42, supporting its effect on the reduced migratory potential of these cells. It is not surprising that Cdc42 activity could be modulated by Golgi-localized CASC4 since Cdc42

localizes to the Golgi apparatus and interacts with regulators of cytoskeleton remodeling and centrosome organization (480). We further demonstrated that shedding of CASC4 into sCASC4 is a critical event that transforms the protective function of CASC4-WT into a pathogenic one due to the generation of the NTD (Figure 2.8). Since shedding likely occurs in the TGN (Furin) or endosomes (PC7), CASC4-5REL would remain as full length until it reaches these intracellular destinations, and would partially participate in reducing invasion in early Golgi compartments (Figure 2.8), like CASC4-WT. This may rationalize the intermediate invasion phenotype observed in cells expressing CASC4-5REL, which when shed later along the secretory pathway would generate an NTD that rather increases podosome formation, known to be associated with enhanced invasion (454, 455). More detailed studies are needed to define the underlying mechanism behind the activity of the NTD in enhancing the formation of podosome-like structures. Since we do not know the physiological function of CASC4, future work will also be needed to investigate the function of the luminal domain of this protein. Similar to other members of the GOLM1 family, CASC4 may act as a co-receptor, as reported for GOLM1/GP73 for the EGF receptor (481).

The fact that experimental expression of different forms of CASC4 (WT, $AA_{65/66}$ or 5REL) leads to different/opposing biological consequences in the context of breast cancer, suggests that this protein might have dual actions depending on the associated activity of PC7/Furin. Breast cancer can be categorized pathologically into three main categories: Estrogen/progesterone receptor (ER/PR) positive, $HER2^{+}$, or Triple-Negative Breast Cancer (TNBC). Interestingly, in two different clinical breast cancer datasets, METABRIC and TCGA, we found that CASC4 expression positively correlates with the ER/PR status (Supplemental Figure 2.2). Correlating the CASC4 mRNA levels to the different molecular subtypes of breast cancer by the PAM50 classification showed similarly that luminal tumors, that are usually ER/PR positive and have best prognosis, express the highest levels of CASC4 (Supplemental Figure 2.2). These evidences strongly pinpoint the significance of exploring the dual roles of CASC4 and its PC7/Furin-shed form in order to better understand the role of CASC4 in different breast cancer subtypes.

Interestingly, analysis of the genes implicated in cancer on chromosome 11, revealed that the locus 11q23.3 is associated with a high incidence of ovarian, breast and uterine cancer (human

cancer proteome database http://canprovar2.zhang-lab.org/chr/chr11.php). Coincidentally, this is the locus of *PCSK7* that resides close to the gene-cluster *APOA5/APOA4/APOC3/APOA1*, a region implicated in the regulation of lipoprotein metabolism (Supplemental Figure 2.3) (299).

In conclusion, our results provide a framework for deciphering the biological functions of CASC4 and more importantly suggest that inhibitors of Furin/PC7 may find clinical applications in breast and ovarian cancers (216, 440, 444).

2.3.6 Acknowledgments

This work was supported by a CIHR Foundation grant # 148363 (NGS), a CIHR Project grant # MOP-142425 to (JFC), a Canada Research Chairs in Precursor Proteolysis (NGS; # 950-231335) and a philanthropic Transat Chair in Breast Cancer Research (JFC). A.A.T and IEE are recipients of FRQS Doctoral studentships. SD and IEE were also supported by philanthropic studentships from Molson-Bombardier through the IRCM Foundation. The authors thank Mouna Derbali for cell culture assistance and Brigitte Mary for editorial help.

2.3.7 Conflict of interest

"The authors declare no conflict of interest"

Chapter III

Shedding of GPP130 by PC7 and Furin sheds light on a Golgi-resident protein with a unique trafficking pathway

(Manuscript *in preparation*)

3.1 Résumé:

Durant ce troisième chapitre nous nous intéresserons à l'étude de GPP130, un deuxième substrat de PC7 identifié dans notre analyse protéomique. Nous avons démontré que GPP130 est aussi clivé par PC7 et Furin mais au niveau des motifs H_{67}RSRLEK$_{73}$↓SL et K_{274}PTR$_{277}$↓EV dans les endosomes/TGN ou à la membrane plasmique. Récemment, GPP130 a été rapporté comme étant impliqué dans la prolifération cellulaire de cancers de la tête et du cou. Nos analyses provenant de la banque de données cBioPortal ont montré que le gène GPP130/GOLIM4 était surexprimé dans 35% des cas de cancer du poumon. Nous avons aussi montré qu'une réduction de GPP130 dans les cellules de cancer de poumon A549 augmente légèrement la prolifération cellulaire. Nous étudions actuellement l'hypothèse que GPP130 transporterait des cargos qui pourraient influencer la prolifération cellulaire.

3.2 Contributions to the chapter:

Conceptualization: Nabil G. Seidah and Stéphanie Duval

Performing experiments: Stéphanie Duval

Result analysis: Stéphanie Duval and Nabil G. Seidah

Writing of the manuscript: Stéphanie Duval

Supervision: Nabil G. Seidah

3.3 Manuscript #2

Shedding of GPP130 by PC7 and Furin sheds light on a Golgi-resident protein with a unique trafficking pathway

Stéphanie Duval[1] and Nabil G. Seidah[1]

1-Laboratory of Biochemical Neuroendocrinology, Clinical Research Institute of Montreal, QC, Canada.

3.3.1 Abstract:

GPP130, or Golgi phosphoprotein of 130 kDa, is a protein that was identified as a potential PC7 substrate from a proteomics screen performed previously. GPP130 is a type-II transmembrane protein with a luminal domain containing endosomal and Golgi-retrieval determinants enabling a unique trafficking route. GPP130 is predicted to be trafficking cargos, and most of the previous work is related to its binding and retrograde trafficking of the Shiga toxin. GPP130 was also recently reported to be implicated in cell cycle progression and cell proliferation in head and neck cancer cells. Our analysis from cBioPortal for Cancer Genomics has shown that the *GPP130/GOLIM4* gene is amplified in up to 35% of the patients with lung cancer. These first observations led us to use the A549 lung cancer cell lines to investigate GPP130 functions and to analyze how is the shedding by PC7/Furin affecting these functions. We first validated that GPP130 is indeed cleaved by PC7 and Furin at two different shedding sites on its luminal domain, at a first site within the motif **H**$_{67}$RSRLE**K**$_{73}$↓SL and at a second site **K**$_{274}$PT**R**$_{277}$↓EV, specific for Furin. We further showed that the shedding requires the formation of COPII-coated vesicles and occurs in acidic endosomes/*trans*-Golgi Network (TGN) and at the plasma membrane. Furthermore, we have preliminary results showing that GPP130 knockdown in A549 cells slightly increases cell proliferation. We have also showed proliferation disadvantage using different GPP130 mutant constructs. We are currently investigating the possibility of GPP130 to be carrying important cargos that would influence cell proliferation. In conclusion, our analysis from this new PC7 and Furin substrate is shedding light on a Golgi-resident protein with unknown

biological functions. Future work will help to decipher its involvement in diseases' progression, and how the shedding by PCs modulate its functions.

3.3.2 Introduction:

The proprotein convertases (PCs) are a family of nine serine secretory proteases implicated in multiple biological mechanisms, from development to viral infections (4). PCs are responsible for the cleavage and maturation of a wide variety of precursor proteins (4). The first seven PCs cleave (↓) precursor proteins at specific single or paired basic amino acid (aa) within the motif (R/K)-$(2X)_n$-(R/K)↓, where n = 0, 1, 2, or 3 spacer aa (4). In the clinic, therapies targeting the PCs have had multiple success (*i.e.* PCSK9 antibodies (320) or the FANG vaccine (226)), but the physiological roles of PC7, the seventh member of the family, are still obscure. Searching for new PC7 substrates, a quantitative proteomics screen for selective enrichment of N-glycosylated polypeptides secreted from hepatic HuH7 cells performed recently (482) have identified another interesting type-II transmembrane protein as potential PC7 substrate; Golgi Phosphoprotein of 130 kDa (GPP130/GOLIM4).

GPP130 is a Golgi protein that has a small cytosolic tail, a 20 amino acids (aa) transmembrane domain and a luminal domain containing features that dictate its trafficking route (241, 423). It was demonstrated that GPP130 is trafficking from the *cis*-Golgi to the plasma membrane and back to the *cis*-Golgi via the TGN38/46 bypass pathway (419, 421). Further investigations have demonstrated that GPP130 is binding the Shiga toxin in early endosomes and help the toxin to traffic back to the endoplasmic reticulum to exert its cytotoxic effect (430). In addition, manganese treatment was also shown to induce GPP130 oligomerization which in turn reroute GPP130 into multivesicular bodies (MVBs) before trafficking to lysosomes for degradation (431). Therefore, GPP130 have been described has a Golgi protein with a unique trafficking route that carries cargos within the secretory pathway. Recently, the *GPP130/GOLIM4* gene was connected to head and neck cancer in a study investigating downstream targets of stromal interaction molecule 1 (STM1), a calcium channel protein member of the Store-operated calcium entry (SOCE), a pathway activated upon reduction in intracellular endoplasmic reticulum Ca^{2+} (483). In this former study, GPP130 expression was shown to be higher in head and neck cancer cells and

it was suggested as a potential downstream target of STM1 (435). Also, Bai *et al.* showed that GPP130 is implicated in cell cycle progression and cell proliferation, by modulating the expression levels of MDM2 and CDK6, in head and neck cancer cells (435). In line with these observations, our analysis from cBioPortal for Cancer Genomics database have shown that the GPP130 gene is amplified in up to 35% of the patients with lung cancer and ~10% in head and neck cancer patients.

We have first investigated the cleavage of GPP130 by PCs in HEK293 cells, where we showed that both PC7 and Furin are cleaving GPP130 at two distinct cleavage sites H_{67}RSRLEK$_{73}$↓SL and at a second site K$_{274}$PTR$_{277}$↓EV, specific for Furin on its luminal domain, releasing two different molecular weight fragments into the media. Also, we characterized the intracellular localization of the cleavage and identified the PC7/Furin cleavage site to be in acidic endosome or TGN, and the Furin-specific site to possibly be at the plasma membrane. Finally, we tested for cell proliferation as shown previously in head and neck cancer cells and we showed a moderate increase in cell proliferation when silencing GPP130 in lung cancer cells. Also, we investigated the consequences of GPP130 cleavage on cell proliferation and showed that the generation of GPP130 secreted luminal domain is inducing a proliferation disadvantage in A549 lung cancer cells.

In conclusion, we showed that GPP130 is a Golgi-localized protein that is cleaved and shed by two proprotein convertases PC7 and Furin in acidic compartments and possibly at the plasma membrane. GPP130's cleavage by PCs could have consequences on cargo binding and consequently be beneficial or detrimental during cancer progression and needs to be further investigated.

3.3.3 Results

3.3.3.1 GPP130 is cleaved and shed by PC7 and Furin

Using a mass spectrometry approach consisting of selective enrichment of N-glycosylated secreted polypeptides performed previously to define novel PC7 substrates (482) our group recently identified a type-II transmembrane protein, GPP130 (Figure 3.1A) as a potential

candidate. In this current study, we are investigating the functional relevance of GPP130 shedding by PC7. To do so, we first validated that GPP130 is processed by PC7 in HEK293 cells overexpressing cDNAs coding for GPP130 with a V5 tag on its C-terminal (Figure 3.1A), PC7, or an empty vector control plasmid (Figure 3.1B). Western blot (WB) analyses revealed that GPP130 is cleaved and shed in the media by PC7 since we observed the release of a ~ 100 kDa fragment in the media in presence of PC7 when using an antibody targeting the V5 tag on its luminal domain, but not in the control cells expressing cDNAs coding for empty vector (Figure 3.1B). In addition, overexpression in HEK293 cells of cDNAs coding for GPP130 with all the basic aa specific PCs (Furin, PC5A, PC5B, PACE4 and PC7), or empty vector control revealed that not only PC7, but also Furin is able to cleave and shed GPP130 into the media (Figure 3.1C). Interestingly, Furin is cleaving GPP130 at two different sites within its luminal domain, since two distinct fragments of different molecular weights ~ 100 kDa and ~75 kDa are detectable in the media (Figure 3.1C).

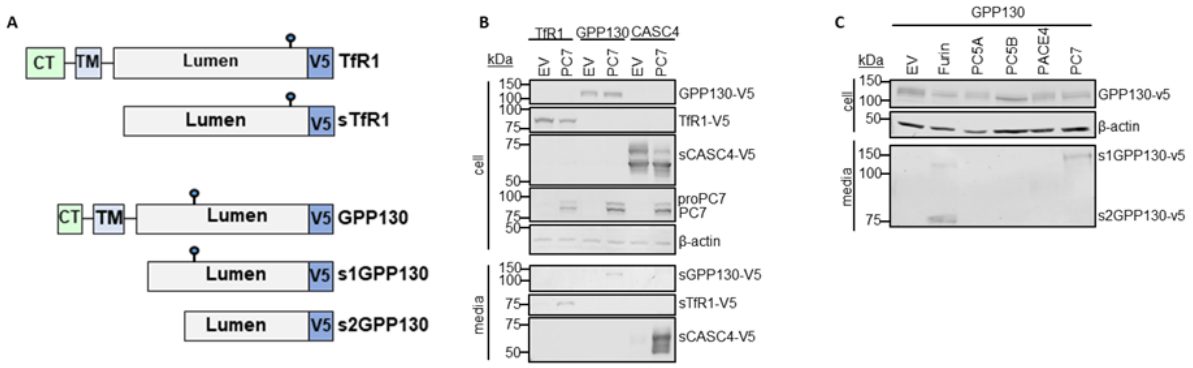

Figure 3.1. PC7 and Furin cleave GPP130.
A) Schematic representation of human transferrin receptor 1 (TfR1) and Golgi Phosphoprotein of 130 kDa (GPP130) identified in the mass spectrometry analysis. Depicted are the cytosolic tail (CT), the transmembrane domain (TM), the luminal domain and the C-terminal V5-tag. The blue circle is depicting a potential N-glycosylation site. B) Western blot analysis of cell lysates and media from HEK293 cells expressing TfR1-V5, GPP130-V5 or CASC4-V5, with either pIRES-empty vector (EV) or human PC7. C) Western blot analysis of cell lysates and media from HEK293 cells expressing GPP130-V5 with all the basic aa PCs or pIRES-empty vector. These results are representative of three independent experiments.

To better understand the trafficking of GPP130, by immunofluorescence analysis we demonstrated that GPP130 colocalizes mainly within the TGN marker Golgin-97, and to a smaller proportion colocalizes with early endosome antigen 1 marker (EEA1), the endoplasmic reticulum

marker calnexin and the plasma membrane marker low density lipoprotein receptor (LDLR) (Figure 3.2), when overexpressed in HeLa cells. These results are coherent with previous publications demonstrating that PC7 and Furin activities are mostly occurring in the TGN and/or endosomal-like structures (235, 238, 239).

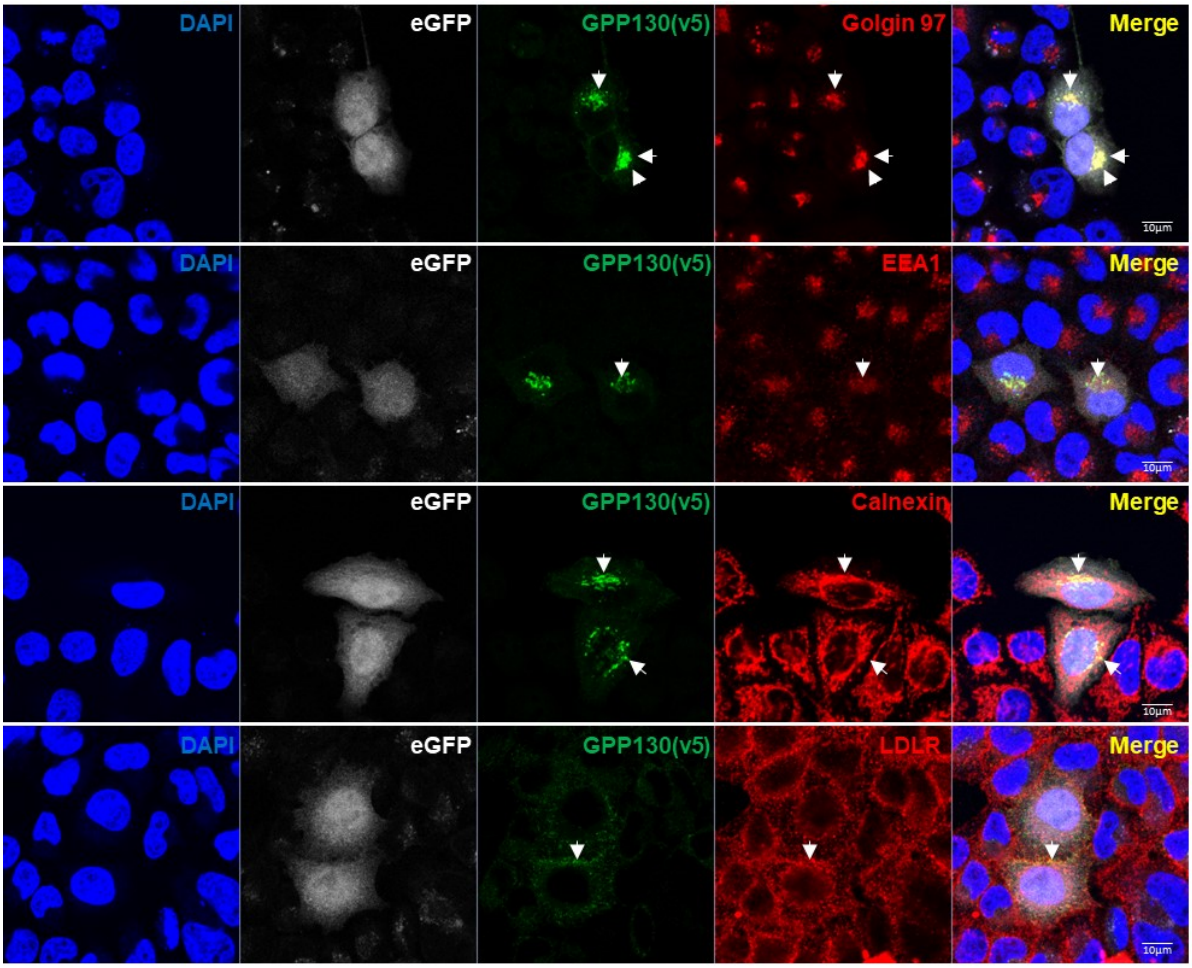

Figure 3.2. GPP130 is localized primarily in the TGN when overexpressed in HeLa cells. Immunofluorescence analysis of permeabilized HeLa cells overexpressing human GPP130-V5 colocalizing (white arrows) with TGN marker (Golgin-97), early endosome marker (EEA1), endoplasmic reticulum marker (calnexin) and plasma membrane marker low density lipoprotein receptor (LDLR) (non-permeabilized condition). These results are representative of three independent experiments. Scale: 10µm

3.3.3.2 Identification of GPP130 shedding sites by PC7 and Furin

To identify GPP130 cleavage sites we replaced arginines or lysines by alanines within potential consensus cleavage motifs (R/K)-X_n-(R/K)↓ using site-directed mutagenesis and assessed the

cleavage activity of GPP130 by analysing its release in the media. Western blot analysis of HEK293 cells overexpressing cDNAs coding for GPP130 WT, its mutant forms (H67A, R68A, R70A, K73A, R148A, K274A or R277A) or an empty vector control, we demonstrated that the R68A and R70A mutants are resistant for PC7 shedding and that residues from H67A to K73A are resistant to Furin shedding within the first motif **H**$_{67}$**R**S**R**LE**K**$_{73}$ (s1-site) (Figures 3.3A-B). Also, while the other mutants did not affect PC7 shedding, the mutants K274A and R277A were resistant for Furin second shedding (s2-site) (Figures 3.3A, B). These results demonstrated that GPP130 is cleaved at **HR**S**R**$_{70}$↓ by both PC7 and Furin, but only Furin cleaves GPP130 at the **K**PT**R**$_{277}$↓EV site (Figure 3.3B). To further emphasis that these are the cleavage sites, we generated mutant proteins harboring an optimized PC recognition site (440) RRRR$_{70}$EL (called 4REL). WB analysis demonstrated that this motif is indeed the cleavage site because the expression in HEK293 cells of cDNAs coding for the GPP130-4REL mutant generated a soluble form of the protein in the media, even when coexpressed with empty vector control, at the same molecular weight then the WT construct coexpressed with PC7 or Furin (Figure 3.3C). Accordingly, the expression of the R70A mutant generated the shedding at only the second site (the Furin cleavage s2 site) in the media when overexpressed with either PC7 or Furin (Figures 3.3B, C).

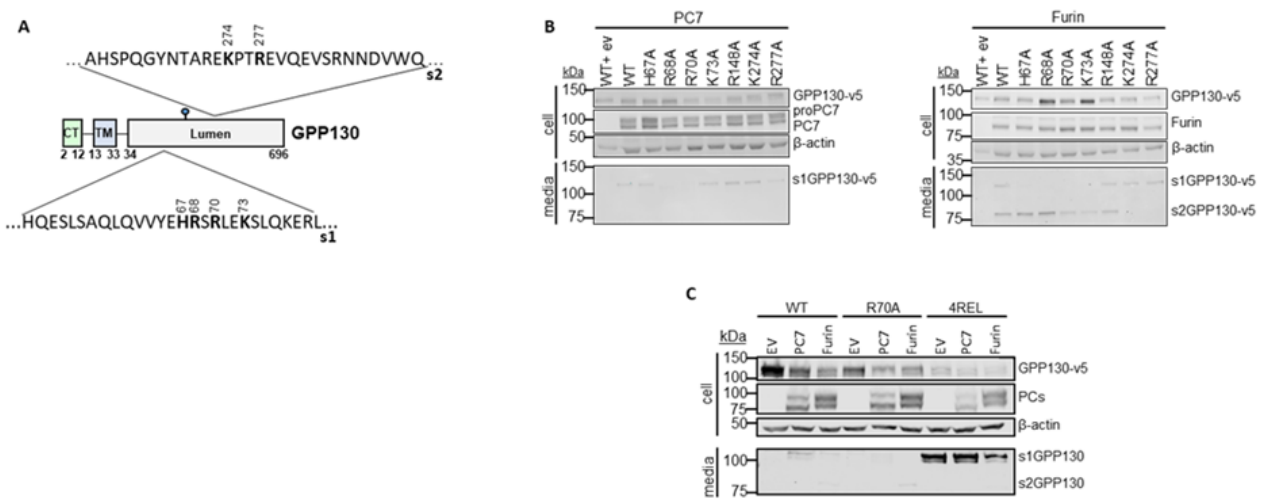

Figure 3.3. GPP130 cleavage by PC7 and Furin occurs at HRSR$_{70}$↓LE and solely at KPTR$_{277}$↓EV for Furin.

A) Schematic representation of GPP130 cleavage motifs and released fragments. B) Western blot analysis of cell lysates and media from HEK293 cells overexpressing GPP130-V5 WT and different point mutation (H67A, R68A, R70A, K73A, R148A, K274A or R277A), with human PC7, human Furin or with pIRES-empty vector (EV). C) Western blot analysis and quantifications of cell lysates and media from HEK293 cells overexpressing GPP130-V5 WT, GPP130 4REL (an optimally cleaved mutant) or GPP130 R70A (a PC non-cleavable mutant) coexpressed with human PC7, human Furin or with pIRES-empty vector. These results are representative of three independent experiments.

3.3.3.3 GPP130 is cleaved in post-ER acidic compartment

In order to determine in which cellular compartments GPP130 is cleaved by PC7 and Furin, we took advantage of different inhibitors and mutant proteins. In HEK293 cells, WB analysis showed that the shedding of GPP130 by PC7 and Furin was abrogated when treated with Brefeldin A (BFA) (Figure 3.4A), an inhibitor that blocks the transport of proteins from the ER to the *cis*-Golgi (470). Shedding was also inhibited when we overexpressed PC7 or Furin in combination with cDNAS coding for the dominant negative Sar1p (H79G) mutant protein (Figure 3.4B), a GTP-restricted mutant that blocks COPII vesicles formation (484). It is interesting to note that GPP130 intracellular levels are affected by both BFA treatment and the coexpression of the Sar1p (H79G) mutant. Indeed, we can observe an increase in intracellular protein levels in these two conditions (Figures 3.4A-B), suggesting that these conditions are blocking the 'normal' degradative route taken by GPP130 when overexpressed in cells. We next used the alkalizing agent ammonium chloride (NH_4Cl) which blocks the acidification of intracellular compartments to test if the

shedding was occurring in acidic pH compartments as previously described (235). Accordingly, treatment of HEK293 cells with NH_4Cl prevented GPP130 shedding (on the first shedding site s1) by PC7 and Furin of into the media (Figure 3.4C), suggesting that the first shedding site occurs in TGN or endosomes and that the second cleavage site is possibly occurring at the plasma membrane. Accordingly, to investigate possible cleavage at the plasma membrane, and because Furin (158, 238) and PC7 (129, 239) also traffic to the plasma membrane, we used the cell permeable pan-PC general inhibitor RVKR-cmk, and the non cell-permeable inhibitor hexapeptide $(D\text{-}Arg)_6$ (D6R). The data demonstrated that treatment with RVKR-cmk abolished almost completely the first shedding site by both PC7 and Furin (Figure 3.4D), emphasising that the processing is PC-specific. On the other hand, D6R treatment failed in preventing the first shedding but reduced the cleavage efficiency of the second site by Furin (Figure 3.4D), suggesting that Furin sheds GPP130 at the plasma membrane. Taken together these data suggest that GPP130 is cleaved in post-ER compartments, acidic TGN or endosomes, and at the plasma membrane for Furin second cleavage site (s2).

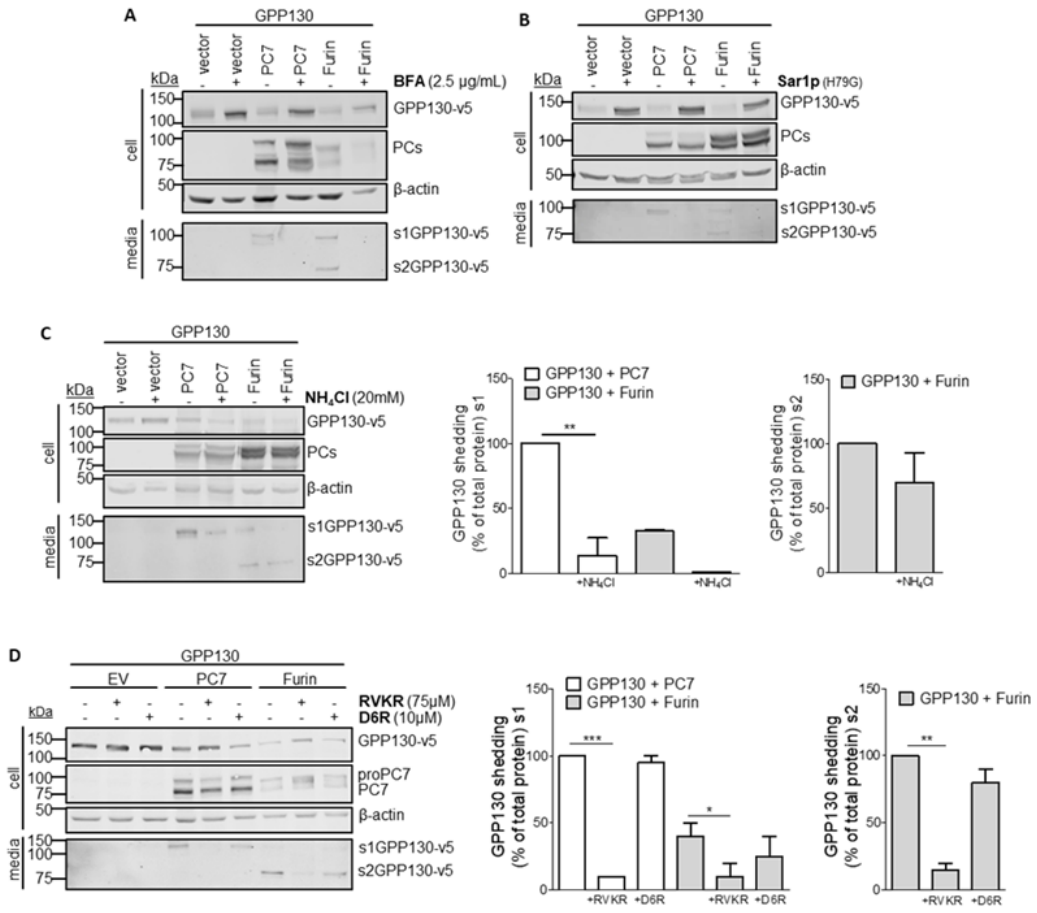

Figure 3.4. GPP130 is cleaved in acidic compartments by both PC7 and Furin, and at the plasma membrane by Furin only.

A) Western blot analysis of cell lysates and media from HEK293 cells overexpressing GPP130-V5 WT with human PC7, human Furin or with pIRES-empty vector (Vector) and treated with Brefeldin A (BFA) (2.5µg/mL). B) Western blot analysis of cell lysates and media from HEK293 cells overexpressing GPP130-V5 WT, pIRES-empty vector or Sar1P-(H79G) with human PC7 or human Furin. C) Western blot analysis of cells lysates and media from HEK293 cells overexpressing GPP130-V5 WT, with human PC7, human Furin or with pIRES-empty vector treated with NH4Cl (20mM). D) Western blot analysis of cells lysates and media from HEK293 cells overexpressing GPP130-V5 WT, with human PC7, human Furin or with pIRES-empty vector treated with RVKR-cmk (75µM) or D6R (10µM). Means +/- S.E.M. are represented. These results are representative of three independent experiments. *, p <0.1 **, p < 0.01; ***, p < 0.001 (Student's t test).

3.3.3.4 GPP130 rerouting to multivesicular bodies (MVB)/lysosomes with manganese abrogates s1 cleavage and induces differential cleavages by PC7 and Furin

Manganese treatment induces GPP130 oligomerization, rerouting to MVBs and subsequent degradation in lysosomes (431). We next sought to investigate if manganese treatment would hamper subcellular localization of GPP130 with PC7 and Furin and therefore interfere with its shedding. In HEK293 cells overexpressing cDNA coding for GPP130 and empty vector, we showed that manganese treatment for 18 hours induces GPP130 degradation (Figure 3.5), in line with previous observations (431). We also showed that the s1 cleavage for both PC7 and Furin is impaired when treated with manganese (Figure 3.5), as we no longer detect the s1 cleavage fragment in the media when overexpressing cDNAs coding for GPP130, PC7 and Furin and followed by a manganese treatment for 18 hours. Surprisingly, manganese treatment also led to the release of shed GPP130 of different molecular weights that were not previously observed when overexpressed with PC7 or Furin (Figure 3.1) and in a more prominent manner in cells expressing cDNAs coding for PC7 (Figure 3.5). Indeed, we observed the generation of a ~75kDa in cells coexpressing GPP130 and PC7 when treated with manganese, a cleaved fragment not observed in untreated cells (Figure 3.5). We also observed the generation of smaller fragments in cells overexpressing Furin and treated with manganese (Figure 3.5), taken together these results indicate a possible rerouting of GPP130 into a cellular compartment more favorable for GPP130 shedding by PCs, and leading to other possible cleavages.

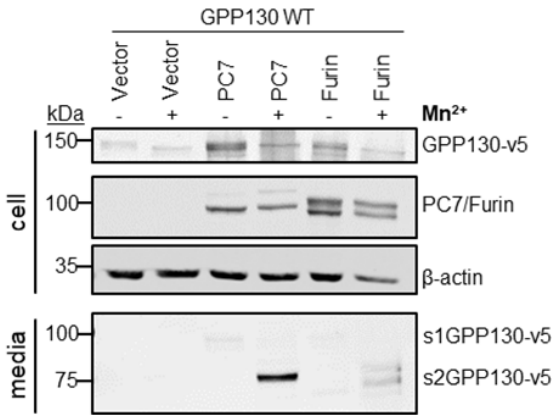

Figure 3.5. Treatment with manganese alters GPP130 s1 cleavage by PCs.
A) Western blot analysis of cell lysates and media from HEK293 cells overexpressing GPP130-v5 WT with human PC7, human Furin or with pIRES-empty vector (Vector) and treated with manganese (Mn2+) (250 µM). These results are representative of three independent experiments.

3.3.3.5 GPP130 influences cell proliferation in lung cancer cells

The *GOLIM4/GPP130* gene was recently demonstrated to be important in cell proliferation via the modulation of key regulators of the cell cycle in head and neck cancer cells (435). We therefore wanted to investigate if GPP130 shedding reported in this current study could also influence cell proliferation. We have assessed the genomics database (cBioPortal for Cancer Genomics) and noted that the *GOLIM4/GPP130* gene is amplified up to ~35% in the lung cancer patients and up to ~10% in head and neck cancer patients (Figure 3.6A). In accord with this observation we decided to continue our analysis using the lung cancer cells A549 to perform cell proliferation assay and cellular apoptosis analysis. Our results showed that GPP130 silencing using siRNA against GPP130 is increasing proliferation of lung cancer cells, although not significantly (Figure 3.6B). On the other hand, we cannot exclude possible off-target effects caused by the siRNAs targeting GPP130, therefore proper control such as a rescue experiment, where GPP130 would be re-introduced, would demonstrate that this effect is due specifically to the GPP130 silencing. Coherent with the previous observation, we showed a reduction of ~50% of cell death, marked by a decrease in Annexin V/propidium iodide double positive staining in cells silenced for GPP130 (Figure 3.6C). We next wanted to assess if the shedding by PCs could affect cell proliferation so we coexpressed cDNAs coding for GPP130 WT, a mutant uncleavable

GPP130 R70A (at the s1 site), an optimally cleaved mutant GPP130 4REL, or a secreted luminal domain protein SP-ΔTM-GPP130 containing a PCSK9 signal peptide (102) to mimic the secreted fragment generated by PC7 and Furin shedding (Figure 3.7A), and confirmed the transfection efficiency (Figure 3.7B). Our results showed that the secreted SP-ΔTM-GPP130 and the non-cleavable form GPP130 R70A are decreasing cell proliferation (Figure 3.7C) when overexpressed in A549 cells.

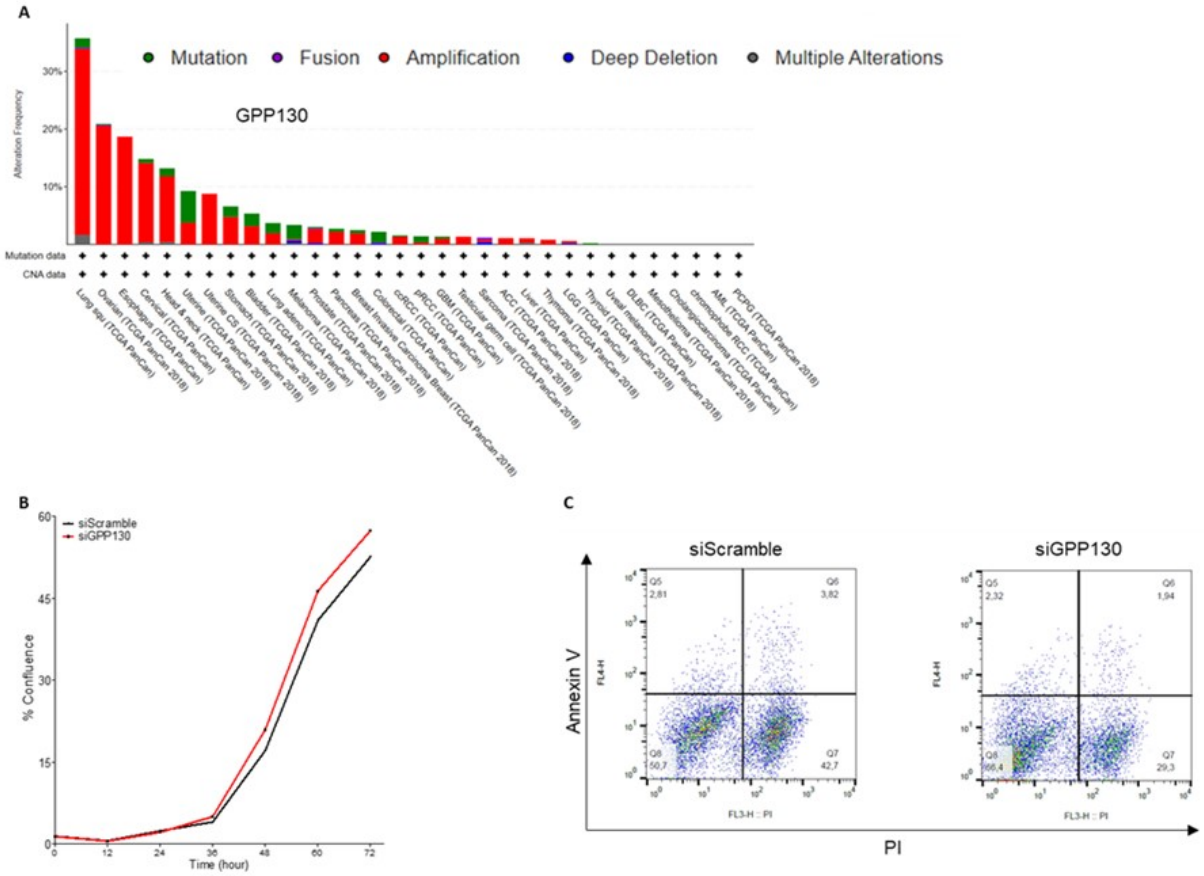

Figure 3.6. Knockdown of GPP130 increases cell proliferation and reduces apoptosis in lung cancer cells.
A) cBioPortal for Cancer Genomics analysis of patients' data with altered expression and reported mutations in the GPP130/GOLIM4 gene. B) Growth curve of proliferating A549 lung cancer cells following siRNA for GPP130 or Scramble control over a 3-day period. C) Representative graphs of cell death by flow cytometry analysis after Annexin-V/ Propidium iodide (PI) dual staining.

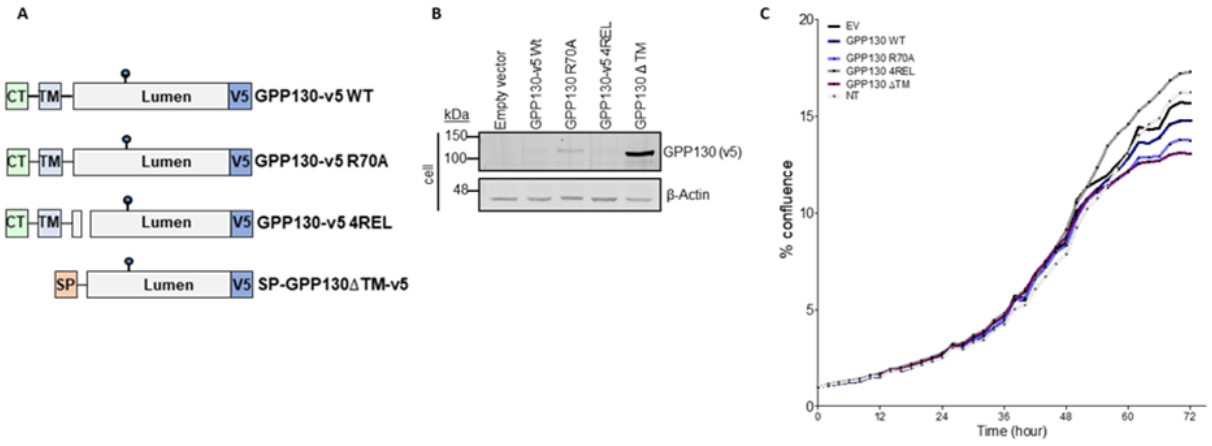

Figure 3.7. GPP130 shedding influences cell proliferation in lung cancer cells.

A) Schematic representation of various GPP130 mutant proteins. Depicted are the cytosolic tail (CT), the transmembrane domain (TM), the luminal domain, the signal peptide (SP) and the C-terminal V5-tag. The blue circle is depicting a potential N-glycosylation site. B) Western blot analyses of cell lysates from A549 cells not transfected (NT) or overexpressing GPP130 WT, GPP130 4REL (an optimally cleaved mutant), GPP130 R70A (a PC non-cleavable mutant), GPP130 ΔTM (a secreted luminal domain protein), or with pIRES-empty vector. C) Growth curve of proliferating A549 lung cancer cells (normalized) following overexpression with various mutant constructs over a 3-day period. These results are representative of three independent experiments.

Taken together, these results suggest that GPP130 may interfere with cell proliferation and that overexpression of some of its mutant (*i.e.* the luminal domain) is promoting a proliferative disadvantage. Investigating GPP130 cargos binding on its luminal domain will help to decipher GPP130's biological function.

3.3.4 Discussion

GPP130 is a Golgi resident protein with a unique trafficking pathway. Most of the literature covering GPP130 is related to its role in transporting the Shiga toxin intracellularly (485). In addition, investigations aiming at targeting GPP130 trafficking for therapeutic uses in the context of Shiga toxin infections have demonstrated that this protein is sensitive to manganese and can be rerouted for degradation following manganese treatments (431). Previous studies have therefore dissected its trafficking route and have demonstrated that GPP130's endosome to

lysosome trafficking is dependant on sortilin, a well characterized sorting protein (367) and the adaptor protein AP-5, a newly described adaptor protein (372, 433). These recent studies suggest that GPP130 is capable of trafficking cargos along the secretory pathway and possibly regulate cargo protein rerouting for degradation, but its biological roles and defined cargos remain unknown. Notably, a group interested in Ca^{2+} signaling during cancer formation has recently highlighted GPP130 as important during cell cycle progression and showed that knockdown of GPP130 severely impacts cell proliferation in head and neck cancer cells.

In this current study we demonstrated that GPP130 is shed by PC7 and Furin in acidic compartments, at two distinct sites on its luminal domain, which could have dramatic consequences on the efficient binding and transport of the Shiga toxin. Also, we demonstrated that treatment with manganese is promoting GPP130 degradation and blocks the first cleavage by PC7 and Furin in acidic compartments. We also showed that manganese treatment possibly allows GPP130 localization within endocytic compartments where it can encounter different active enzymes (maybe in MVBs) and be cleaved to generate multiple cleaved fragments of unknown biological impacts. Lastly, we have further investigated GPP130's role in cancer progression and we demonstrated that the shedding of GPP130 and its luminal domain secretion decreases cell proliferation in lung cancer cells. We suggest that future work should investigate GPP130 cargos, to better define how its knockdown or overexpression would influence signaling molecules or downstream targets. In line with this, recent reports investigating the role of GP73, a Golgi resident protein overexpressed in hepatocellular carcinomas (15), have shown that GP73 is trafficking a matrix metalloprotease (MMP-7) and helps in its secretion which increases the invasion potential in hepatocellular carcinoma cells (439). We thus hypothesize that GPP130 could be having similar types of cargos and that the shedding by PCs could interfere with cargo binding. Also, it is noteworthy to mention that GPP130 was originally identified in head and neck cancer as a protein downstream of a calcium channel protein STM1 (435), therefore its role in calcium and manganese homeostasis should be investigated. It would not be surprising to identify calcium or manganese transporters as potential GPP130 cargos which would be in line with GPP130 overexpression in various cancers and the known roles of calcium signaling in tumour formation (483, 486).

In conclusion, we showed for the first time that GPP130 is cleaved by PC7 and Furin, in a similar way than a very oncogenic protein GP73 (15, 438), and that this shedding could lead to the release of an ectodomain fragment which impedes cell proliferation. This original work is shedding light on a poorly characterized Golgi-resident protein and future work will help to elucidate its biological role, binding partners and how the PCs modulate its functions.

3.3.5 Material and methods

3.3.5.1 Plasmids

Human CASC4 WT (Thermo Scientific, Open Bioscience), GPP130 WT (Thermo Scientific, Open Bioscience) and its mutants (H67A, R68A, R70A, K73A, R148A, K274A or R277A, SP-GPP130ΔTM and 4REL) were subcloned, with a V5 tag at the C-terminus into pIRES2-EGFP vector (Clontech). All constructions (human transferrin receptor 1, human Furin, mouse PC5A, mouse PC5B, human PACE4, full-length human PC7, soluble rat PC7, soluble human PC7 and Sar1P-(H79G) were cloned in pIRES2-EGFP vector (Clontech).

3.3.5.2 Cell Culture, Transfections, and Cell Treatments

HEK293 cells were grown in Dulbecco's modified Eagle's medium (DMEM, Invitrogen) with 10% fetal bovine serum (FBS, Invitrogen), MDA-MB-231 cells were grown in Dulbecco's modified Eagle's medium (DMEM, Invitrogen) with 10% fetal bovine serum (FBS, Invitrogen), A549 cells were grown in Kaighn's Modification of Ham's F-12 Medium (F12K, Invitrogen) supplemented with 10% FBS, Invitrogen. All cells were maintained at 37°C under 5% CO. HEK293 cells were cotransfected with equimolar quantities (0,5µg) of each plasmid using Jetprime Polyplus, A549 cells were transfected with equimolar quantities (1,0µg) of each plasmid using FuGene HD, using manufacturer's instructions. MDA-MB-231 cells were transfected using GenJetTM In Vitro DNA Transfection Reagent for MDA-MB231 Cells (SignaGen Laboratories) with equimolar quantities of plasmids (1.5-2µg) using manufacturer’s instructions. At 24 hours post transfection, cells were washed in serum-free medium followed by an additional 20 hours alone or in incubation with 2,5µg/mL brefeldin A (BFA; Cabiochem), 20mM ammonium chloride (NH_4Cl; Sigma), or manganese (250µM, Baker Analyzed® ACS, J.T), cells and media were collected for western blot analysis.

3.3.5.3 Western blot analysis and antibodies

Cells were lysed in cold Radio-Immunoprecipitation Assay (RIPA) buffer (100mM Tris-HCL pH 8, 300mM NaCl, 0,2% SDS, 2% NP-40, 1% Na deoxycholate) containing protease inhibitors (Roche Applied Bioscience). Proteins were analysed by SDS-PAGE on 8-12% Tris-Glycine and transferred on a nitrocellulose membrane (GE Healthcare Life Science, No. 10600003) followed by 1h blocking in Li-Cor blocking buffer (Li-Cor) or in 5% milk in TBST-T. Membranes were then incubated with primary antibodies overnight. Proteins were visualized using mouse anti-V5 (1/2000, Invitrogen), rabbit anti-PC7 (1:10,000, homemade or 1:5000 Cell Signaling Technologies), Furin (1:5000, Invitrogen), rabbit anti β-actin (1:5,000, Sigma-Aldrich), or a horseradish peroxidase (HRP)-conjugated mAb V5 (1:10,000, Sigma-Aldrich). Bound primary antibodies were detected with corresponding species-specific fluorescent anti-mouse antibody 680 (Mandel) (1:10 000) or anti-rabbit Ab 800 (Mandel), and revealed using LiCor Bioscience, or with corresponding species-specific HRP-labelled secondary antibodies (1:10,000, Invitrogen) and revealed by enhanced chemiluminescence (ECL; Amersham). Quantifications were done using Image Studio Lite v.4.0 and Image J software (National Institutes of Health).

3.3.5.4 Microscopy Analysis and Antibodies

Cells were grown on coverslips and fixed with warm paraformaldehyde (4%) for 10 min and permeabilized with PBS 1X + Triton 0.1%. Followed permeabilization or PBS incubation, cells were stained for primary antibodies: anti EEA1 (Abcam), anti-Golgin 97 (Santa Cruz Biotechnology), anti-LDLR (R&D Systems), anti-calnexin (Abcam), or anti-V5 (Invitrogen) for 1 hour followed by incubation with fluorescent corresponding secondary antibodies for 1 hour in the dark. Coverslips were then mounted on microscope slide (Fisher Scientific) with ProLong Gold antifade with DAPI (Invitrogen) to stain for nucleus. Co-localization of fluorescently labeled protein was quantified with IMARIS analysis software (8.2.1) along with aXTension script named Colocalize Spots. We used the same approach as mention in Rajan et al. (456). Positive signals were found using the Imaris function spots from each fluorescent marker images. The spot diameter used was 1.2 µm with the same quality factor for each image. The Colocalize Spots script considers colocalization between two spots when their center to center distance is equal of inferior to 0.8 µm.

3.3.5.5 Cell proliferation and cell cycle analysis

For cell proliferation assays, cells were seeded into 6 well plate (Greiner) at low cellular density (200 000 cell/well) and place into the Incucyte imager for up to 72 hours. Images were taken every 2 hours to generate cellular density (% of confluence) and results were graphed over time. For cell cycle analysis, after 2 days in culture cells were washed with 1X PBS, fixed and permeabilized with ethanol 70% for 2h at room temperature. Following fixation, cells were treated with 2mg of ribonuclease-A (RNase-A; Sigma-Aldrich) in 900 µL of DPBS for 2 h at 37 °C. Finally, cells were stained with 100 µL of propidium iodide (PI) 0.2 mg/mL (Sigma-Aldrich), analysed with a FACScalibur system (BD Biosciences) and data were analyzed and calculated using FlowJo software.

3.3.5.6 Cell apoptosis analysis

Cell apoptosis was evaluated by Annexin V Apoptosis Detection Kit APC (88-8007, BD Bioscience). Cells were grown in culture for 2 days before they were harvested and stained according to manufacturer's protocol. Data acquisition and analysis were performed in a FACScalibur system (BD Biosciences) and data were analyzed using FlowJo software.

3.3.6 Acknowledgements:

This work was supported by a Canada Research Chairs in Precursor Proteolysis (NGS; # 950-231335). The authors thank Mouna Derbali for technical assistance with the cell culture.

Chapter IV

Are PC7 KO mice protected from diet-induced obesity anxiety-like behavior?

(Manuscript *in preparation*)

4.1 Résumé:

Durant le chapitre 4 de cette thèse nous avons poursuivi la caractérisation des souris PC7 KO dans le but de mieux comprendre les rôles physiologiques de PC7. Nous avons fait la connexion avec des études récentes montrant un effet anxiogène d'une alimentation riche en gras saturé chez la souris. Comme les souris PC7 KO ont précédemment montré un phénotype marqué par la diminution de l'anxiété, nous avons émis l'hypothèse que ces souris seraient protégées d'un effet anxiogène causé par l'obésité induite par l'alimentation. Nous avons montré que les souris PC7 KO ont une tendance à être moins affectées par la diète riche en gras saturé. Nous avons aussi montré que les souris PC7 ont une réponse déficiente face au stress.

4.2 Contributions to the chapter:

Conceptualization: Nabil Seidah, Stephanie Fulton and Stéphanie Duval

Performing experiments: Stéphanie Duval and Léa Décarie-Spain

Result analysis: Stéphanie Duval and Léa Décarie-Spain

Writing of the manuscript: Stéphanie Duval

Generating the mice colonies: Stéphanie Duval with the help of Annik Prat

Supervision: Nabil Seidah

4.3 Manuscript #3

Are PC7 KO mice protected from diet-induced obesity anxiety-like behavior?

Duval S.[1], Décarie-Spain L.[2], Fulton S.[2], Prat A.[1], and Seidah NG.[1]

1-Laboratory of Biochemical Neuroendocrinology, Clinical Research Institute of Montreal, QC, Canada.

2-Centre de Recherche du CHUM, Université de Montréal, Quebec, Canada; Montreal Diabetes Research Centre, Université de Montréal, Quebec, Canada; Department of Neuroscience, Université de Montréal, Quebec, Canada.

4.3.1 Abstract

In contrast to other proprotein convertases knockout (KO) mice that result in gross physical abnormalities and/or embryonical death, the PC7 KO mice are viable and do not present any flagrant physical defects, therefore making it challenging to define specific function. However, by performing behavioral phenotyping to further analyze the PC7 KO mice, our group have previously observed impaired episodic memory as well as an anxiolytic phenotype which were caused by the aberrant maturation of brain-derived neurotrophic factor (BDNF) in the amygdala and hippocampus. Of particular interest, increased levels of BDNF in brain regions (nucleus accumbens, ventral tegmental area, amygdala and dorsolateral striatum) was shown to promote anxiety- and depression-like behavior in mice chronically fed a high fat diet (HFD). We thus suggest that the PC7 KO mice should be protected from diet-induced obesity (DIO) anxiety-like behavior. We have placed WT and PC7 KO mice on a saturated HFD (palm oil) and a control diet for 12 weeks and then proceed with behavioral phenotyping. The mice were also subjected to restraint stress to evaluate their basal levels and post-stress corticosterone levels. Different brain areas were also dissected for protein extractions and quantification of mature BDNF by western blot analysis. In our analysis, we have observed a trend for protection of the anxiety-like phenotype induced by the HFD in some of the behavioral tests in the PC7 KO mice. We also observed a significant increase in marble burying and in immobility time during the force swim test in the PC7 KO mice on ND. Interestingly, these abnormal behaviors can be associated with

obsessive-compulsive disorder (OCD). In addition, we have also observed a blunt in the corticosterone secretion after restraint stress in the PC7 KO mice fed a HFD, suggesting aberrant stress response, but to confirm these observations as well as the behavioral observations more mice experiments are needed. Finally, this study provided more information on the development of anxiety- and depression-like symptoms when consuming a saturated high-fat diet in the PC7 KO mice. Future work should aim to define the PC7 KO mice OCD-like phenotype in relationship to BDNF processing and possibly other neuropeptide substrates in various regions of the brain.

4.3.2 Introduction

The prevalence of obesity is escalating rapidly and is a major public health concern. Obesity can be defined as a medical condition where global health is compromised due to the accumulation of excess lipid (487). Many elements influence body weight gain such as inherited biological traits, life experiences, behavior, environmental and social factors (488). The consequences of being overweight or obese are affecting a wide spectrum of health issues such as increased risk of metabolic syndrome, type 2 diabetes, cardiovascular disease, developing certain types of cancers, respiratory conditions, fatty liver disease, depression and mood disorders (489, 490).

The availability, the constant exposure and the palatable qualities of high fat/high sugar foods are increasing the consumption of such foods in absence of nutriment requirement, which is a main driver of obesity. Accordingly, high-fat and high-sugar foods have been demonstrated to modulate the brain motivation and reward circuit (265, 274, 491, 492). The neural connections responsible for motivation and reward are composed of dopamine (DA) neurons and these connections are transmitting sensory, cognitive and emotional information related to searching and consuming food (493). DA signaling, which regulates inhibitory mechanisms within the reward system, is often impaired or deficient in obese humans which leads to increase food consumption to compensate for desensitization of these pathways (494). The signaling mediated by DA neurons modulates BDNF, pCREB and ΔFosB (a truncated splice variant) in the reward circuit. Interestingly, accumulation of ΔFosB in the nucleus accumbens also increases sensitivity of the rewarding responses mediated by cocaine (495, 496). These mechanistic neural modifications lead to increase the effects of drugs and natural rewards which consequently

perpetuate compulsive usage (495, 496). In addition, feeding a high-fat diet for 12 weeks in mice was shown to cause DIO anxiety- and depressive-like behaviors that is accompanied by a significant increase in BDNF, ΔFosB and pCREB in the nucleus accumbens, ventral tegmental area and dorsolateral striatum. Chronic feeding of a saturated HFD for 12 weeks in mice have also shown an increase in circulating corticosterone at basal levels and following restraint stress (265). These results are demonstrating that DIO is inducing anxiety-like behavior caused by neuronal changes in the reward circuit, promoting negative emotional state (265).

Our group has recently reported that the PC7 KO mice displayed impaired episodic memory, as well as an anxiolytic phenotype (259). These phenotypes were rationalized by the demonstration of a significant decrease in mature BDNF signaling in the amygdala and the hippocampus and was rescued using a tyrosine receptor kinase B (TrkB) agonist (7,8-dihydroxyflavone) prior to behavioral testing (259). In this current study we thus hypothesised that the PC7 KO mice should be protected from diet-induced obesity anxiety-like behavior. In this current study, we aimed at understanding the impact of diet-induced obesity in our PC7 KO mice model to better understand the intimate relationship between obesity and increased risk of depression and anxiety. We have undertaken a series of behavior testing to analyse the cognitive performance of the PC7 KO mice when fed a saturated HFD. We were also interested in the corticosterone secretion levels following a restraint stress in our PC7 KO mice, and finally we dissected different brain regions for investigation of BDNF maturation.

Taken together, in this study we have reproduced in our wild-type (WT) animals the behavior phenotypes previously observed when fed a HFD for 12 weeks (265), although more mice are needed to clearly demonstrate that there is a protective effect in the PC7 KO on a HFD. Finally, we have preliminary results suggesting potential obsessive-compulsive behavior in the PC7 KO mice that needs to be investigated further with more behavior testing and biochemical analysis.

4.3.3 Results

4.3.3.1 Body weight and caloric intake

We first assessed the changes in body weights within our different cohorts. Comparing WT mice to PC7 KO mice on a normal diet (ND) throughout the 12-week diet, we observed that the PC7 KO mice are smaller and maintain the body weight difference throughout the study on the ND, Figure 4.1A. Mice on a HFD gained more weight independently of the genotypes which was expected from the consumption of a high-fat foods, but a small reduction of the body weight gain is noticed in the HFD PC7 KO mice, Figures 4.1A-B. To evaluate the palatability between the two diets and the food consumption between the genotypes, cumulative food intake was analyzed and we observed an increase in food intake both in WT and PC7 KO mice on the HFD starting around 5 week of consumption, Figure 4.1C. Interestingly, the PC7 KO mice have a tendency to consume less food on ND, Figure 4.1C and this trend can also be observed in the HFD PC7 KO mice.

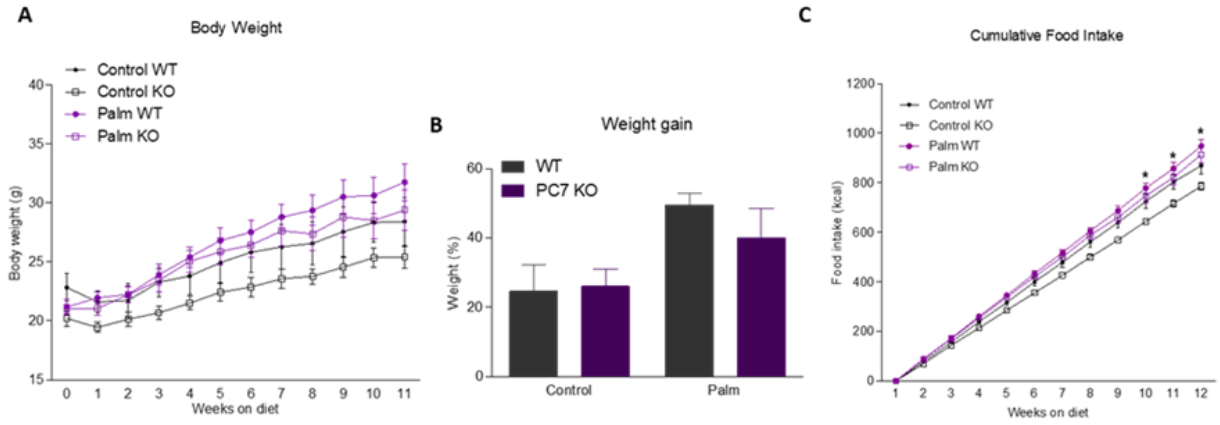

Figure 4.1. Body weight gain and cumulative food intake of WT and PC7 KO mice on a ND and a HFD.

A) Increase in body weight (g) for the 12-week period of feeding. B) Associated body weight gain (%). C) Cumulative food intake (kcal) between ND and HFD through the 12-week period. *n*= 4-6 mice/group. Means ± s.e.m.

4.3.3.2 Body fat mass and lean mass composition

To further characterize the body mass composition of the WT and PC7 KO mice on the two different diets, we analyzed the lean mass and fat mass by echoMRI. No changes were observed in lean mass (g) between diets or genotypes after the 12-week ND, Figure 4.2A. A significant and anticipated change was observed in mice fed a HFD, as we observed a ~2 fold increase in the fat mass (g) of HFD mice both in the WT and KO mice, Figure 4.2B. This is further corroborated with an increase in % of fat mass in HFD mice in both genotypes, Figure 4.2C.

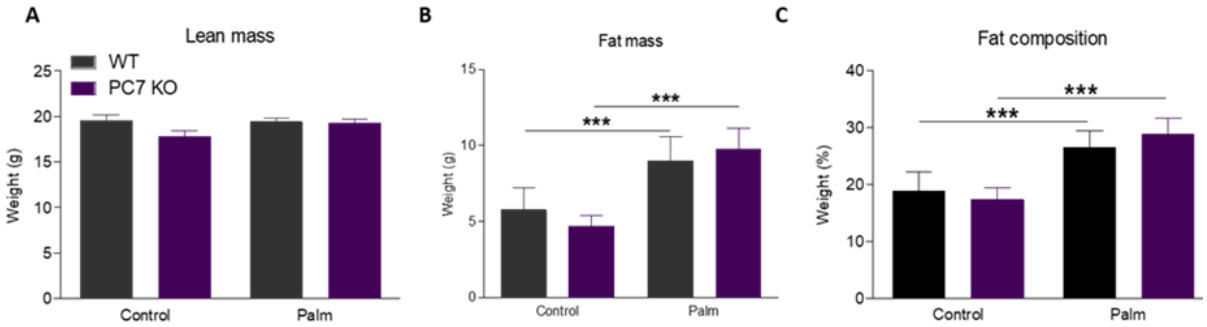

Figure 4.2. Lean and fat mass composition between WT and PC7 KO mice on a ND and a HFD. A) lean mass and B) Fat mass and in grams (g). C) Percentage (%) of fat composition of each mice at the end of the 12-week period relative to their total body weight. *n*= 4-6 mice/group. Means ± s.e.m.

4.3.3.3 Energy balance

We next investigated the metabolic changes in these mice by placing the mice in metabolic cages for 2 days and measured locomotion, energy expenditure and respiratory exchange rate. First, the locomotion during dark phase shown no significant changes between WT and PC7 KO, although the PC7 KO mice have a slight trend for increase locomotion compared to WT and is also appreciable during light phase, on ND. As for differences between diets, a decrease is observed in locomotion for both WT and PC7 KO in HFD mice with a significant decrease for the PC7 KO mice, during dark phase, Figures 4.3A-B. The respiratory exchange rate confirmed in the WT and PC7 KO mice chronically exposed to a HFD a greater utilisation of lipids by having a significant decrease in the respiratory exchange rate ratio, Figures 4.3C-D. Interestingly, the PC7 KO mice on ND have a significant increase in respiratory exchange rate, Figures 4.3C-D. The analysis for energy expenditure showed that under both ND and HFD, the PC7 KO mice have a

significant decrease in energy expenditure during the dark phase, but this decrease is only significant on the HFD during the light phase. Lastly, there is a significant increase in energy expenditure in the WT and PC7 KO mice on a HFD compared to mice on a ND, Figures 4.3E-F.

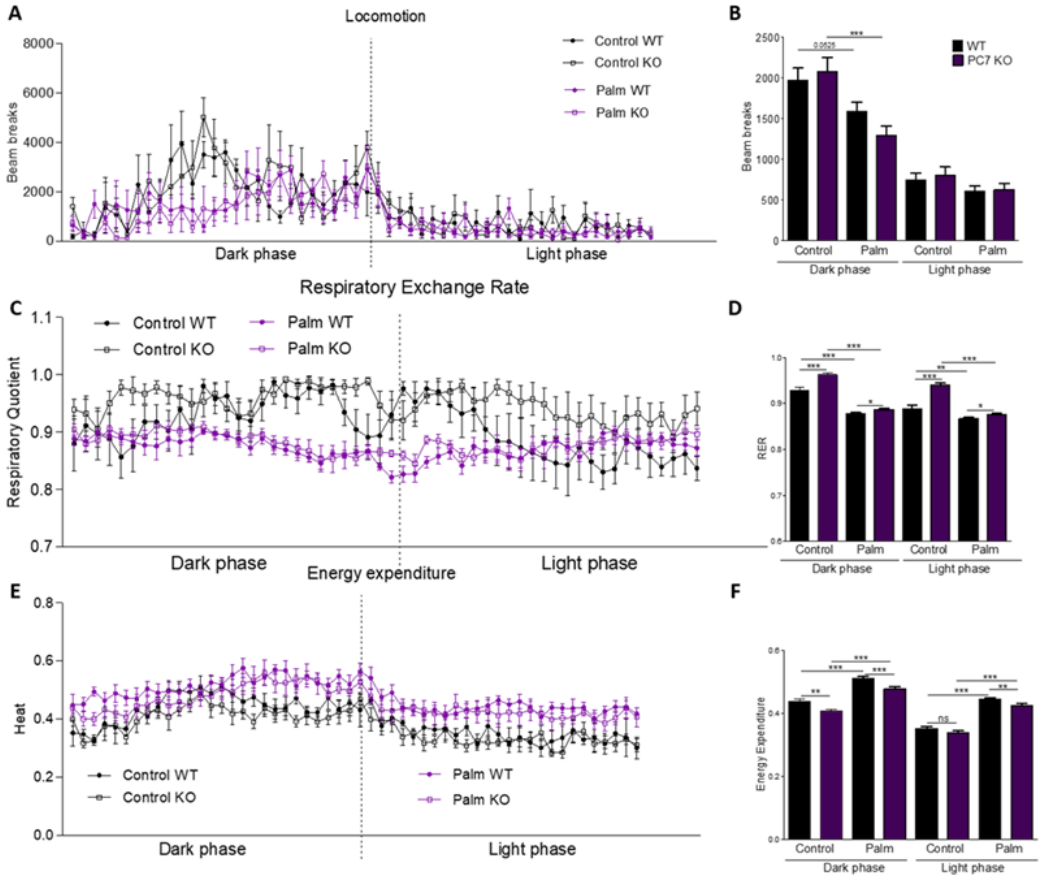

Figure 4.3. Energy balance in WT and PC7 KO mice on a ND and a HFD.
A) Beam breaks measured over dark and light phases show a HFD decrease in locomotion in both WT and KO mice. B) Beam breaks quantifications. C-D) Respiratory exchange rate was decreased in HFD relative to LFD consistent with greater lipid utilization, in both WT and PC7 KO mice during dark phase. Increase in RER during light phase in the PC7 KO mice under ND. E-F) HFD increases energy expenditure in both WT and PC7 KO mice. *n* =4-6 mice/group. Means ± s.e.m.

4.3.3.4 Diet-induced obesity (DIO) anxiety-like and depressive-like behavior

We next determined the consequences of diet-induced obesity on anxiety- and depressive-like behaviors in the WT and PC7 KO mice using different tests, such as the elevated-plus maze (EPM), the open field test (OFT), the force swim test (FST) and the marble burying test (MBT). Our results have shown that like previously described in WT mice, DIO is not affecting the number of entries

in the EPM, neither the distance travelled Figures 4.4A-B, but decreases the percentage (%) of time spent in the open arms, Figure 4.4C. Consistent with the previously described anxiolytic phenotype, the PC7 KO mice on a ND have a trend for spending more time in the open arms, in comparison with the WT mice, Figure 4.4C. Interestingly, the PC7 KO mice on the HFD shown an increase in time spent in the open arms compared to WT mice on HFD, Figure 4.4C, suggesting a protective effect in the PC7 KO mice when chronically exposed to a HFD. The results from the OFT have shown that the PC7 KO mice on a ND had a significant increase in distance travelled in comparison to the WT mice on a ND, Figure 4.5A. No changes in the number of entries or % of time spent in the center was observed in the OFT for the PC7 KO mice, Figures 4.5B-C. On the other hand, WT mice on a HFD had no changes in entries or distance travelled, Figures 4.5A-B, but have shown a reduction in time spent in the center of the OFT, Figure 4.5C, coherent with previous observations (265). We have also performed marble burying test, an experimental method based on the interpretation that mice will burry any harmful objects in their environment, Figure 4.6A. The data showed that WT mice buried significantly more marbles when on a HFD compared to mice on a ND, Figure 4.6B, which can suggest an anxiogenic phenotype, consistent with previous results (265). Surprisingly, the PC7 KO mice have also shown a significant increase in marble burying on a ND in comparison to WT mice, Figure 4.6B, which can appear to be in opposition with the previously described anxiolytic phenotype in the PC7 KO mice when based on our interpretations of the marble burying results in WT mice on HFD. However, recognizing that data interpretation in the marble burying test can be very complex and that many publications have associated an increase in marble burying in mice with obsessive-compulsive disorder (497), we are suggesting that the increase in marble burying observed in the PC7 KO mice could be indicative of a possible obsessive-compulsive behavior when analysed in combination with other behavior results presented in this manuscript.

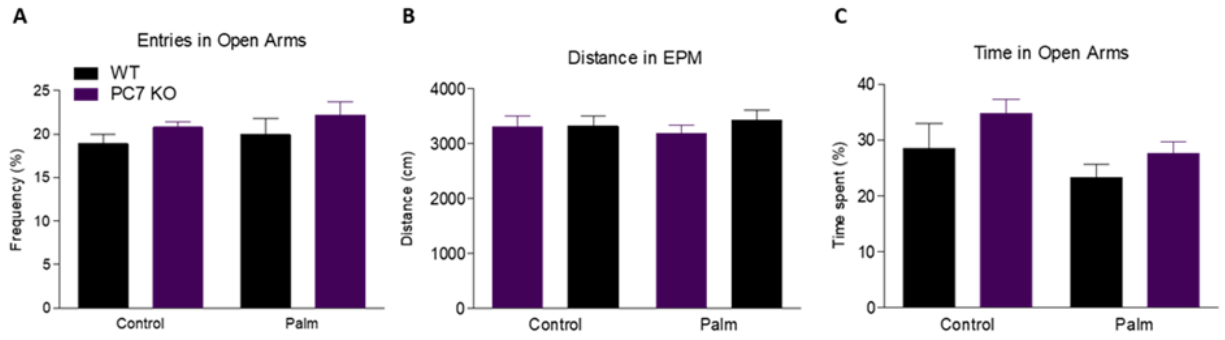

Figure 4.4. PC7 KO mice are protected from DIO anxiogenic behavior in the elevated plus maze (EPM).

A) Similar number of entries between WT and KO mice fed a ND and a HFD into the open arms. B) Similar distance travelled during the experiment between the WT and KO mice fed a ND and HFD C) HFD decreases % time spent in the open arms in WT mice, but KO mice are mildly protected. *n*=4-6 mice/group. Means ± s.e.m.

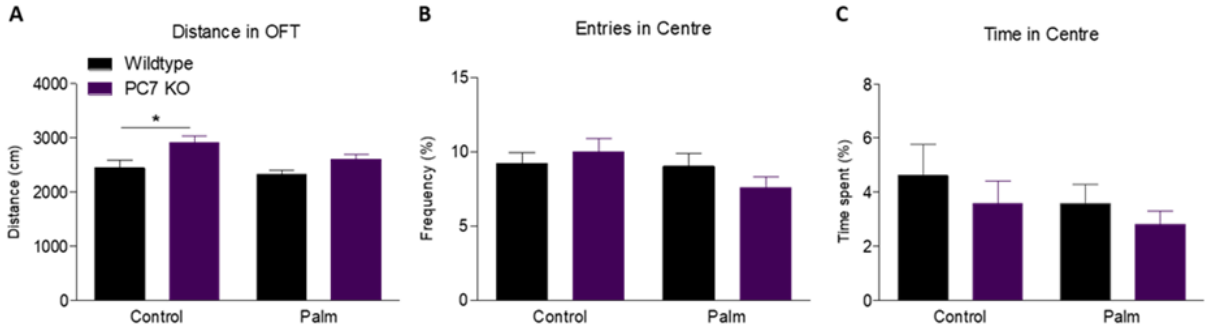

Figure 4.5. PC7 KO mice on a ND show a significant increase in distance travelled in open field test (OFT).

A) Increase distance travelled (cm) during OFT in PC7 KO mice compared to WT mice. B) Similar % of entries into the center of the arena in OFT between the diets and the genotypes. C) Decrease time in center (%) in the OFT in the PC7 KO mice, both on ND and HFD. n= 4-6 mice/group. Means ± s.e.m.

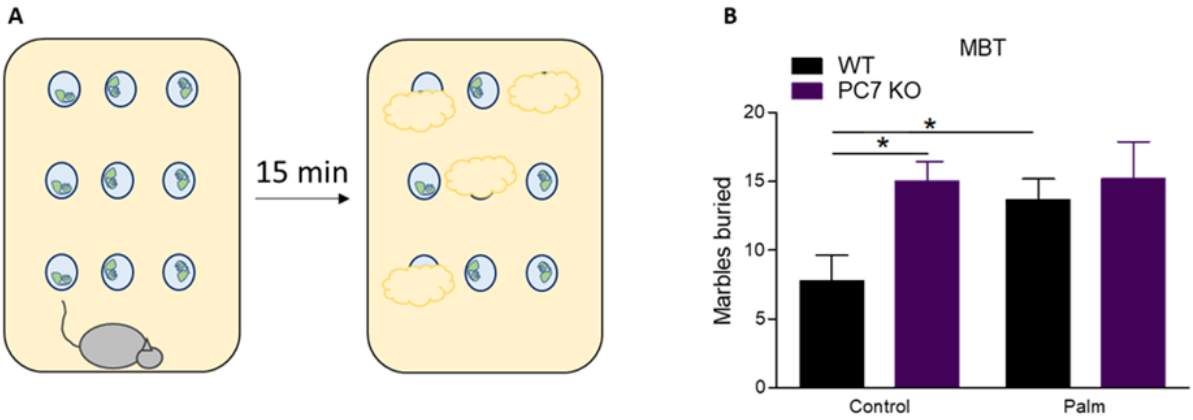

Figure 4.6. PC7 KO mice have repetitive behavior in the marble burying test.
A) Schematic representation of the experimental design. B) PC7 KO mice present an obsessive behavior by burying more marbles in both diets. n=4-6 mice/group. Means ± s.e.m.

To test for depressive-like behavior in our cohorts we performed FST and measured immobility time. The results showed that WT mice on a HFD had a significant increase in immobility time (%) in comparison with WT mice fed a ND, Figure 4.7A, consistent with what was previously demonstrated that DIO increases behavioural despair (265). Interestingly, the PC7 KO mice on a ND seems to also have a trend for increased immobility compared to WT mice even when fed a ND, and this trend is not exacerbated in PC7 KO mice fed a HFD, Figure 4.7A. This immobility was not caused by a deficit in swimming abilities since there was not change in swim velocity between the genotypes in the different diets, Figure 4.7B.

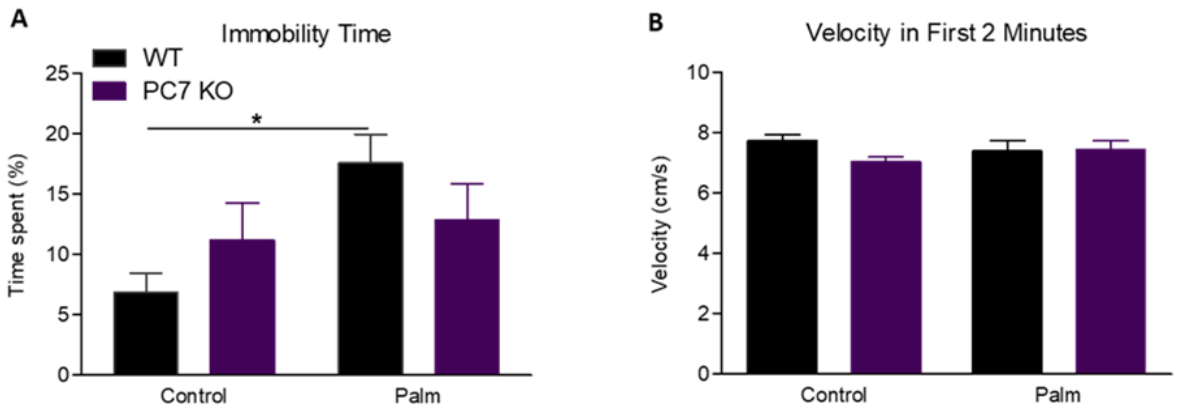

Figure 4.7. PC7 KO mice present self-destructive behavior in the force swim test (FST).
A) PC7 KO mice engaged in self destructive behavior during the FST when fed ND and HFD. WT mice on a HFD are showing depressive-like behavior. B) These observations are not due to modulation of the mice velocity capacity. n=4-6 mice/group. Means ± s.e.m.

4.3.3.5 HFD potentiate stress response in WT mice but the PC7 KO mice on a HFD have a blunted stress response

It was previously reported that a saturated HFD consumption in WT mice increases the basal level of corticosterone secretion and that this effect is potentiated after restraint stress (265). We therefore tested if the PC7 KO mice when chronically exposed to a HFD would have a variation in corticosterone secretion at basal level and after restraint stress, Figure 4.8A. We have validated in our experiments that the WT mice on a HFD had an increase in corticosterone levels both at basal levels as well as post 15 min of restraint stress, Figures 4.8B-D. Interestingly, the PC7 KO mice on a ND had a slight increase in corticosterone secreted at basal levels, but the levels of corticosterone did not change after the stress restraint, Figures 4.8B-D. This blunt effect observed in the PC7 KO mice in comparison with the WT mice on a HFD is suggesting that the PC7 KO mice are defective in stress-coping following dual combination of chronic consumption of a saturated HFD and exposed to stress restraint.

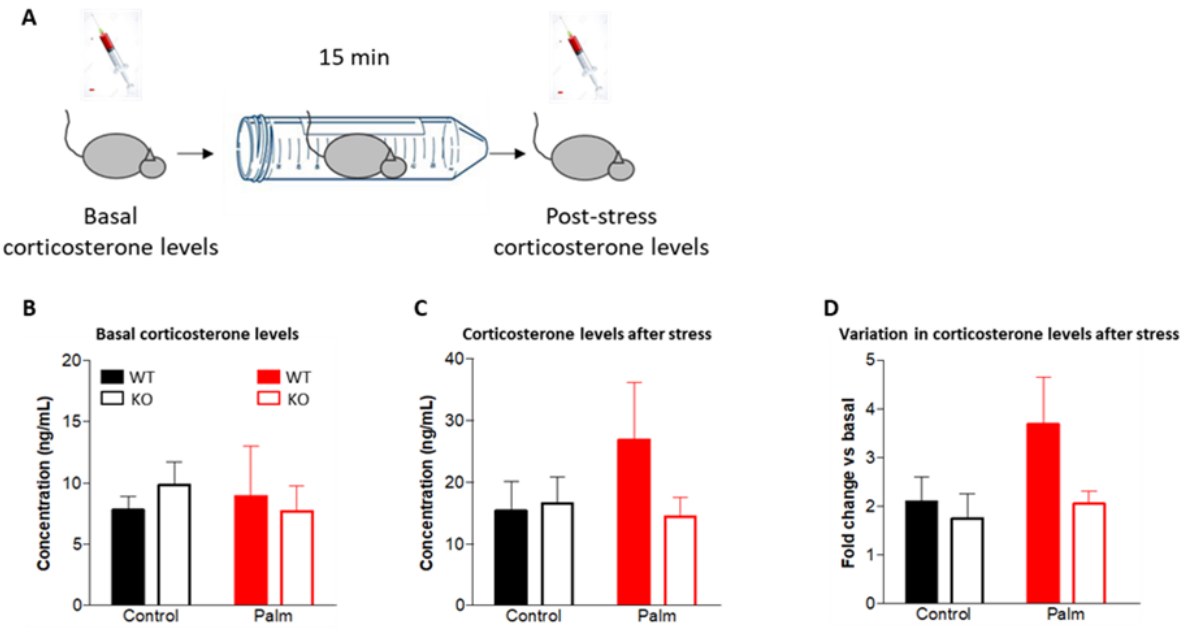

Figure 4.8. PC7 KO mice on HFD show a blunted corticosterone response after restraint stress. A) Schematic representation of experimental design. B) Corticosterone measurements before experiment. C) Corticosterone measurement after 15-minute restraint stress experiment. D) Ratio of post vs basal corticosterone levels show a blunt response in PC7 KO mice fed a HFD. n=4-6 mice/group. Means ± s.e.m.

4.3.3.6 Novel object recognition memory (NORM)

We have previously observed in the PC7 KO mice a deficit in episodic memory caused by aberrant processing of BDNF in the amygdala, a brain area responsible for memory plasticity (498). We therefore aimed to further investigate the effect of DIO on the cognitive performance in these mice. We subjected the mice to Novel Object Recognition Memory tests (NORM) in which the mice were presented, in the same arena used for the open field test, with two objects. One hour later (short-term memory: STM) or 24 hour later (long-term memory: LTM) mice were presented with the same familiar object, and a novel object. The time spent investigating the novel object was quantified, and the more time spent with the novel object is suggesting that the mice recognize the old one. Our results showed that the PC7 KO mice had a reduced preference for the novel object in the STM test in comparison with WT mice on ND Figure 4.9A, consistent with previous results, but not in the LTM test, Figure 4.9B. The HFD WT mice had lower preference for the novel object in the STM test, Figure 4.9A. Interestingly, the HFD WT mice had a slight increase

in their preference for the novel object in the LTM test, Figure 4.9B, in comparison to ND WT mice. These results were not related to a reduced or increased exploration of the objects, as both genotypes explored for the same duration in each diet (Figure Supplemental 1).

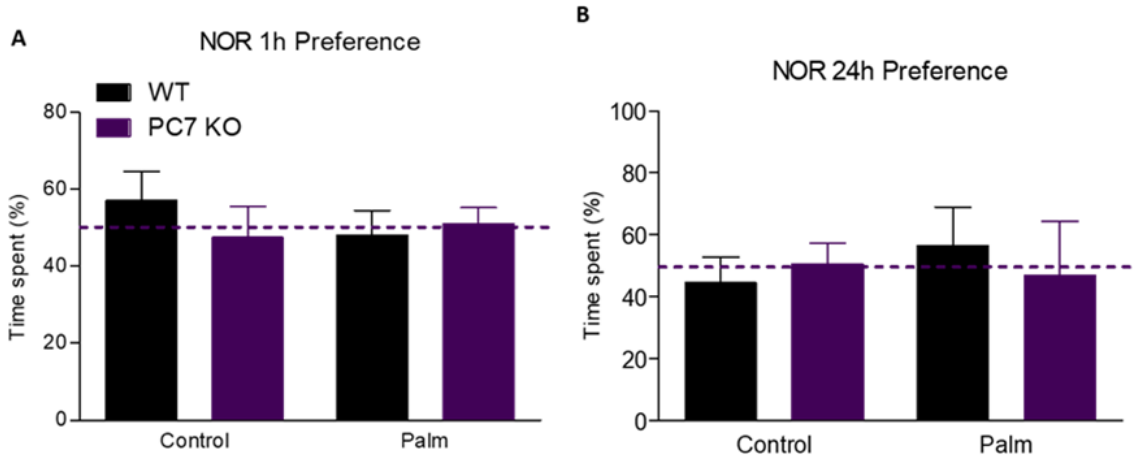

Figure 4.9. PC7 KO mice show impaired STM.
A) Preference scores for novel object in the NORM test at 1-hour post exploration. B) Preference scores for the novel object in the NORM test at 24-hour post exploration. *n*=4-6 mice/group. Means ± s.e.m.

4.3.3.7 proBDNF maturation

As previously demonstrated (259), we observed a reduction of BDNF maturation in the nucleus accumbens of the PC7 KO mice on a ND, Figure 4.10A. Surprisingly, no significant decrease was observed in the amygdala of these mice, Figure 4.10B. No significant changes were observed in the maturation of BDNF in the amygdala sections in both genotypes on HFD, although a trend is observed similar to the nucleus accumbens sections, Figure 4.10B. Also, we have reproduced the previous observations showing that chronic exposure to a saturated HFD increases the maturation of BDNF in the nucleus accumbens in the WT mice and also demonstrated that this increase is moderate in the PC7 KO mice on a HFD, Figure 4.10A.

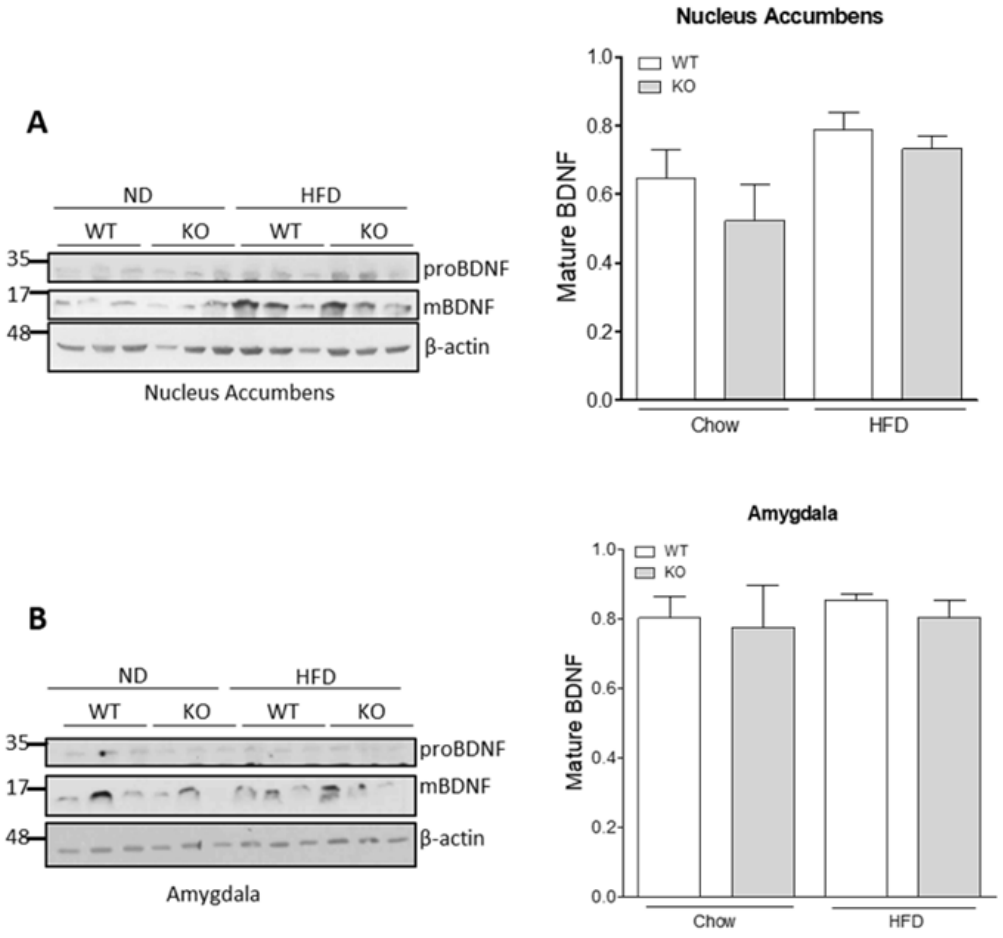

Figure 4.10. PC7 KO mice show impaired processing of BDNF in the nucleus accumbens.
A) Western blot analysis of WT and PC7 KO mice brain section (nucleus accumbens) extracts. B) Western blot analysis of WT and PC7 KO mice brain section (amygdala) extracts. n=3 mice/group. Means ± s.e.m.

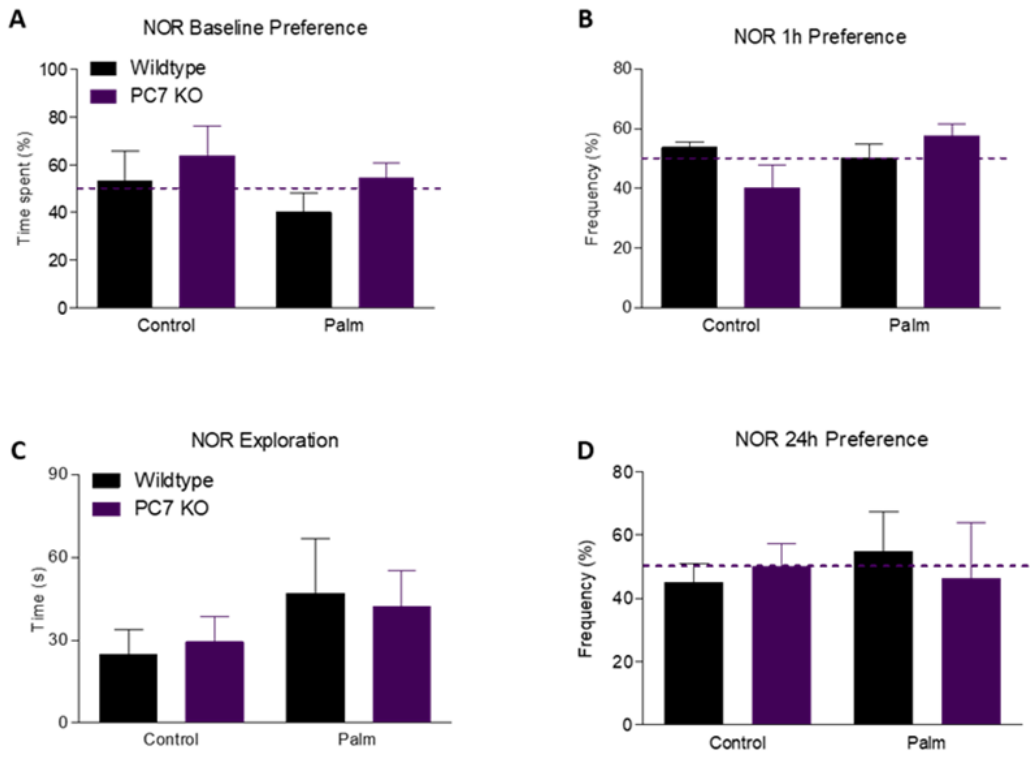

Supplemental Figure 4.1. Baseline preference and exploration in WT and PC7 KO mice.
A) NOR baseline preference measured in time spent (%) with each object. B) Frequency with each object (%) after 1h. C) Time spent (s). D) Frequency with each object (%) after 24h.

4.3.4 Discussion

As obesity and mood disorders have become public health concerns, we aimed to elucidate brain reward circuitry in relationship to diet-induced obesity and the maturation of neuropeptides. Our laboratory is interested in the maturation of precursor proteins and previous publications have highlighted the role for PC7 in the maturation of BDNF and related cognitive impairments (259, 499).

In this work we have reproduced what was previously described as DIO anxiety-like behavior (265) in our WT mice in most of our behavior experiments even with a small number of mice (*n* between 4 and 6 mice). We also confirmed our previously demonstrated anxiolytic phenotype in the PC7 KO mice in the EPM experiment and in the OFT in PC7 KO mice on ND. Interestingly, the combination of chronic consumption of an anxiogenic saturated HFD and the anxiolytic PC7 KO phenotype have shown intermediate phenotypes in some of the behavioral and biochemical

analyses. Accordingly, during the EPM the decrease in time spent (%) in the open arms for the PC7 KO mice is not as severe as the decrease observed for the WT mice on HFD. To further validate these observations, we will need to increase the number of mice in our behavior tests as well as in the biochemical analysis of BDNF maturation. In addition, we will need to investigate other brain sections such as the ventral tegmental area (VTA), the hippocampus and the dorsolateral striatum for mature BDNF but also for the dopamine signaling such as ΔFosB and pCREB. Dopamine regulates inhibitory signaling in the reward circuit which is often decreased in obese rodent models and based on our current observation that PC7 KO mice seem to consume less of the palatable foods we suggest that their dopamine signaling could be impaired. In line with this, elevation of CREB within the nucleus accumbens in rodents have been shown to induce anhedonia-like symptoms and increase immobility time in the FST (500, 501), reinforcing that DA signaling in the nucleus accumbens of our mice should be investigated in the future.

During this current study we have also made some novel observations in our PC7 KO mice. Indeed, we have observed abnormal self-destructive behavior in the PC7 KO mice during the FST, a behavior that could be both explained by behavioral despair but can also be associated with OCD (502). In addition, we have noted that the PC7 KO mice have a significant increase in the distance travelled in the OFT on ND, which could suggest a possible perseverative hyperlocomotion also observed in OCD (503). Similarly, the observed increase in the number of marbles buried in the PC7 KO mice could also be associated with an anxiety-like phenotype but based on previous observations (259, 499) and current observations we have connected these results to abnormal repetitive behavior in line with the symptoms of OCD previously described in mice (497). Of note, it was recently demonstrated that the Galectin-1 (Gal-1) and galectin-3 (Gal-3) KO mice displayed similar behavior phenotypes (impaired stress-coping and compulsive behaviors) accompanied by a decrease in BDNF in the prefrontal cortex (502). We therefore suggest that the PC7 KO mice possibly have an obsessive-compulsive disorder, that will need further investigations. Other regions of the brain need to be analysed for BDNF processing, such as the prefrontal cortex to solidify our conclusions.

Also, we showed that chronically exposed to a saturated HFD, the PC7 KO have their corticosterone response blunted in comparison to WT mice after a second stress. These results

are suggesting a possible hypothalamus-pituitary-adrenal (HPA) axis impairment (265) and reiterate aberrant stress coping in PC7 KO mice. Indeed, the HPA axis functions are affected by both metabolic and mood disorders (504, 505). Accordingly, future work should investigate gene expression of stress-related genes in the hypothalamus such as corticotrophin-releasing-hormone (CRH), a gene implicated in glucocorticoid (GC) negative-feedback. Future work should also investigate the mRNA levels of other prohormone processing enzymes, such as PC1/PC2 in the pituitary of the PC7 KO mice. The levels of PC1/PC2 could have been increased as a compensatory mechanism and could have affected CRH processing leading to HPA axis defects, PC2 levels which are also known to be affected by nutrition status (111, 506, 507).

Lastly, we reported the same episodic memory deficit in the PC7 KO mice (STM) in the NORM experiment, but there was no change in the LTM, possibly due to a small number of mice. Taken this data together, we confirm that the PC7 KO mice have impaired STM, but that the consumption of HFD does not seem to be beneficial or to exacerbate the phenotype in these mice.

In conclusions, in this study we have demonstrated that the chronic consumption of a saturated HFD in mice is promoting anxiogenic behavior as previously described in WT mice (265). We have also shown that the PC7 KO mice not only have an anxiolytic behavior as previously described (259), but also have a severe dampening of corticosterone secretion in situation where the mice are exposed to long-term HFD in combination with a second stressor. Finally, the PC7 KO mice on normal diet also showed symptoms of OCD-like behaviors in three different experiments and should be investigated in future work to better understand the overall aberrant stress-coping phenotypes reported here.

4.3.5 Material and method

4.3.5.1 Animals and diet:

All procedures involving the use of animals were approved by the CRCHUM and IRCM Animal Care Committee in accordance with Canadian Council on Animal Care guidelines. Eight weeks old C57BL/6J male WT mice and PC7 KO mice were single-housed under reverse cycle (lights off at

10am) in environmentally controlled rooms (22–24 °C) with ad libitum access to water and food. Mice were fed standard chow (ND) or high-fat (HFD) diet, see table 1, as described by Hryhorczuk *et al.*, 2016. The amount of food consumed over 24 h was measured right before the onset of the dark cycle. All behavioural testing and sacrifices below were carried out in the dark phase of the light -- dark cycle.

Table 4.1 Diet composition

	CTL	PALM
Fat source	Soybean oil	Palm oil
Fat (g/kg)	70	270
Casein (g/kg)	200	200
L-Cystine (g/kg)	3	3
Sucrose (g/kg)	100	100
Cornstarch (g/kg)	397.5	197.5
Dyetrose (g/kg)	132	132
Mineral Mix (g/kg)	35	35
Vitamine Mix (g/kg)	10	10
% Kcal Fat	17	50
% Kcal carbohydrates	62	43
% Kcal proteins	21	7
Total Kcal/g	3.8	4.8
% palmitic acid (C16:0)	10.2	44.5
% stearic acid (C18:0)	4.5	4.2
% oleic acid (C18:1)	22.7	39.4
% linoleic acid (C18:2)	54.8	9.5
% linolenic acid (C18:3)	7.8	N/A
% saturated fat	15	51.1
% monounsaturated fat	23.4	38.8
% polyunsaturated fat	61.2	9.7

4.3.5.2 Metabolic cages: locomotor activity and energy expenditure

Mice were habituated to metabolic cages (Comprehensive Lab Animal Monitoring System CLAMS, Columbus, OH) for 2 days prior to testing. Locomotor activity (X-Y-Z beambreaks) was measured for 12 hours. Body mass composition was also measured using echoMRI.

4.3.5.3 Anxiety: Elevated-plus maze

In order to assess anxiety-like behaviour following the diets consumption mice were tested in both the elevated-plus maze and open field test (below). The EPM apparatus consists of two closed arms that oppose two open arms in a plus design (Med Associates, Inc., St Albans, VT, USA). Decreased time spent in the open, exposed arm is an indicator of increased anxiety-like behaviour. The apparatus is placed 60 cm above the floor and has a video camera fixed overhead.

Each mouse was placed in the middle of the maze facing the open arm opposing the experimenter. Movement in the maze was recorded and tracked for 5 min by an overhead video camera connected to a PC with Ethovision XT software (Med Associates, Inc.).

4.3.5.4 Anxiety: Open field test

We used the open field test as an additional measure of anxiety-like behaviour. The open field test was carried out 1 day before the EPM task. The open field consisted of a Plexiglas box (50x50x30 cm) in a brightly lit room. Each mouse was placed in the middle of the arena and allowed to explore the field for 5 min. Movement in the field was recorded and tracked by an overhead video camera connected to a PC with Ethovision XT software.

4.3.5.5 Depression: Forced swim test

The FST is widely used to screen and validate antidepressants. In this test, animals display 'behavioural despair' as indicated by increased immobility and less escape-oriented behaviours. When forced to swim in a glass cylinder filled with water in which they are confined mice eventually cease escape attempts and become immobile. The increasing immobility time reflects a state of helplessness and despair. After 12 weeks of HFD or LFD, all the mice were forced to swim in a glass cylinder (height, 15 cm; diameter, 12 cm) containing water (23 °C) at a 10-cm depth. A video camera located above the apparatus recorded each test. The duration of immobility during the last 4 min of the 6-min testing period (2 min habituation) was calculated.

4.3.5.6 Anxiety and obsessive behavior: Marble burying test

Marble-burying test (MBT) is a tool for assessing a compulsive-like behavior or anxiety behavior. The apparatus used were clean plastic cages (28 × 17 × 13 cm) containing approximately 5 cm of clean sawdust layer covering its floor. Twenty glass marbles (15 mm diameter) were distributed in 4 rows evenly spaced in each cage. The animals were individually placed in the center of the marble-containing cage for 15 min, and the number of marbles buried (those with at least two-thirds under sawdust) was counted afterwards (508, 509).

4.3.5.7 Novel Object Recognition Memory test

Mice are placed for 5 minutes in the same arena then the open field test and presented with two identical objects. On day 1 of NORM testing, time spent near each object is measured. One hour (STM) and 24 h (LTM) later mice were presented with the now familiar and a novel object (510). If mice spend more time (preference score) examining the novel object, it suggests that they recognize and remember the old one. Analysis close to 50% indicates no preference.

4.3.5.8 Corticosterone levels

Both basal and stress-potentiated plasma corticosterone levels were measured. To measure basal corticosterone, blood samples were collected 3 days after behavior experiments. Each mouse was restrained for 15 min in decapicones (Braintree Scientific Inc., Braintree, MA, USA) and blood samples obtained immediately afterwards. Plasma corticosterone was measured by an ELISA corticosterone kit (Enzo Life Sciences, Farmingdale, NY, USA).

4.3.5.9 Western blot and antibodies

Mice were decapitated under isoflurane anaesthesia. Brains were rapidly dissected and stored at -80 °C. Frozen brains were sliced into 0.5mm coronal sections using a brain matrix. Coronal sections were mounted onto slides and maintained on dry ice. Nuclei were microdissected using brain tissue punches (Stoelting, Inc., Wood Dale, IL, USA). Bilateral punches of 0.75mm diameter were obtained from the VTA and 1.0mm diameter punches from the nucleus accumbens and amygdala. Microdissected tissues were homogenized on ice in 100 ml of cell lysis buffer (20mM Tris, pH 7.5; 150mM NaCl; 1mM Na2EDTA; 1mM EGTA; 1% Triton; 2.5mM sodium pyrophosphate; 1mM b-glycerophosphate; 1mM Na3VO4; 1mgml^{-1} leupeptin) with added complete protease cocktail inhibitors (Roche) in 1.5 ml tubes. Tubes containing homogenates were centrifuged for 15 min at 14 000 g. Protein concentrations were measured using BCA protein assay (Pierce Biotechnology, Rockford, IL, USA). Protein samples (20 mg) were separated by electrophoresis on a 10% polyacrylamide gel and electrotransferred onto a nitrocellulose

membrane (GE Healthcare Life Science, No. 10600003) and blocked for 1 hour in 5% milk in TBS-T and then incubated with anti-BDNF (1:500; Santa Cruz Biotechnology, Santa Cruz, CA, USA) or anti-actin (1:5,000, Sigma-Aldrich). Bound primary antibodies were detected with corresponding species-specific HRP-labelled secondary antibodies (1:10,000, Invitrogen) and revealed by enhanced chemiluminescence (ECL; Amersham). Quantifications were done using Image J software (National Institutes of Health).

4.3.5.10 Statistical analysis

Data were analysed using GraphPad Prism 5 software (http://www. graphpad.com). A two-way analysis of variance with Bonferonni post-tests was used to calculate data collected from food intake, body weight, OFT, EPM test, MBT, NORM, plasma corticosterone and western blotting.

4.3.6 Acknowledgements:

This work was supported by a Canada Research Chairs in Precursor Proteolysis (NGS; # 950-231335). The authors thank Suzie Riverin for fantastic technical assistance in the animal care facility.

Chapter V:

Discussion and Conclusion

5.1 Discussion:

In this PhD thesis, we have presented mechanisms and examples to better appreciate the powerful roles of the proprotein convertases in both health and diseases. Since no apparent defects were observed in the PC7 KO mice model it has remained a challenge to identify specific functions for the seventh member of the proprotein convertases family. Therefore, the original objective of this thesis was to define PC7 specific substrates, and here we focused on two type-II transmembrane proteins, like the unique PC7 specific substrate TfR1. In the chapters II and III we demonstrated that these two substrates, CASC4 and GPP130, are shed not only by PC7, but also by Furin, reiterating the functional redundancies between PC7 and its close family member Furin. We showed like many other groups that Golgi proteins are crucial in maintaining cellular homeostasis but that they can also be driving diseases and should not be overlooked. In chapter IV of this thesis we have pursued the work on the PC7 KO mice, since behavior phenotyping previously highlighted PC7-specific function in mood disorders, in relationship to proBDNF cleavage. In the sections below we will discuss key findings from this thesis as well as avenues for future work and significance. Lastly, perspectives regarding PC7 and the ongoing work will be presented.

5.1.1 CASC4

5.1.1.1 CASC4 full-length protein and cellular architecture

During the second chapter of this thesis we have investigated the biological functions of CASC4, a candidate substrate identified from a N-glycosylated secretome enrichment proteomics screen performed to discover new PC7 substrates. Previous publications have highlighted aberrant splicing events in the *CASC4* gene in breast cancer (415) and in glioblastoma (416), suggesting potential roles in cancer progression. Accordingly, we showed that CASC4 is influencing cell architecture by blunting the Rho-GTPase Cdc42 activation. This decrease in Cdc42 activation is causing perturbations of the focal adhesions, marked by increase paxillin-positive staining and decreased cell migration. Cdc42 is a GTPase known to be localized at the Golgi to sustain cell polarity (404), it is therefore not surprising to find its activity modulated by the overexpression of a Golgi-resident protein. However, how is CASC4 interfering with Cdc42 inactivation still need

to be fully characterized. Short term goals should aim at characterizing the relationship between CASC4 and Cdc42, to do so we aim to perform live imaging in cells overexpressing CASC4 and analyze the focal adhesion turnovers. Also, performing staining's for both CASC4 and active Cdc42 in migrating and non-migrating cells will help to investigate our hypothesis that CASC4 possibly binds Cdc42 and sequesters it at the Golgi membrane during directional migration. CASC4 binding of Cdc42 at the Golgi membrane would retain Cdc42 from activating downstream effectors, such as p65PAK or WASp (511) which would normally enhance cell migration. It is noteworthy to mention that other Golgi-localized proteins have been demonstrated to be relevant in Golgi-reorientation, cell migration and protein trafficking relevant to cancer progression, namely Golgin-160, GM130, GOLPH3 and GP73 (15, 404, 407-409, 412, 439, 480, 512). Indeed, our observations are coherent with what was previously observed by other Golgi proteins in other cellular context and add to the appreciation that Golgi-localized proteins are important players in cancer progression.

It is also important to note that we showed the role of full-length CASC4 in actin structure remodeling, but we have only assessed the full-length isoform and not the spliced isoforms reported (415, 416). As mentioned previously, CASC4 is alternatively spliced in certain types of cancer compared to normal cells. Therefore, the increase in *CASC4* alternative splicing and the relevance of these isoforms regarding their functions and their cleavage efficiency by PCs need to be investigated.

5.1.1.2 CASC4 N-terminal domain and podosome formation

On the other hand, we also showed that CASC4 cleavage by PC7 and Furin generates a cleaved fragment (N-terminal domain) which is endowed with novel function. We demonstrated that this N-terminal domain fragment is involved in the generation of podosome-like structures and the mechanisms remain to be characterized. Podosomes are actin structures rich in metalloproteases that are needed for degradation of the extracellular matrix, thus we hypothesize that CASC4, and specifically its N-terminal domain, could help in trafficking proteins such as matrix metalloproteases to these protrusions. Therefore, overexpression of CASC4 N-terminal domain could exacerbate the formation of podosome structures within the breast cancer cell lines (MDA-

MB-231 cells). One way to better define the role of CASC4 in the formation of these structures could be to identify binding partners using approaches such as BioID (513), to identify cargos transported by CASC4 on its cytosolic tail (representing the N-terminal domain).

We have also shown that only PC7 and not Furin correlates with CASC4 in influencing differential survival rates in breast cancer patients, suggesting a PC7-specific regulation of this deleterious shedding event. Accordingly, high *CASC4* seems to be beneficial for patient's survival, consistent with our observation that CASC4 decreases cell migration but conversely high *CASC4* and high *PCSK7* is detrimental for patient's survival, reinforcing our hypothesis that PC7 induces a detrimental CASC4 shed fragment. We have also observed from the clinical METABRIC data, that the *CASC4* gene is differentially expressed between normal tissues and patients' tumours from multiple types of cancers, see annexe I. We therefore suggest that CASC4 shedding and ectodomain release in the plasma could be detected in the plasma as a diagnostic tool. Long term goals and physiological relevance of this work could be to investigate circulating CASC4 as potential biomarker for cancers that have poor survival rate, such as ovarian cancers which is also difficult to diagnose (514). We are also interested to develop approaches to better detect and inhibit the deleterious CASC4 shedding by PC7 early during the disease progression. We therefore conclude that the shedding reported here is regulated by complex mechanisms and that derailed proteolysis could be involved in the metastases process, but how exactly needs to be investigated.

5.1.2 GPP130

5.1.2.1 Cleavage and Shiga toxin binding

In the third chapter of this thesis we have investigated the processing of GPP130, a Golgi resident protein with a unique trafficking route. GPP130 is a protein that received most of its attention because of its binding in endosomes and retrograde transport of the Shiga toxin. Manganese treatments in cells expressing GPP130 and infected with the Shiga toxin were showing protecting results since manganese is inducing GPP130 oligomerization and rerouting to the lysosomes for degradation with concomitant Shiga toxin degradation (430-432, 515). In line with these observations, we showed that PC7 and Furin cleave GPP130 at two different sites on its luminal

domain which would release the luminal domain ~20 aa after the binding site necessary for the toxin. We thus suggest that increasing GPP130 shedding by the PCs could potentially block the infection since GPP130 luminal domain could drastically change its conformation after the shedding and it could interfere with the toxin binding, although future work is needed to explore this hypothesis. In addition, it is possible that the Shiga toxin is not the only toxin taking advantage of the bypass pathway and strategies aiming at rerouting GPP130 as a protective mechanism could be relevant for other diseases in the future.

5.1.2.2 Manganese and calcium homeostasis

The previous studies on GPP130 and its manganese sensitivity have helped to elucidate GPP130 trafficking pathways (431, 433, 485, 515) but have also highlighted possible biological functions. GPP130 was shown to be rerouted to MVBs and lysosomes when treated with manganese, but it will be interesting to investigate if GPP130 could also influence manganese homeostasis inside the Golgi lumen. From protein-protein interactions depository (BioGRID) we observed that GPP130 could potentially interact with a calcium transporter (ATP2B2) and a potassium channel (KCNS3), hence we suggest that manganese transporters could also be binding partners. Manganese homeostasis, as well as calcium homeostasis, is crucial for multiple biological reactions including protein glycosylation. Indeed, a recent report has highlighted the intimate relationship between protein glycosylation defects observed in congenital disorder of glycosylation (CDG) and manganese homeostasis (516). Accumulating evidences have shown that CDG could also be caused by a deficit of the vesicular transport within the Golgi or by disruption of the pH homeostasis (517). As a relevant example, the Golgi transmembrane protein TMEM165 was recently identified as an important actor of Golgi Mn^{2+} homeostasis. The data showed that TMEM165-deficient cells have abnormal glycosylation patterns caused by reduced levels of Mn^{2+} entry inside the Golgi lumen (516). We can hypothesize that if GPP130 is also implicated in Mn^{2+} homeostasis like TMEM165, it could have similar drastic consequences on protein glycosylation. We suggest that identification of GPP130 cargos would greatly help in understanding GPP130's function by defining potential interactions. One strategy would be to isolate different organelles, such as endosomes, and identify proteins that are enriched/decreased in absence of GPP130. The identification of luminal cargos for protein trafficking along the secretory has remained an

important challenge since the luminal environment of the secretory pathway does not allow for efficient proximity labeling approaches such as traditional BioID using biotinylation by the BirA enzyme (513). However, recent techniques have been shown to be very efficient in biotinylating proteins in the endoplasmic reticulum such as TurboID and miniTurbo (518) and could be optimized to identify cargo proteins trafficked by GPP130 along the secretory pathway. Also, we should investigate glycosylation patterns in cells silenced for GPP130. Lastly, it is important to mention that GPP130 was reported in a study interested in calcium homeostasis and was further shown to be modulating cell survival in head and neck cancer cells (435). Since it is well established that calcium signaling is modulated during cancer progression (483), long-term goals should investigate how GPP130 could be related to calcium homeostasis as well. Additionally, our CbioPortal for Cancer Genomics analysis have highlighted that the *GPP130* gene is amplified in up to 35% in lung cancer, potential research avenues should investigate how this amplification could be connected to calcium signaling.

In addition, it was also reported that GPP130 is binding sortilin and AP-5 in order to traffic from TGN to lysosomes (433). We suggest that GPP130 sorting and rerouting to lysosomes for degradation could also be relevant in protein turnover, a mechanism often altered in neurodegenerative diseases (519-521). Indeed, it could be possible that defects observed in AP-5 knockdown (accumulation of endolysosomes) were also caused by defects in protein targeted for degradation by GPP130 (372).

5.1.2.3 Conclusion chapters CASC4 and GPP130

Our work demonstrated that PC7 and Furin can cleave and shed two poorly characterized Golgi-resident proteins and that the interplay between the full-length form and the cleaved form could have opposite functional consequences. Also, from that original N-glycoproteome screen, we had identified other possible substrates that would be interesting to investigate, see Chapter II Tables 2.1 and 2.2. Indeed, multiple potential substrates are related to cancer progression, *i.e.* Fibulin and GDF15, hence reiterating that PC7 plays a role during cancer development. Also, one strategy that we can use in order to better define potential substrates in the future would be to perform siRNA screen instead of PC7 overexpression, to highlight more physiological substrates using

different cell types. Lastly, derailed or increased PC activity can lead to cancer development, therefore efforts to inhibit PCs in certain types of cancer have led to promising results (156) but a better understanding of these newly described proteins could lead to better treatments targeting the substrates directly avoiding PC inhibition side effects.

5.1.3 PC7 KO mice behavior analysis

5.1.3.1 Protection from DIO anxiety and depression-like behavior

In the fourth chapter of this thesis we have pursued the behavioral phenotyping of the PC7 KO mice. Previous work had demonstrated that the PC7 KO mice displayed impaired episodic memory as well as an anxiolytic phenotype (259). To follow-up on these observations, we wanted to combine our previous results with the recently described anxiogenic phenotype associated with the chronic consumption of a HFD (265) to investigate a possible protection from diet-induced obesity anxiety-like behavior in our PC7 KO mice. To do so, we have challenged WT and PC7 KO mice with a chronic consumption of saturated HFD and have observed in some of the behavior tests that the PC7 KO mice would not be impaired as much as the WT mice by the anxiogenic effects of the saturated HFD but more mice are needed to validate these observations. Indeed, the PC7 KO mice seemed to be protected from the anxiogenic consequences of the HFD but only in the force swim test, but since we had a small number of mice and that the biochemistry was analysed for BDNF processing only in two brain sections, it is impossible to generate solid conclusions for now. In addition, we have confirmed that the WT mice on a HFD had short-term memory deficit, and because these deficits were previously explained in part by an increase in inflammation markers such as TNF-α and IL-1β (290) in the amygdala and hippocampus, it would be interesting to test for these markers in our PC7 KO mice on ND and HFD.

5.1.3.2 OCD-like symptoms

We have also made some novel observations about the PC7 KO mice that will need to be further investigated and will help to decipher new PC7 physiological functions. Indeed, we have shown that the PC7 KO mice had abnormal behaviors that could be associated with obsessive and compulsive-like disorders (OCD) in the force swim test and the marble burying test. Accordingly,

since our previous results showed an anxiolytic phenotype, we were surprised to observe longer immobility period in the PC7 KO mice during the force swim test, and similarly with the increase in marble burying. These two phenotypes can also be associated with OCD-like symptoms and have been described previously as "self-destructive" when observed during the FST, and as repetitive movement when observed during the MBT (497). Interestingly, a similar OCD phenotype was characterized recently in a different mice model (502) and was explained by a decrease in mature BDNF in the pre-frontal cortex. Therefore, to further validate our observations, we should investigate in our PC7 KO mice the levels of mature BDNF in the prefrontal cortex and perform more behavior testing's such as tail suspension tests and monitor self-grooming.

5.1.3.3 Impaired stress coping

We have also observed a severe blunt in corticosterone secretion following restraint stress in the PC7 KO mice on a high fat diet. In this context, we suggested that the PC7 KO mice may have an impaired hypothalamic-pituitary-adrenal (HPA) signaling. To further investigate this observation we should analyze the neuroendocrine peptides present in the hypothalamus, pituitary and adrenal gland to possibly identify peptides differentially modulated, in a similar manner as performed previously for PC1 and PC2 in the mouse spinal cord (522). In line with this, most of our behavior observations have been linked previously to BDNF processing in specific regions of the brain, therefore we suggest that the downstream pathways, such as $p75^{NTR}$ and tropomyosin-related kinase B (TrkB) receptor signaling pathways should be dissected further in the PC7 KO mice. Previous studies have also highlighted that pCREB and ΔFos are modulated by saturated high-fat diets in the reward circuit in mice (265), therefore a better understanding of the modifications within these circuits in the PC7 KO mice is needed.

proBDNF is also cleaved by other enzymes such as PC1 and Furin. For future work, it will be interesting to generate different mouse models with complete PC7 KO in addition to PC1 and Furin conditional KOs in specific region of the brain to reduce the processing of BDNF in the reward circuit, or in the pre-frontal cortex and perform behavioral and biochemical analyses. Finally, this ongoing work could greatly help developing new therapeutic avenues for mood

disorders in relationship with diet-induced obesity. For long term goals we are interested in identifying patients with SNPs within the *PCSK7* gene in association with OCD, anxiety or depressive behaviors.

5.1.4 Perspectives for PC7

5.1.4.1 Localization of active enzymes in health and diseases

Proprotein convertases are synthetized as zymogens and inhibitory mechanisms control the release of active enzymes when the cognate subcellular compartment is reached (4). Together with the trafficking signals on their cytosolic tails, complex mechanisms of regulations are needed to limit unwanted proteolysis. In addition, natural inhibitors are being discovered, such as PAR1, GBP2 and GBP5 (204, 225), which have been demonstrated to inhibit Furin in various contexts. These recently discovered natural inhibitors could explain, in part, why proteases do not always cleave the same substrates, especially when a substrate is sharing consensus cleavage motifs targeted by multiple enzymes. It suggests that in some contexts Furin, or possibly other proteases, are retained in an inactive state by an inhibitory protein. It is a complex orchestration between zymogen activation, cellular localization and natural inhibitors balance that will allow a substrate to be cleaved or not, but a lot is still to learn. In line with this, during the second chapter of this thesis we observed that both PC7 and Furin were expressed in non-cancerous (MCF10a) and cancerous triple negative breast cancer cell lines (MDA-MB-231 cells) but that CASC4 was only cleaved in triple negative breast cancer cells and not in the non-cancerous cells. We decided to analyze for *PAR1*, *GBP2* and *GBP5* and found that *PAR1* is significantly more expressed, at the mRNA levels, in the non-cancerous cells, annexe II. This result suggests a regulatory mechanism to inhibit/limit deleterious consequences generated by the PC7/Furin cleavage in the non-cancerous cell lines and will need to be further analyzed.

Multiple groups are currently investigating the pathways of activation of proprotein convertases (238) or other protease (523) to specifically probe active enzymes in various systems. Better defining the sub-cellular localization of active enzymes can also lead to ground-breaking clinical application such as the generation of active proteases imaging probes for optical surgical guidance (524). Our understanding of the activation and trafficking of PC7 is emerging and recent

work by our group (239) have help to better define its unique trafficking pathway in hope of answering remaining questions such as 1) how does PC7 traffic to the plasma membrane via the unconventional secretory pathway? and 2) where is PC7 loosing its inhibitory prosegment? Answering these fundamental questions would help to better understand the biological function of this enzyme.

5.1.4.2 Inflammation

As mentioned in the introduction, one important feature of PC7 is that it is highly expressed in the immune system and specifically in the thymus (230). Nevertheless, the role of PC7 in the immune system has not been studied thoroughly apart from one study reporting that Foxp3 is cleaved by PC7 and PC1 in activated $CD4^+$ T cells. Foxp3 is a transcription factor important for the development and function of regulatory T cells (Tregs) (525). This cleavage was shown to induce the activation of downstream Tregs genes such as interleukin-1l (IL-10), an anti-inflammatory and immunosuppressive cytokine, which suggests alternate signaling pathways between full-length Foxp3 and the C-terminal cleaved form. Similar to PC7, Tregs are expressed in the thymus (526), hence physiological relevance of studying the immune responses in PC7 KO mice using various immune activation stimuli would be relevant. Importantly, a major concern from this former study is the fact that Foxp3 is a cytoplasmic and nuclear transcription factor, and PC7 is a transmembrane enzyme localized within the secretory pathway, hence the likelihood of these two proteins to interact remain an important question.

5.1.4.3 Proprotein convertases' non enzymatic functions

5.1.4.3.1 Lipid metabolism

Accumulating evidences have led to the connection of PC7 with lipid metabolism (298), and more precisely the apolipoproteins. Coherent with previous genomics associations, our group have recently demonstrated that PC7 is responsible for the degradation of apoA-V in an non-enzymatic fashion (299). For future work, we are interested in investigating the decrease in circulating apoB levels and the reduced triglyceride levels observed in the liver of the PC7 KO mice. Accordingly, we are currently studying the impact of high-fat and high-sugar diet on the development of liver cirrhosis in WT and PC7 KO mice. Importantly, we want to analyze the recovery from high-fat

high-sugar diet withdrawal in our PC7 KO mice as we hypothesize that they should recover faster then WT from cirrhosis, as a proof of concept to utilize PC7 inhibition as a therapeutic avenue in the clinic for liver cirrhosis.

5.1.4.3.2 Cancer

For PC7 in cancer studies it is only the tip of the iceberg as we are only starting to examine PC7 regulatory mechanisms that could be non-enzymatic, such as the HIF-1α (304). One barely studied avenue that should be investigated is the *PCSK7* gene duplication. Indeed, as mentioned in the introduction, the *PCSK7* gene has a duplication in exons 13 to 17, 60 Kb downstream of its coding region but the mechanisms of regulation in *cis* or in *trans* have not been studied yet. With our data showing a relationship between the *CASC4* gene and *PCSK7*, and not *Furin*, in breast cancer patients, it would be interesting to investigate potential regulatory mechanisms between *CASC4* and *PCSK7* in a breast cancer context. Lastly, future work should also investigate the *PCSK7* gene duplication regulation mechanisms in the context of hypoxia since it was previously reported to be relevant for *PC7* and *Furin* expression in squamous carcinoma cells (304).

Non-enzymatic functions for other members of the family like PCSK9 (*i.e.* LDLR degradation (317)) have been described but those of PC7 are only emerging. Our current knowledge of the PCs is mostly revolving around their associated substrates but to discover non-enzymatic functions for PC7 is opening up a vast and exciting new area of research which should shed light on this enzyme.

5.1.5 2019-nCoV

Lastly, as this thesis is being written, the COVID-19 infection has reached a global pandemic. This new coronavirus which emerged in China during the fall 2019 has now reached the 3 million people infected across 204 countries as of April 2020 and is deadly in the most vulnerable members of our societies due to severe respiratory distress (527). No vaccines or antiviral treatments are available yet, hence a race for a better understanding of its infectiosity is ongoing. Our group has very recently described that the surface spike protein-S contains a Furin-like cleavage site close to its maturation site (210), suggesting that the surface viral glycoprotein may need cleavage by PCs to infect. Multiple examples of such maturation by PCs in other coronavirus

have been reported in the past such as the MERS-CoV (528) and the HKU1 (529) and this maturation/cleavage step enables viral fusion with the host cells (530). Even though the focus of this thesis was not revolving around viral infection, the knowledge applied to protein cleavage and maturation is relevant to this infection and using that information to target PCs with Furin-like inhibitors could potentially decrease infections in humans at risk (210).

5.2 Conclusion

As a general conclusion for this work, throughout the different chapters of this thesis we have highlighted novel PC7 and Furin biological functions and demonstrated their resemblance in activity but also their uniqueness. Also, we are only starting to define PC7 non-enzymatic functions and this area should be further investigated in hope of finding better treatments or more specific approaches for diagnostics. Finally, during the PC7 KO mice behavior study we have reiterated the anxiolytic behavior phenotypes observed in the PC7 KO mice and discovered novel behavior phenotypes relevant to obsessive disorders that remain to be fully characterized. Taking advantage of the bioinformatics tools and the genomics data available we can hope to better define the PCSK7 gene regulation and identifying specific substrates in human diseases in the future.

Finally, we believe that even if the proprotein convertases are part of the "golden age" of biochemistry, their fundamental mechanisms of action are still extremely relevant today and many more novel therapeutic applications are still to come.

Annexe I: *CASC4* expression levels

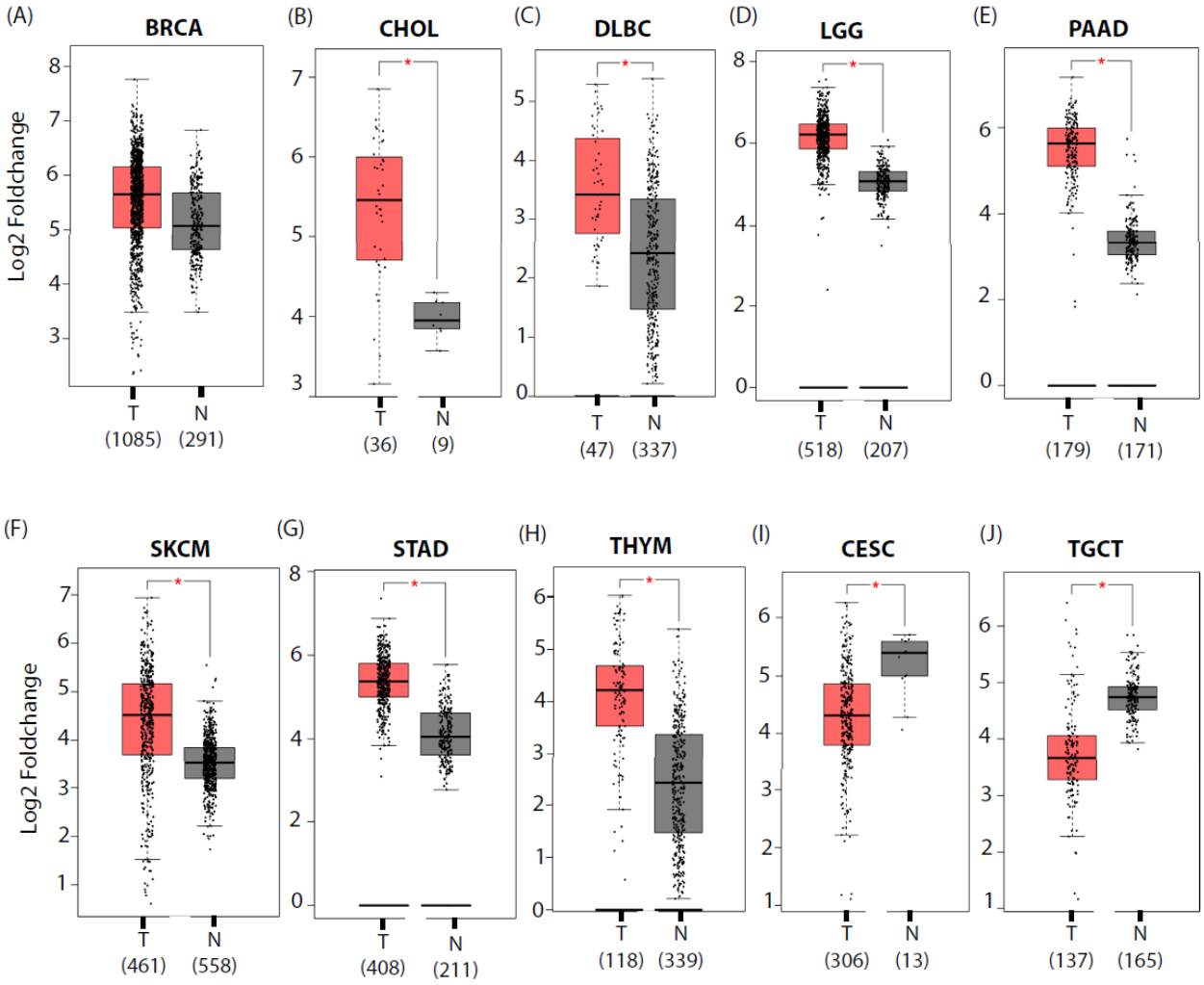

Legend

BRCA= Breast- invasive carcinoma
CHOL = Cholangiocarcinoma
DLBC= Lymphoid Neoplasm -Diffuse Large B-cell Lymphoma
LGG= Brain- Lower Grade Glioma
PAAD= Pancreatic adenocarcinoma
SKCM = Skin -Cutaneous Melanoma
STAD = Stomach adenocarcinoma
THYM= Thyroid carcinoma
CESC= Cervical squamous cell carcinoma and endocervical adenocarcinoma
TGCT = Testicular Germ Cell Tumors
T= Tumor
N = Normal

CASC4 levels in patients with various cancers compared to normal donors from TCGA database.

Annexe II: Natural inhibitors

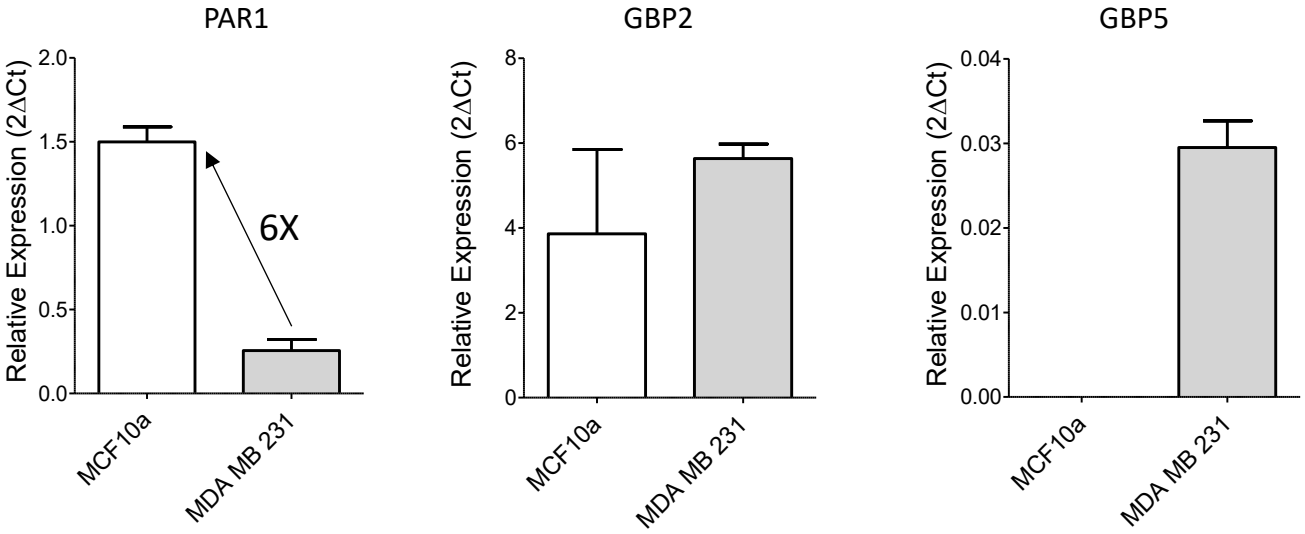

PAR1, GBP2 and GBP5 mRNA levels in MCF10a and in MDA-MB-231 cells. n=2/sample, represented is the mean +/- s.d.

References

1. Ladunga I. Large-scale predictions of secretory proteins from mammalian genomic and EST sequences. Curr Opin Biotechnol. 2000;11(1):13-8.
2. Roth J. Protein N-glycosylation along the secretory pathway: relationship to organelle topography and function, protein quality control, and cell interactions. Chem Rev. 2002;102(2):285-303.
3. Jensen ON. Interpreting the protein language using proteomics. Nat Rev Mol Cell Biol. 2006;7(6):391-403.
4. Seidah NG, Prat A. The biology and therapeutic targeting of the proprotein convertases. Nat Rev Drug Discov. 2012;11(5):367-83.
5. Pascovici D, Wu JX, McKay MJ, Joseph C, Noor Z, Kamath K, et al. Clinically Relevant Post-Translational Modification Analyses-Maturing Workflows and Bioinformatics Tools. Int J Mol Sci. 2018;20(1).
6. Han ZJ, Feng YH, Gu BH, Li YM, Chen H. The post-translational modification, SUMOylation, and cancer (Review). Int J Oncol. 2018;52(4):1081-94.
7. Shults K, Flye L, Green L, Daly T, Manro JR, Lahn M. Patient-derived acute myeloid leukemia (AML) bone marrow cells display distinct intracellular kinase phosphorylation patterns. Cancer Manag Res. 2009;1:49-59.
8. Rapundalo ST. Cardiac protein phosphorylation: functional and pathophysiological correlates. Cardiovasc Res. 1998;38(3):559-88.
9. Kingsley DM, Krieger M. Receptor-mediated endocytosis of low density lipoprotein: somatic cell mutants define multiple genes required for expression of surface-receptor activity. Proc Natl Acad Sci U S A. 1984;81(17):5454-8.
10. Incani M, Sentinelli F, Perra L, Pani MG, Porcu M, Lenzi A, et al. Glycated hemoglobin for the diagnosis of diabetes and prediabetes: Diagnostic impact on obese and lean subjects, and phenotypic characterization. J Diabetes Investig. 2015;6(1):44-50.
11. Milde-Langosch K, Schutze D, Oliveira-Ferrer L, Wikman H, Muller V, Lebok P, et al. Relevance of betaGal-betaGalNAc-containing glycans and the enzymes involved in their synthesis for invasion and survival in breast cancer patients. Breast Cancer Res Treat. 2015;151(3):515-28.
12. Shaw LM, Vanderstichele H, Knapik-Czajka M, Clark CM, Aisen PS, Petersen RC, et al. Cerebrospinal fluid biomarker signature in Alzheimer's disease neuroimaging initiative subjects. Ann Neurol. 2009;65(4):403-13.
13. Chen IH, Xue L, Hsu CC, Paez JS, Pan L, Andaluz H, et al. Phosphoproteins in extracellular vesicles as candidate markers for breast cancer. Proc Natl Acad Sci U S A. 2017;114(12):3175-80.
14. Foulds PG, Diggle P, Mitchell JD, Parker A, Hasegawa M, Masuda-Suzukake M, et al. A longitudinal study on alpha-synuclein in blood plasma as a biomarker for Parkinson's disease. Sci Rep. 2013;3:2540.
15. Marrero JA, Romano PR, Nikolaeva O, Steel L, Mehta A, Fimmel CJ, et al. GP73, a resident Golgi glycoprotein, is a novel serum marker for hepatocellular carcinoma. J Hepatol. 2005;43(6):1007-12.
16. Kawahara R, Ortega F, Rosa-Fernandes L, Guimaraes V, Quina D, Nahas W, et al. Distinct urinary glycoprotein signatures in prostate cancer patients. Oncotarget. 2018;9(69):33077-97.
17. Ghosh P, Vaidya A, Sahoo R, Goldfine A, Herring N, Bry L, et al. Glycation of the complement regulatory protein CD59 is a novel biomarker for glucose handling in humans. J Clin Endocrinol Metab. 2014;99(6):E999-e1006.

18. Stanta JL, Saldova R, Struwe WB, Byrne JC, Leweke FM, Rothermund M, et al. Identification of N-glycosylation changes in the CSF and serum in patients with schizophrenia. J Proteome Res. 2010;9(9):4476-89.
19. Mueller TM, Meador-Woodruff JH. Post-translational protein modifications in schizophrenia. NPJ Schizophr. 2020;6(1):5.
20. Ma W, Kantarjian H, Zhang X, Wang X, Estrov Z, O'Brien S, et al. Ubiquitin-proteasome system profiling in acute leukemias and its clinical relevance. Leuk Res. 2011;35(4):526-33.
21. Ohrfelt A, Johansson P, Wallin A, Andreasson U, Zetterberg H, Blennow K, et al. Increased Cerebrospinal Fluid Levels of Ubiquitin Carboxyl-Terminal Hydrolase L1 in Patients with Alzheimer's Disease. Dement Geriatr Cogn Dis Extra. 2016;6(2):283-94.
22. Rawlings ND, Barrett AJ, Bateman A. MEROPS: the database of proteolytic enzymes, their substrates and inhibitors. Nucleic Acids Res. 2012;40(Database issue):D343-50.
23. Hershko A, Ciechanover A. The ubiquitin system. Annu Rev Biochem. 1998;67:425-79.
24. Klein T, Eckhard U, Dufour A, Solis N, Overall CM. Proteolytic Cleavage-Mechanisms, Function, and "Omic" Approaches for a Near-Ubiquitous Posttranslational Modification. Chem Rev. 2018;118(3):1137-68.
25. Julius D, Blair L, Brake A, Sprague G, Thorner J. Yeast alpha factor is processed from a larger precursor polypeptide: the essential role of a membrane-bound dipeptidyl aminopeptidase. Cell. 1983;32(3):839-52.
26. Julius D, Brake A, Blair L, Kunisawa R, Thorner J. Isolation of the putative structural gene for the lysine-arginine-cleaving endopeptidase required for processing of yeast prepro-alpha-factor. Cell. 1984;37(3):1075-89.
27. Fuller RS, Sterne RE, Thorner J. Enzymes required for yeast prohormone processing. Annu Rev Physiol. 1988;50:345-62.
28. Leibowitz MJ, Wickner RB. A chromosomal gene required for killer plasmid expression, mating, and spore maturation in Saccharomyces cerevisiae. Proc Natl Acad Sci U S A. 1976;73(6):2061-5.
29. Rockwell NC, Thorner JW. The kindest cuts of all: crystal structures of Kex2 and furin reveal secrets of precursor processing. Trends Biochem Sci. 2004;29(2):80-7.
30. Chretien M, Li CH. Isolation, purification, and characterization of gamma-lipotropic hormone from sheep pituitary glands. Can J Biochem. 1967;45(7):1163-74.
31. Li CH, Geschwind, II, Cole RD, Raacke ID, Harris JI, Dixon JS. Amino-acid sequence of alpha-corticotropin. Nature. 1955;176(4484):687-9.
32. Chretien M, Mbikay M. 60 YEARS OF POMC: From the prohormone theory to pro-opiomelanocortin and to proprotein convertases (PCSK1 to PCSK9). J Mol Endocrinol. 2016;56(4):T49-62.
33. Sanger F. Chemistry of insulin; determination of the structure of insulin opens the way to greater understanding of life processes. Science. 1959;129(3359):1340-4.
34. Sanger F. Sequences, sequences, and sequences. Annu Rev Biochem. 1988;57:1-28.
35. Douglass J, Civelli O, Herbert E. Polyprotein gene expression: generation of diversity of neuroendocrine peptides. Annu Rev Biochem. 1984;53:665-715.
36. Chance RE, Ellis RM, Bromer WW. Porcine proinsulin: characterization and amino acid sequence. Science. 1968;161(3837):165-7.
37. Steiner DF, Cunningham D, Spigelman L, Aten B. Insulin biosynthesis: evidence for a precursor. Science. 1967;157(3789):697-700.
38. Steiner DF, Hallund O, Rubenstein A, Cho S, Bayliss C. Isolation and properties of proinsulin, intermediate forms, and other minor components from crystalline bovine insulin. Diabetes. 1968;17(12):725-36.
39. Chretien M. How the prohormone theory solved two important controversies in hormonal and neural Peptide biosynthesis. Front Endocrinol (Lausanne). 2013;4:148.

40. Puente XS, Sanchez LM, Overall CM, Lopez-Otin C. Human and mouse proteases: a comparative genomic approach. Nat Rev Genet. 2003;4(7):544-58.
41. Chen S, Yim JJ, Bogyo M. Synthetic and biological approaches to map substrate specificities of proteases. Biol Chem. 2019;401(1):165-82.
42. Rockwell NC, Wang GT, Krafft GA, Fuller RS. Internally consistent libraries of fluorogenic substrates demonstrate that Kex2 protease specificity is generated by multiple mechanisms. Biochemistry. 1997;36(7):1912-7.
43. Siezen RJ, Leunissen JA. Subtilases: the superfamily of subtilisin-like serine proteases. Protein Sci. 1997;6(3):501-23.
44. Schechter I, Berger A. On the size of the active site in proteases. I. Papain. Biochem Biophys Res Commun. 1967;27(2):157-62.
45. Vizovisek M, Vidmar R, Drag M, Fonovic M, Salvesen GS, Turk B. Protease Specificity: Towards In Vivo Imaging Applications and Biomarker Discovery. Trends Biochem Sci. 2018;43(10):829-44.
46. Kleifeld O, Doucet A, auf dem Keller U, Prudova A, Schilling O, Kainthan RK, et al. Isotopic labeling of terminal amines in complex samples identifies protein N-termini and protease cleavage products. Nat Biotechnol. 2010;28(3):281-8.
47. Verhamme IM, Leonard SE, Perkins RC. Proteases: Pivot Points in Functional Proteomics. Methods Mol Biol. 2019;1871:313-92.
48. Brown MS, Ye J, Rawson RB, Goldstein JL. Regulated intramembrane proteolysis: a control mechanism conserved from bacteria to humans. Cell. 2000;100(4):391-8.
49. Lichtenthaler SF, Steiner H. Sheddases and intramembrane-cleaving proteases: RIPpers of the membrane. Symposium on regulated intramembrane proteolysis. EMBO Rep. 2007;8(6):537-41.
50. Urban S. A guide to the rhomboid protein superfamily in development and disease. Semin Cell Dev Biol. 2016;60:1-4.
51. Urban S, Dickey SW. The rhomboid protease family: a decade of progress on function and mechanism. Genome Biol. 2011;12(10):231.
52. Lichtenthaler SF, Haass C, Steiner H. Regulated intramembrane proteolysis--lessons from amyloid precursor protein processing. J Neurochem. 2011;117(5):779-96.
53. Hardy J, Selkoe DJ. The amyloid hypothesis of Alzheimer's disease: progress and problems on the road to therapeutics. Science. 2002;297(5580):353-6.
54. Cao X, Sudhof TC. Dissection of amyloid-beta precursor protein-dependent transcriptional transactivation. J Biol Chem. 2004;279(23):24601-11.
55. Cao X, Sudhof TC. A transcriptionally [correction of transcriptively] active complex of APP with Fe65 and histone acetyltransferase Tip60. Science. 2001;293(5527):115-20.
56. Furukawa K, Sopher BL, Rydel RE, Begley JG, Pham DG, Martin GM, et al. Increased activity-regulating and neuroprotective efficacy of alpha-secretase-derived secreted amyloid precursor protein conferred by a C-terminal heparin-binding domain. J Neurochem. 1996;67(5):1882-96.
57. Meziane H, Dodart JC, Mathis C, Little S, Clemens J, Paul SM, et al. Memory-enhancing effects of secreted forms of the beta-amyloid precursor protein in normal and amnestic mice. Proc Natl Acad Sci U S A. 1998;95(21):12683-8.
58. Rice HC, de Malmazet D, Schreurs A, Frere S, Van Molle I, Volkov AN, et al. Secreted amyloid-β precursor protein functions as a GABA(B)R1a ligand to modulate synaptic transmission. Science. 2019;363(6423).
59. Lichtenthaler SF, Lemberg MK, Fluhrer R. Proteolytic ectodomain shedding of membrane proteins in mammals-hardware, concepts, and recent developments. Embo j. 2018;37(15).
60. Black PH. Shedding from normal and cancer-cell surfaces. N Engl J Med. 1980;303(24):1415-6.
61. Ehlers MR, Riordan JF. Membrane proteins with soluble counterparts: role of proteolysis in the release of transmembrane proteins. Biochemistry. 1991;30(42):10065-74.

62. Kapeller M, Gal-Oz R, Grover NB, Doljanski F. Natural shedding of carbohydrate-containing macromolecules from cell surfaces. Exp Cell Res. 1973;79(1):152-8.
63. Laurent SA, Hoffmann FS, Kuhn PH, Cheng Q, Chu Y, Schmidt-Supprian M, et al. gamma-Secretase directly sheds the survival receptor BCMA from plasma cells. Nat Commun. 2015;6:7333.
64. De Strooper B, Annaert W, Cupers P, Saftig P, Craessaerts K, Mumm JS, et al. A presenilin-1-dependent gamma-secretase-like protease mediates release of Notch intracellular domain. Nature. 1999;398(6727):518-22.
65. Laskar A, Rodger EJ, Chatterjee A, Mandal C. Modeling and structural analysis of PA clan serine proteases. BMC Res Notes. 2012;5:256.
66. Puente XS, Sanchez LM, Gutierrez-Fernandez A, Velasco G, Lopez-Otin C. A genomic view of the complexity of mammalian proteolytic systems. Biochem Soc Trans. 2005;33(Pt 2):331-4.
67. Barrett AJ, Rawlings ND. Families and clans of serine peptidases. Arch Biochem Biophys. 1995;318(2):247-50.
68. Gohara DW, Di Cera E. Allostery in trypsin-like proteases suggests new therapeutic strategies. Trends Biotechnol. 2011;29(11):577-85.
69. Patel S. A critical review on serine protease: Key immune manipulator and pathology mediator. Allergol Immunopathol (Madr). 2017;45(6):579-91.
70. Barr PJ. Mammalian subtilisins: the long-sought dibasic processing endoproteases. Cell. 1991;66(1):1-3.
71. Van de Ven WJ, Roebroek AJ, Van Duijnhoven HL. Structure and function of eukaryotic proprotein processing enzymes of the subtilisin family of serine proteases. Crit Rev Oncog. 1993;4(2):115-36.
72. Hedstrom L. Serine protease mechanism and specificity. Chem Rev. 2002;102(12):4501-24.
73. Perona JJ, Craik CS. Structural basis of substrate specificity in the serine proteases. Protein Sci. 1995;4(3):337-60.
74. Page MJ, Di Cera E. Evolution of peptidase diversity. J Biol Chem. 2008;283(44):30010-4.
75. David P. Clark NJP. Chapter 9 - Proteomics2016. Pages 295-333 p.
76. Di Cera E. Serine proteases. IUBMB Life. 2009;61(5):510-5.
77. Gailani D, Renne T. Intrinsic pathway of coagulation and arterial thrombosis. Arterioscler Thromb Vasc Biol. 2007;27(12):2507-13.
78. Rothman SS. The digestive enzymes of the pancreas: a mixture of inconstant proportions. Annu Rev Physiol. 1977;39:373-89.
79. Olsen JV, Ong SE, Mann M. Trypsin cleaves exclusively C-terminal to arginine and lysine residues. Mol Cell Proteomics. 2004;3(6):608-14.
80. Heutinck KM, ten Berge IJ, Hack CE, Hamann J, Rowshani AT. Serine proteases of the human immune system in health and disease. Mol Immunol. 2010;47(11-12):1943-55.
81. de Koning PJ, Kummer JA, de Poot SA, Quadir R, Broekhuizen R, McGettrick AF, et al. Intracellular serine protease inhibitor SERPINB4 inhibits granzyme M-induced cell death. PLoS One. 2011;6(8):e22645.
82. Tanabe LM, List K. The role of type II transmembrane serine protease-mediated signaling in cancer. Febs j. 2017;284(10):1421-36.
83. Jaaks P, Bernasconi M. The proprotein convertase furin in tumour progression. Int J Cancer. 2017;141(4):654-63.
84. Martin CE, List K. Cell surface-anchored serine proteases in cancer progression and metastasis. Cancer Metastasis Rev. 2019;38(3):357-87.
85. Loessner D, Goettig P, Preis S, Felber J, Bronger H, Clements JA, et al. Kallikrein-related peptidases represent attractive therapeutic targets for ovarian cancer. Expert Opin Ther Targets. 2018;22(9):745-63.

86. Prassas I, Eissa A, Poda G, Diamandis EP. Unleashing the therapeutic potential of human kallikrein-related serine proteases. Nat Rev Drug Discov. 2015;14(3):183-202.
87. Diamandis EP, Borgono CA, Scorilas A, Yousef GM, Harbeck N, Dorn J, et al. Immunofluorometric quantification of human kallikrein 5 expression in ovarian cancer cytosols and its association with unfavorable patient prognosis. Tumour Biol. 2003;24(6):299-309.
88. Diamandis EP, Scorilas A, Fracchioli S, Van Gramberen M, De Bruijn H, Henrik A, et al. Human kallikrein 6 (hK6): a new potential serum biomarker for diagnosis and prognosis of ovarian carcinoma. J Clin Oncol. 2003;21(6):1035-43.
89. Koh SC, Huak CY, Lutan D, Marpuang J, Ketut S, Budiana NG, et al. Combined panel of serum human tissue kallikreins and CA-125 for the detection of epithelial ovarian cancer. J Gynecol Oncol. 2012;23(3):175-81.
90. Dorn J, Schmitt M, Kates R, Schmalfeldt B, Kiechle M, Scorilas A, et al. Primary tumor levels of human tissue kallikreins affect surgical success and survival in ovarian cancer patients. Clin Cancer Res. 2007;13(6):1742-8.
91. Geng X, Liu Y, Diersch S, Kotzsch M, Grill S, Weichert W, et al. Clinical relevance of kallikrein-related peptidase 9, 10, 11, and 15 mRNA expression in advanced high-grade serous ovarian cancer. PLoS One. 2017;12(11):e0186847.
92. Seidah NG. The proprotein convertases, 20 years later. Methods Mol Biol. 2011;768:23-57.
93. Mizuno K, Nakamura T, Ohshima T, Tanaka S, Matsuo H. Yeast KEX2 genes encodes an endopeptidase homologous to subtilisin-like serine proteases. Biochem Biophys Res Commun. 1988;156(1):246-54.
94. Seidah NG, Gaspar L, Mion P, Marcinkiewicz M, Mbikay M, Chretien M. cDNA sequence of two distinct pituitary proteins homologous to Kex2 and furin gene products: tissue-specific mRNAs encoding candidates for pro-hormone processing proteinases. DNA Cell Biol. 1990;9(6):415-24.
95. Thomas G, Thorne BA, Thomas L, Allen RG, Hruby DE, Fuller R, et al. Yeast KEX2 endopeptidase correctly cleaves a neuroendocrine prohormone in mammalian cells. Science. 1988;241(4862):226-30.
96. Bourbonnais Y, Germain D, Ash J, Thomas DY. Cleavage of prosomatostatins by the yeast Yap3 and Kex2 endoprotease. Biochimie. 1994;76(3-4):226-33.
97. van de Ven WJ, Voorberg J, Fontijn R, Pannekoek H, van den Ouweland AM, van Duijnhoven HL, et al. Furin is a subtilisin-like proprotein processing enzyme in higher eukaryotes. Mol Biol Rep. 1990;14(4):265-75.
98. Smeekens SP, Avruch AS, LaMendola J, Chan SJ, Steiner DF. Identification of a cDNA encoding a second putative prohormone convertase related to PC2 in AtT20 cells and islets of Langerhans. Proc Natl Acad Sci U S A. 1991;88(2):340-4.
99. Smeekens SP, Steiner DF. Identification of a human insulinoma cDNA encoding a novel mammalian protein structurally related to the yeast dibasic processing protease Kex2. J Biol Chem. 1990;265(6):2997-3000.
100. Seidah NG, Marcinkiewicz M, Benjannet S, Gaspar L, Beaubien G, Mattei MG, et al. Cloning and primary sequence of a mouse candidate prohormone convertase PC1 homologous to PC2, Furin, and Kex2: distinct chromosomal localization and messenger RNA distribution in brain and pituitary compared to PC2. Mol Endocrinol. 1991;5(1):111-22.
101. Espenshade PJ, Cheng D, Goldstein JL, Brown MS. Autocatalytic processing of site-1 protease removes propeptide and permits cleavage of sterol regulatory element-binding proteins. J Biol Chem. 1999;274(32):22795-804.
102. Seidah NG, Benjannet S, Wickham L, Marcinkiewicz J, Jasmin SB, Stifani S, et al. The secretory proprotein convertase neural apoptosis-regulated convertase 1 (NARC-1): liver regeneration and neuronal differentiation. Proc Natl Acad Sci U S A. 2003;100(3):928-33.

103. Turpeinen H, Kukkurainen S, Pulkkinen K, Kauppila T, Ojala K, Hytonen VP, et al. Identification of proprotein convertase substrates using genome-wide expression correlation analysis. BMC Genomics. 2011;12:618.
104. Zhou A, Martin S, Lipkind G, LaMendola J, Steiner DF. Regulatory roles of the P domain of the subtilisin-like prohormone convertases. J Biol Chem. 1998;273(18):11107-14.
105. Mbikay M, Seidah NG, Chretien M. Neuroendocrine secretory protein 7B2: structure, expression and functions. Biochem J. 2001;357(Pt 2):329-42.
106. Hsi KL, Seidah NG, De Serres G, Chretien M. Isolation and NH2-terminal sequence of a novel porcine anterior pituitary polypeptide. Homology to proinsulin, secretin and Rous sarcoma virus transforming protein TVFV60. FEBS Lett. 1982;147(2):261-6.
107. Benjannet S, Reudelhuber T, Mercure C, Rondeau N, Chretien M, Seidah NG. Proprotein conversion is determined by a multiplicity of factors including convertase processing, substrate specificity, and intracellular environment. Cell type-specific processing of human prorenin by the convertase PC1. J Biol Chem. 1992;267(16):11417-23.
108. Malide D, Seidah NG, Chretien M, Bendayan M. Electron microscopic immunocytochemical evidence for the involvement of the convertases PC1 and PC2 in the processing of proinsulin in pancreatic beta-cells. J Histochem Cytochem. 1995;43(1):11-9.
109. Day R, Schafer MK, Watson SJ, Chretien M, Seidah NG. Distribution and regulation of the prohormone convertases PC1 and PC2 in the rat pituitary. Mol Endocrinol. 1992;6(3):485-97.
110. Vazquez-Martinez R, Gasman S. The regulated secretory pathway in neuroendocrine cells. Front Endocrinol (Lausanne). 2014;5:48.
111. Dong W, Seidel B, Marcinkiewicz M, Chretien M, Seidah NG, Day R. Cellular localization of the prohormone convertases in the hypothalamic paraventricular and supraoptic nuclei: selective regulation of PC1 in corticotrophin-releasing hormone parvocellular neurons mediated by glucocorticoids. J Neurosci. 1997;17(2):563-75.
112. Billova S, Galanopoulou AS, Seidah NG, Qiu X, Kumar U. Immunohistochemical expression and colocalization of somatostatin, carboxypeptidase-E and prohormone convertases 1 and 2 in rat brain. Neuroscience. 2007;147(2):403-18.
113. Feng Y, Reznik SE, Fricker LD. Distribution of proSAAS-derived peptides in rat neuroendocrine tissues. Neuroscience. 2001;105(2):469-78.
114. Schafer MK, Day R, Cullinan WE, Chretien M, Seidah NG, Watson SJ. Gene expression of prohormone and proprotein convertases in the rat CNS: a comparative in situ hybridization analysis. J Neurosci. 1993;13(3):1258-79.
115. Tanaka S, Kurabuchi S, Mochida H, Kato T, Takahashi S, Watanabe T, et al. Immunocytochemical localization of prohormone convertases PC1/PC3 and PC2 in rat pancreatic islets. Arch Histol Cytol. 1996;59(3):261-71.
116. Kurabuchi S, Tanaka S. Immunocytochemical localization of prohormone convertases PC1 and PC2 in the mouse thyroid gland and respiratory tract. J Histochem Cytochem. 2002;50(7):903-9.
117. Damholt AB, Buchan AM, Holst JJ, Kofod H. Proglucagon processing profile in canine L cells expressing endogenous prohormone convertase 1/3 and prohormone convertase 2. Endocrinology. 1999;140(10):4800-8.
118. Benjannet S, Rondeau N, Day R, Chretien M, Seidah NG. PC1 and PC2 are proprotein convertases capable of cleaving proopiomelanocortin at distinct pairs of basic residues. Proc Natl Acad Sci U S A. 1991;88(9):3564-8.
119. Kaufmann JE, Irminger JC, Mungall J, Halban PA. Proinsulin conversion in GH3 cells after coexpression of human proinsulin with the endoproteases PC2 and/or PC3. Diabetes. 1997;46(6):978-82.

120. Irminger JC, Meyer K, Halban P. Proinsulin processing in the rat insulinoma cell line INS after overexpression of the endoproteases PC2 or PC3 by recombinant adenovirus. Biochem J. 1996;320 (Pt 1):11-5.
121. Zhu X, Zhou A, Dey A, Norrbom C, Carroll R, Zhang C, et al. Disruption of PC1/3 expression in mice causes dwarfism and multiple neuroendocrine peptide processing defects. Proc Natl Acad Sci U S A. 2002;99(16):10293-8.
122. Furuta M, Zhou A, Webb G, Carroll R, Ravazzola M, Orci L, et al. Severe defect in proglucagon processing in islet A-cells of prohormone convertase 2 null mice. J Biol Chem. 2001;276(29):27197-202.
123. Furuta M, Yano H, Zhou A, Rouille Y, Holst JJ, Carroll R, et al. Defective prohormone processing and altered pancreatic islet morphology in mice lacking active SPC2. Proc Natl Acad Sci U S A. 1997;94(13):6646-51.
124. O'Rahilly S, Gray H, Humphreys PJ, Krook A, Polonsky KS, White A, et al. Brief report: impaired processing of prohormones associated with abnormalities of glucose homeostasis and adrenal function. N Engl J Med. 1995;333(21):1386-90.
125. Stijnen P, Ramos-Molina B, O'Rahilly S, Creemers JW. PCSK1 Mutations and Human Endocrinopathies: From Obesity to Gastrointestinal Disorders. Endocr Rev. 2016;37(4):347-71.
126. Jackson RS, Creemers JW, Ohagi S, Raffin-Sanson ML, Sanders L, Montague CT, et al. Obesity and impaired prohormone processing associated with mutations in the human prohormone convertase 1 gene. Nat Genet. 1997;16(3):303-6.
127. Benzinou M, Creemers JW, Choquet H, Lobbens S, Dina C, Durand E, et al. Common nonsynonymous variants in PCSK1 confer risk of obesity. Nat Genet. 2008;40(8):943-5.
128. Gyamera-Acheampong C, Sirois F, Denis NJ, Mishra P, Figeys D, Basak A, et al. The precursor to the germ cell-specific PCSK4 proteinase is inefficiently activated in transfected somatic cells: evidence of interaction with the BiP chaperone. Mol Cell Biochem. 2011;348(1-2):43-52.
129. Rousselet E, Benjannet S, Hamelin J, Canuel M, Seidah NG. The proprotein convertase PC7: unique zymogen activation and trafficking pathways. J Biol Chem. 2011;286(4):2728-38.
130. Seidah NG, Day R, Hamelin J, Gaspar A, Collard MW, Chretien M. Testicular expression of PC4 in the rat: molecular diversity of a novel germ cell-specific Kex2/subtilisin-like proprotein convertase. Mol Endocrinol. 1992;6(10):1559-70.
131. Gyamera-Acheampong C, Tantibhedhyangkul J, Weerachatyanukul W, Tadros H, Xu H, van de Loo JW, et al. Sperm from mice genetically deficient for the PCSK4 proteinase exhibit accelerated capacitation, precocious acrosome reaction, reduced binding to egg zona pellucida, and impaired fertilizing ability. Biol Reprod. 2006;74(4):666-73.
132. Gyamera-Acheampong C, Mbikay M. Proprotein convertase subtilisin/kexin type 4 in mammalian fertility: a review. Hum Reprod Update. 2009;15(2):237-47.
133. Li M, Mbikay M, Arimura A. Pituitary adenylate cyclase-activating polypeptide precursor is processed solely by prohormone convertase 4 in the gonads. Endocrinology. 2000;141(10):3723-30.
134. Cho C, Bunch DO, Faure JE, Goulding EH, Eddy EM, Primakoff P, et al. Fertilization defects in sperm from mice lacking fertilin beta. Science. 1998;281(5384):1857-9.
135. Shamsadin R, Adham IM, Nayernia K, Heinlein UA, Oberwinkler H, Engel W. Male mice deficient for germ-cell cyritestin are infertile. Biol Reprod. 1999;61(6):1445-51.
136. Gyamera-Acheampong C, Vasilescu J, Figeys D, Mbikay M. PCSK4-null sperm display enhanced protein tyrosine phosphorylation and ADAM2 proteolytic processing during in vitro capacitation. Fertil Steril. 2010;93(4):1112-23.
137. Lusson J, Vieau D, Hamelin J, Day R, Chretien M, Seidah NG. cDNA structure of the mouse and rat subtilisin/kexin-like PC5: a candidate proprotein convertase expressed in endocrine and nonendocrine cells. Proc Natl Acad Sci U S A. 1993;90(14):6691-5.

138. Essalmani R, Hamelin J, Marcinkiewicz J, Chamberland A, Mbikay M, Chretien M, et al. Deletion of the gene encoding proprotein convertase 5/6 causes early embryonic lethality in the mouse. Mol Cell Biol. 2006;26(1):354-61.
139. Seidah NG, Mayer G, Zaid A, Rousselet E, Nassoury N, Poirier S, et al. The activation and physiological functions of the proprotein convertases. Int J Biochem Cell Biol. 2008;40(6-7):1111-25.
140. Nakagawa T, Hosaka M, Torii S, Watanabe T, Murakami K, Nakayama K. Identification and functional expression of a new member of the mammalian Kex2-like processing endoprotease family: its striking structural similarity to PACE4. J Biochem. 1993;113(2):132-5.
141. Nakagawa T, Murakami K, Nakayama K. Identification of an isoform with an extremely large Cys-rich region of PC6, a Kex2-like processing endoprotease. FEBS Lett. 1993;327(2):165-71.
142. Essalmani R, Zaid A, Marcinkiewicz J, Chamberland A, Pasquato A, Seidah NG, et al. In vivo functions of the proprotein convertase PC5/6 during mouse development: Gdf11 is a likely substrate. Proc Natl Acad Sci U S A. 2008;105(15):5750-5.
143. McPherron AC, Lawler AM, Lee SJ. Regulation of anterior/posterior patterning of the axial skeleton by growth/differentiation factor 11. Nat Genet. 1999;22(3):260-4.
144. Szumska D, Pieles G, Essalmani R, Bilski M, Mesnard D, Kaur K, et al. VACTERL/caudal regression/Currarino syndrome-like malformations in mice with mutation in the proprotein convertase Pcsk5. Genes Dev. 2008;22(11):1465-77.
145. Iatan I, Dastani Z, Do R, Weissglas-Volkov D, Ruel I, Lee JC, et al. Genetic variation at the proprotein convertase subtilisin/kexin type 5 gene modulates high-density lipoprotein cholesterol levels. Circ Cardiovasc Genet. 2009;2(5):467-75.
146. Stawowy P, Fleck E. Proprotein convertases furin and PC5: targeting atherosclerosis and restenosis at multiple levels. J Mol Med (Berl). 2005;83(11):865-75.
147. Sun X, Essalmani R, Seidah NG, Prat A. The proprotein convertase PC5/6 is protective against intestinal tumorigenesis: in vivo mouse model. Mol Cancer. 2009;8:73.
148. Hoac B, Susan-Resiga D, Essalmani R, Marcinkiweicz E, Seidah NG, McKee MD. Osteopontin as a novel substrate for the proprotein convertase 5/6 (PCSK5) in bone. Bone. 2018;107:45-55.
149. Tsuji A, Sakurai K, Kiyokage E, Yamazaki T, Koide S, Toida K, et al. Secretory proprotein convertases PACE4 and PC6A are heparin-binding proteins which are localized in the extracellular matrix. Potential role of PACE4 in the activation of proproteins in the extracellular matrix. Biochim Biophys Acta. 2003;1645(1):95-104.
150. Nour N, Mayer G, Mort JS, Salvas A, Mbikay M, Morrison CJ, et al. The cysteine-rich domain of the secreted proprotein convertases PC5A and PACE4 functions as a cell surface anchor and interacts with tissue inhibitors of metalloproteinases. Mol Biol Cell. 2005;16(11):5215-26.
151. Mesnard D, Donnison M, Fuerer C, Pfeffer PL, Constam DB. The microenvironment patterns the pluripotent mouse epiblast through paracrine Furin and Pace4 proteolytic activities. Genes Dev. 2011;25(17):1871-80.
152. Tortorella MD, Arner EC, Hills R, Gormley J, Fok K, Pegg L, et al. ADAMTS-4 (aggrecanase-1): N-terminal activation mechanisms. Arch Biochem Biophys. 2005;444(1):34-44.
153. Liu J, Afroza H, Rader DJ, Jin W. Angiopoietin-like protein 3 inhibits lipoprotein lipase activity through enhancing its cleavage by proprotein convertases. J Biol Chem. 2010;285(36):27561-70.
154. Xiao Y, Chen G, Richard J, Rougeau N, Li H, Seidah NG, et al. Cell-surface processing of extracellular human immunodeficiency virus type 1 Vpr by proprotein convertases. Virology. 2008;372(2):384-97.
155. Constam DB, Robertson EJ. SPC4/PACE4 regulates a TGFbeta signaling network during axis formation. Genes Dev. 2000;14(9):1146-55.
156. D'Anjou F, Routhier S, Perreault JP, Latil A, Bonnel D, Fournier I, et al. Molecular Validation of PACE4 as a Target in Prostate Cancer. Transl Oncol. 2011;4(3):157-72.

157. Couture F, Sabbagh R, Kwiatkowska A, Desjardins R, Guay SP, Bouchard L, et al. PACE4 Undergoes an Oncogenic Alternative Splicing Switch in Cancer. Cancer Res. 2017;77(24):6863-79.
158. Thomas G. Furin at the cutting edge: from protein traffic to embryogenesis and disease. Nat Rev Mol Cell Biol. 2002;3(10):753-66.
159. Plaimauer B, Mohr G, Wernhart W, Himmelspach M, Dorner F, Schlokat U. 'Shed' furin: mapping of the cleavage determinants and identification of its C-terminus. Biochem J. 2001;354(Pt 3):689-95.
160. Griffiths G, Simons K. The trans Golgi network: sorting at the exit site of the Golgi complex. Science. 1986;234(4775):438-43.
161. Molloy SS, Anderson ED, Jean F, Thomas G. Bi-cycling the furin pathway: from TGN localization to pathogen activation and embryogenesis. Trends Cell Biol. 1999;9(1):28-35.
162. Bosshart H, Humphrey J, Deignan E, Davidson J, Drazba J, Yuan L, et al. The cytoplasmic domain mediates localization of furin to the trans-Golgi network en route to the endosomal/lysosomal system. J Cell Biol. 1994;126(5):1157-72.
163. Schafer W, Stroh A, Berghofer S, Seiler J, Vey M, Kruse ML, et al. Two independent targeting signals in the cytoplasmic domain determine trans-Golgi network localization and endosomal trafficking of the proprotein convertase furin. Embo j. 1995;14(11):2424-35.
164. Takahashi S, Nakagawa T, Banno T, Watanabe T, Murakami K, Nakayama K. Localization of furin to the trans-Golgi network and recycling from the cell surface involves Ser and Tyr residues within the cytoplasmic domain. J Biol Chem. 1995;270(47):28397-401.
165. Teuchert M, Schafer W, Berghofer S, Hoflack B, Klenk HD, Garten W. Sorting of furin at the trans-Golgi network. Interaction of the cytoplasmic tail sorting signals with AP-1 Golgi-specific assembly proteins. J Biol Chem. 1999;274(12):8199-207.
166. Wan L, Molloy SS, Thomas L, Liu G, Xiang Y, Rybak SL, et al. PACS-1 defines a novel gene family of cytosolic sorting proteins required for trans-Golgi network localization. Cell. 1998;94(2):205-16.
167. Roebroek AJ, Umans L, Pauli IG, Robertson EJ, van Leuven F, Van de Ven WJ, et al. Failure of ventral closure and axial rotation in embryos lacking the proprotein convertase Furin. Development. 1998;125(24):4863-76.
168. Constam DB, Robertson EJ. Tissue-specific requirements for the proprotein convertase furin/SPC1 during embryonic turning and heart looping. Development. 2000;127(2):245-54.
169. Cui Y, Hackenmiller R, Berg L, Jean F, Nakayama T, Thomas G, et al. The activity and signaling range of mature BMP-4 is regulated by sequential cleavage at two sites within the prodomain of the precursor. Genes Dev. 2001;15(21):2797-802.
170. Susan-Resiga D, Essalmani R, Hamelin J, Asselin MC, Benjannet S, Chamberland A, et al. Furin is the major processing enzyme of the cardiac-specific growth factor bone morphogenetic protein 10. J Biol Chem. 2011;286(26):22785-94.
171. Teng HK, Teng KK, Lee R, Wright S, Tevar S, Almeida RD, et al. ProBDNF induces neuronal apoptosis via activation of a receptor complex of p75NTR and sortilin. J Neurosci. 2005;25(22):5455-63.
172. Logeat F, Bessia C, Brou C, LeBail O, Jarriault S, Seidah NG, et al. The Notch1 receptor is cleaved constitutively by a furin-like convertase. Proc Natl Acad Sci U S A. 1998;95(14):8108-12.
173. Mumm JS, Schroeter EH, Saxena MT, Griesemer A, Tian X, Pan DJ, et al. A ligand-induced extracellular cleavage regulates gamma-secretase-like proteolytic activation of Notch1. Mol Cell. 2000;5(2):197-206.
174. Bush G, diSibio G, Miyamoto A, Denault JB, Leduc R, Weinmaster G. Ligand-induced signaling in the absence of furin processing of Notch1. Dev Biol. 2001;229(2):494-502.
175. Roebroek AJ, Taylor NA, Louagie E, Pauli I, Smeijers L, Snellinx A, et al. Limited redundancy of the proprotein convertase furin in mouse liver. J Biol Chem. 2004;279(51):53442-50.
176. Bhattacharyya N, Chong WH, Gafni RI, Collins MT. Fibroblast growth factor 23: state of the field and future directions. Trends Endocrinol Metab. 2012;23(12):610-8.

177. White KE, Carn G, Lorenz-Depiereux B, Benet-Pages A, Strom TM, Econs MJ. Autosomal-dominant hypophosphatemic rickets (ADHR) mutations stabilize FGF-23. Kidney Int. 2001;60(6):2079-86.
178. Kato K, Jeanneau C, Tarp MA, Benet-Pages A, Lorenz-Depiereux B, Bennett EP, et al. Polypeptide GalNAc-transferase T3 and familial tumoral calcinosis. Secretion of fibroblast growth factor 23 requires O-glycosylation. J Biol Chem. 2006;281(27):18370-7.
179. Tagliabracci VS, Wiley SE, Guo X, Kinch LN, Durrant E, Wen J, et al. A Single Kinase Generates the Majority of the Secreted Phosphoproteome. Cell. 2015;161(7):1619-32.
180. Tagliabracci VS, Engel JL, Wiley SE, Xiao J, Gonzalez DJ, Nidumanda Appaiah H, et al. Dynamic regulation of FGF23 by Fam20C phosphorylation, GalNAc-T3 glycosylation, and furin proteolysis. Proc Natl Acad Sci U S A. 2014;111(15):5520-5.
181. Roberts AB, Anzano MA, Lamb LC, Smith JM, Sporn MB. New class of transforming growth factors potentiated by epidermal growth factor: isolation from non-neoplastic tissues. Proc Natl Acad Sci U S A. 1981;78(9):5339-43.
182. Padua D, Massague J. Roles of TGFbeta in metastasis. Cell Res. 2009;19(1):89-102.
183. Muraoka-Cook RS, Dumont N, Arteaga CL. Dual role of transforming growth factor beta in mammary tumorigenesis and metastatic progression. Clin Cancer Res. 2005;11(2 Pt 2):937s-43s.
184. McMahon S, Laprise MH, Dubois CM. Alternative pathway for the role of furin in tumor cell invasion process. Enhanced MMP-2 levels through bioactive TGFbeta. Exp Cell Res. 2003;291(2):326-39.
185. Hsia HE, Tushaus J, Brummer T, Zheng Y, Scilabra SD, Lichtenthaler SF. Functions of 'A disintegrin and metalloproteases (ADAMs)' in the mammalian nervous system. Cell Mol Life Sci. 2019;76(16):3055-81.
186. Sato H, Takino T, Okada Y, Cao J, Shinagawa A, Yamamoto E, et al. A matrix metalloproteinase expressed on the surface of invasive tumour cells. Nature. 1994;370(6484):61-5.
187. Ohuchi E, Imai K, Fujii Y, Sato H, Seiki M, Okada Y. Membrane type 1 matrix metalloproteinase digests interstitial collagens and other extracellular matrix macromolecules. J Biol Chem. 1997;272(4):2446-51.
188. Maret D, Sadr MS, Sadr ES, Colman DR, Del Maestro RF, Seidah NG. Opposite roles of furin and PC5A in N-cadherin processing. Neoplasia. 2012;14(10):880-92.
189. Ma YC, Fan WJ, Rao SM, Gao L, Bei ZY, Xu ST. Effect of Furin inhibitor on lung adenocarcinoma cell growth and metastasis. Cancer Cell Int. 2014;14:43.
190. Bassi DE, Mahloogi H, Al-Saleem L, Lopez De Cicco R, Ridge JA, Klein-Szanto AJ. Elevated furin expression in aggressive human head and neck tumors and tumor cell lines. Mol Carcinog. 2001;31(4):224-32.
191. Bassi DE, Mahloogi H, Lopez De Cicco R, Klein-Szanto A. Increased furin activity enhances the malignant phenotype of human head and neck cancer cells. Am J Pathol. 2003;162(2):439-47.
192. Lopez de Cicco R, Watson JC, Bassi DE, Litwin S, Klein-Szanto AJ. Simultaneous expression of furin and vascular endothelial growth factor in human oral tongue squamous cell carcinoma progression. Clin Cancer Res. 2004;10(13):4480-8.
193. Aznavoorian S, Moore BA, Alexander-Lister LD, Hallit SL, Windsor LJ, Engler JA. Membrane type I-matrix metalloproteinase-mediated degradation of type I collagen by oral squamous cell carcinoma cells. Cancer Res. 2001;61(16):6264-75.
194. Cepeda MA, Evered CL, Pelling JJH, Damjanovski S. Inhibition of MT1-MMP proteolytic function and ERK1/2 signalling influences cell migration and invasion through changes in MMP-2 and MMP-9 levels. J Cell Commun Signal. 2017;11(2):167-79.
195. Scamuffa N, Sfaxi F, Ma J, Lalou C, Seidah N, Calvo F, et al. Prodomain of the proprotein convertase subtilisin/kexin Furin (ppFurin) protects from tumor progression and metastasis. Carcinogenesis. 2014;35(3):528-36.

196. Cheng M, Xu N, Iwasiow B, Seidah N, Chretien M, Shiu RP. Elevated expression of proprotein convertases alters breast cancer cell growth in response to estrogen and tamoxifen. J Mol Endocrinol. 2001;26(2):95-105.
197. Page RE, Klein-Szanto AJ, Litwin S, Nicolas E, Al-Jumaily R, Alexander P, et al. Increased expression of the pro-protein convertase furin predicts decreased survival in ovarian cancer. Cell Oncol. 2007;29(4):289-99.
198. Jaaks P, D'Alessandro V, Grob N, Buel S, Hajdin K, Schafer BW, et al. The Proprotein Convertase Furin Contributes to Rhabdomyosarcoma Malignancy by Promoting Vascularization, Migration and Invasion. PLoS One. 2016;11(8):e0161396.
199. Mercapide J, Lopez De Cicco R, Bassi DE, Castresana JS, Thomas G, Klein-Szanto AJP. Inhibition of furin-mediated processing results in suppression of astrocytoma cell growth and invasiveness. Clin Cancer Res. 2002;8(6):1740-6.
200. Fu J, Bassi DE, Zhang J, Li T, Nicolas E, Klein-Szanto AJ. Transgenic overexpression of the proprotein convertase furin enhances skin tumor growth. Neoplasia. 2012;14(4):271-82.
201. Montalbano M, Rastellini C, McGuire JT, Prajapati J, Shirafkan A, Vento R, et al. Role of Glypican-3 in the growth, migration and invasion of primary hepatocytes isolated from patients with hepatocellular carcinoma. Cell Oncol (Dordr). 2018;41(2):169-84.
202. Basak A, Zhong M, Munzer JS, Chretien M, Seidah NG. Implication of the proprotein convertases furin, PC5 and PC7 in the cleavage of surface glycoproteins of Hong Kong, Ebola and respiratory syncytial viruses: a comparative analysis with fluorogenic peptides. Biochem J. 2001;353(Pt 3):537-45.
203. Moulard M, Chaloin L, Canarelli S, Mabrouk K, Darbon H. Retroviral envelope glycoprotein processing: structural investigation of the cleavage site. Biochemistry. 1998;37(13):4510-7.
204. Kim W, Zekas E, Lodge R, Susan-Resiga D, Marcinkiewicz E, Essalmani R, et al. Neuroinflammation-Induced Interactions between Protease-Activated Receptor 1 and Proprotein Convertases in HIV-Associated Neurocognitive Disorder. Mol Cell Biol. 2015;35(21):3684-700.
205. Dubay JW, Dubay SR, Shin HJ, Hunter E. Analysis of the cleavage site of the human immunodeficiency virus type 1 glycoprotein: requirement of precursor cleavage for glycoprotein incorporation. J Virol. 1995;69(8):4675-82.
206. Hallenberger S, Bosch V, Angliker H, Shaw E, Klenk HD, Garten W. Inhibition of furin-mediated cleavage activation of HIV-1 glycoprotein gp160. Nature. 1992;360(6402):358-61.
207. Volchkov VE, Feldmann H, Volchkova VA, Klenk HD. Processing of the Ebola virus glycoprotein by the proprotein convertase furin. Proc Natl Acad Sci U S A. 1998;95(10):5762-7.
208. Volchkov VE, Volchkova VA, Stroher U, Becker S, Dolnik O, Cieplik M, et al. Proteolytic processing of Marburg virus glycoprotein. Virology. 2000;268(1):1-6.
209. Stieneke-Grober A, Vey M, Angliker H, Shaw E, Thomas G, Roberts C, et al. Influenza virus hemagglutinin with multibasic cleavage site is activated by furin, a subtilisin-like endoprotease. Embo j. 1992;11(7):2407-14.
210. Coutard B, Valle C, de Lamballerie X, Canard B, Seidah NG, Decroly E. The spike glycoprotein of the new coronavirus 2019-nCoV contains a furin-like cleavage site absent in CoV of the same clade. Antiviral Res. 2020;176:104742.
211. Couture F, Kwiatkowska A, Dory YL, Day R. Therapeutic uses of furin and its inhibitors: a patent review. Expert Opin Ther Pat. 2015;25(4):379-96.
212. Anderson ED, Thomas L, Hayflick JS, Thomas G. Inhibition of HIV-1 gp160-dependent membrane fusion by a furin-directed alpha 1-antitrypsin variant. J Biol Chem. 1993;268(33):24887-91.
213. Cameron A, Appel J, Houghten RA, Lindberg I. Polyarginines are potent furin inhibitors. J Biol Chem. 2000;275(47):36741-9.

214. Henrich S, Cameron A, Bourenkov GP, Kiefersauer R, Huber R, Lindberg I, et al. The crystal structure of the proprotein processing proteinase furin explains its stringent specificity. Nat Struct Biol. 2003;10(7):520-6.
215. Sachan V, Lodge R, Mihara K, Hamelin J, Power C, Gelman BB, et al. HIV-induced neuroinflammation: impact of PAR1 and PAR2 processing by Furin. Cell Death Differ. 2019;26(10):1942-54.
216. Tome M, Pappalardo A, Soulet F, Lopez JJ, Olaizola J, Leger Y, et al. Inactivation of Proprotein Convertases in T Cells Inhibits PD-1 Expression and Creates a Favorable Immune Microenvironment in Colorectal Cancer. Cancer Res. 2019;79(19):5008-21.
217. Basak A, Lotfipour F. Modulating furin activity with designed mini-PDX peptides: synthesis and in vitro kinetic evaluation. FEBS Lett. 2005;579(21):4813-21.
218. Lu W, Zhang W, Molloy SS, Thomas G, Ryan K, Chiang Y, et al. Arg15-Lys17-Arg18 turkey ovomucoid third domain inhibits human furin. J Biol Chem. 1993;268(20):14583-5.
219. Kibler KV, Miyazato A, Yedavalli VS, Dayton AI, Jacobs BL, Dapolito G, et al. Polyarginine inhibits gp160 processing by furin and suppresses productive human immunodeficiency virus type 1 infection. J Biol Chem. 2004;279(47):49055-63.
220. Sarac MS, Peinado JR, Leppla SH, Lindberg I. Protection against anthrax toxemia by hexa-D-arginine in vitro and in vivo. Infect Immun. 2004;72(1):602-5.
221. Karicherla P, Hobden JA. Nona-D-arginine therapy for Pseudomonas aeruginosa keratitis. Invest Ophthalmol Vis Sci. 2009;50(1):256-62.
222. Karicherla P, Aras S, Aiyar A, Hobden JA. Nona-D-arginine amide suppresses corneal cytokines in Pseudomonas aeruginosa keratitis. Cornea. 2010;29(11):1308-14.
223. Gagnon H, Beauchemin S, Kwiatkowska A, Couture F, D'Anjou F, Levesque C, et al. Optimization of furin inhibitors to protect against the activation of influenza hemagglutinin H5 and Shiga toxin. J Med Chem. 2014;57(1):29-41.
224. Remacle AG, Gawlik K, Golubkov VS, Cadwell GW, Liddington RC, Cieplak P, et al. Selective and potent furin inhibitors protect cells from anthrax without significant toxicity. Int J Biochem Cell Biol. 2010;42(6):987-95.
225. Braun E, Hotter D, Koepke L, Zech F, Gross R, Sparrer KMJ, et al. Guanylate-Binding Proteins 2 and 5 Exert Broad Antiviral Activity by Inhibiting Furin-Mediated Processing of Viral Envelope Proteins. Cell Rep. 2019;27(7):2092-104.e10.
226. Senzer N, Barve M, Kuhn J, Melnyk A, Beitsch P, Lazar M, et al. Phase I trial of "bi-shRNAi(furin)/GMCSF DNA/autologous tumor cell" vaccine (FANG) in advanced cancer. Mol Ther. 2012;20(3):679-86.
227. Meerabux J, Yaspo ML, Roebroek AJ, Van de Ven WJ, Lister TA, Young BD. A new member of the proprotein convertase gene family (LPC) is located at a chromosome translocation breakpoint in lymphomas. Cancer Res. 1996;56(3):448-51.
228. Cabanillas F, Pathak S, Trujillo J, Grant G, Cork A, Hagemeister FB, et al. Cytogenetic features of Hodgkin's disease suggest possible origin from a lymphocyte. Blood. 1988;71(6):1615-7.
229. DeCoteau JF, Reis MD, Griesser H, Lorenzana A, al-Hashmi I, Hawley RG, et al. SBH-1, a novel Reed-Sternberg-like cell line capable of inducing tumors in SCID mice: immunophenotypic, cytogenetic, and cytokine expression profiles. Blood. 1995;85(10):2829-38.
230. Seidah NG, Hamelin J, Mamarbachi M, Dong W, Tardos H, Mbikay M, et al. cDNA structure, tissue distribution, and chromosomal localization of rat PC7, a novel mammalian proprotein convertase closest to yeast kexin-like proteinases. Proc Natl Acad Sci U S A. 1996;93(8):3388-93.
231. Declercq J, Meulemans S, Plets E, Creemers JW. Internalization of proprotein convertase PC7 from plasma membrane is mediated by a novel motif. J Biol Chem. 2012;287(12):9052-60.

232. Munzer JS, Basak A, Zhong M, Mamarbachi A, Hamelin J, Savaria D, et al. In vitro characterization of the novel proprotein convertase PC7. J Biol Chem. 1997;272(32):19672-81.
233. Sergeeva OA, van der Goot FG. Anthrax toxin requires ZDHHC5-mediated palmitoylation of its surface-processing host enzymes. Proc Natl Acad Sci U S A. 2019;116(4):1279-88.
234. Rousselet E, Benjannet S, Marcinkiewicz E, Asselin MC, Lazure C, Seidah NG. Proprotein convertase PC7 enhances the activation of the EGF receptor pathway through processing of the EGF precursor. J Biol Chem. 2011;286(11):9185-95.
235. Guillemot J, Canuel M, Essalmani R, Prat A, Seidah NG. Implication of the proprotein convertases in iron homeostasis: proprotein convertase 7 sheds human transferrin receptor 1 and furin activates hepcidin. Hepatology. 2013;57(6):2514-24.
236. van de Loo JW, Teuchert M, Pauli I, Plets E, Van de Ven WJ, Creemers JW. Dynamic palmitoylation of lymphoma proprotein convertase prolongs its half-life, but is not essential for trans-Golgi network localization. Biochem J. 2000;352 Pt 3:827-33.
237. Declercq J, Ramos-Molina B, Sannerud R, Brouwers B, Pruniau V, Meulemans S, et al. Endosome to trans-Golgi network transport of Proprotein Convertase 7 is mediated by a cluster of basic amino acids and palmitoylated cysteines. Eur J Cell Biol. 2017;96(5):432-9.
238. Ginefra P, Filippi BGH, Donovan P, Bessonnard S, Constam DB. Compartment-Specific Biosensors Reveal a Complementary Subcellular Distribution of Bioactive Furin and PC7. Cell Rep. 2018;22(8):2176-89.
239. Durand L, Duval S, Evagelidis A, Guillemot J, Dianati V, Sikorska E, et al. The motif ExExxxL in the cytosolic tail of the secretory human proprotein convertase PC7 regulates its trafficking and cleavage activity. J Biol Chem. 2020.
240. Kelly BT, McCoy AJ, Spate K, Miller SE, Evans PR, Honing S, et al. A structural explanation for the binding of endocytic dileucine motifs by the AP2 complex. Nature. 2008;456(7224):976-9.
241. Linstedt AD, Mehta A, Suhan J, Reggio H, Hauri HP. Sequence and overexpression of GPP130/GIMPc: evidence for saturable pH-sensitive targeting of a type II early Golgi membrane protein. Mol Biol Cell. 1997;8(6):1073-87.
242. Oexle K, Ried JS, Hicks AA, Tanaka T, Hayward C, Bruegel M, et al. Novel association to the proprotein convertase PCSK7 gene locus revealed by analysing soluble transferrin receptor (sTfR) levels. Hum Mol Genet. 2011;20(5):1042-7.
243. Turpeinen H, Oksanen A, Kivinen V, Kukkurainen S, Uusimaki A, Ramet M, et al. Proprotein convertase subtilisin/kexin type 7 (PCSK7) is essential for the zebrafish development and bioavailability of transforming growth factor beta1a (TGFbeta1a). J Biol Chem. 2013;288(51):36610-23.
244. Senturker S, Thomas JT, Mateshaytis J, Moos M, Jr. A homolog of Subtilisin-like Proprotein Convertase 7 is essential to anterior neural development in Xenopus. PLoS One. 2012;7(6):e39380.
245. Siegfried G, Basak A, Cromlish JA, Benjannet S, Marcinkiewicz J, Chretien M, et al. The secretory proprotein convertases furin, PC5, and PC7 activate VEGF-C to induce tumorigenesis. J Clin Invest. 2003;111(11):1723-32.
246. Siegfried G, Khatib AM, Benjannet S, Chretien M, Seidah NG. The proteolytic processing of pro-platelet-derived growth factor-A at RRKR(86) by members of the proprotein convertase family is functionally correlated to platelet-derived growth factor-A-induced functions and tumorigenicity. Cancer Res. 2003;63(7):1458-63.
247. Canaff L, Bennett HP, Hou Y, Seidah NG, Hendy GN. Proparathyroid hormone processing by the proprotein convertase-7: comparison with furin and assessment of modulation of parathyroid convertase messenger ribonucleic acid levels by calcium and 1,25-dihydroxyvitamin D3. Endocrinology. 1999;140(8):3633-42.

248. Anyetei-Anum EN, Blum A, Seidah NG, Beinfeld MC. Prohormone convertase 7 is necessary for the normal processing of cholecystokinin in mouse brain. Biochem Biophys Res Commun. 2017;482(4):1190-3.
249. Bessonnard S, Mesnard D, Constam DB. PC7 and the related proteases Furin and Pace4 regulate E-cadherin function during blastocyst formation. J Cell Biol. 2015;210(7):1185-97.
250. Lei X, Shi F, Basu D, Huq A, Routhier S, Day R, et al. Proteolytic processing of angiopoietin-like protein 4 by proprotein convertases modulates its inhibitory effects on lipoprotein lipase activity. J Biol Chem. 2011;286(18):15747-56.
251. Anders A, Gilbert S, Garten W, Postina R, Fahrenholz F. Regulation of the alpha-secretase ADAM10 by its prodomain and proprotein convertases. Faseb j. 2001;15(10):1837-9.
252. Couture F, D'Anjou F, Desjardins R, Boudreau F, Day R. Role of proprotein convertases in prostate cancer progression. Neoplasia. 2012;14(11):1032-42.
253. Scamuffa N, Siegfried G, Bontemps Y, Ma L, Basak A, Cherel G, et al. Selective inhibition of proprotein convertases represses the metastatic potential of human colorectal tumor cells. J Clin Invest. 2008;118(1):352-63.
254. Elhage R, Cherai M, Levacher B, Darrasse-Jeze G, Baillou C, Zhao X, et al. C-terminal cleavage of human Foxp3 at a proprotein convertase motif abrogates its suppressive function. Scand J Immunol. 2015;81(4):229-39.
255. Ozden S, Lucas-Hourani M, Ceccaldi PE, Basak A, Valentine M, Benjannet S, et al. Inhibition of Chikungunya virus infection in cultured human muscle cells by furin inhibitors: impairment of the maturation of the E2 surface glycoprotein. J Biol Chem. 2008;283(32):21899-908.
256. Basak A, Mitra A, Basak S, Pasko C, Chretien M, Seaton P. A fluorogenic peptide containing the processing site of human SARS corona virus S-protein: kinetic evaluation and NMR structure elucidation. Chembiochem. 2007;8(9):1029-37.
257. Bergeron E, Vincent MJ, Wickham L, Hamelin J, Basak A, Nichol ST, et al. Implication of proprotein convertases in the processing and spread of severe acute respiratory syndrome coronavirus. Biochem Biophys Res Commun. 2005;326(3):554-63.
258. Wouters S, Decroly E, Vandenbranden M, Shober D, Fuchs R, Morel V, et al. Occurrence of an HIV-1 gp160 endoproteolytic activity in low-density vesicles and evidence for a distinct density distribution from endogenously expressed furin and PC7/LPC convertases. FEBS Lett. 1999;456(1):97-102.
259. Wetsel WC, Rodriguiz RM, Guillemot J, Rousselet E, Essalmani R, Kim IH, et al. Disruption of the expression of the proprotein convertase PC7 reduces BDNF production and affects learning and memory in mice. Proc Natl Acad Sci U S A. 2013;110(43):17362-7.
260. Kowianski P, Lietzau G, Czuba E, Waskow M, Steliga A, Morys J. BDNF: A Key Factor with Multipotent Impact on Brain Signaling and Synaptic Plasticity. Cell Mol Neurobiol. 2018;38(3):579-93.
261. Woo NH, Teng HK, Siao CJ, Chiaruttini C, Pang PT, Milner TA, et al. Activation of p75NTR by proBDNF facilitates hippocampal long-term depression. Nat Neurosci. 2005;8(8):1069-77.
262. Mowla SJ, Farhadi HF, Pareek S, Atwal JK, Morris SJ, Seidah NG, et al. Biosynthesis and post-translational processing of the precursor to brain-derived neurotrophic factor. J Biol Chem. 2001;276(16):12660-6.
263. Seidah NG, Benjannet S, Pareek S, Chretien M, Murphy RA. Cellular processing of the neurotrophin precursors of NT3 and BDNF by the mammalian proprotein convertases. FEBS Lett. 1996;379(3):247-50.
264. Marcinkiewicz M, Savaria D, Marcinkiewicz J. The pro-protein convertase PC1 is induced in the transected sciatic nerve and is present in cultured Schwann cells: comparison with PC5, furin and PC7, implication in pro-BDNF processing. Brain Res Mol Brain Res. 1998;59(2):229-46.

265. Sharma S, Fulton S. Diet-induced obesity promotes depressive-like behaviour that is associated with neural adaptations in brain reward circuitry. Int J Obes (Lond). 2013;37(3):382-9.
266. Murphy M, Mercer JG. Diet-regulated anxiety. Int J Endocrinol. 2013;2013:701967.
267. Scott KM, McGee MA, Wells JE, Oakley Browne MA. Obesity and mental disorders in the adult general population. J Psychosom Res. 2008;64(1):97-105.
268. Decarie-Spain L, Sharma S, Hryhorczuk C, Issa-Garcia V, Barker PA, Arbour N, et al. Nucleus accumbens inflammation mediates anxiodepressive behavior and compulsive sucrose seeking elicited by saturated dietary fat. Mol Metab. 2018;10:1-13.
269. Sanchez-Villegas A, Martinez-Gonzalez MA. Diet, a new target to prevent depression? BMC Med. 2013;11:3.
270. Peet M, Murphy B, Shay J, Horrobin D. Depletion of omega-3 fatty acid levels in red blood cell membranes of depressive patients. Biol Psychiatry. 1998;43(5):315-9.
271. Lai JS, Oldmeadow C, Hure AJ, McEvoy M, Hiles SA, Boyle M, et al. Inflammation mediates the association between fatty acid intake and depression in older men and women. Nutr Res. 2016;36(3):234-45.
272. Wei W, Pham K, Gammons JW, Sutherland D, Liu Y, Smith A, et al. Diet composition, not calorie intake, rapidly alters intrinsic excitability of hypothalamic AgRP/NPY neurons in mice. Sci Rep. 2015;5:16810.
273. Leigh SJ, Lee F, Morris MJ. Hyperpalatability and the Generation of Obesity: Roles of Environment, Stress Exposure and Individual Difference. Curr Obes Rep. 2018;7(1):6-18.
274. Davis JF, Tracy AL, Schurdak JD, Tschop MH, Lipton JW, Clegg DJ, et al. Exposure to elevated levels of dietary fat attenuates psychostimulant reward and mesolimbic dopamine turnover in the rat. Behav Neurosci. 2008;122(6):1257-63.
275. Russo SJ, Nestler EJ. The brain reward circuitry in mood disorders. Nat Rev Neurosci. 2013;14(9):609-25.
276. Johnson PM, Kenny PJ. Dopamine D2 receptors in addiction-like reward dysfunction and compulsive eating in obese rats. Nat Neurosci. 2010;13(5):635-41.
277. Stice E, Spoor S, Bohon C, Small DM. Relation between obesity and blunted striatal response to food is moderated by TaqIA A1 allele. Science. 2008;322(5900):449-52.
278. Wang GJ, Volkow ND, Fowler JS. The role of dopamine in motivation for food in humans: implications for obesity. Expert Opin Ther Targets. 2002;6(5):601-9.
279. Lumeng CN, Saltiel AR. Inflammatory links between obesity and metabolic disease. J Clin Invest. 2011;121(6):2111-7.
280. Liu Y, Al-Sayegh H, Jabrah R, Wang W, Yan F, Zhang J. Association between C-reactive protein and depression: modulated by gender and mediated by body weight. Psychiatry Res. 2014;219(1):103-8.
281. Daly M. The relationship of C-reactive protein to obesity-related depressive symptoms: a longitudinal study. Obesity (Silver Spring). 2013;21(2):248-50.
282. Thaler JP, Yi CX, Schur EA, Guyenet SJ, Hwang BH, Dietrich MO, et al. Obesity is associated with hypothalamic injury in rodents and humans. J Clin Invest. 2012;122(1):153-62.
283. Valdearcos M, Robblee MM, Benjamin DI, Nomura DK, Xu AW, Koliwad SK. Microglia dictate the impact of saturated fat consumption on hypothalamic inflammation and neuronal function. Cell Rep. 2014;9(6):2124-38.
284. Cazettes F, Cohen JI, Yau PL, Talbot H, Convit A. Obesity-mediated inflammation may damage the brain circuit that regulates food intake. Brain Res. 2011;1373:101-9.
285. Prasad A, Prasad C. Short-term consumption of a diet rich in fat decreases anxiety response in adult male rats. Physiol Behav. 1996;60(3):1039-42.
286. Sweeney P, O'Hara K, Xu Z, Yang Y. HFD-induced energy states-dependent bidirectional control of anxiety levels in mice. Int J Obes (Lond). 2017;41(8):1237-45.

287. Souza CG, Moreira JD, Siqueira IR, Pereira AG, Rieger DK, Souza DO, et al. Highly palatable diet consumption increases protein oxidation in rat frontal cortex and anxiety-like behavior. Life Sci. 2007;81(3):198-203.
288. Avena NM, Bocarsly ME, Rada P, Kim A, Hoebel BG. After daily bingeing on a sucrose solution, food deprivation induces anxiety and accumbens dopamine/acetylcholine imbalance. Physiol Behav. 2008;94(3):309-15.
289. Ohland CL, Pankiv E, Baker G, Madsen KL. Western diet-induced anxiolytic effects in mice are associated with alterations in tryptophan metabolism. Nutr Neurosci. 2016;19(8):337-45.
290. Beilharz JE, Maniam J, Morris MJ. Short exposure to a diet rich in both fat and sugar or sugar alone impairs place, but not object recognition memory in rats. Brain Behav Immun. 2014;37:134-41.
291. Burchfield JG, Kebede MA, Meoli CC, Stockli J, Whitworth PT, Wright AL, et al. High dietary fat and sucrose results in an extensive and time-dependent deterioration in health of multiple physiological systems in mice. J Biol Chem. 2018;293(15):5731-45.
292. Attuquayefio T, Stevenson RJ, Boakes RA, Oaten MJ, Yeomans MR, Mahmut M, et al. A high-fat high-sugar diet predicts poorer hippocampal-related memory and a reduced ability to suppress wanting under satiety. J Exp Psychol Anim Learn Cogn. 2016;42(4):415-28.
293. Stickel F, Buch S, Zoller H, Hultcrantz R, Gallati S, Osterreicher C, et al. Evaluation of genome-wide loci of iron metabolism in hereditary hemochromatosis identifies PCSK7 as a host risk factor of liver cirrhosis. Hum Mol Genet. 2014;23(14):3883-90.
294. Huang T, Huang J, Qi Q, Li Y, Bray GA, Rood J, et al. PCSK7 genotype modifies effect of a weight-loss diet on 2-year changes of insulin resistance: the POUNDS LOST trial. Diabetes Care. 2015;38(3):439-44.
295. Hoogeveen RC, Gaubatz JW, Sun W, Dodge RC, Crosby JR, Jiang J, et al. Small dense low-density lipoprotein-cholesterol concentrations predict risk for coronary heart disease: the Atherosclerosis Risk In Communities (ARIC) study. Arterioscler Thromb Vasc Biol. 2014;34(5):1069-77.
296. Peloso GM, Auer PL, Bis JC, Voorman A, Morrison AC, Stitziel NO, et al. Association of low-frequency and rare coding-sequence variants with blood lipids and coronary heart disease in 56,000 whites and blacks. Am J Hum Genet. 2014;94(2):223-32.
297. Guillemot J, Essalmani R, Hamelin J, Seidah NG. Is there a link between proprotein convertase PC7 activity and human lipid homeostasis? FEBS Open Bio. 2014;4:741-5.
298. Sarwar N, Sandhu MS, Ricketts SL, Butterworth AS, Di Angelantonio E, Boekholdt SM, et al. Triglyceride-mediated pathways and coronary disease: collaborative analysis of 101 studies. Lancet. 2010;375(9726):1634-9.
299. Ashraf Y, Duval S, Sachan V, Essalmani R, Susan-Resiga D, Roubtsova A, et al. Proprotein convertase 7 (PCSK7) reduces apoA-V levels. Febs j. 2020.
300. Ke Q, Costa M. Hypoxia-inducible factor-1 (HIF-1). Mol Pharmacol. 2006;70(5):1469-80.
301. McMahon S, Grondin F, McDonald PP, Richard DE, Dubois CM. Hypoxia-enhanced expression of the proprotein convertase furin is mediated by hypoxia-inducible factor-1: impact on the bioactivation of proproteins. J Biol Chem. 2005;280(8):6561-9.
302. Arsenault D, Lucien F, Dubois CM. Hypoxia enhances cancer cell invasion through relocalization of the proprotein convertase furin from the trans-Golgi network to the cell surface. J Cell Physiol. 2012;227(2):789-800.
303. Silvestri L, Pagani A, Camaschella C. Furin-mediated release of soluble hemojuvelin: a new link between hypoxia and iron homeostasis. Blood. 2008;111(2):924-31.
304. Fu J, Zhang J, Gong Y, Testa CL, Klein-Szanto AJ. Regulation of HIF-1 alpha by the proprotein convertases furin and PC7 in human squamous carcinoma cells. Mol Carcinog. 2015;54(9):698-706.

305. Elagoz A, Benjannet S, Mammarbassi A, Wickham L, Seidah NG. Biosynthesis and cellular trafficking of the convertase SKI-1/S1P: ectodomain shedding requires SKI-1 activity. J Biol Chem. 2002;277(13):11265-75.
306. da Palma JR, Cendron L, Seidah NG, Pasquato A, Kunz S. Mechanism of Folding and Activation of Subtilisin Kexin Isozyme-1 (SKI-1)/Site-1 Protease (S1P). J Biol Chem. 2016;291(5):2055-66.
307. Seidah NG, Mowla SJ, Hamelin J, Mamarbachi AM, Benjannet S, Toure BB, et al. Mammalian subtilisin/kexin isozyme SKI-1: A widely expressed proprotein convertase with a unique cleavage specificity and cellular localization. Proc Natl Acad Sci U S A. 1999;96(4):1321-6.
308. Pullikotil P, Benjannet S, Mayne J, Seidah NG. The proprotein convertase SKI-1/S1P: alternate translation and subcellular localization. J Biol Chem. 2007;282(37):27402-13.
309. Marschner K, Kollmann K, Schweizer M, Braulke T, Pohl S. A key enzyme in the biogenesis of lysosomes is a protease that regulates cholesterol metabolism. Science. 2011;333(6038):87-90.
310. Pasquato A, Pullikotil P, Asselin MC, Vacatello M, Paolillo L, Ghezzo F, et al. The proprotein convertase SKI-1/S1P. In vitro analysis of Lassa virus glycoprotein-derived substrates and ex vivo validation of irreversible peptide inhibitors. J Biol Chem. 2006;281(33):23471-81.
311. Goldstein JL, DeBose-Boyd RA, Brown MS. Protein sensors for membrane sterols. Cell. 2006;124(1):35-46.
312. Llarena M, Bailey D, Curtis H, O'Hare P. Different mechanisms of recognition and ER retention by transmembrane transcription factors CREB-H and ATF6. Traffic. 2010;11(1):48-69.
313. Yang J, Goldstein JL, Hammer RE, Moon YA, Brown MS, Horton JD. Decreased lipid synthesis in livers of mice with disrupted Site-1 protease gene. Proc Natl Acad Sci U S A. 2001;98(24):13607-12.
314. Blanchet MH, Le Good JA, Mesnard D, Oorschot V, Baflast S, Minchiotti G, et al. Cripto recruits Furin and PACE4 and controls Nodal trafficking during proteolytic maturation. Embo j. 2008;27(19):2580-91.
315. Lenz O, ter Meulen J, Klenk HD, Seidah NG, Garten W. The Lassa virus glycoprotein precursor GP-C is proteolytically processed by subtilase SKI-1/S1P. Proc Natl Acad Sci U S A. 2001;98(22):12701-5.
316. Vincent MJ, Sanchez AJ, Erickson BR, Basak A, Chretien M, Seidah NG, et al. Crimean-Congo hemorrhagic fever virus glycoprotein proteolytic processing by subtilase SKI-1. J Virol. 2003;77(16):8640-9.
317. Benjannet S, Rhainds D, Essalmani R, Mayne J, Wickham L, Jin W, et al. NARC-1/PCSK9 and its natural mutants: zymogen cleavage and effects on the low density lipoprotein (LDL) receptor and LDL cholesterol. J Biol Chem. 2004;279(47):48865-75.
318. Abifadel M, Varret M, Rabes JP, Allard D, Ouguerram K, Devillers M, et al. Mutations in PCSK9 cause autosomal dominant hypercholesterolemia. Nat Genet. 2003;34(2):154-6.
319. Maxwell KN, Breslow JL. Adenoviral-mediated expression of Pcsk9 in mice results in a low-density lipoprotein receptor knockout phenotype. Proc Natl Acad Sci U S A. 2004;101(18):7100-5.
320. Seidah NG, Prat A, Pirillo A, Catapano AL, Norata GD. Novel strategies to target proprotein convertase subtilisin kexin 9: beyond monoclonal antibodies. Cardiovasc Res. 2019;115(3):510-8.
321. Nishikido T, Ray KK. Non-antibody Approaches to Proprotein Convertase Subtilisin Kexin 9 Inhibition: siRNA, Antisense Oligonucleotides, Adnectins, Vaccination, and New Attempts at Small-Molecule Inhibitors Based on New Discoveries. Front Cardiovasc Med. 2018;5:199.
322. Zhu R, Zacharias L, Wooding KM, Peng W, Mechref Y. Glycoprotein Enrichment Analytical Techniques: Advantages and Disadvantages. Methods Enzymol. 2017;585:397-429.
323. Wolters DA, Washburn MP, Yates JR, 3rd. An automated multidimensional protein identification technology for shotgun proteomics. Anal Chem. 2001;73(23):5683-90.
324. Yates JR, 3rd. Mass spectral analysis in proteomics. Annu Rev Biophys Biomol Struct. 2004;33:297-316.

325. Vandermarliere E, Mueller M, Martens L. Getting intimate with trypsin, the leading protease in proteomics. Mass Spectrom Rev. 2013;32(6):453-65.
326. Woods RJ, Edge CJ, Dwek RA. Protein surface oligosaccharides and protein function. Nat Struct Biol. 1994;1(8):499-501.
327. Zielinska DF, Gnad F, Wisniewski JR, Mann M. Precision mapping of an in vivo N-glycoproteome reveals rigid topological and sequence constraints. Cell. 2010;141(5):897-907.
328. North SJ, Huang HH, Sundaram S, Jang-Lee J, Etienne AT, Trollope A, et al. Glycomics profiling of Chinese hamster ovary cell glycosylation mutants reveals N-glycans of a novel size and complexity. J Biol Chem. 2010;285(8):5759-75.
329. Madera M, Mann B, Mechref Y, Novotny MV. Efficacy of glycoprotein enrichment by microscale lectin affinity chromatography. J Sep Sci. 2008;31(14):2722-32.
330. Ongay S, Boichenko A, Govorukhina N, Bischoff R. Glycopeptide enrichment and separation for protein glycosylation analysis. J Sep Sci. 2012;35(18):2341-72.
331. Wang D, Hincapie M, Rejtar T, Karger BL. Ultrasensitive characterization of site-specific glycosylation of affinity-purified haptoglobin from lung cancer patient plasma using 10 mum i.d. porous layer open tubular liquid chromatography-linear ion trap collision-induced dissociation/electron transfer dissociation mass spectrometry. Anal Chem. 2011;83(6):2029-37.
332. Kolb HC, Finn MG, Sharpless KB. Click Chemistry: Diverse Chemical Function from a Few Good Reactions. Angew Chem Int Ed Engl. 2001;40(11):2004-21.
333. Zacharias LG, Hartmann AK, Song E, Zhao J, Zhu R, Mirzaei P, et al. HILIC and ERLIC Enrichment of Glycopeptides Derived from Breast and Brain Cancer Cells. J Proteome Res. 2016;15(10):3624-34.
334. Ning Z, Seebun D, Hawley B, Chiang CK, Figeys D. From cells to peptides: "one-stop" integrated proteomic processing using amphipols. J Proteome Res. 2013;12(3):1512-9.
335. Chen R, Seebun D, Ye M, Zou H, Figeys D. Site-specific characterization of cell membrane N-glycosylation with integrated hydrophilic interaction chromatography solid phase extraction and LC-MS/MS. J Proteomics. 2014;103:194-203.
336. Wong E, Maretzky T, Peleg Y, Blobel CP, Sagi I. The Functional Maturation of A Disintegrin and Metalloproteinase (ADAM) 9, 10, and 17 Requires Processing at a Newly Identified Proprotein Convertase (PC) Cleavage Site. J Biol Chem. 2015;290(19):12135-46.
337. Farquhar MG, Palade GE. The Golgi apparatus (complex)-(1954-1981)-from artifact to center stage. J Cell Biol. 1981;91(3 Pt 2):77s-103s.
338. Anitei M, Hoflack B. Exit from the trans-Golgi network: from molecules to mechanisms. Curr Opin Cell Biol. 2011;23(4):443-51.
339. Dick G, Akslen-Hoel LK, Grondahl F, Kjos I, Prydz K. Proteoglycan synthesis and Golgi organization in polarized epithelial cells. J Histochem Cytochem. 2012;60(12):926-35.
340. Mellman I, Simons K. The Golgi complex: in vitro veritas? Cell. 1992;68(5):829-40.
341. Jackson CL. Mechanisms of transport through the Golgi complex. J Cell Sci. 2009;122(Pt 4):443-52.
342. Stanley P. Golgi glycosylation. Cold Spring Harb Perspect Biol. 2011;3(4).
343. Day KJ, Staehelin LA, Glick BS. A three-stage model of Golgi structure and function. Histochem Cell Biol. 2013;140(3):239-49.
344. Rabouille C, Hui N, Hunte F, Kieckbusch R, Berger EG, Warren G, et al. Mapping the distribution of Golgi enzymes involved in the construction of complex oligosaccharides. J Cell Sci. 1995;108 (Pt 4):1617-27.
345. Glick BS, Luini A. Models for Golgi traffic: a critical assessment. Cold Spring Harb Perspect Biol. 2011;3(11):a005215.
346. Saraste J, Prydz K. A New Look at the Functional Organization of the Golgi Ribbon. Front Cell Dev Biol. 2019;7:171.

347. Palade GE. Membrane biogenesis: an overview. Methods Enzymol. 1983;96:xxix-lv.
348. Seemann J, Jokitalo E, Pypaert M, Warren G. Matrix proteins can generate the higher order architecture of the Golgi apparatus. Nature. 2000;407(6807):1022-6.
349. Ronchi P, Tischer C, Acehan D, Pepperkok R. Positive feedback between Golgi membranes, microtubules and ER exit sites directs de novo biogenesis of the Golgi. J Cell Sci. 2014;127(Pt 21):4620-33.
350. Rothman JE, Wieland FT. Protein sorting by transport vesicles. Science. 1996;272(5259):227-34.
351. Mironov AA, Weidman P, Luini A. Variations on the intracellular transport theme: maturing cisternae and trafficking tubules. J Cell Biol. 1997;138(3):481-4.
352. Bonifacino JS, Glick BS. The mechanisms of vesicle budding and fusion. Cell. 2004;116(2):153-66.
353. Glick BS, Elston T, Oster G. A cisternal maturation mechanism can explain the asymmetry of the Golgi stack. FEBS Lett. 1997;414(2):177-81.
354. Barlowe CK, Miller EA. Secretory protein biogenesis and traffic in the early secretory pathway. Genetics. 2013;193(2):383-410.
355. Myers MD, Payne GS. Clathrin, adaptors and disease: insights from the yeast Saccharomyces cerevisiae. Front Biosci (Landmark Ed). 2013;18:862-91.
356. Schmid SL. Clathrin-coated vesicle formation and protein sorting: an integrated process. Annu Rev Biochem. 1997;66:511-48.
357. Goud B, Liu S, Storrie B. Rab proteins as major determinants of the Golgi complex structure. Small GTPases. 2018;9(1-2):66-75.
358. Witkos TM, Lowe M. The Golgin Family of Coiled-Coil Tethering Proteins. Front Cell Dev Biol. 2015;3:86.
359. Blackburn JB, Kudlyk T, Pokrovskaya I, Lupashin VV. More than just sugars: Conserved oligomeric Golgi complex deficiency causes glycosylation-independent cellular defects. Traffic. 2018;19(6):463-80.
360. Blackburn JB, D'Souza Z, Lupashin VV. Maintaining order: COG complex controls Golgi trafficking, processing, and sorting. FEBS Lett. 2019;593(17):2466-87.
361. Chen YA, Scheller RH. SNARE-mediated membrane fusion. Nat Rev Mol Cell Biol. 2001;2(2):98-106.
362. Sollner T, Bennett MK, Whiteheart SW, Scheller RH, Rothman JE. A protein assembly-disassembly pathway in vitro that may correspond to sequential steps of synaptic vesicle docking, activation, and fusion. Cell. 1993;75(3):409-18.
363. Boman AL. GGA proteins: new players in the sorting game. J Cell Sci. 2001;114(Pt 19):3413-8.
364. Bonifacino JS. The GGA proteins: adaptors on the move. Nat Rev Mol Cell Biol. 2004;5(1):23-32.
365. Dell'Angelica EC, Puertollano R, Mullins C, Aguilar RC, Vargas JD, Hartnell LM, et al. GGAs: a family of ADP ribosylation factor-binding proteins related to adaptors and associated with the Golgi complex. J Cell Biol. 2000;149(1):81-94.
366. Puertollano R, Aguilar RC, Gorshkova I, Crouch RJ, Bonifacino JS. Sorting of mannose 6-phosphate receptors mediated by the GGAs. Science. 2001;292(5522):1712-6.
367. Nielsen MS, Madsen P, Christensen EI, Nykjaer A, Gliemann J, Kasper D, et al. The sortilin cytoplasmic tail conveys Golgi-endosome transport and binds the VHS domain of the GGA2 sorting protein. Embo j. 2001;20(9):2180-90.
368. Collins BM, Watson PJ, Owen DJ. The structure of the GGA1-GAT domain reveals the molecular basis for ARF binding and membrane association of GGAs. Dev Cell. 2003;4(3):321-32.
369. Puertollano R, Randazzo PA, Presley JF, Hartnell LM, Bonifacino JS. The GGAs promote ARF-dependent recruitment of clathrin to the TGN. Cell. 2001;105(1):93-102.
370. Robinson MS, Bonifacino JS. Adaptor-related proteins. Curr Opin Cell Biol. 2001;13(4):444-53.
371. Tan JZA, Gleeson PA. Cargo Sorting at the trans-Golgi Network for Shunting into Specific Transport Routes: Role of Arf Small G Proteins and Adaptor Complexes. Cells. 2019;8(6).

372. Hirst J, Itzhak DN, Antrobus R, Borner GHH, Robinson MS. Role of the AP-5 adaptor protein complex in late endosome-to-Golgi retrieval. PLoS Biol. 2018;16(1):e2004411.
373. Zhang X, Wang Y. GRASPs in Golgi Structure and Function. Front Cell Dev Biol. 2015;3:84.
374. Xiang Y, Wang Y. GRASP55 and GRASP65 play complementary and essential roles in Golgi cisternal stacking. J Cell Biol. 2010;188(2):237-51.
375. Tang D, Zhang X, Huang S, Yuan H, Li J, Wang Y. Mena-GRASP65 interaction couples actin polymerization to Golgi ribbon linking. Mol Biol Cell. 2016;27(1):137-52.
376. Barr FA, Preisinger C, Kopajtich R, Korner R. Golgi matrix proteins interact with p24 cargo receptors and aid their efficient retention in the Golgi apparatus. J Cell Biol. 2001;155(6):885-91.
377. Preisinger C, Korner R, Wind M, Lehmann WD, Kopajtich R, Barr FA. Plk1 docking to GRASP65 phosphorylated by Cdk1 suggests a mechanism for Golgi checkpoint signalling. Embo j. 2005;24(4):753-65.
378. Zhang X, Wang Y. GRASP55 facilitates autophagosome maturation under glucose deprivation. Mol Cell Oncol. 2018;5(4):e1494948.
379. Lane JD, Lucocq J, Pryde J, Barr FA, Woodman PG, Allan VJ, et al. Caspase-mediated cleavage of the stacking protein GRASP65 is required for Golgi fragmentation during apoptosis. J Cell Biol. 2002;156(3):495-509.
380. Barr FA, Puype M, Vandekerckhove J, Warren G. GRASP65, a protein involved in the stacking of Golgi cisternae. Cell. 1997;91(2):253-62.
381. Shorter J, Watson R, Giannakou ME, Clarke M, Warren G, Barr FA. GRASP55, a second mammalian GRASP protein involved in the stacking of Golgi cisternae in a cell-free system. Embo j. 1999;18(18):4949-60.
382. Xiang Y, Zhang X, Nix DB, Katoh T, Aoki K, Tiemeyer M, et al. Regulation of protein glycosylation and sorting by the Golgi matrix proteins GRASP55/65. Nat Commun. 2013;4:1659.
383. Puthenveedu MA, Bachert C, Puri S, Lanni F, Linstedt AD. GM130 and GRASP65-dependent lateral cisternal fusion allows uniform Golgi-enzyme distribution. Nat Cell Biol. 2006;8(3):238-48.
384. Rabouille C, Linstedt AD. GRASP: A Multitasking Tether. Front Cell Dev Biol. 2016;4:1.
385. Nakamura N, Wei JH, Seemann J. Modular organization of the mammalian Golgi apparatus. Curr Opin Cell Biol. 2012;24(4):467-74.
386. Zhang X, Wang Y. Glycosylation Quality Control by the Golgi Structure. J Mol Biol. 2016;428(16):3183-93.
387. Xiang Y, Wang Y. New components of the Golgi matrix. Cell Tissue Res. 2011;344(3):365-79.
388. Wong M, Gillingham AK, Munro S. The golgin coiled-coil proteins capture different types of transport carriers via distinct N-terminal motifs. BMC Biol. 2017;15(1):3.
389. Munro S. The golgin coiled-coil proteins of the Golgi apparatus. Cold Spring Harb Perspect Biol. 2011;3(6).
390. Derby MC, Lieu ZZ, Brown D, Stow JL, Goud B, Gleeson PA. The trans-Golgi network golgin, GCC185, is required for endosome-to-Golgi transport and maintenance of Golgi structure. Traffic. 2007;8(6):758-73.
391. Luke MR, Kjer-Nielsen L, Brown DL, Stow JL, Gleeson PA. GRIP domain-mediated targeting of two new coiled-coil proteins, GCC88 and GCC185, to subcompartments of the trans-Golgi network. J Biol Chem. 2003;278(6):4216-26.
392. Makhoul C, Gosavi P, Duffield R, Delbridge B, Williamson NA, Gleeson PA. Intersectin-1 interacts with the golgin GCC88 to couple the actin network and Golgi architecture. Mol Biol Cell. 2019;30(3):370-86.
393. Sperling RA, Aisen PS, Beckett LA, Bennett DA, Craft S, Fagan AM, et al. Toward defining the preclinical stages of Alzheimer's disease: recommendations from the National Institute on Aging-

Alzheimer's Association workgroups on diagnostic guidelines for Alzheimer's disease. Alzheimers Dement. 2011;7(3):280-92.
394. Joshi G, Chi Y, Huang Z, Wang Y. Abeta-induced Golgi fragmentation in Alzheimer's disease enhances Abeta production. Proc Natl Acad Sci U S A. 2014;111(13):E1230-9.
395. Sun KH, de Pablo Y, Vincent F, Johnson EO, Chavers AK, Shah K. Novel genetic tools reveal Cdk5's major role in Golgi fragmentation in Alzheimer's disease. Mol Biol Cell. 2008;19(7):3052-69.
396. Joshi G, Bekier ME, 2nd, Wang Y. Golgi fragmentation in Alzheimer's disease. Front Neurosci. 2015;9:340.
397. Trojanowski JQ, Goedert M, Iwatsubo T, Lee VM. Fatal attractions: abnormal protein aggregation and neuron death in Parkinson's disease and Lewy body dementia. Cell Death Differ. 1998;5(10):832-7.
398. Wakabayashi K, Hayashi S, Kakita A, Yamada M, Toyoshima Y, Yoshimoto M, et al. Accumulation of alpha-synuclein/NACP is a cytopathological feature common to Lewy body disease and multiple system atrophy. Acta Neuropathol. 1998;96(5):445-52.
399. Fujita Y, Ohama E, Takatama M, Al-Sarraj S, Okamoto K. Fragmentation of Golgi apparatus of nigral neurons with alpha-synuclein-positive inclusions in patients with Parkinson's disease. Acta Neuropathol. 2006;112(3):261-5.
400. Lashuel HA, Hirling H. Rescuing defective vesicular trafficking protects against alpha-synuclein toxicity in cellular and animal models of Parkinson's disease. ACS Chem Biol. 2006;1(7):420-4.
401. Sundaramoorthy V, Sultana JM, Atkin JD. Golgi fragmentation in amyotrophic lateral sclerosis, an overview of possible triggers and consequences. Front Neurosci. 2015;9:400.
402. Bellouze S, Baillat G, Buttigieg D, de la Grange P, Rabouille C, Haase G. Stathmin 1/2-triggered microtubule loss mediates Golgi fragmentation in mutant SOD1 motor neurons. Mol Neurodegener. 2016;11(1):43.
403. Millarte V, Farhan H. The Golgi in cell migration: regulation by signal transduction and its implications for cancer cell metastasis. ScientificWorldJournal. 2012;2012:498278.
404. Baschieri F, Confalonieri S, Bertalot G, Di Fiore PP, Dietmaier W, Leist M, et al. Spatial control of Cdc42 signalling by a GM130-RasGRF complex regulates polarity and tumorigenesis. Nat Commun. 2014;5:4839.
405. Farhan H, Hsu VW. Cdc42 and Cellular Polarity: Emerging Roles at the Golgi. Trends Cell Biol. 2016;26(4):241-8.
406. Buschman MD, Rahajeng J, Field SJ. GOLPH3 links the Golgi, DNA damage, and cancer. Cancer Res. 2015;75(4):624-7.
407. Dippold HC, Ng MM, Farber-Katz SE, Lee SK, Kerr ML, Peterman MC, et al. GOLPH3 bridges phosphatidylinositol-4- phosphate and actomyosin to stretch and shape the Golgi to promote budding. Cell. 2009;139(2):337-51.
408. Xing M, Peterman MC, Davis RL, Oegema K, Shiau AK, Field SJ. GOLPH3 drives cell migration by promoting Golgi reorientation and directional trafficking to the leading edge. Mol Biol Cell. 2016;27(24):3828-40.
409. Kuna RS, Field SJ. GOLPH3: a Golgi phosphatidylinositol(4)phosphate effector that directs vesicle trafficking and drives cancer. J Lipid Res. 2019;60(2):269-75.
410. Farber-Katz SE, Dippold HC, Buschman MD, Peterman MC, Xing M, Noakes CJ, et al. DNA damage triggers Golgi dispersal via DNA-PK and GOLPH3. Cell. 2014;156(3):413-27.
411. Yadav S, Puri S, Linstedt AD. A primary role for Golgi positioning in directed secretion, cell polarity, and wound healing. Mol Biol Cell. 2009;20(6):1728-36.
412. Tang CX, Luan L, Zhang L, Wang Y, Liu XF, Wang J, et al. Golgin-160 and GMAP210 play an important role in U251 cells migration and invasion initiated by GDNF. PLoS One. 2019;14(1):e0211501.
413. Deakin NO, Turner CE. Paxillin comes of age. J Cell Sci. 2008;121(Pt 15):2435-44.

414. Oh JJ, Grosshans DR, Wong SG, Slamon DJ. Identification of differentially expressed genes associated with HER-2/neu overexpression in human breast cancer cells. Nucleic Acids Res. 1999;27(20):4008-17.
415. Anczukow O, Akerman M, Clery A, Wu J, Shen C, Shirole NH, et al. SRSF1-Regulated Alternative Splicing in Breast Cancer. Mol Cell. 2015;60(1):105-17.
416. Babenko VN, Gubanova NV, Bragin AO, Chadaeva IV, Vasiliev GV, Medvedeva IV, et al. Computer Analysis of Glioma Transcriptome Profiling: Alternative Splicing Events. J Integr Bioinform. 2017;14(3).
417. Pandey P, Sliker B, Peters HL, Tuli A, Herskovitz J, Smits K, et al. Amyloid precursor protein and amyloid precursor-like protein 2 in cancer. Oncotarget. 2016;7(15):19430-44.
418. Ozaki T, Nakagawara A. Role of p53 in Cell Death and Human Cancers. Cancers (Basel). 2011;3(1):994-1013.
419. Bachert C, Lee TH, Linstedt AD. Lumenal endosomal and Golgi-retrieval determinants involved in pH-sensitive targeting of an early Golgi protein. Mol Biol Cell. 2001;12(10):3152-60.
420. Munro S. Localization of proteins to the Golgi apparatus. Trends Cell Biol. 1998;8(1):11-5.
421. Puri S, Bachert C, Fimmel CJ, Linstedt AD. Cycling of early Golgi proteins via the cell surface and endosomes upon lumenal pH disruption. Traffic. 2002;3(9):641-53.
422. Mallet WG, Maxfield FR. Chimeric forms of furin and TGN38 are transported with the plasma membrane in the trans-Golgi network via distinct endosomal pathways. J Cell Biol. 1999;146(2):345-59.
423. Natarajan R, Linstedt AD. A cycling cis-Golgi protein mediates endosome-to-Golgi traffic. Mol Biol Cell. 2004;15(11):4798-806.
424. Mallard F, Antony C, Tenza D, Salamero J, Goud B, Johannes L. Direct pathway from early/recycling endosomes to the Golgi apparatus revealed through the study of shiga toxin B-fragment transport. J Cell Biol. 1998;143(4):973-90.
425. Fraser ME, Chernaia MM, Kozlov YV, James MN. Crystal structure of the holotoxin from Shigella dysenteriae at 2.5 A resolution. Nat Struct Biol. 1994;1(1):59-64.
426. Endo Y, Tsurugi K, Yutsudo T, Takeda Y, Ogasawara T, Igarashi K. Site of action of a Vero toxin (VT2) from Escherichia coli O157:H7 and of Shiga toxin on eukaryotic ribosomes. RNA N-glycosidase activity of the toxins. Eur J Biochem. 1988;171(1-2):45-50.
427. St Hilaire PM, Boyd MK, Toone EJ. Interaction of the Shiga-like toxin type 1 B-subunit with its carbohydrate receptor. Biochemistry. 1994;33(48):14452-63.
428. Hagnerelle X, Plisson C, Lambert O, Marco S, Rigaud JL, Johannes L, et al. Two-dimensional structures of the Shiga toxin B-subunit and of a chimera bound to the glycolipid receptor Gb3. J Struct Biol. 2002;139(2):113-21.
429. Johannes L, Popoff V. Tracing the retrograde route in protein trafficking. Cell. 2008;135(7):1175-87.
430. Mukhopadhyay S, Redler B, Linstedt AD. Shiga toxin-binding site for host cell receptor GPP130 reveals unexpected divergence in toxin-trafficking mechanisms. Mol Biol Cell. 2013;24(15):2311-8.
431. Mukhopadhyay S, Bachert C, Smith DR, Linstedt AD. Manganese-induced trafficking and turnover of the cis-Golgi glycoprotein GPP130. Mol Biol Cell. 2010;21(7):1282-92.
432. Tewari R, Bachert C, Linstedt AD. Induced oligomerization targets Golgi proteins for degradation in lysosomes. Mol Biol Cell. 2015;26(24):4427-37.
433. Venkat S, Linstedt AD. Manganese-induced trafficking and turnover of GPP130 is mediated by sortilin. Mol Biol Cell. 2017;28(19):2569-78.
434. Lefrancois S, Zeng J, Hassan AJ, Canuel M, Morales CR. The lysosomal trafficking of sphingolipid activator proteins (SAPs) is mediated by sortilin. Embo j. 2003;22(24):6430-7.
435. Bai Y, Cui X, Gao D, Wang Y, Wang B, Wang W. Golgi integral membrane protein 4 manipulates cellular proliferation, apoptosis, and cell cycle in human head and neck cancer. Biosci Rep. 2018;38(4).

436. Wei H, Li B, Zhang R, Hao X, Huang Y, Qiao Y, et al. Serum GP73, a marker for evaluating progression in patients with chronic HBV infections. PLoS One. 2013;8(2):e53862.
437. Zhu K, Dai Z, Zhou J. Biomarkers for hepatocellular carcinoma: progression in early diagnosis, prognosis, and personalized therapy. Biomark Res. 2013;1(1):10.
438. Hann HW, Wang M, Hafner J, Long RE, Kim SH, Ahn M, et al. Analysis of GP73 in patients with HCC as a function of anti-cancer treatment. Cancer Biomark. 2010;7(6):269-73.
439. Liu Y, Zhou S, Shi J, Zhang X, Shentu L, Chen Z, et al. c-Myc transactivates GP73 and promotes metastasis of hepatocellular carcinoma cells through GP73-mediated MMP-7 trafficking in a mildly hypoxic microenvironment. Oncogenesis. 2019;8(10):58.
440. Seidah NG, Prat A. The biology and therapeutic targeting of the proprotein convertases. Nat Rev Drug Discov 2012;11(5):367-83.
441. Seidah NG, Chretien M. Proprotein and prohormone convertases: a family of subtilases generating diverse bioactive polypeptides. Brain Res. 1999;848(1-2):45-62.
442. Dubois CM, Blanchette F, Laprise MH, Leduc R, Grondin F, Seidah NG. Evidence that furin is an authentic transforming growth factor-beta1- converting enzyme. Am J Pathol. 2001;158(1):305-16.
443. Yana I, Weiss SJ. Regulation of membrane type-1 matrix metalloproteinase activation by proprotein convertases. Mol Biol Cell. 2000;11(7):2387-401.
444. Bassi DE, Fu J, Lopez de Cicco R, Klein-Szanto AJ. Proprotein convertases: "master switches" in the regulation of tumor growth and progression. Mol Carcinog. 2005;44(3):151-61.
445. Khatib AM, Siegfried G, Chretien M, Metrakos P, Seidah NG. Proprotein convertases in tumor progression and malignancy : novel targets in cancer therapy. Am J Pathol 2002;160(6):1921-35.
446. Fu J, Zhang J, Gong Y, Testa CL, Klein-Szanto AJ. Regulation of HIF-1 alpha by the proprotein convertases furin and PC7 in human squamous carcinoma cells. Mol Carcinog 2015;54(9):698-706.
447. Wetsel WC, Rodriguiz RM, Guillemot J, Rousselet E, Essalmani R, Kim IH, et al. Disruption of the expression of the proprotein convertase PC7 reduces BDNF production and affects learning and memory in mice. Proc Natl Acad Sci U S A. 2013;110(43):17362-7.
448. Thomas G. Furin at the cutting edge: from protein traffic to embryogenesis and disease. Nature Reviews Molecular Cell Biology. 2002;3(10):753-66.
449. Declercq J, Meulemans S, Plets E, Creemers JW. Internalization of the proprotein convertase PC7 from the plasma membrane is mediated by a novel motif. J Biol Chem. 2012;287(12):9052-60.
450. Durand L, Duval S, Evagelidis A, Guillemot J, Dianati V, Sikorska E, et al. The motif EXEXXXL in the cytosolic tail of the secretory human proprotein convertase PC7 regulates its trafficking and cleavage activity. J Biol Chem. 2020;295(7):2068-83.
451. Oh JJ, Grosshans DR, Wong SG, Slamon DJ. Identification of differentially expressed genes associated with HER-2/neu overexpression in human breast cancer cells. Nucleic Acids Res. 1999;27(20):4008-17.
452. Anczukow O, Akerman M, Clery A, Wu J, Shen C, Shirole NH, et al. SRSF1-Regulated Alternative Splicing in Breast Cancer. Mol Cell. 2015;60(1):105-17.
453. Boersema PJ, Geiger T, Wisniewski JR, Mann M. Quantification of the N-glycosylated secretome by super-SILAC during breast cancer progression and in human blood samples. Mol Cell Proteomics. 2013;12(1):158-71.
454. Paterson EK, Courtneidge SA. Invadosomes are coming: new insights into function and disease relevance. Febs j. 2018;285(1):8-27.
455. Seals DF, Azucena EF, Jr., Pass I, Tesfay L, Gordon R, Woodrow M, et al. The adaptor protein Tks5/Fish is required for podosome formation and function, and for the protease-driven invasion of cancer cells. Cancer Cell. 2005;7(2):155-65.
456. Rajan SG, Gallik KL, Monaghan JR, Uribe RA, Bronner ME, Saxena A. Tracking neural crest cell cycle progression in vivo. Genesis. 2018;56(6-7):e23214.

457. Horzum U, Ozdil B, Pesen-Okvur D. Step-by-step quantitative analysis of focal adhesions. MethodsX. 2014;1:56-9.
458. Curtis C, Shah SP, Chin SF, Turashvili G, Rueda OM, Dunning MJ, et al. The genomic and transcriptomic architecture of 2,000 breast tumours reveals novel subgroups. Nature. 2012;486(7403):346-52.
459. Pereira B, Chin SF, Rueda OM, Vollan HK, Provenzano E, Bardwell HA, et al. The somatic mutation profiles of 2,433 breast cancers refines their genomic and transcriptomic landscapes. Nat Commun. 2016;7:11479.
460. Ciriello G, Gatza ML, Beck AH, Wilkerson MD, Rhie SK, Pastore A, et al. Comprehensive Molecular Portraits of Invasive Lobular Breast Cancer. Cell. 2015;163(2):506-19.
461. Cerami E, Gao J, Dogrusoz U, Gross BE, Sumer SO, Aksoy BA, et al. The cBio cancer genomics portal: an open platform for exploring multidimensional cancer genomics data. Cancer Discov. 2012;2(5):401-4.
462. Gao J, Aksoy BA, Dogrusoz U, Dresdner G, Gross B, Sumer SO, et al. Integrative analysis of complex cancer genomics and clinical profiles using the cBioPortal. Sci Signal. 2013;6(269):pl1.
463. Chen R, Zou H, Figeys D. Detergent-Assisted Glycoprotein Capture: A Versatile Tool for In-Depth N-Glycoproteome Analysis. J Proteome Res. 2016;15(6):2080-6.
464. Aebi M. N-linked protein glycosylation in the ER. Biochim Biophys Acta. 2013;1833(11):2430-7.
465. Kornfeld R, Kornfeld S. Assembly of asparagine-linked oligosaccharides. Annu Rev Biochem. 1985;54:631-64.
466. Anderson ED, VanSlyke JK, Thulin CD, Jean F, Thomas G. Activation of the furin endoprotease is a multiple-step process: requirements for acidification and internal propeptide cleavage. EMBO J. 1997;16(7):1508-18.
467. Schechter I, Berger A. On the active site of proteases. 3. Mapping the active site of papain; specific peptide inhibitors of papain. Biochem Biophys Res Commun. 1968;32(5):898-902.
468. Benjannet S, Rhainds D, Hamelin J, Nassoury N, Seidah NG. The proprotein convertase PCSK9 is inactivated by furin and/or PC5/6A: Functional consequences of natural mutations and post-translational modifications. J Biol Chem. 2006;281(41):30561-72.
469. Krieger M, Brown MS, Goldstein JL. Isolation of Chinese hamster cell mutants defective in the receptor-mediated endocytosis of low density lipoprotein. J Mol Biol. 1981;150(2):167-84.
470. Lippincott-Schwartz J, Yuan L, Tipper C, Amherdt M, Orci L, Klausner RD. Brefeldin A's effects on endosomes, lysosomes, and the TGN suggest a general mechanism for regulating organelle structure and membrane traffic. Cell. 1991;67(3):601-16.
471. Nobes CD, Hall A. Rho, rac, and cdc42 GTPases regulate the assembly of multimolecular focal complexes associated with actin stress fibers, lamellipodia, and filopodia. Cell. 1995;81(1):53-62.
472. Bagci H, Sriskandarajah N, Robert A, Boulais J, Elkholi IE, Tran V, et al. Mapping the proximity interaction network of the Rho-family GTPases reveals signalling pathways and regulatory mechanisms. Nat Cell Biol. 2020;22(1):120-34.
473. Sells MA, Knaus UG, Bagrodia S, Ambrose DM, Bokoch GM, Chernoff J. Human p21-activated kinase (Pak1) regulates actin organization in mammalian cells. Curr Biol. 1997;7(3):202-10.
474. Manser E, Huang HY, Loo TH, Chen XQ, Dong JM, Leung T, et al. Expression of constitutively active alpha-PAK reveals effects of the kinase on actin and focal complexes. Mol Cell Biol. 1997;17(3):1129-43.
475. Buccione R, Orth JD, McNiven MA. Foot and mouth: podosomes, invadopodia and circular dorsal ruffles. Nat Rev Mol Cell Biol. 2004;5(8):647-57.
476. Seidah NG, Benjannet S, Wickham L, Marcinkiewicz J, Jasmin SB, Stifani S, et al. The secretory proprotein convertase neural apoptosis-regulated convertase 1 (NARC-1): liver regeneration and neuronal differentiation. Proc Natl Acad Sci U S A. 2003;100(3):928-33.

477. Seidah NG, Sadr MS, Chretien M, Mbikay M. The multifaceted Proprotein Convertases: their unique, redundant, complementary and opposite functions. J Biol Chem. 2013;288:21473-81.
478. Braun E, Sauter D. Furin-mediated protein processing in infectious diseases and cancer. Clin Transl Immunology. 2019;8(8):e1073.
479. Oexle K, Ried JS, Hicks AA, Tanaka T, Hayward C, Bruegel M, et al. Novel association to the proprotein convertase PCSK7 gene locus revealed by analysing soluble transferrin receptor (sTfR) levels. Hum Mol Genet. 2011;20(5):1042-7.
480. Kodani A, Kristensen I, Huang L, Sutterlin C. GM130-dependent control of Cdc42 activity at the Golgi regulates centrosome organization. Mol Biol Cell. 2009;20(4):1192-200.
481. Ye QH, Zhu WW, Zhang JB, Qin Y, Lu M, Lin GL, et al. GOLM1 Modulates EGFR/RTK Cell-Surface Recycling to Drive Hepatocellular Carcinoma Metastasis. Cancer Cell. 2016;30(3):444-58.
482. Duval S. A-TA, Elkholi E. I., Chen R., Seebun D., Mayne J., Côté J.F., Figeys D., Seidah N. G. Shedding of Cancer Susceptibility Candidate 4 (CASC4) by the Convertases PC7/Furin Unravels a Novel Secretory Protein Implicated in Cancer Progression. in revision 2020.
483. Monteith GR, Prevarskaya N, Roberts-Thomson SJ. The calcium-cancer signalling nexus. Nat Rev Cancer. 2017;17(6):367-80.
484. Aridor M, Bannykh SI, Rowe T, Balch WE. Sequential coupling between COPII and COPI vesicle coats in endoplasmic reticulum to Golgi transport. J Cell Biol. 1995;131(4):875-93.
485. Tewari R, Jarvela T, Linstedt AD. Manganese induces oligomerization to promote down-regulation of the intracellular trafficking receptor used by Shiga toxin. Mol Biol Cell. 2014;25(19):3049-58.
486. Roderick HL, Cook SJ. Ca2+ signalling checkpoints in cancer: remodelling Ca2+ for cancer cell proliferation and survival. Nat Rev Cancer. 2008;8(5):361-75.
487. Ogden CL, Yanovski SZ, Carroll MD, Flegal KM. The epidemiology of obesity. Gastroenterology. 2007;132(6):2087-102.
488. Morris MJ, Beilharz JE, Maniam J, Reichelt AC, Westbrook RF. Why is obesity such a problem in the 21st century? The intersection of palatable food, cues and reward pathways, stress, and cognition. Neurosci Biobehav Rev. 2015;58:36-45.
489. Flegal KM, Graubard BI, Williamson DF, Gail MH. Cause-specific excess deaths associated with underweight, overweight, and obesity. Jama. 2007;298(17):2028-37.
490. Simon GE, Von Korff M, Saunders K, Miglioretti DL, Crane PK, van Belle G, et al. Association between obesity and psychiatric disorders in the US adult population. Arch Gen Psychiatry. 2006;63(7):824-30.
491. Geiger BM, Haburcak M, Avena NM, Moyer MC, Hoebel BG, Pothos EN. Deficits of mesolimbic dopamine neurotransmission in rat dietary obesity. Neuroscience. 2009;159(4):1193-9.
492. Teegarden SL, Nestler EJ, Bale TL. Delta FosB-mediated alterations in dopamine signaling are normalized by a palatable high-fat diet. Biol Psychiatry. 2008;64(11):941-50.
493. Fulton S. Appetite and reward. Front Neuroendocrinol. 2010;31(1):85-103.
494. Wang GJ, Volkow ND, Logan J, Pappas NR, Wong CT, Zhu W, et al. Brain dopamine and obesity. Lancet. 2001;357(9253):354-7.
495. Russo SJ, Bolanos CA, Theobald DE, DeCarolis NA, Renthal W, Kumar A, et al. IRS2-Akt pathway in midbrain dopamine neurons regulates behavioral and cellular responses to opiates. Nat Neurosci. 2007;10(1):93-9.
496. Hyman SE, Malenka RC, Nestler EJ. Neural mechanisms of addiction: the role of reward-related learning and memory. Annu Rev Neurosci. 2006;29:565-98.
497. Ahmari SE. Using mice to model Obsessive Compulsive Disorder: From genes to circuits. Neuroscience. 2016;321:121-37.

498. Maren S. The amygdala, synaptic plasticity, and fear memory. Ann N Y Acad Sci. 2003;985:106-13.
499. Besnard J, Ruda GF, Setola V, Abecassis K, Rodriguiz RM, Huang XP, et al. Automated design of ligands to polypharmacological profiles. Nature. 2012;492(7428):215-20.
500. Barrot M, Wallace DL, Bolanos CA, Graham DL, Perrotti LI, Neve RL, et al. Regulation of anxiety and initiation of sexual behavior by CREB in the nucleus accumbens. Proc Natl Acad Sci U S A. 2005;102(23):8357-62.
501. Pliakas AM, Carlson RR, Neve RL, Konradi C, Nestler EJ, Carlezon WA, Jr. Altered responsiveness to cocaine and increased immobility in the forced swim test associated with elevated cAMP response element-binding protein expression in nucleus accumbens. J Neurosci. 2001;21(18):7397-403.
502. Sartim AG, Sartim MA, Cummings RD, Dias-Baruffi M, Joca SR. Impaired Emotional Response to Stress in Mice Lacking Galectin-1 or Galectin-3. Physiol Behav. 2020:112862.
503. Oberlander C, Demassey Y, Verdu A, Van de Velde D, Bardelay C. Tolerance to the serotonin 5-HT1 agonist RU 24969 and effects on dopaminergic behaviour. Eur J Pharmacol. 1987;139(2):205-14.
504. Faravelli C, Lo Sauro C, Lelli L, Pietrini F, Lazzeretti L, Godini L, et al. The role of life events and HPA axis in anxiety disorders: a review. Curr Pharm Des. 2012;18(35):5663-74.
505. Hryhorczuk C, Decarie-Spain L, Sharma S, Daneault C, Rosiers CD, Alquier T, et al. Saturated high-fat feeding independent of obesity alters hypothalamus-pituitary-adrenal axis function but not anxiety-like behaviour. Psychoneuroendocrinology. 2017;83:142-9.
506. Toorie AM, Cyr NE, Steger JS, Beckman R, Farah G, Nillni EA. The Nutrient and Energy Sensor Sirt1 Regulates the Hypothalamic-Pituitary-Adrenal (HPA) Axis by Altering the Production of the Prohormone Convertase 2 (PC2) Essential in the Maturation of Corticotropin-releasing Hormone (CRH) from Its Prohormone in Male Rats. J Biol Chem. 2016;291(11):5844-59.
507. Nillni EA. The metabolic sensor Sirt1 and the hypothalamus: Interplay between peptide hormones and pro-hormone convertases. Mol Cell Endocrinol. 2016;438:77-88.
508. Thomas A, Burant A, Bui N, Graham D, Yuva-Paylor LA, Paylor R. Marble burying reflects a repetitive and perseverative behavior more than novelty-induced anxiety. Psychopharmacology (Berl). 2009;204(2):361-73.
509. Tosta CL, Silote GP, Fracalossi MP, Sartim AG, Andreatini R, Joca SRL, et al. S-ketamine reduces marble burying behaviour: Involvement of ventromedial orbitofrontal cortex and AMPA receptors. Neuropharmacology. 2019;144:233-43.
510. Porton B, Rodriguiz RM, Phillips LE, Gilbert JWt, Feng J, Greengard P, et al. Mice lacking synapsin III show abnormalities in explicit memory and conditioned fear. Genes Brain Behav. 2010;9(3):257-68.
511. Etienne-Manneville S. Cdc42--the centre of polarity. J Cell Sci. 2004;117(Pt 8):1291-300.
512. Bergeron JJM, Au CE, Thomas DY, Hermo L. Proteomics Identifies Golgi phosphoprotein 3 (GOLPH3) with A Link Between Golgi Structure, Cancer, DNA Damage and Protection from Cell Death. Mol Cell Proteomics. 2017;16(12):2048-54.
513. Lambert JP, Tucholska M, Go C, Knight JD, Gingras AC. Proximity biotinylation and affinity purification are complementary approaches for the interactome mapping of chromatin-associated protein complexes. J Proteomics. 2015;118:81-94.
514. Matulonis UA. Ovarian Cancer. Hematol Oncol Clin North Am. 2018;32(6):xiii-xiv.
515. Mukhopadhyay S, Linstedt AD. Manganese blocks intracellular trafficking of Shiga toxin and protects against Shiga toxicosis. Science. 2012;335(6066):332-5.
516. Potelle S, Morelle W, Dulary E, Duvet S, Vicogne D, Spriet C, et al. Glycosylation abnormalities in Gdt1p/TMEM165 deficient cells result from a defect in Golgi manganese homeostasis. Hum Mol Genet. 2016;25(8):1489-500.

517. Kornak U, Reynders E, Dimopoulou A, van Reeuwijk J, Fischer B, Rajab A, et al. Impaired glycosylation and cutis laxa caused by mutations in the vesicular H+-ATPase subunit ATP6V0A2. Nat Genet. 2008;40(1):32-4.
518. Branon TC, Bosch JA, Sanchez AD, Udeshi ND, Svinkina T, Carr SA, et al. Efficient proximity labeling in living cells and organisms with TurboID. Nat Biotechnol. 2018;36(9):880-7.
519. Guardia CM, De Pace R, Mattera R, Bonifacino JS. Neuronal functions of adaptor complexes involved in protein sorting. Curr Opin Neurobiol. 2018;51:103-10.
520. Ciechanover A, Kwon YT. Degradation of misfolded proteins in neurodegenerative diseases: therapeutic targets and strategies. Exp Mol Med. 2015;47:e147.
521. Yerbury JJ, Ooi L, Dillin A, Saunders DN, Hatters DM, Beart PM, et al. Walking the tightrope: proteostasis and neurodegenerative disease. J Neurochem. 2016;137(4):489-505.
522. Saidi M, Beaudry F. Targeted high-resolution quadrupole-Orbitrap mass spectrometry analyses reveal a significant reduction of tachykinin and opioid neuropeptides level in PC1 and PC2 mutant mouse spinal cords. Neuropeptides. 2017;65:37-44.
523. Shaulov-Rotem Y, Merquiol E, Weiss-Sadan T, Moshel O, Salpeter S, Shabat D, et al. A novel quenched fluorescent activity-based probe reveals caspase-3 activity in the endoplasmic reticulum during apoptosis. Chem Sci. 2016;7(2):1322-37.
524. Walker E, Liu Y, Kim I, Biro M, Iyer SR, Ezaldein H, et al. A Protease-Activated Fluorescent Probe Allows Rapid Visualization of Keratinocyte Carcinoma During Excision. Cancer Res. 2020.
525. Wan YY, Flavell RA. Regulatory T-cell functions are subverted and converted owing to attenuated Foxp3 expression. Nature. 2007;445(7129):766-70.
526. Geiger TL, Tauro S. Nature and nurture in Foxp3(+) regulatory T cell development, stability, and function. Hum Immunol. 2012;73(3):232-9.
527. Phua J, Weng L, Ling L, Egi M, Lim CM, Divatia JV, et al. Intensive care management of coronavirus disease 2019 (COVID-19): challenges and recommendations. Lancet Respir Med. 2020.
528. Millet JK, Whittaker GR. Host cell entry of Middle East respiratory syndrome coronavirus after two-step, furin-mediated activation of the spike protein. Proc Natl Acad Sci U S A. 2014;111(42):15214-9.
529. Chan CM, Woo PC, Lau SK, Tse H, Chen HL, Li F, et al. Spike protein, S, of human coronavirus HKU1: role in viral life cycle and application in antibody detection. Exp Biol Med (Maywood). 2008;233(12):1527-36.
530. Izaguirre G. The Proteolytic Regulation of Virus Cell Entry by Furin and Other Proprotein Convertases. Viruses. 2019;11(9).